JOINT TRANSPORTATION
RESEARCH PROGRAM
INDIANA DEPARTMENT OF TRANSPORTATION
AND PURDUE UNIVERSITY

Long-Term Project and Network-Level NDT Implementation Plan for Indiana

Yunhui Jia, Christopher S. Williams, Prince Baah, Mark D. Bowman

SPR-4445 • Report Number: FHWA/IN/JTRP-2022/31 • DOI: 10.5703/1288284317582

RECOMMENDED CITATION

Jia, Y., Williams, C. S., Baah, P., & Bowman, M. D. (2022). *Long-term project and network-level NDT implementation plan for Indiana* (Joint Transportation Research Program Publication No. FHWA/IN/JTRP-2022/31). West Lafayette, IN: Purdue University. https://doi.org/10.5703/1288284317582

AUTHORS

Yunhui Jia
Graduate Researcher
Lyles School of Civil Engineering
Purdue University

Christopher S. Williams, PhD
Assistant Professor of Civil Engineering
Lyles School of Civil Engineering
Purdue University

Prince Baah, PhD, PE
Bridge Research Engineer
Indiana Department of Transportation

Mark D. Bowman, PhD, PE
Professor of Civil Engineering
Lyles School of Civil Engineering
Purdue University
(765) 494-2220
bowmanmd@purdue.edu
Corresponding Author

JOINT TRANSPORTATION RESEARCH PROGRAM

The Joint Transportation Research Program serves as a vehicle for INDOT collaboration with higher education institutions and industry in Indiana to facilitate innovation that results in continuous improvement in the planning, design, construction, operation, management and economic efficiency of the Indiana transportation infrastructure. https://engineering.purdue.edu/JTRP/index_html

Published reports of the Joint Transportation Research Program are available at http://docs.lib.purdue.edu/jtrp/.

NOTICE

TECHNICAL REPORT DOCUMENTATION PAGE

1. Report No. FHWA/IN/JTRP-2022/31	**2. Government Accession No.**	**3. Recipient's Catalog No.**
4. Title and Subtitle Long-Term Project and Network-Level NDT Implementation Plan for Indiana		**5. Report Date** November 2022 **6. Performing Organization Code**
7. Author(s) Yunhui Jia, Christopher S. Williams, Prince Baah, and Mark D. Bowman		**8. Performing Organization Report No.** FHWA/IN/JTRP-2022/31
9. Performing Organization Name and Address Joint Transportation Research Program Hall for Discovery and Learning Research (DLR), Suite 204 207 S. Martin Jischke Drive West Lafayette, IN 47907		**10. Work Unit No.** **11. Contract or Grant No.** SPR-4445
12. Sponsoring Agency Name and Address Indiana Department of Transportation (SPR) State Office Building 100 North Senate Avenue Indianapolis, IN 46204		**13. Type of Report and Period Covered** Final Report **14. Sponsoring Agency Code**

15. Supplementary Notes
Conducted in cooperation with the U.S. Department of Transportation, Federal Highway Administration.

16. Abstract

Bridge deck condition assessments in Indiana are primarily reliant on visual inspection. The condition of bridge decks, however, is highly dependent on deterioration under the surface, which includes the corrosion of steel reinforcement and concrete delamination. The implementation of reliable nondestructive testing (NDT) methods can provide information about such internal deterioration, but considering the multiple NDT methods currently available, guidance is needed to find the best approach for assessing bridge decks in the state's bridge inventory. A research program was conducted to examine various NDT methods with the objective of recommending an effective NDT strategy for network-level and project-level bridge inspections in Indiana that will complement information from traditional bridge inspections and provide asset engineers with improved information for long-term programming decisions. For the study, several consultants used various NDT methods to inspect a set of bridge decks that represented a range of desired test variables. Based on the test results, it was determined that aerial infrared thermography (IRT) is a good network-level method that is capable of scanning a large number of bridges and providing an initial assessment of bridge deck conditions. If significant delamination activity is detected, then follow-up network-level scanning limited to the problematic bridge decks should be performed using vehicle-mounted IRT. For project-level scanning of individual bridge decks, impact echo was found to be reliable and repeatable. For bridges with high-traffic volume for which project-level scanning is needed, a pole-mounted IRT system was found to be effective for evaluating the deck condition.

17. Key Words bridge deck, nondestructive testing, delamination, corrosion, condition assessment	**18. Distribution Statement** No restrictions. This document is available through the National Technical Information Service, Springfield, VA 22161.

19. Security Classif. (of this report) Unclassified	**20. Security Classif. (of this page)** Unclassified	**21. No. of Pages** 239 including appendices	**22. Price**

Form DOT F 1700.7 (8-72) Reproduction of completed page authorized

EXECUTIVE SUMMARY

Introduction

The Indiana Department of Transportation (INDOT) has traditionally paired visual inspection with bridge deck age to assess the condition of bridge decks and make programming decisions about possible future work actions. While chain dragging and hammer sounding are used by bridge inspectors to complement the information obtained from visual inspection, the internal condition of bridge decks cannot be accurately evaluated unless nondestructive inspection methods are employed. Considering the multiple NDT (nondestructive testing) methods that are available, INDOT needs guidance to select NDT methods that effectively assess the condition of large numbers of bridge decks on a network-wide basis and are also effective on a case-by-case, project-level basis for individual bridges. Consequently, the purpose of this study is to examine various NDT methods and develop recommendations for an NDT strategy for network-level and project-level bridge inspections in Indiana that will complement bridge information from traditional bridge inspections and provide asset engineers with improved information for long-term programming decisions.

Findings

Several different factors were considered for the development of the nondestructive testing plan for the research study. These included different bridge deck characteristics, such as the type of bridge deck, type of supporting structure, reinforcement protection (plain or epoxy-coated), bridge NBI deck and wearing surface conditions, presence, type of overlay (latex modified concrete or epoxy overlay), depth of top reinforcement layer, and geographic location within the state. Several different NDT methods that were suitable for ease of implementation were also considered, such as ground penetrating radar (GPR), automated sounding, impact echo (IE), and infrared thermography (IRT). For each of these NDT methods, a different way of collecting the nondestructive data was used. Lastly, a limited number of concrete cores was collected and used to assess the results from the nondestructive scanning.

The next step in the research plan was to select a variety of consultants who provide NDT services to collect NDT data from a set of bridge decks that represented various combinations of the bridge deck characteristics noted previously. The INDOT Division of Research also collected NDT data. Many of the consultants nondestructively scanned the same set of bridge decks so that a broad spectrum of NDT information could be compared. A total of nine different NDT consultants plus INDOT collected NDT information. The testing was conducted in two rounds—the first in the fall of 2020 and the second in the summer to fall of 2021. Some of the consultants conducted more than one NDT method when scanning the bridge decks, while others conducted only a single test method. The NDT results from different consultants were compared to gauge the degree of agreement in the deck conditions for a given test method. The results of different test methods were also compared to understand the relative sensitivity of the NDT methods. It was recognized that comparing different NDT methods may be problematic because different methods detect different types of deck distress conditions.

Based upon the comparisons and the results observed in this study, the following findings were discovered.

- IE results compare reasonably well, and the method was found to be repeatable. Selective concrete cores extracted from some of the bridge decks universally confirmed the IE results.
- IRT results for delamination detection were found to be somewhat comparable between entities. However, it was also determined that the IRT method can be notably affected by shaded deck areas, moisture, and small temperature differences. Percentage delamination values detected by IRT were routinely less than those found by IE, but they were greater than the values from automated sounding for most bridges.
- GPR was used to both detect the concrete cover thickness above the top reinforcement and assess the condition of the bridge deck.
  - Both air-launched GPR and ground-coupled GPR were found to be very effective in detecting the location of the top layer of reinforcement and determining the amount of concrete cover for the top reinforcement layer. Either method is suitable for verifying the concrete cover of a bridge deck.
  - Bridge deck deterioration results detected by both air-launched and ground-coupled GPR were found to have significant variations in both values and locations. Therefore, the method is not believed to be consistently repeatable, and it is not recommended as a sole method to evaluate bridge deck condition. Nevertheless, it is believed that it can provide valuable information about the possible likelihood of corrosion activity in a bridge deck and is useful when combined with other primary NDT information, such as IRT or IE.
- Automated sounding results were found to provide low delamination detection values compared to other methods.
- There is a need for ground-truth testing to clearly identify the actual bridge deck condition so that suitable comparisons with nondestructive testing can be verified. A follow-up study is recommended to fill in this missing information and develop additional confidence in the results found herein.

Implementation

There is a significant need by INDOT to complement current bridge inspection information based upon visual inspection data and bridge age with reliable nondestructive testing data. The combination of visual information and internal deck condition information will help bridge inspectors evaluate the deck and wearing surface conditions more accurately. Improved condition assessments will provide asset engineers with further information that can be used strategically in future programing of major bridge deck work actions.

The following recommendations were made for network-level NDT inspection and project-level NDT inspection of bridge decks in Indiana.

- Aerial IRT is recommended as the initial network-level inspection method to scan a large number of bridges and effectively conduct a triage of bridge deck condition. If significant delamination activity is detected, then follow-up network-level scanning on only the problematic bridge decks should be performed using vehicle-mounted IRT. It may be

advantageous to also add vehicle-mounted air-launched GPR to complement the IRT information to assess the probability of corrosion activity.

- IE is recommended as a project-level test for future NDT assessment to detect delamination discontinuities in bridge decks.
- Pole-mounted IRT-UTD is recommended as a secondary project-level test for bridges with very high-volume traffic because of its ease of installation and removal in the field.

The recommended network-level inspection methods should be employed to evaluate the entire network of interstate bridge decks and NHS bridge decks. Additional state road bridges can also be included in the rotation of bridge assessments depending upon available funds and personnel. These condition assessments can be refreshed every 2 to 4 years so that the condition assessments can be compared and changes in bridge deck condition tracked, much like routine medical assessments are conducted for people.

If the condition of the bridge decks evaluated in the network-level assessments deteriorate to a significant extent, then project-level inspections may be initiated to gather information for making decisions regarding the application of an overlay or even a deck replacement on specific bridges. Use of reliable nondestructive test information of the actual bridge deck condition is much more reliable than simply using visual inspection and bridge deck age alone to make major programming decisions that can cost several millions of dollars.

CONTENTS

LIST OF TABLES

LIST OF FIGURES

1. INTRODUCTION

To make programming decisions for bridge decks, the present INDOT protocol integrates visual bridge inspection data with the age of the bridge deck. Although it is a good starting point to detect the damage level of bridges, visual inspection cannot assess what is happening inside the structure or under the bridge due to deck pans. Nondestructive testing (NDT) of a bridge deck is a methodology used to detect deterioration and damage under the deck surface. The NDT information can provide additional reliable results on the deck condition that can be used to complement the visual inspection information. There are many different NDT methods that can be used for different applications, such as ground penetrating radar (GPR), infrared thermography (IRT), impact echo (IE), etc. (Gucunski et al., 2013). Delamination and probability of corrosion are two major bridge deck deterioration parameters that NDT technologies can identify.

After 20 years of service, INDOT often initiates a significant construction operation for bridge decks, such as the installation of an overlay or a deck replacement. As a result, a typical bridge service life would be 80 years, with an overlay after 20 years of bridge service life, a deck replacement after 40 years, another overlay after 60 years, and bridge replacement after 80 years. As part of a study conducted by Taylor et al. (2016), this model was compared to the service life of the decks—and the related cost—if non-destructive testing (NDT) was used to determine significant work action decisions. The lowest cost option available through the programming actions currently used by INDOT is always more costly than the use of NDT to determine the main bridge deck work actions; it is estimated to be 23% to 54% more expensive (Taylor et al., 2018). The savings were enormous when the cost reductions were applied to Indiana's full network of bridges. A number of studies have been conducted to show the numerous benefits of adopting NDT to assess bridge deck conditions, including the aforementioned study for Indiana (Taylor et al., 2016).

INDOT previously contracted with an NDT consultant (Consultant J) to test 259 bridge decks using air-launched GPR scanning. However, the bridge deck type and the nondestructive testing method were not always coordinated. Some of the decks were reinforced concrete with no overlay, while others had different types and thicknesses of overlay material. Consequently, there was significant variation in the results, creating some concerns about the reliability and apparent usefulness of bridge deck NDT information in evaluating the condition of bridge decks.

The purpose of the research discussed herein is (1) to examine the reliability of various NDT test methods and their usefulness in assessing the condition of bridge decks and (2) to make recommendations of viable NDT methods for network-level and project-level bridge deck inspections.

2. BACKGROUND INFORMATION

Both project-level and network-level evaluations are good candidates for NDT bridge deck inspections. Project-level testing is a detailed bridge deck inspection that normally involves maintenance of traffic (MOT), whereas network-level testing is the assessment of a large number of bridges at highway speeds in an abbreviated period and, in most cases, without MOT.

Project-level (PL) inspections are often performed when the number of bridges to be evaluated is limited and detailed inspection protocols need to be carried out. Chain dragging and hammer sounding, half-cell potential, IE testing, chloride ion penetration testing, and ground coupled GPR scanning are some of the inspection methods commonly used. The results of these more detailed inspection techniques are frequently more accurate and detailed than the results of network-level inspections, which are more limited.

Network-level (NL) inspections are often used to scan or analyze a large set of bridge decks and to acquire a better knowledge of the INDOT bridge inventory. NDT testing methods performed during such inspections are designed to collect bridge deck condition data quickly. Many entities apply infrared thermography and air-launched ground penetrating radar to collect NDT data at highway speeds. The precision of these bridge deck scans is often lower than project-level inspection methods. The NDT findings produced during network-level scanning, on the other hand, are still reasonably accurate and can be used as an initial scanning or screening method to evaluate decks and identify those decks that may be good candidates for further project-level inspection.

In the research described in this report, five major NDT methods were used to evaluate the condition of selected bridge decks: GPR, sounding, IE, IRT, and destructive sampling. GPR and IRT testing were used in both project-level and network-level testing. Air-launched GPR was used for network-level scanning and ground-coupled GPR was used for project-level testing. IRT testing was completed in different ways, such as aerial IRT, pole-mounted IRT, vehicle-mounted IRT, and drone-mounted IRT. Pole-mounted IRT needed traffic control for installation and removal, so it is categorized as project-level testing. IE, concrete cores, and automatic sounding methods were only used in project-level testing. Detailed information about each testing method is provided below.

2.1 Ground Penetrating Radar

GPR is a common NDT method used to quickly examine the conditions of a structure. Electromagnetic waves that are transmitted into the bridge deck and pass through the top reinforcement level are used to evaluate the condition of bridge decks. Reinforcement cover thickness, the configuration of reinforcement, the probability of corrosion of reinforcement, and concrete deterioration are major condition assessments

that GPR can provide. The results from deck scanning are used to create a subsurface contour map. Deicing salt chlorides are a common cause of concrete deck reinforcing steel corrosion, and chloride concentrations in concrete attenuate GPR signals. Therefore, a relative comparison of data throughout the deck can identify locations of possible corrosion. The operating frequency of the antennas can be set as needed to allow for different levels of detail and penetration depth. GPR can be divided into two types: air-launched GPR and ground-coupled GPR (Romero & Roberts, 2002). Data are collected at traffic speed using air-launched GPR, which commonly has antenna mounts on a vehicle (Figure 2.1). Using air-launched GPR, a large amount of data can be collected in a short period. A ground-coupled GPR antenna usually is installed on a pushcart (Figure 2.2). Inspectors take repeated passes to push the cart across the bridge deck. By directly touching, or nearly touching, the bridge surface, the antenna transmits and receives waves. When comparing the two types of GPR tests, air-launched GPR is better for evaluating many bridges, while ground-coupled GPR is better for more precise measurements.

2.2 Sounding Inspection Methods

Two general sounding inspection methods are commonly used to detect delaminated regions in a bridge deck: manual sounding and automated sounding inspection.

Figure 2.1 Example of air-launched GPR equipment.

Chain dragging and hammer sounding are two traditional manual sounding inspection methods that are used by many state DOTs. Elastic sound waves are sent into the bridge deck by either dragging chains or striking the deck with a hammer. Operators listen to the sound, and especially changes in the sound, to determine the condition of the bridge deck. A sound deck has a distinct ringing sound, but a delaminated deck has an echoing or muffled sound. The manual sounding inspection method mainly applies to bridge decks with significant delamination. The limitation of the manual sounding method is that minor delamination is hard to distinguish by the human ear, and results rely on the skill and experience of operators.

An automated sounding method performs an inspection similar in nature to that used in manual inspections, but deck sounding and the sound collection is performed in an automated fashion (Figure 2.3). Automated sounding equipment may use, for example, chains mounted to wheels or a number of impact hammers to generate the deck sounding. Isolated microphones are used to record the induced dynamic sound excitation. The microphones capture sound and vibration amplitudes as a function of time, then convert the data to the frequency domain for analysis.

Instead of human judgment, the method adjusts and compares acoustic data to classify the deck condition. The data are classified as either "intact" or "delaminated."

2.3 Impact Echo

The impact echo (IE) technique is a project-level method for detecting delaminations in concrete (see Figure 2.4). Waves are sent into the bridge deck by impacting or striking the surface and measuring the time needed for the wave to pass through the deck by monitoring the reflected waves. This is accomplished by striking the surface of the bridge deck being tested and measuring the response using a neighboring sensor (Sansalone & Carino, 1989). The dominant return frequency from the bottom of the deck would indicate intact concrete, while a delaminated region within the deck will produce a shift in the return frequency and indicate an internal discontinuity.

Figure 2.2 Example of ground-coupled GPR equipment.


Figure 2.3 Example of equipment for automated sounding inspection (used with permission from consultant).

Figure 2.4 Example of IE equipment.

Figure 2.5 Example of a plane for aerial IRT (used with permission from consultant).

Figure 2.6 Example of the vehicle-mounted IRT equipment (used with permission from consultant).

Figure 2.7 Example of drone-mounted IRT equipment (used with permission from consultant).

2.4 Infrared Thermography

IR thermography (IRT) is a common NDT method used to discover subsurface delamination. Surface radiation of electromagnetic waves associated with temperature fluctuations at infrared wavelengths is used to analyze the condition of a bridge deck. The heating and cooling behavior of the resultant material is compared to the surrounding material. Temperature difference within a bridge deck is measured by infrared cameras, which subsequently transforms the information into a signal. These signals are then analyzed to generate temperature maps in the structure. Variable parameters, such as density and thermal conductivity of the material, temperature of the surrounding area, and humidity of air can affect the testing results. IRT is commonly used to detect delaminations at or above the top reinforcement level and debonding between the overlay and bridge deck (Maierhofer, et al., 2002, 2004, 2006; Maser & Bernhardt, 2000). IR thermography testing can be collected in different ways: mounted on an airplane (aerial IRT), mounted on a vehicle (vehicle-mounted IRT), mounted on a drone (drone-mounted IRT), and mounted on a pole (pole-mounted IRT) (see Figure 2.5 through Figure 2.8). The data collection system may influence the accuracy of the results in terms of testing speed, distance from the surface of a deck, and presence of an overlay.

Figure 2.8 Example of pole-mounted IRT equipment (used with permission from consultant).

Figure 2.9 Example of a concrete core.

2.5 Destructive Sampling

Core drilling is a reliable approach for obtaining representative samples from concrete structures. Concrete cores of the actual bridge deck material offer samples for laboratory tests to determine the presence of steel, condition of concrete, chemical contents, etc. Cores are commonly cut with a rotary cutting tool equipped with diamond bits. Depending on the purpose of the concrete core, the size of the cylindrical specimen can be varied. A typical specimen is depicted in Figure 2.9. If the core is located in a region of the deck that exhibits deterioration, it can provide visual evidence of delamination inside the deck caused by reinforcement corrosion or debonding at the interface between the original concrete deck and a surface overlay.

3. TESTING INFORMATION

3.1 Bridge Selection

Two rounds of testing were conducted for the research study. The first and second rounds of deck scanning were performed in fall 2020 and summer/fall 2021, respectively. In the first round of testing, 20 bridges were selected for network-level testing. Out of these bridges, 10 were then selected for project-level testing. In addition, a total 38 bridges along I-65 were chosen for aerial IRT testing; only a couple of these bridges were included in the set of network-level bridges to be tested. Lastly, ten bridges with newly-constructed bridge decks were selected to nondestructively measure the concrete cover depth to the top reinforcing bars in the deck. In the second round of testing, 10 bridges were selected for both project-level and network-level testing, while 14 bridges along SR 18 and 27 bridges along I-69 were chosen for aerial IRT testing.

The bridges that were selected for nondestructive evaluation were chosen based on the inclusion of various critical factors that may influence the test results. During the selection process, parameters such as superstructure type, type of wearing surface, type of

design, deck protection, facility carried, age of deck, age of overlay, deck rating, and wearing surface rating were taken into account. The explanation of each factor is listed below.

Steel, concrete, and prestressed concrete were three superstructure types that were considered in bridge selection. Second, the three major types of wearing surfaces considered were latex concrete overlay, epoxy overlay, and monolithic concrete (no overlay). This study did not include decks with an asphalt overlay. Furthermore, slab bridges, girder bridges, and truss bridges were included as different types of bridge design. Bridges were selected from each of these three types. Then, deck protection was concerned with the presence of epoxy-coated reinforcement in the deck. Selected bridge decks included those with black steel and others with epoxy-coated reinforcement. Moreover, the type of roads carried by most bridges that were evaluated were interstate, state road, and US Highway; few bridges carried city roads. In addition, the ages of the decks and overlays were an important consideration. Newer bridge decks or overlays would be expected to have few defects, which would not be ideal for detecting delamination or degradation. As a result, for testing, bridges with older decks or overlays were selected. Finally, bridge decks with deck and wearing surface NBI ratings of 8, 9, and less than 4 were not used in this study.

3.2 Bridge Information

For the first round of scanning, 61 bridges were tested by seven different NDT methods, and six entities (INDOT and five consultants) were involved. For the second round of testing, 56 bridges were tested by eight different NDT methods, and eight entities (INDOT and seven consultants) were involved. Table 3.1 is a summary table of the 24 bridges evaluated by NL and PL testing for both rounds. Locations of these bridges are shown in Figure 3.1. A total of 75 bridges were selected for the two rounds of aerial IRT testing, and summarized information is provided in Table 3.2. The locations of these bridges are marked in Figure 3.2. Summary information for new bridges decks is listed in Table 3.3, and locations are presented in Figure 3.3. Detailed information of all tested bridges for both rounds is presented in Appendix A.

3.3 Entities Information

Ten different entities comprised of various NDT consultants and INDOT participated in this study. A summary of testing information for each entity is provided in Table 3.4. Information about the entities and the NDT equipment as well as the scanning results is sourced from reports prepared by each entity and is used with permission.

TABLE 3.1
Summary of bridges evaluated by NL and PL testing

Structure Number	Test Round	Super-Structure Type	Type of Design	Overlay	Reinf. Bar Protection	Type of Road Carried	Age of Deck	Age of Overlay	Deck Rating	Wearing Surface Rating
1310	1 & 2	Concrete	Slab	Latex	None	SR	63	35	5	5
1347	1 & 2	PC[1]	Girder	None	Coated	SR	32	–	7	6
4845	2	Steel	Girder	None	Coated	SR	39	–	5	5
4930	2	PC[1]	Girder	Latex	None	SR	50	24	4	5
5230	1	Steel	Girder	None	None	US Hwy	3		5	6
8630	2	PC[1]	Girder	Latex	Coated	US Hwy	43	28	5	4
11940	1	Steel	Girder	Latex	Coated	US Hwy	38	20	7	7
16500	1 & 2	Concrete	Slab	Epoxy	Coated	SR	40	5	6	8
17940	2	Steel	Truss	Epoxy	Coated	SR	8	26	6	7
18770	1 & 2	Steel	Girder	Latex	Coated	US Hwy	30	2	5	5
18870	1	Concrete	Slab	Latex	Coated	US Hwy	38	19	5	6
19640	1 & 2	Steel	Girder	Latex	Coated	SR	41	15	6	6
20610	1 & 2	Steel	Girder	Latex	None	SR	50	27	6	5
22690	1 & 2	Steel	Girder	Latex	None	SR	54	32	6	6
24220	2	Concrete	Girder	Latex	None	SR	49	19	6	6
31080	1 & 2	PC[1]	Girder	None	None	SR	46	–	5	5
35520	1 & 2	Steel	Arch	Latex	Coated	Interstate	26	1	7	6
37070	1 & 2	Steel	Girder	None	Coated	Interstate	28	–	7	7
37100	1 & 2	Concrete	Slab	Latex	None	Interstate	62	27	5	5
37150	1 & 2	Steel	Girder	Epoxy	Coated	Interstate	63	28	7	8
41810	1 & 2	Concrete	Slab	Latex	None	Interstate	4	–	6	6
41870	1 & 2	Steel	Girder	None	Coated	Interstate	27	–	6	6
49180	2	Steel	Girder	Latex	None	Interstate	6	–	7	7
49200	1 & 2	Steel	Girder	Latex	None	Interstate	40	5	5	6
76140	1	Steel	Girder	Epoxy	Coated	Interstate	32	7	7	8

[1]PC indicates prestressed concrete.

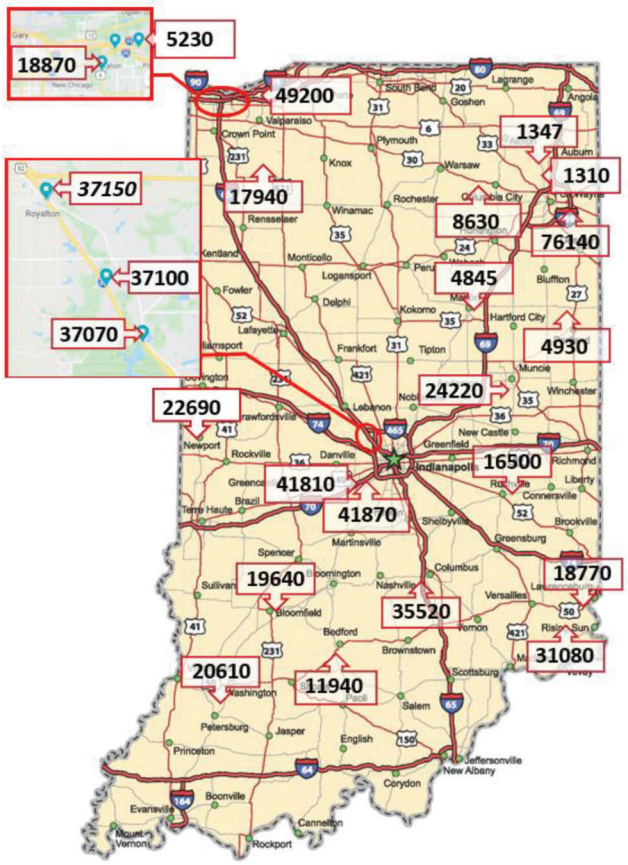

Figure 3.1 Locations of bridges listed by structure number for PL and NL testing.

3.3.1 Consultant A

3.3.1.1 Equipment and setting. Consultant A used an automated sounding system (Figure 3.4) to evaluate bridges for this research. The system uses chains to repeatedly hit the bridge deck like a manual chain drag test but in an automated manner. Testing speed is 15 mph. A proprietary algorithm is used to analyze the response sound from the chains, and the software is able to categorize the sound as "intact" or "delaminated." Results are also verified by inspectors. Moreover, deck imaging data are collected during the testing, and the imaging data can help to identify cracks, patches, and spalls.

3.3.1.2 Tested bridges. Table 3.5 presents the number of bridges that were tested by Consultant A. Detailed information for each bridge can be found in Appendix A.

3.3.2 Consultant B

3.3.2.1 Equipment and setting

3.3.2.1.1 Automated sounding. Consultant B used their automated sounding system to complete NDT testing for this research. The system in Figure 3.5 uses 12 impactor and sensor pairs that are uniformly positioned at 1-ft intervals. The traveling speed is around 3 mph, and the width of each scan is 12 ft. The frequency of impacts is 2 Hz, with each impact separated by approximately 40 ms to avoid crosstalk between channels. The setting can eliminate interference across channels. The system uses the microphones to capture sound and vibration amplitudes as a function of time, then converts the data to the frequency domain for analysis. This sounding method does not need to terminate traffic as is done when using manual sounding. A large amount of data can be generated in a short period of time.

3.3.2.1.2 Ground-coupled GPR. Consultant B used a Proceq GP8000 CWSF antenna to complete ground-coupled GPR tests for this research. The equipment, which is shown in Figure 3.6, was used to scan the bridge deck along lines in the longitudinal direction at intervals spaced at 5-ft transversely. Only the transverse reinforcing bars are measured for condition and cover depth.

3.3.2.1.3 Infrared thermography. Consultant B used a Vision Aerial SwitchBlade-Elite 2.0 tricopter drone with a FLIR Duo Pro R 640 thermal camera attached to collect IRT data. The camara has a 13-mm lens with the frame rate 30 Hz. Figure 3.7 shows the system. The system flies adjacent to the bridge decks to record the IRT information for the deck surface. The IRT data are analyzed by Pix4d to provide information of delamination and debonding.

3.3.2.2 Tested bridges. Table 3.6 presents the number of bridges that were tested by Consultant B. Detailed information for each bridge can be found in Appendix A.

3.3.3 INDOT In-House NDT

3.3.3.1 Equipment and setting

3.3.3.1.1 Concrete cores drilled. Concrete cores were drilled based on visual inspection of the deck. The intent of taking the cores was to confirm the accuracy of the IE NDT results. Three or four cores were drilled on each bridge selected for the concrete core test; 14 cores were taken for Round 1 and 6 cores for Round 2. For the first round of testing, the diameter of core bit used was 3 in. However, 4-in. diameter cores were used for the second round of testing. The depth to which cores were drilled varied due to factors such as cores breaking at weak concrete depth locations. The typical coring equipment that INDOT used is shown in Figure 3.8.

3.3.3.1.2 Impact echo (INDOT). A push-cart IE scanner, manufactured by Consultant F, was used for the testing. Figure 3.9 shows the scanner used in this study. The IE scanner method is based on

TABLE 3.2
Summary of bridges evaluated by aerial IRT testing

	Structure Number	Superstructure Type	Type of Design	Overlay	Reinf. Bar Protection	Age of Deck	Age of Overlay	Type of Road Carried	Deck Rating	Wearing Surface Rating
I-65 (round 1)	36070	Steel	Girder	None	Coated	5	–	Interstate	8	8
	36130	Steel	Girder	None	Coated	25	–	Interstate	7	7
	36150	Steel	Girder	None	Coated	25	–	Interstate	7	7
	36170	Steel	Girder	None	Coated	25	–	Interstate	7	7
	36190	Steel	Girder	None	Coated	25	–	Interstate	7	7
	36210	Steel	Girder	None	Coated	25	–	Interstate	6	6
	36230	Steel	Girder	None	Coated	25	–	Interstate	7	7
	36250	Steel	Girder	None	Coated	25	–	Interstate	7	7
	36270	Steel	Girder	None	Coated	25	–	Interstate	7	6
	36290	Steel	Girder	None	Coated	25	–	Interstate	7	7
	36320	Steel	Girder	None	None	3	–	Interstate	6	6
	36330	Steel	Girder	None	Coated	7	–	Interstate	7	7
	36520	Steel	Girder	Latex	None	48	19	Interstate	6	5
	36660	Steel	Girder	Latex	None	50	2	Interstate	6	6
	36680	Steel	Girder	Latex	None	52	3	Interstate	6	8
	36690	Steel	Girder	Latex	None	52	3	Interstate	5	8
	36700	Steel	Girder	Latex	None	53	3	Interstate	6	8
	36720	Steel	Girder	None	Coated	17	–	Interstate	7	7
	36730	Steel	Girder	None	Coated	17	–	Interstate	7	7
	36740	Steel	Girder	None	Coated	17	–	Interstate	7	7
	36750	Concrete	Slab	None	Coated	17	–	Interstate	6	6
	36760	Steel	Girder	None	Coated	17	–	Interstate	7	7
	36770	Steel	Girder	None	Coated	17	–	Interstate	7	6
	36780	Steel	Girder	None	Coated	17	–	Interstate	7	6
	36790	Steel	Girder	None	Coated	26	–	Interstate	7	7
	36800	Steel	Girder	None	Coated	26	–	Interstate	6	6
	36850	Steel	Girder	None	Coated	26	–	Interstate	7	7
	36880	Steel	Girder	None	Coated	22	–	Interstate	7	7
	36900	Steel	Girder	None	Coated	22	–	Interstate	7	7
	36920	Steel	Girder	None	Coated	22	–	Interstate	6	6
	36950	Steel	Girder	None	Coated	22	–	Interstate	7	9
	36980	Steel	Girder	None	Coated	22	–	Interstate	7	7
	37030	Steel	Girder	None	Coated	28	–	Interstate	6	6
	37060	Concrete	Girder	Latex	None	62	27	Interstate	4	4
	37070	Steel	Girder	None	Coated	28	–	Interstate	7	7
	37100	Concrete	Slab	Latex	None	62	26	Interstate	5	5
	37120	Concrete	Girder	Latex	None	62	27	Interstate	5	6
	50720	Steel	Girder	None	Coated	28	–	Interstate	7	7
I-69 (round 2)	39620	PC[1]	Girder	None	Coated	29	–	Interstate	7	7
	39630	PC[1]	Girder	None	Coated	29	–	Interstate	7	6
	39640	Steel	Girder	None	Coated	29	–	Interstate	7	6
	39650	Steel	Girder	None	Coated	29	–	Interstate	6	6
	39740	Concrete	Slab	Latex	None	59	6	Interstate	6	7
	39770	Concrete	Slab	Latex	None	59	21	Interstate	6	6
	39780	Concrete	Slab	Latex	None	59	21	Interstate	6	5
	39850	Concrete	Slab	None	Coated	9	–	Interstate	6	6
	39860	Concrete	Slab	None	Coated	9	–	Interstate	7	7
	39870	Steel	Girder	None	Coated	26	–	Interstate	6	6
	39880	Steel	Girder	None	Coated	26	–	Interstate	7	7
	39910	Concrete	Girder	Latex	None	59	26	Interstate	6	7
	39920	Concrete	Girder	Latex	None	59	26	Interstate	6	6
	40000	Steel	Girder	None	Coated	12	–	Interstate	7	7
	40010	Steel	Girder	None	Coated	29	–	Interstate	6	6
	40130	Concrete	Slab	Latex	None	59	29	Interstate	5	5
	40140	Concrete	Slab	Latex	None	59	29	Interstate	5	4
	40220	Steel	Girder	Latex	Coated	29	18	Interstate	7	6
	40230	Steel	Girder	Latex	Coated	29	18	Interstate	7	6

Continued on next page

TABLE 3.2
(Continued)

	Structure Number	Superstructure Type	Type of Design	Overlay	Reinf. Bar Protection	Age of Deck	Age of Overlay	Type of Road Carried	Deck Rating	Wearing Surface Rating
	40330	PC[1]	Girder	Latex	Coated	30	17	Interstate	7	7
	40340	PC[1]	Girder	Latex	Coated	30	18	Interstate	6	5
	40350	PC[1]	Girder	Latex	Coated	30	19	Interstate	7	6
	40360	PC[1]	Girder	Latex	Coated	30	19	Interstate	7	6
SR 18 (round 2)	4708	Concrete	Slab	Latex	Coated	41	16	SR	7	6
	4710	Concrete	Slab	None	Coated	31	–	SR	7	7
	4730	Concrete	Slab	Latex	Coated	37	6	SR	7	6
	4740	Concrete	Slab	Latex	Coated	38	6	SR	7	7
	4750	PC[1]	Girder	None	Coated	32	–	SR	7	7
	4770	Steel	Girder	None	Coated	38	–	SR	7	7
	4820	Steel	Girder	Latex	Coated	46	19	SR	6	6
	4830	Steel	Girder	Latex	Coated	46	19	SR	7	7
	4845	Steel	Girder	None	Coated	39	–	SR	5	5
	4859	Concrete	Slab	Latex	None	58	33	SR	6	6
	4860	Concrete	Slab	None	Coated	29	–	SR	6	6
	4910	Concrete	Slab	Latex	Coated	36	8	SR	7	6
	4920	PC[1]	Girder	None	Coated	32	–	SR	7	7
	4930	PC[1]	Girder	Latex	None	50	24	SR	5	4

[1]PC indicates prestressed concrete.

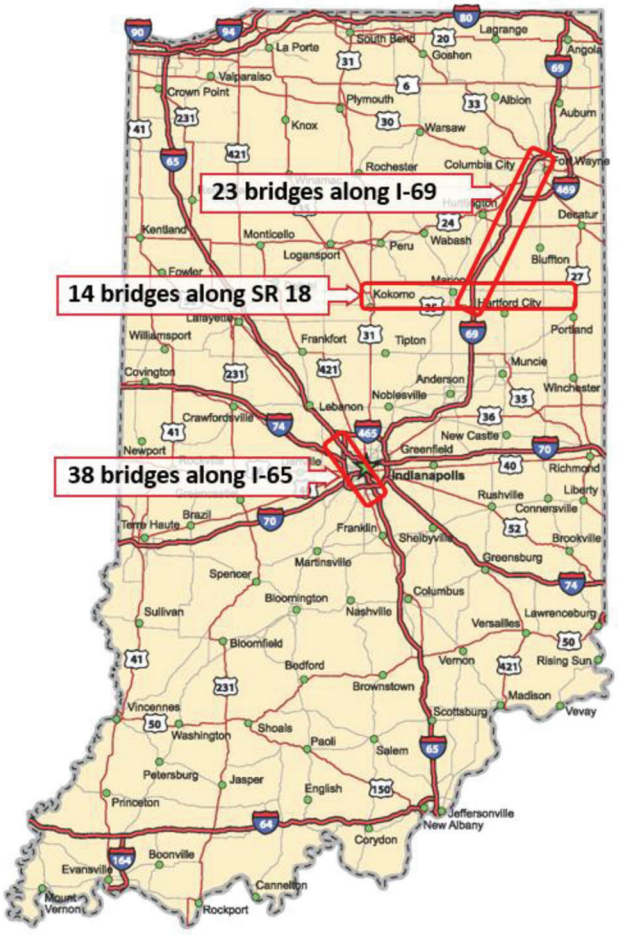

Figure 3.2 Locations of bridges listed by structure number for aerial IRT testing.

Consultant F's technology of a rolling transducer and automated impactor to evaluate the deck thickness and detect flaws in the structural concrete. The scanner system allows the user to collect data along two lines with the test points spaced at 0.5-ft increments along the test lines. A scanning rate of around 1 ft/s was used for best-quality results. As the technician moves the IE scanner forward on the bridge deck and the two sensor wheels turn, the automatic solenoids on the side of the sensor wheels impact the deck surface.

3.3.3.1.3 Ground-coupled GPR. GSSI equipment was used to collect GPR data from the bridge decks. An SIR-20 control unit with a 1.6 GHz ground connected antenna (Model 51600) was used to collect GPR data, and a 1.5-ft grid spacing was used to control the scanned area. The information was obtained using 24 traces per foot along the track being scanned. Figure 3.10 shows the equipment.

3.3.3.2 Data processing and analysis procedure

3.3.3.2.1 Concrete cores drilled. Concrete cores were returned to the lab for additional investigation. At this point, measurements such as overlay thickness and reinforcing bar cover depth were recorded. Delamination/debonding or vertical cracks can be identified by inspecting the condition of a concrete core. The information was used to confirm NDT results collected by other testing methods.

3.3.3.2.2 Impact echo (INDOT). The IE delamination/debonding maps indicate areas of delamination/debonding detected by the IE survey. It is important to

TABLE 3.3
Summary of new bridges for reinforcing bar cover depth measurement (round 1)

Structure Number	Superstructure Type	Type of Design	Wearing Surface	Reinf. Bar Protection	Age of Deck	Type of Road Carried	Deck Rating	Wearing Surface Rating
13321	PC[1]	Girder	None	Coated	3	SR	9	9
16171	Steel	Girder	None	Coated	3	US Hwy	9	9
16811	Concrete	Slab	None	Coated	3	SR	9	9
28326	Steel	Girder	None	Coated	3	SR	9	9
32675	Steel	Girder	None	Coated	4	City Road	8	8
33500	Steel	Girder	None	Coated	5	Interstate	8	8
44090	Steel	Girder	None	Coated	3	Interstate	8	8
17051	PC[1]	Tee Beam	None	Coated	3	SR	9	9
28430	Steel	Girder	None	Coated	2	SR	8	8
44120	Steel	Girder	None	Coated	4	Interstate	8	8

[1]PC indicates prestressed concrete.

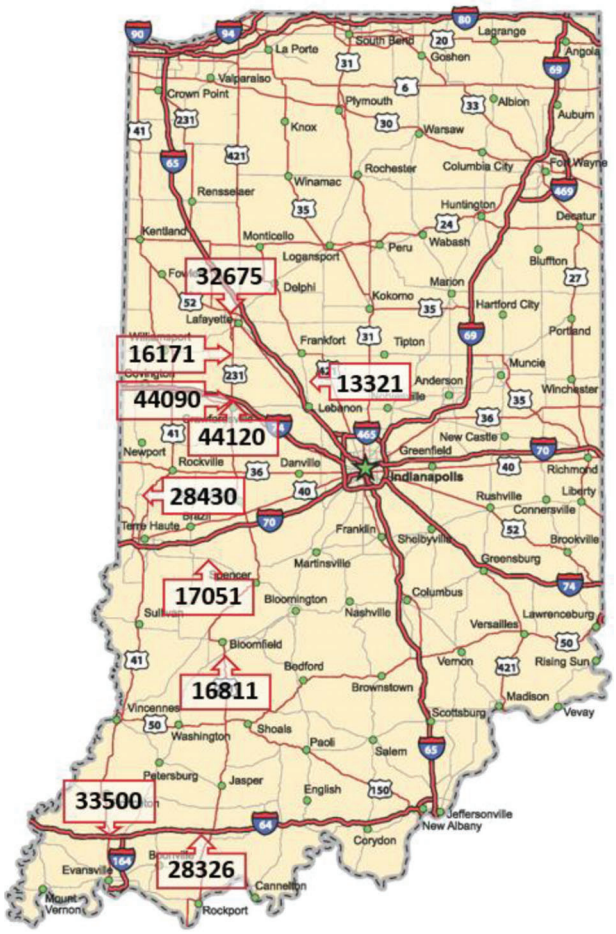

Figure 3.3 Locations of bridges listed by structure number for reinforcing bar cover depth measurement.

note that the analysis results focused primarily on delamination/debonding within the top half of the overall thickness of the structural deck, with or without an overlay on the top surface.

The bridge deck, with or without an overlay, was assessed using thickness echo results provided by the IE NDT technique. Sound concrete areas/regions generally have a thickness echo corresponding to the overall depth of the bridge deck with/without an overlay. For simplicity and easy to interpret results by bridge inspectors and bridge asset engineers, two color codes were used to show sound concrete and deteriorated concrete regions in the deck. For a typical bridge concrete deck, sound concrete regions denoted with grey color typically have an echo thickness which falls within $\pm$10–15% of the nominal IE thickness. A red color denotes total areas at the surface or within the deck with flaws such as delamination/debonding. These red regions generally have a smaller thickness echo (typically less than 10% of the nominal IE thickness) or have apparent thickness appreciably higher (typically 20% more than the nominal IE thickness) than the nominal IE thickness. Analysis assumed concrete compressional wave velocity of 12,000 ft/s.

3.3.3.2.3 Ground-coupled GPR. The procedure utilized to process the GPR data is described in the flowchart in Figure 3.11. The data correction plots include a plot of the regression lines used to make the time amplitude corrections. The raw and migrated amplitudes were corrected using two different methodologies. For the first method, the "Linear" method, one linear regression line was produced based upon the population without the outliers. For the second methodology, "POLY", a 5th order polynomial curve was fitted to the time amplitude data, followed by a group of line segments. All points within the bounds of the line segments were then corrected individually. Next, thresholds for the corrected populations were determined using a statistical methodology. Plots of the thresholds and populations are included. Contour maps of the estimated area of the bridge deck with a higher probability of corrosion for the different populations and thresholds were then developed. There was little difference in the results between the "Linear" and "POLY" methodologies

TABLE 3.4
Summary of entities involved in NDT evaluations

Entity	Round of Testing	Method	Equipment	Number of Bridges
Consultant A	2nd round	Automated sounding	Deck acoustic response system	20
Consultant B	1st round	Automated sounding	Deck acoustic response system	10
		Ground-coupled GPR	Proceq GP8000 antenna	10
		Drone-mounted IRT	FLIR Duo Pro R 640 Thermal Camera/13 mm/ 30 HZ mounted on a Switchblade-Elite drone	10
INDOT	1st round	IE	Pushcart IE Scanner	10
		Ground-coupled GPR	SIR-20 control unit with a 1.6 GHz antenna model 51600	3
		Concrete cores	Concrete Core Drill	4
	2nd round	IE	Pushcart IE Scanner	10
		Ground-coupled GPR	SIR-20 control unit with a 1.6 GHz antenna model 51600	3
		Concrete cores	Concrete Core Drill	2
Consultant C	2nd round	Drone-mounted IRT	DJI Matrice 210 V2 RTK drone with a DJI Zenmuse XT2 infrared and visual imaging system	10
Consultant D	1st round	Air-launched GPR	Dual 1-GHz horn antenna vehicle-based system	20
		Vehicle-mounted IRT	640 × 512-pixel FLIR Systems Model A6701sc infrared camera and a Sony-Alpha a7sii 4K resolution visual camera	20
		Aerial IRT	Fixed-wing airplane with IR camara	38
		Ground-coupled GPR	GSSI 1.6 GHz antennas	10
	2nd round	Air-launched 3D GPR	DX1821 antenna	10
		Aerial IRT	Fixed-wing airplane with IR camara	41
Consultant E	1st round	Vehicle-mounted IRT	Vehicle-mounted imaging system	20
	2nd round	Vehicle-mounted IRT	Vehicle-mounted imaging system	10
Consultant F	2nd round	IE	Pushcart IE Scanner	5
		Ground-coupled GPR	A GSSI SIR-4000 data acquisition unit with a ground-coupled 1,600 MHz antenna	5
Consultant G	1st round	Air-launched GPR	GSSI RoadScan 30 system	10
Consultant H	2nd round	Ground-coupled Multichannel GPR	IDS GeoRadar RIS Hi-BrigHT	10
Consultant I	1st round	Pole-mounted IRT	Pole-mounted IRT system	2
	2nd round	Pole-mounted IRT	Pole-mounted IRT system	4

for the tested bridges. The raw amplitude and migrated amplitude results were similar. The plot that best describes the "Corrosion potential" higher probability of corrosion is the RAW 1.5-3 dB threshold.

3.3.3.3 Tested bridges. Table 3.7 presents the number of bridges that were tested by INDOT. Detailed information for each bridge can be found in Appendix A.

3.3.4 Consultant C

3.3.4.1 Equipment and setting. Consultant C used a high-resolution infrared imaging device placed on a drone as shown in Figure 3.12. The device includes a FLIR Model DJI Zenmuse XT2 imager attached on a Matrice 210 V2 RTK drone. The drone follows the predefined flight routes to fly adjacent to each bridge deck at heights varying from 175 ft to 300 ft above the deck surface.

3.3.4.2 Data processing and analysis procedure. The IRT data were processed and analyzed offsite by Consultant C. A computer-assisted interpretation of the IRT data is performed for the observation of unexpected thermal differences and other signs of interior concrete delamination.

3.3.4.3 Tested bridges. Table 3.8 presents the number of bridges that were tested by Consultant C. Detailed information for each bridge can be found in Appendix A.

3.3.5 Consultant D

3.3.5.1 Equipment and setting

3.3.5.1.1 Ground-coupled GPR. Two GSSI 1.6 GHz antennas were attached on the rear of a survey truck, and an SIR 30 data acquisition system was installed inside for the ground-coupled GPR test (see

Figure 3.4 Automated sounding system from Consultant A (used with permission from consultant).

Figure 3.5 Automated sounding system (left); individual impactor and microphone (right) (used with permission from consultant).

TABLE 3.5
Number of bridges evaluated by Consultant A

Round of Testing	Method	Overlay	Number of Bridges
2nd Round	Automated sounding	None	5
		Latex	12
		Epoxy	3

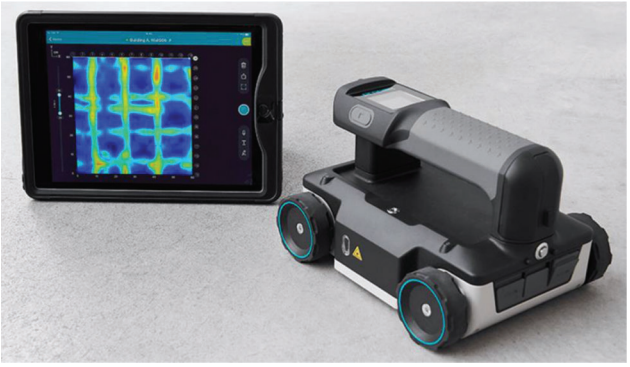

Figure 3.6 Photo of Proceq GP8000 antenna with tablet PC for remote data acquisition (used with permission from consultant).

Figure 3.13). Scans were completed at a rate of 60 scans per foot in the direction of traffic with distance control provided by an attached encoder wheel. The test was taken at a maximum speed of 5 mph in a series of lines spaced 1 ft transversely across the width of each deck. The distance measuring instrument (DMI) data were also recorded with each GPR data point, so GPR results can be presented with distance information.

3.3.5.1.2 Air-launched 3D GPR. The air-launched 3D GPR test was completed by using a system manufactured by 3D Radar, which is known as a Geoscope (Figure 3.14). The system includes an air-launched DX1821 antenna and a data gathering device. The antenna generates 21 data channels, and each channel is separated 3 in. laterally for a total coverage width of 5 ft. Three data passes were performed for each lane to provide comprehensive lateral coverage. The scanning procedure created an overlap of data, thereby preventing gaps to appear between passes. Each shoulder received one pass as well. Data were collected with DMI data at a regular driving speed.

Figure 3.7 Photo of a FLIR Duo Pro R 640 Thermal Camera/13 mm/30 HZ mounted on a Switchblade-Elite drone (used with permission from consultant).

TABLE 3.6
Number of bridges evaluated by Consultant B

Round of Testing	Method	Overlay	Number of Bridges
1st Round	Automated sounding	None	2
	Ground-coupled GPR	Latex	6
	Drone-mounted IRT	Epoxy	2

Figure 3.8 INDOT typical core drill equipment.

A 3-in. (transverse) by 2-in. (longitudinal) testing grid was used because the longitudinal collection rate was one set of transverse scans per 2 in. of longitudinal motion. An external GPS device was mounted on the top of the testing truck to record GPS coordinates for data analysis. The 3D Radar technology is a stepped frequency system where the data are generated in a stepped fashion by sending out a series of sine waves at a set of predetermined frequencies. The frequency range for the system applied in this research was 150 to 2,990 MHz, with frequency increments of 20 MHz.

Figure 3.9 IE push-cart scanner used by INDOT.

3.3.5.1.3 Air-launched GPR. The air-launched GPR surveys were conducted using a dual 1-GHz horn antenna vehicle-based system (see Figure 3.15). The GPR data were collected at regular highway speeds

Figure 3.10 Ground-coupled GPR equipment used by INDOT.

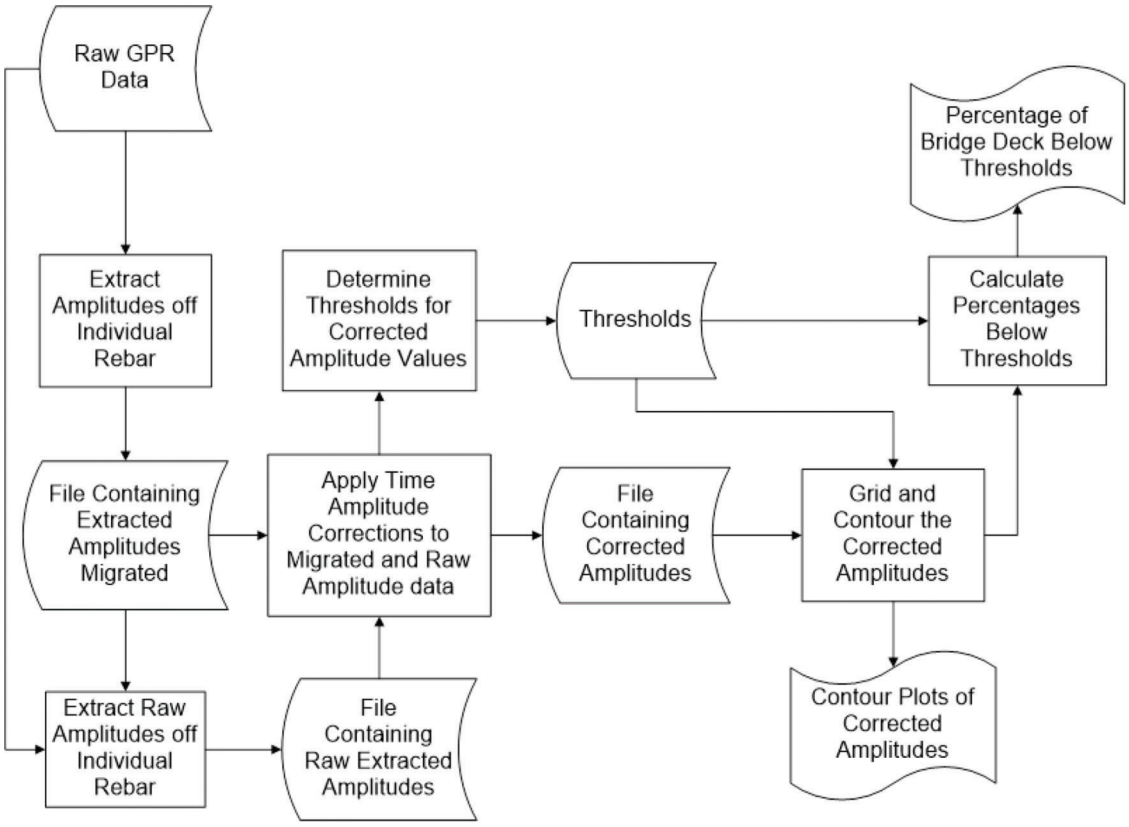

Figure 3.11 The procedure utilized to process the GPR data (Harris, 2021).

throughout the width of each deck in a series of lines with a maximum spacing of 3 ft. The DMI distance data were continually entered into each GPR record, resulting in a distance for each GPR data scan.

3.3.5.1.4 IRT by vehicle. The IRT and high-resolution visual (HRV) surveys were conducted using a 640 × 512-pixel FLIR Systems Model A6701sc infrared camera and a Sony–Alpha a7sii 4K resolution visual camera. Both devices were mounted on top of the survey vehicle (Figure 3.15) and controlled remotely in the vehicle. One pass per driving lane and shoulder over each deck was used to gather the IR and HRV data. A 15-ft deck width is covered by each pass. For precise position reference, a DMI is coupled to the IR and HRV cameras.

TABLE 3.7
Number of bridges evaluated by INDOT

Round of Testing	Method	Overlay	Number of Bridges
1st Round	Concrete cores drilled	None	2
		Latex	0
		Epoxy	0
	IE	None	2
		Latex	6
		Epoxy	2
	Ground-coupled GPR	None	2
		Latex	1
		Epoxy	0
2nd Round	Concrete cores drilled	None	0
		Latex	2
		Epoxy	0
	IE	None	2
		Latex	7
		Epoxy	1
	Ground-coupled GPR	None	1
		Latex	2
		Epoxy	0

TABLE 3.8
Number of bridges evaluated by Consultant C

Round of Testing	Method	Overlay	Number of Bridges
2nd Round	Drone-mounted IRT	None	2
		Latex	7
		Epoxy	1

Figure 3.12 High-resolution infrared imaging equipment and drone equipment (used with permission from consultant).

3.3.5.1.5 Aerial IRT. A consultant hired by Consultant D was used to collect the aerial infrared data. The aerial IRT data were obtained with high-resolution visual data from a fixed-wing airplane that was piloted by a licensed pilot (see Figure 3.16). The airplane was 500 to 1,000 ft above each bridge when the IRT data were collected. The data were sent to Consultant D using a file sharing platform for quality assurance evaluation.

3.3.5.1.6 Impact echo. The IE testing was performed using an IE scanner equipment as depicted in Figure 3.17. The testing sites were chosen to verify the deterioration identified in the NL GPR and IR data.

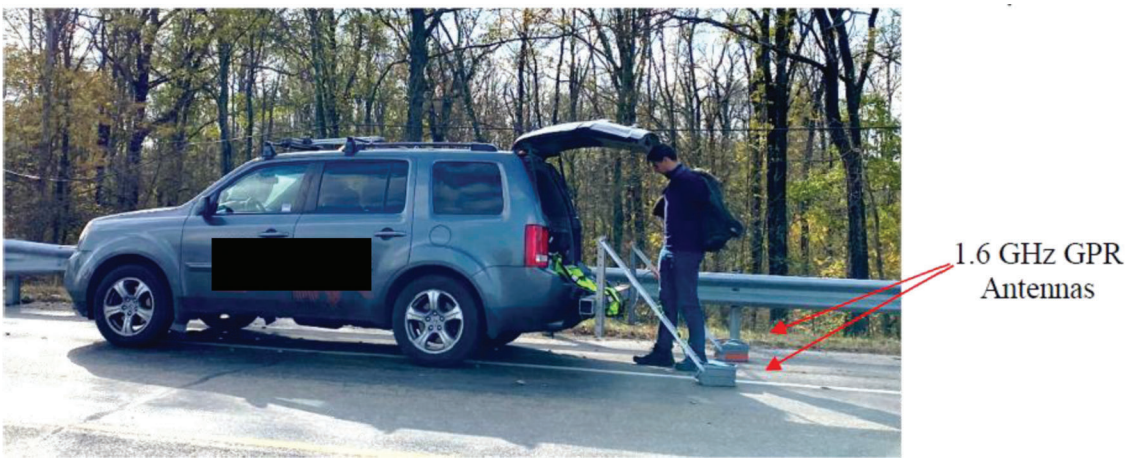

Figure 3.13 Ground-coupled PL GPR survey—antenna mounting to vehicle (used with permission from consultant).

Figure 3.14 Air-launched 3D GPR equipment (used with permission from consultant).

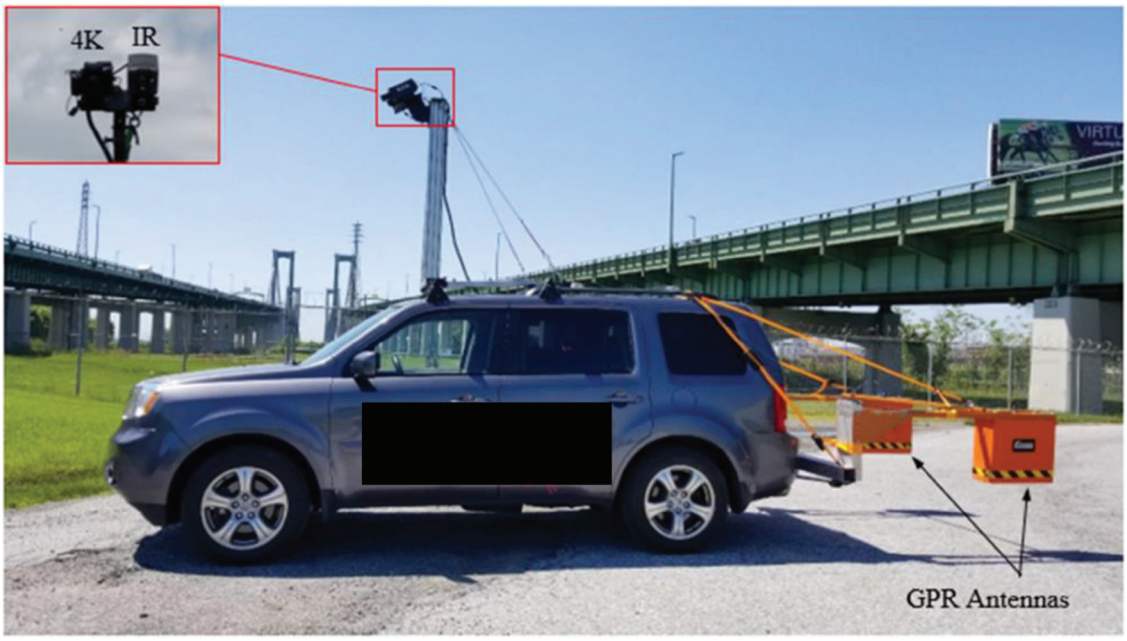

Figure 3.15 Consultant D survey vehicle with GPR, HRV, and IR equipment (used with permission from consultant).

Figure 3.16 Fixed-wing airplane used for aerial IR surveys (used with permission from consultant).

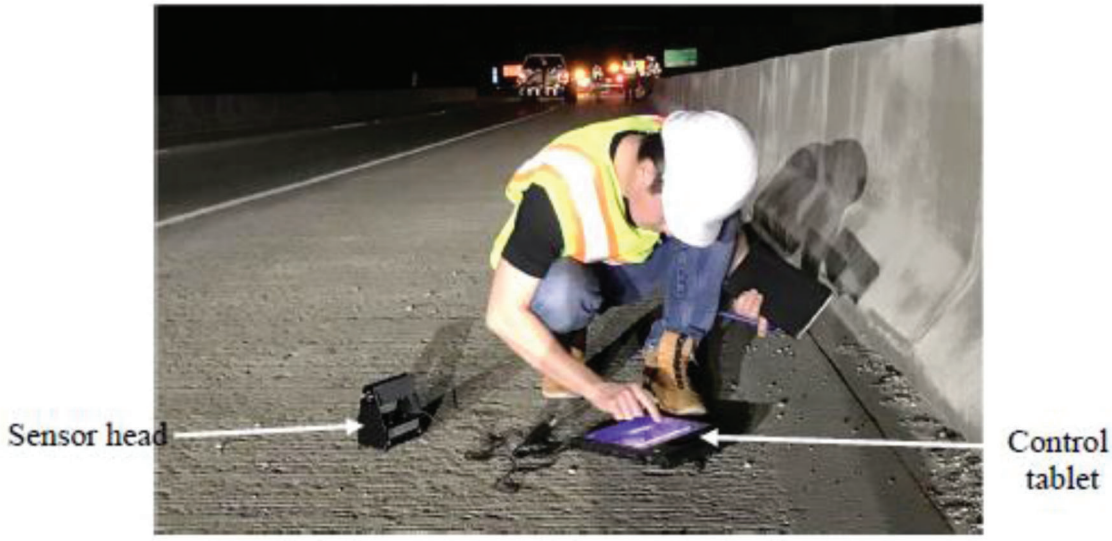

Figure 3.17 IE system from Consultant D (used with permission from consultant).

The final maps show the locations of verified delamination and/or deterioration.

3.3.5.1.7 Hammer sounding. Hammer sounding was conducted in a few spots to verify delaminations detected by IR data obtained earlier on tested bridge decks. When a hollow sound was detected while sounding, it was affirmed that the region was indeed delaminated. Delaminations that were confirmed were reported and are shown in the final maps.

3.3.5.2 Data processing and analysis procedure

3.3.5.2.1 Ground-coupled GPR. Deterioration at the level of reinforcement was quantified and mapped using ground-coupled GPR data. The deterioration maps are made by plotting computed amplitudes of the GPR signal response to construct contour maps.

3.3.5.2.2 Air-launched 3D GPR. Because the recorded data includes a set of reactions to each of the frequency steps, the response is referred to as being in the "frequency domain." A brief broadband pulse is created by an impulse radar system, and the reaction to this pulse is generated in the "time domain." The 3D GPR data is transformed to time domain as most GPR analysis is performed in the time domain. The data files are placed on a plan view map once the data has been translated into the time domain. The result map of a bridge deck has several data files that are spliced together to form one full file. The top layer of reinforcement in bridge decks can be tracked once the full file is created. Amplitudes at the reinforcement level were computed to conduct the deterioration analysis using Consultant D's software. Contour plots are used to present the analyzed GPR data.

3.3.5.2.3 Air-launched GPR. The air-launched GPR analysis is carried out with Consultant D's proprietary software using the following procedure. First, the beginning and end of the structure are located, and the GPR distance data are compared with

the dimension of the bridge deck. Dielectric discontinuities in the GPR data are then recognized, and the corresponding features are identified. Last, concrete attenuation, reinforcing bar depth, and concrete dielectric constant are calculated. Contour plots are used to present the analyzed GPR data.

3.3.5.2.4 IRT by vehicle. Surface features (discoloration, oil stains, sand, rust deposits, etc.) that appear in the results but are unrelated to subsurface conditions were compared to the infrared data to distinguish delaminated areas from surface features. Each image has a "snip" taken from it and is calibrated to capture an area 1 ft in the direction of travel and 12 ft across. Then, the snips are composed together to generate a single strip image for each pass. Each deck's composite thermal and visual pictures are created by aligning the separate strip images. Delaminations or overlay debonding are shown by white blotchy patches on the IRT picture that do not correlate to surface features. Due to the thermal barrier created by the delaminations, these are "hot spots" where the surface temperatures are greater. These thermal differences in decks with overlays might be caused by debonding of the overlay or delamination at the level of the reinforcement. Debonding of the overlay will be more intensive in general. Each map's delaminated and debonded regions are traced, and the sum of the highlighted areas yields an estimate of each deck's percentage of delamination and debonding. It is important to note that the IRT technique identifies the difference in surface temperature induced by subsurface debonding and delamination. The depth to which it can reliably detect anomalies is restricted to 4 in.

3.3.5.2.5 Aerial IRT. The amount of overlay debonding and/or delamination at the level of the reinforcement as well as patching were estimated using aerial IRT plan-views by an experienced analyst. The quantity estimations were obtained by tracing the "hot spots" in the IRT and using a mapping application to quantify the regions expected to be delaminated. In a similar way, evidence of patching in visual imagery was defined and measured.

3.3.5.3 Tested bridges. Table 3.9 presents the number of bridges that were tested by Consultant D. Detailed information for each bridge can be found in Appendix A.

3.3.6 Consultant E

3.3.6.1 Equipment and setting. Figure 3.18 shows a transportable imaging platform installed on a truck. An IRT camera, two line-scanning cameras, a GPS device, and a speedometer unit are all part of the system. These sensors work together to detect surface and sub-surface problems on highways and bridge decks. The IRT camera is positioned on the back of the vehicle and captures a 15-ft-wide swath. The two cameras are set on either end of the rear frame in a similar fashion, and each capture a 13-ft swath. They capture a total of 18 ft when mounted in a single row, with some overlap in the middle to allow for picture-stitching. The system operates at speeds ranging from 10 to 70 mph, obviating the need for lane closures.

3.3.6.2 Data processing and analysis procedure. The IRT camera, line-scanning cameras, distance/speed data, and GPS information are all extracted from the recording vehicle and converted using IrSUITE, JeSUITE, and Kuraves, three different but interconnected software systems. The software program determines the best placement for each recorded image based on the distance pitches acquired from the distance/speed data. This process is known as "image stitching," and it requires capturing individual photos, applying different perspective correction procedures to them, and then arranging them in rows to create a composite image. Each bridge was thoroughly inspected by Consultant E's analysts in compliance with AASHTO bridge element-level inspection criteria (Figure 3.19).

3.3.6.3 Tested bridges. Table 3.10 presents the number of bridges that were tested by Consultant E. Detailed information for each bridge can be found in Appendix A.

3.3.7 Consultant F

3.3.7.1 Equipment and setting

3.3.7.1.1 Impact echo. Consultant F used the pushcart IE scanner system (Figure 3.20) to run an IE test every 6 in. on two scan lines at a speed of around 1.0 mph. Scan lines were positioned 1 ft apart and operated longitudinally throughout the whole width of the bridge. The IE technique detects voids if they exist and is mostly sensitive to cracking, delamination, and debonding that is parallel to the test surface. The approach utilizes a tiny impact solenoid to administer a low-strain impact, and a displacement transducer positioned in the rolling sensor wheels to measure the resonant concrete thickness/delamination response echoes. A typical IE pulse was assumed to travel through concrete at a velocity of 12,000 ft/s. If there is no damage, the IE tests will provide sharp and consistent resonant echo frequencies that match to the thickness of the concrete deck at that test location.

3.3.7.1.2 Ground-coupled GPR. GPR testing was performed using GSSI SIR-4000 equipment with a ground-coupled 1,600 MHz antenna (Figure 3.21) to assess the possibility for corrosion due to chloride presence by analyzing steel reinforcement reflection amplitude changes over the bridge deck area. The GPR data were normally acquired while the cart was rolled

TABLE 3.9
Number of bridges evaluated by Consultant D

Round of Testing	Method	Overlay	Number of Bridges
1st Round	Air-launched GPR	None	4
		Latex	12
		Epoxy	4
	Vehicle-mounted IRT	None	4
		Latex	12
		Epoxy	4
	Ground-coupled GPR	None	2
		Latex	6
		Epoxy	2
	Aerial IRT	None	29
		Latex	9
		Epoxy	0
2nd Round	Air-launched 3D GPR	None	2
		Latex	7
		Epoxy	1
	Aerial IRT	None	16
		Latex	21
		Epoxy	0

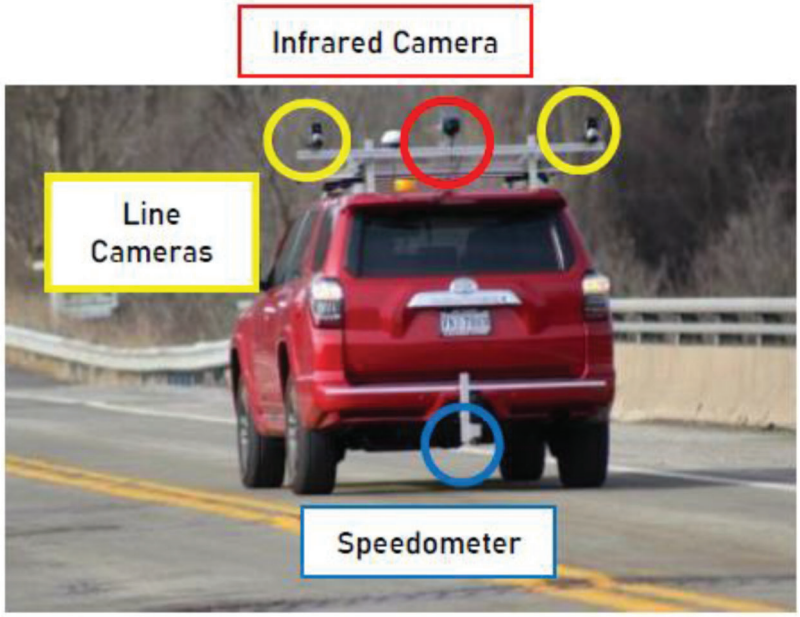

Figure 3.18 Vehicle-mounted imaging system (used with permission from consultant).

across the bridge along longitudinal scan lines with a 1-ft transverse spacing (same configuration as used for the IE scanning). However, two of the five assessed bridges had longitudinal reinforcement closest to the test surface, necessitating transverse scans at 1-ft longitudinal intervals.

On both NDE systems, integrated RTK GPS devices recorded the exact locations of each test point. An Emlid Reach GPS device was installed in both the GPR and IE systems, allowing all data to be georeferenced. Consultant F used the Indiana Continuously Operating Reference Station (InCORS) network to send real-time adjustments to the push-cart units and offered RTK correction with a 10-cm accuracy estimate. A 2-ft transverse grid was laid out across each bridge to ensure complete coverage during data collection and to aid in testing with the IE scanner system and GPR system in straight longitudinal passes when the top deck steel was transverse to the traffic direction.

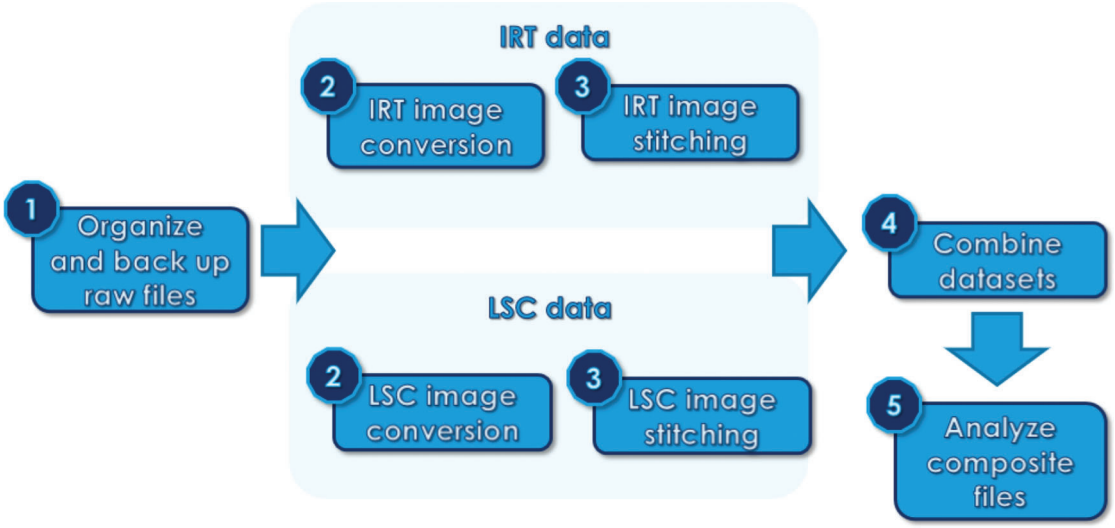

Figure 3.19 Data processing procedure by Consultant E (used with permission from consultant).

Figure 3.20 Pushcart IE scanner system.

Figure 3.21 Ground-coupled GPR equipment from Consultant F.

TABLE 3.10
Number of bridges evaluated by Consultant E

Round of Testing	Method	Overlay	Number of Bridges
1st Round	Vehicle-mounted IRT	None	4
		Latex	12
		Epoxy	4
2nd Round	Vehicle-mounted IRT	None	2
		Latex	7
		Epoxy	1

3.3.7.2 Data Processing and Analysis Procedure

3.3.7.2.1 Impact echo. The thickness of the generated resonant echo is used to illustrate the IE results. If there are near-surface delaminations inside the concrete slab, often in the top 3 in, the delaminated concrete replies with a low-frequency, undamped flexural resonance response that appears considerably thicker than the actual deck thickness. If the concrete is sound on the surface but has internal horizontal cracking, an echo resonance is detected to determine the depth of the internal cracking, which might be delaminations caused by deep top steel or delaminations at the bottom of the deck caused by bottom steel corrosion.

3.3.7.2.2 Ground-coupled GPR. The ground-coupled GPR reflection for each top layer reinforcing bar is collected and the depth and amplitude of this reflection are tabulated. This enables the creation of an accurate steel reinforcement concrete cover depth map as well as a map of deck condition based on relative GPR reflection amplitude. Consultant F considered a

number of signal attenuation values due to reinforcing bar depth changes in order to identify effects caused by chloride concentrations. Because GPR reflection amplitudes are analyzed as a relative measurement, multiple cut-off values were chosen to determine which areas are possibly delaminated and which areas are in good condition. Consultant F provided numerous versions of the GPR results, each with different cut-off values of 10%, 20%, and 30%.

3.3.7.3 Tested bridges. Table 3.11 presents the number of bridges that were tested by Consultant F. Detailed information for each bridge can be found in Appendix A.

3.3.8 Consultant G

3.3.8.1 Equipment and setting. Consultant G reported that the ASTM D6087(2008) (ASTM, 2008) *Standard Test Method for Evaluating Asphalt-Covered Concrete Bridge Decks Using Ground Penetrating Radar* was employed using a GSSI RoadScanTM 30 system (Figure 3.22) equipped with a 2 GHz air-launched horn antenna and a submeter GPS as positional assistance. The collected profiles for each bridge were separated at 3-ft intervals. Data was collected at a speed of 45 mph or greater with six scans per foot. The GPR survey was limited to within the vehicle lanes (i.e., inside line to outside line) for some of the bridges due to shoulder width restrictions.

3.3.8.2 Data processing and analysis procedure. GSSI Radan 7 GPR software with the BridgeScan module was used to estimate the depths and normalize amplitude responses (in dB) from the top of the interpreted upper transverse layer of embedded steel reinforcement. The data are also used to estimate the concrete cover dielectric. Consultant G performed extra analytical processes to create a more quantitative data analysis associated to possible deterioration since signal attenuation is directly related to depth. A 90th percentile linear regression was used to calculate trends in signal attenuation by mapping normalized amplitude responses versus depth, which assumed that at least 10% of the top transverse bars were not deteriorated. The final depth adjusted amplitudes were calculated using these trends. Consultant G evaluated the cumulative percentage from histograms that were created from the depth-corrected amplitudes to interpret statistical threshold criteria of the severity that was associated with the prospective areas of deterioration. The final estimated data, which were comprised of concrete cover depth, calculated dielectric of the concrete cover, normalized amplitudes, and depth adjusted amplitudes, were grided and shown using Golden Software's Surfer.

3.3.8.3 Tested bridges. Table 3.12 presents the number of bridges that were tested by Consultant G. Detailed information for each bridge can be found in Appendix A.

3.3.9 Consultant H

3.3.9.1 Equipment and setting. To gather data across the bridge deck, Consultant H used a ground-coupled

TABLE 3.11
Number of bridges evaluated by Consultant F

Round of Testing	Method	Overlay	Number of Bridges
2nd Round	Vehicle-mounted IRT	None	2
	Ground-coupled GPR	Latex	3
		Epoxy	0

Figure 3.22 GSSI RoadScan 30 system (used with permission from consultant).

Multichannel Ground Penetrating Radar (MCGPR) system consisting of an IDS GeoRadar Hi-BrigHT scanner mounted to a push-cart that is shown in Figure 3.23. The IDS GeoRadar Hi-BrigHT system includes 16 channels that operate at a 2,000 MHz antenna frequency that are oriented in both the horizontal (8 channels) and vertical (8 channels) dipole directions. This enables the collection of large amounts of data in a single run. The data were georeferenced with sub-meter precision using an instrument-mounted Leica GG04 and using the bridge deck expansion joints to locate when available.

3.3.9.2 Data processing and analysis procedure. IDS GeoRadar's GRED software package was used to post-process the MCGPR data. Position correction, background removal (filtering), and data visual assessment were all part of the MCGPR post-processing. For deterioration evaluation, the GPR data were analyzed by applying the signature of the depth of the top reinforcement as well as the amplitude of that signature.

3.3.9.3 Tested bridges. Table 3.13 presents the number of bridges that were tested by Consultant H. Detailed information for each bridge can be found in Appendix A.

3.3.10 Consultant I

3.3.10.1 Equipment and setting. Consultant I used their pole-mounted IRT system to scan bridge decks. The measurements are collected over a two-day period. A shoulder closure of about one-hour was required to install the pole-mounted IRT systems on the right barrier rail of each bridge. A typical top deck installation is shown in Figure 3.24. The entire width of the bridge deck (shoulder plus two lanes) was measured for a length of 100 to 120 ft in each direction from the setup position using the pole-mounted IRT technology. The devices collected data automatically during the scanning period. Views of various parts of the bridge deck can be recorded from a single setup point by using the pan and tilt functions of the pole-mounted IRT camera head.

3.3.10.2 Data processing and analysis procedure. The daily temperature variations heat up and cool down the deck structure being examined. Pole-mounted IRT data are collected over a relatively long period of time to capture these daily changes, resulting in increased sensitivity to IRT data collected over a short time-frame. When delamination indications are investigated during the heating and cooling cycles, they usually show symmetric color representations. Shallower delamination indications can heat up more quickly

Figure 3.23 Ground-coupled MCGPR equipment (IDS GeoRadar RIS Hi-BrigHT).

TABLE 3.12
Number of bridges evaluated by Consultant G

Round of Testing	Method	Overlay	Number of Bridges
1st Round	Vehicle-mounted IRT	None	2
	Ground-coupled GPR	Latex	6
		Epoxy	2

TABLE 3.13
Number of bridges evaluated by Consultant H

Round of Testing	Method	Overlay	Number of Bridges
2nd Round	Ground-coupled MCGPR	None	2
		Latex	6
		Epoxy	1

Figure 3.24 Typical top deck equipment setup on the barrier rail (used with permission from consultant).

TABLE 3.14
Number of bridges evaluated by Consultant I

Round of Testing	Method	Overlay	Number of Bridges
1st Round	Pole-mounted IRT	None	0
		Latex	2
		Epoxy	0
2nd Round	Pole-mounted IRT	None	1
		Latex	3
		Epoxy	0

and appear lighter in color, but deeper delamination indications will appear darker in color during the cooling process because they cool down quicker than sound concrete. To estimate the depth of a delamination, and define the dynamic reaction of the deck temperature, pole-mounted IRT data are processed using the heating cycle, cooling cycle, or both.

3.3.10.3 Tested bridges. Table 3.14 presents the number of bridges that were tested by Consultant I. Detailed information for each bridge can be found in Appendix A.

4. RESULTS AND DISCUSSION

In this chapter, test results are presented and discussed based on the comparison between different entities and testing methods.

4.1 Existing Test Results

Consultant J had previously examined 259 bridges in all six INDOT districts using vehicle-mounted air-launched GPR with data collected at highway speeds. The number of bridges inspected in each district is provided in Table 4.1. A 1-GHz antenna was used to collect GPR data. The results were shown on maps to demonstrate the condition of deterioration of each deck. Furthermore, Consultant J produced color maps for each bridge deck showing the reinforcing bar cover depth. Additionally, during the GPR scan, visual inspections of the bridge deck surfaces were performed, and photos were taken of any substantial problems seen on the decks.

4.2 Result Comparison for Same Method

In this section, testing results for air-launched GPR, ground-coupled GPR, IE, IRT, automated

TABLE 4.1
Number of bridges tested by Consultant J in each district

District	Crawfordsville	Fort Wayne	Greenfield	LaPorte	Seymour	Vincennes
Number of Bridges	56	7	77	44	29	46

sounding, and reinforcing bar cover depth are presented and discussed based on the comparison between different entities using the same NDT method. The purpose of the comparison of results between entities is to check if the NDT method examined can produce consistent and repeatable results. The test results and deterioration maps provided herein are sourced from reports prepared by each entity and are used with permission.

4.2.1 Air-launched GPR Results

In the first round of testing, Consultant D evaluated 20 bridges with their air-launched GPR equipment, while Consultant G examined 10 of these bridges. In the second round of testing, Consultant D evaluated 10 bridges by using an air-launched 3D GPR system. Consultant J tested nine bridges before this study, and the results were compared to the air-launched GPR results from Consultant D and Consultant G. Consultant D provided the percentage of deterioration using one value. Depending on the severity of the deterioration, areas of deterioration are highlighted in dark blue and transitions to pink with increasing severity. Delaminations are also highlighted in red on the result maps but are not discussed in this section as these defects were detected by IRT. The legend for Consultant D's maps is shown in Figure 4.1a. Consultant G divided the percentage of deterioration into four levels: good, fair, poor, and severe. In Figure 4.1b, each severity level is defined by various colors. Location of deterioration is represented by different colors on plan view maps. Consultant J divided the percentage of deterioration into five levels and used various colors to represent severity (Figure 4.1c). The deterioration percentage values detected by the three entities are summarized in Table 4.2. In the table, only poor and severe levels were considered for results from Consultant G, and only medium and high deterioration severity levels were used for Consultant J. Detailed result tables can be found in Appendix B.

For the first round of testing, Consultant D indicated that four bridges had deterioration percentages greater than 10% of their scanned area. Other bridges had a minor amount of deterioration in the bridge deck, which Consultant J concurred with. If only the severe level of deterioration indicated by Consultant G is used to compare with other entities, they all agreed that the examined bridges exhibited minor deterioration. However, when the poor and severe condition levels for Consultant G were compared with other entities, the comparison was not good. Because it was unclear which severity levels should be utilized to compare between entities' data, comparing percentage values for each bridge may not be the best approach. Nevertheless, it is reasonable to compare six bridges tested by Consultant D in the two rounds of testing. The average absolute difference between the 3D GPR survey and the conventional air-launched GPR survey is 2.7%, which indicates relatively good agreement between the two methods overall.

Bridge 31080 and Bridge 37100 were selected to provide an example of the comparison between the results maps for the first round of testing. Figure 4.2a shows the result map from Consultant D for Bridge 31080. The location of bridge deck concrete delamination and deterioration can be seen on the plan view map. The map has a 4-ft increment distance scale along the length of the bridge deck. Figure 4.2b shows the result map for Bridge 31080 provided by Consultant G. The last result map for Bridge 31080 provided in Figure 4.2c is from Consultant J. The plan view map shows the location of bridge deck concrete deterioration and a 2-ft increment distance scale along the length and width of the bridge deck. Similarly, Figure 4.3 depicts the result maps from the three entities for Bridge 37100.

Overall, locations of deteriorated areas compare well for Bridge 31080, but poor comparisons are observed for Bridge 37100 between result maps from Consultant D, Consultant G, and Consultant J. When comparing the result maps for Bridge 31080, it is clear that deterioration is likely occurring along the pier locations. However, maps for Bridge 37100 only show some agreement between Consultant G and Consultant J at the right end of the span. At the same position, Consultant D did not identify any deterioration. Furthermore, other entities did not have good agreement with other deteriorated areas highlighted on the map from Consultant G.

Bridge 20610 was selected for the comparison between the first round and the second round of testing. Consultant D participated in both rounds, so the result map collected with a conventional GPR was compared to the 3D GPR result map. Figure 4.4a shows the result map from the first round of testing, and Figure 4.4b shows the map from the second round of testing.

It was discovered that the 3D GPR result map and the conventional air-launched GPR result map did not always compare well; while the average deterioration difference was only 2.7%, the deterioration location varied considerably. Consultant D indicated that RF noise interference was present in a portion of the frequency spectrum, preventing the clear detection of

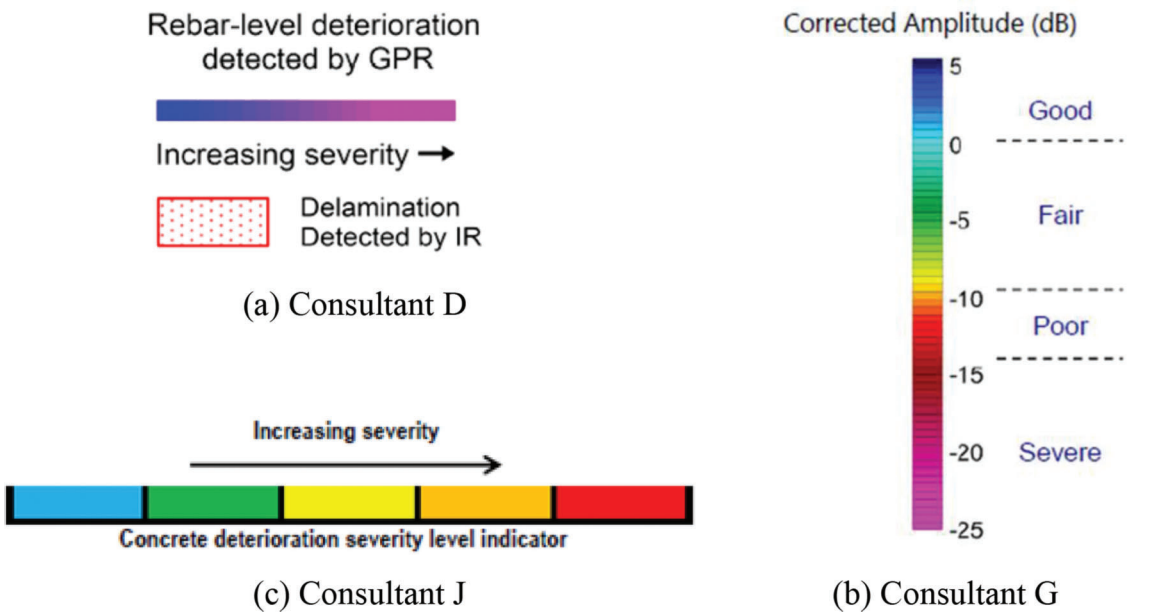

Figure 4.1 Legends for air-launched GPR result maps (used with permission from consultant).

TABLE 4.2
Summary table of air-launched GPR results

			Consultant G			Consultant J		
			Deterioration (% of Area Surveyed for Different Levels of Severity)			Deterioration (% of Area Surveyed for Different Levels of Severity)		
	Consultant D	Consultant D	First Round			Previous Testing		
Structure Number	First Round	Second Round	Poor & Severe	Severe	Poor	Medium & High	High	Medium
01310	3.1	4.7	–	–	–	–	–	–
01347	2.3	3.5	–	–	–	–	–	–
04845	–	10.7	–	–	–	–	–	–
04930	–	9.6	–	–	–	–	–	–
05230	2.6	–	–	–	–	–	–	–
08630	–	–	–	–	–	–	–	–
11940	3	–	–	–	–	–	–	–
16500	10.1	–	19.3	4.5	14.8	–	–	–
17940	9.6	16.3	–	–	–	–	–	–
18770	1.7	–	15.8	5.5	10.3	5.6	0.8	4.8
18870	10.4	–	–	–	–	–	–	–
19640	6.5	8.7	–	–	–	–	–	–
20610	6.5	9.1	–	–	–	2.1	0.3	1.8
22690	2.0	–	22.5	7.1	15.5	2.7	0.4	2.3
24220	–	–	–	–	–	–	–	–
31080	–	–	17.7	5.6	12.1	6.6	0.6	6.0
35520	12.1	–	17.7	6.4	11.3	2.0	0.1	1.9
37070	6.8	–	13.9	3.2	10.6	1.0	0.0	1.0
37100	1.5	–	15.8	6.8	9.0	3.5	0.7	2.8
37150	3.5	–	17.9	5.2	12.7	4.7	0.7	4.0
41810	9.1	–	16.5	4.6	11.9	–	–	–
41870	5.9	–	13.0	2.9	10.1	3.9	0.7	3.2
49200	13.5	11.9	–	–	–	–	–	–
76140	3.7	–	–	–	–	–	–	–

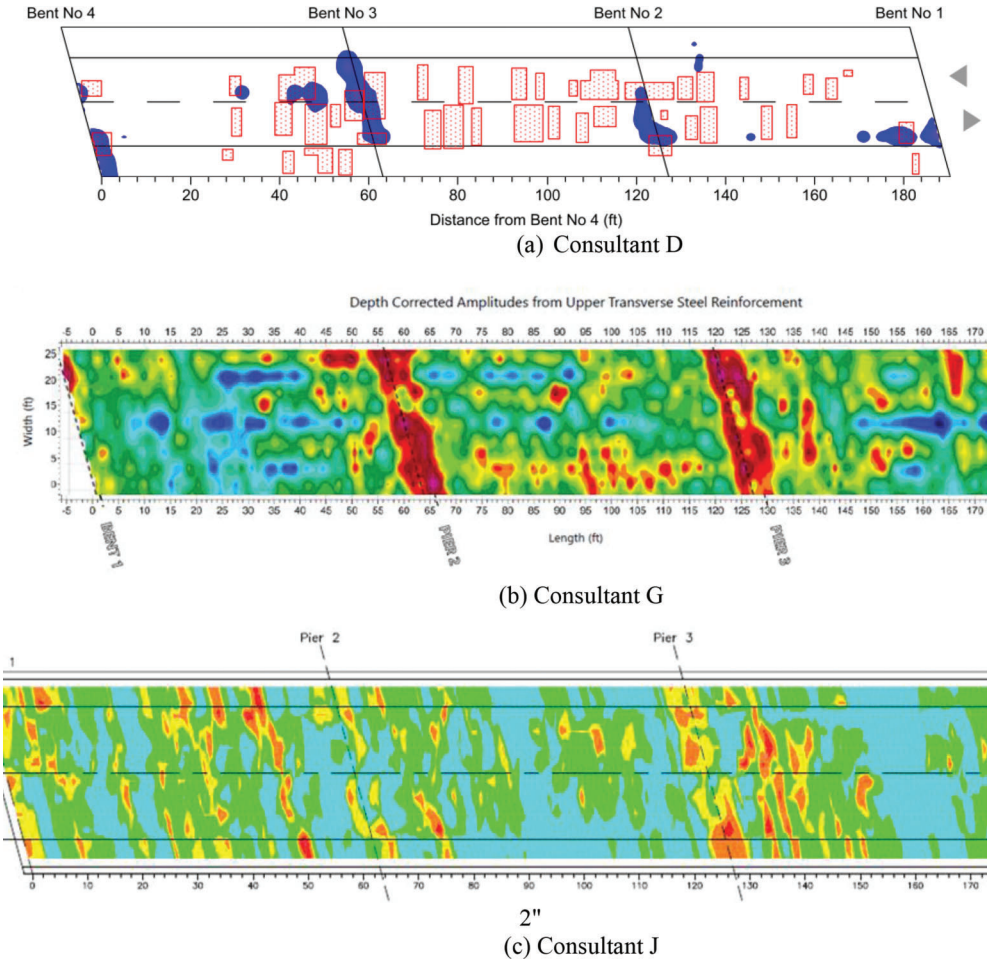

Figure 4.2 Air-launched GPR result maps for Bridge 31080 (used with permission from consultant).

the reinforcing bars. The problem occurred on the other five bridges as well. As a result, the 3D GPR data was not believed to be particularly reliable for these tests. Result maps for other bridges can be found in Appendix C.

Overall, comparing the deterioration percentage of the area surveyed and the result maps for all bridges listed in Table 4.2, poor comparisons for the air-launched GPR results are generally found between the results from Consultant D, Consultant G, and Consultant J. The selection of the frequency threshold associated with deterioration is believed to be the major issue causing the observed discrepancy.

4.2.2 Ground-coupled GPR Results

In the first round of testing, Consultant D and Consultant B used their ground-coupled GPR equipment to assess ten bridges. In the second round of testing, Consultant H used their multichannel GPR equipment to test ten bridges, and Consultant F used ground-coupled GPR to test five of these bridges. INDOT also evaluated three bridges using a ground-coupled GPR antenna in each round of testing. Consultant D provided the percentage of deterioration using one value. Depending on the severity of the deterioration, areas of deterioration are highlighted in dark blue or pink on the result maps. The delamination and patched areas that are not considered in this section of the report are highlighted in red and green, respectively. The legend for Consultant D's map is provided in Figure 4.5a. Consultant B divided the percentage of deterioration into four levels: intact, fair, poor, and severe. In Figure 4.5b, each severity level is defined by various colors. Consultant H used three colors to represent the deterioration potential. Figure 4.5c shows that green, yellow, and red are used to correspond to low, medium, and high potentials. INDOT uses red to indicate deteriorated areas, and Consultant F uses yellow. The deterioration percentage values detected by the four entities are summarized in Table 4.3. Because Consultant F provided three result maps for the scanned bridges and each map had a cut-off value of 10%, 20%, and 30% of the data, result values cannot be present in the table. Only poor and severe levels are considered for results from Consultant B, and medium and high deterioration potential are considered for results from Consultant H in the table. Detailed results can be found in Appendix B.

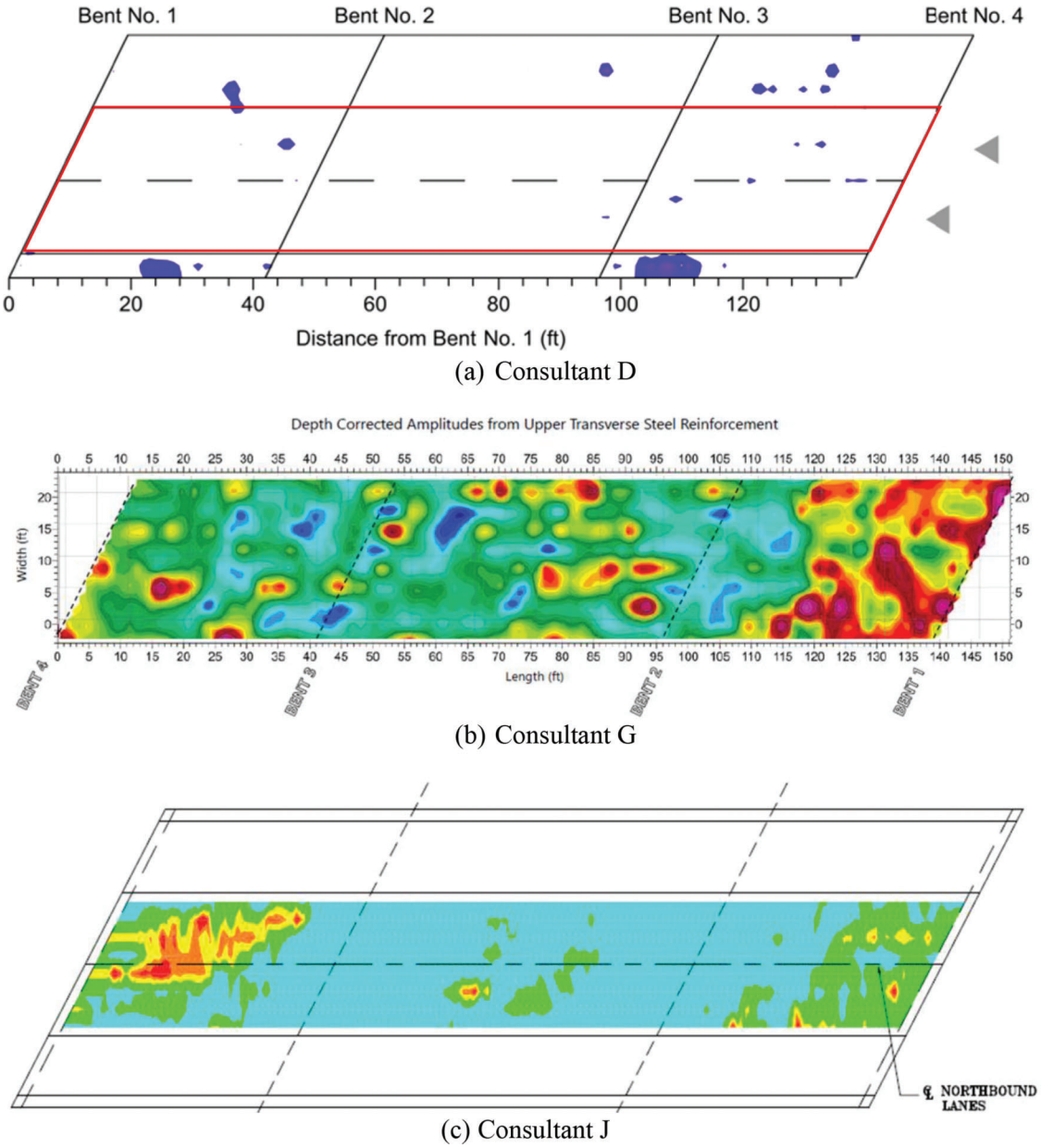

Figure 4.3 Air-launched GPR result maps for Bridge 37100 (used with permission from consultant).

For the first round of testing, Consultant D indicated that all ten bridges had deterioration percentages of less than 10% of the scanned area. Consultant B concurred with the results if the severe and poor levels of deterioration are added together, except for Bridge 37070 and Bridge 37100. When comparing these two bridges, Consultant B detected more deterioration when only the severe level from Consultant B was used. Moreover, INDOT identified more deterioration than Consultant D and Consultant B for Bridge 41810. Because it was unclear which severity levels should be utilized to compare between entities' data and the thresholds chosen by each entity were different, comparing percentage values for each bridge is not the best approach.

The percentage value of deterioration for three bridges can be compared between INDOT and Consultant H's results in the second round of testing. Bridges 20610 and 24220 show severe deterioration on their bridge decks, and Bridge 04845 has less deterioration than the others, notwithstanding the differences in percentage values. The choice of the thresholds, as noted in the discussion of the first round of testing, is believed to be the primary reason for differences in the percentage values. The low repeatability of deterioration percentage values in ground-coupled GPR data was observed.

For the map comparison for ground-coupled GPR, Bridge 22690 and Bridge 41810 are selected as examples for the first round of testing. Figure 4.6a shows the

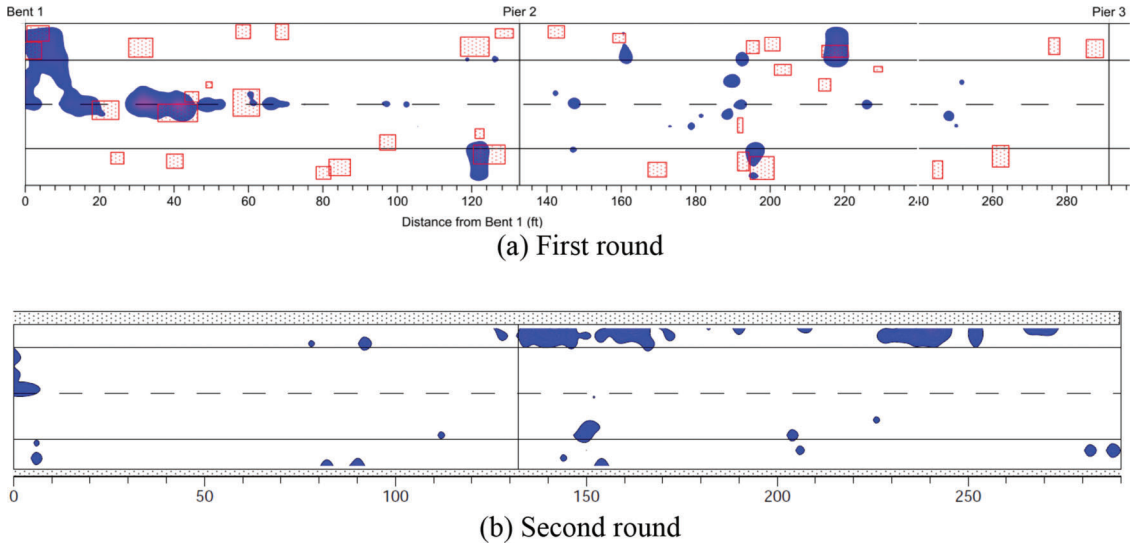

Figure 4.4 Air-launched GPR result maps for Bridge 20610 (used with permission from consultant).

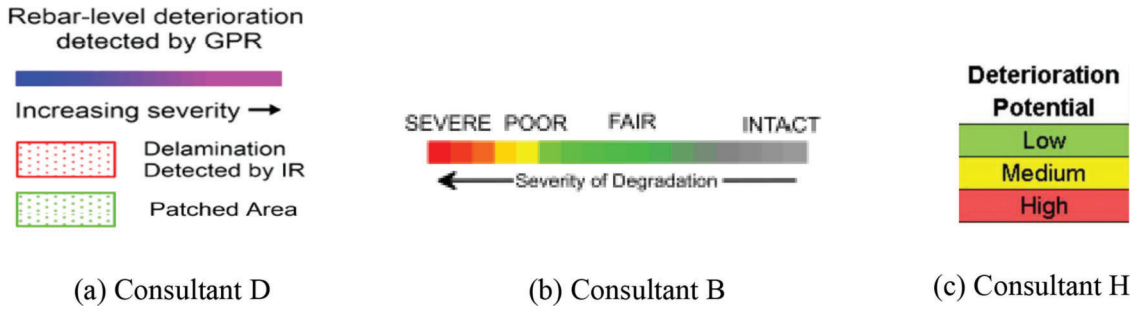

Figure 4.5 Legends for ground-coupled GPR result maps (used with permission from consultant).

result map from Consultant D for Bridge 22690. The location of the bridge deck concrete deterioration can be observed on the plan view map. The map has a 4-ft increment distance scale along the length of the bridge deck. Consultant B provides the second result map for Bridge 22690 in Figure 4.6b. The map includes a distance scale with 20-ft increments throughout the length of the bridge deck. The third result map for Bridge 22690 provided in Figure 4.6c is from INDOT. The plan view map shows the location of bridge deck concrete deterioration and a 20-ft increment distance scale along the length and a 5-ft increment along the width of the bridge deck. Similarly, Figure 4.7 shows result maps for Bridge 41810 from the three entities.

Poor comparison is found when comparing locations of deteriorated areas between the result maps from Consultant D, Consultant B, and INDOT for Bridge 22690, but they compare better for Bridge 41810. From Consultant B's results, a large amount of deterioration is present along the shoulder of the bridge, but it is not confirmed by Consultant D and INDOT for Bridge 22690. Consultant B scanned bridges in the longitudinal direction with test grids of 5-ft spacing in the lateral direction, so the result map shows GPR results in a series of lines related to the 5-ft spacing. This undoubtedly caused some inaccuracy in the results. Moreover, weather conditions were not controlled carefully in the first round of testing. Entities tested bridges on different days, and weather conditions were therefore not consistent. The moisture content of the deck can affect GPR results. It may also be a contributing factor to the discrepancies observed. When comparing the result maps for Bridge 41810, deterioration is occurring along the pier locations. Overall, result map comparisons for the ten bridges that were tested in the first round of testing are not ideal.

For the second round of testing, Bridge 04845 is selected for the comparison of the deteriorated areas. The bridge was tested by INDOT, Consultant H, and Consultant F with their ground-coupled GPR equipment. Figure 4.8a shows the result map from INDOT, and Figure 4.8b shows the map from Consultant H. The result map with 10% of data from Consultant F was selected to compare with the other entities, and the map is shown in Figure 4.8c.

For bridge 04845, the result maps from the three entities compare well overall. They all agree that the location at the first pier from the left end of the deck exhibits some degree of deterioration. Other bridges were examined in the second round of testing by the

TABLE 4.3
Summary table of ground-coupled GPR results

	Consultant D	Consultant B			INDOT		Consultant H		
	Deterioration (% of Area Surveyed)	Deterioration (% of Area Surveyed)			Deterioration (% of Area Surveyed)		Deterioration (% of Area Surveyed)		
		First Round					Second Round		
Structure Number	First Round	Poor & Severe	Severe	Poor	First Round	Second Round	High & Medium	High	Medium
01310	–	–	–	–	–	–	62	3	59
01347	–	–	–	–	–	–	9	<1	9
04845	–	–	–	–	–	8.5	13	<1	13
04930	–	–	–	–	–	–	33	1	61
08630	–	–	–	–	–	–	6	<1	6
16500	8.9	6.1	1.7	4.4	–	–	–	–	–
17940	–	–	–	–	–	–	10	<1	9
18770	7.2	6.3	3.3	3.0	–	–	–	–	–
19640	–	–	–	–	–	–	16	<1	16
20610	–	–	–	–	–	44.9	66	4	62
22690	1.3	5.7	2.2	3.5	7.9	–	–	–	–
24220	–	–	–	–	–	38.7	40	4	37
31080	3.0	3.8	0.7	3.1	–	–	–	–	–
35520	9.6	3.6	0.9	2.7	–	–	–	–	–
37070	9.8	21.6	17.2	4.4	–	–	–	–	–
37100	7.6	25	17.0	8.0	–	–	–	–	–
37150	3.2	2.6	0.6	2.0	–	–	–	–	–
41810	4.9	5.5	2.1	3.4	18.5	–	–	–	–
41870	5.9	7.3	6.0	1.3	9.0	–	–	–	–
49180	–	–	–	–	–	–	4	<1	3

ground-coupled GPR method and also provided a fair comparison for the location of deteriorated area between the three entities. Weather conditions were more carefully controlled during this round of testing. Result maps for other bridges can be found in Appendix C.

Overall, comparing the deterioration percentage of the area surveyed and the result maps for all bridges listed in Table 4.3, poor comparison is observed for the first round of testing between results from Consultant D, Consultant B, and INDOT. The results from the second round of testing performed well in terms of the locations of deterioration, but selecting the appropriate threshold remains a challenge for GPR testing.

4.2.3 Impact Echo Results

INDOT used the IE method to evaluate ten bridges in each round of testing and provided the percentage of delamination using a single value. INDOT used red to indicate delaminated areas in the result maps. Consultant F tested five bridges with their IE equipment in the second round of testing. Depending on the location of the delamination through the depth of the deck, delamination is separated into six categories, each represented by a different color on the result maps. The legend used by Consultant F is provided in Figure 4.9. The delamination percentage values detected by the two entities are summarized in Table 4.4. For the results from Consultant F, only near surface delamination, likely top delamination, and deep top delamination are considered for the results. Detailed results can be found in Appendix B.

Five bridges can be compared between INDOT and Consultant F's results in the second round of testing. In the table, the summation percentage values of the three delamination categories considered for Consultant F are provided. Both entities agree that Bridge 01310, Bridge 04930, and Bridge 24220 have more delamination than the other two bridges. Bridge 01347 and Bridge 04845 are likely in good condition. However, the relative percentage values between the results from the two entities are quite different for Bridge 04845. Because Consultant F divided the delamination results into six categories, choosing which categories to compare with the results from INDOT is a challenge. The percentage results and the result maps should both be compared to make a better judgment.

For the map comparison, Bridge 01347 and Bridge 24220 are selected as examples for the second round of testing. Figure 4.10a shows the result map from INDOT for Bridge 01347. The location of delamination can be observed on the plan view map. The map has a 10-ft increment distance scale along the length and a 5-ft increment distance scale along the width of the bridge

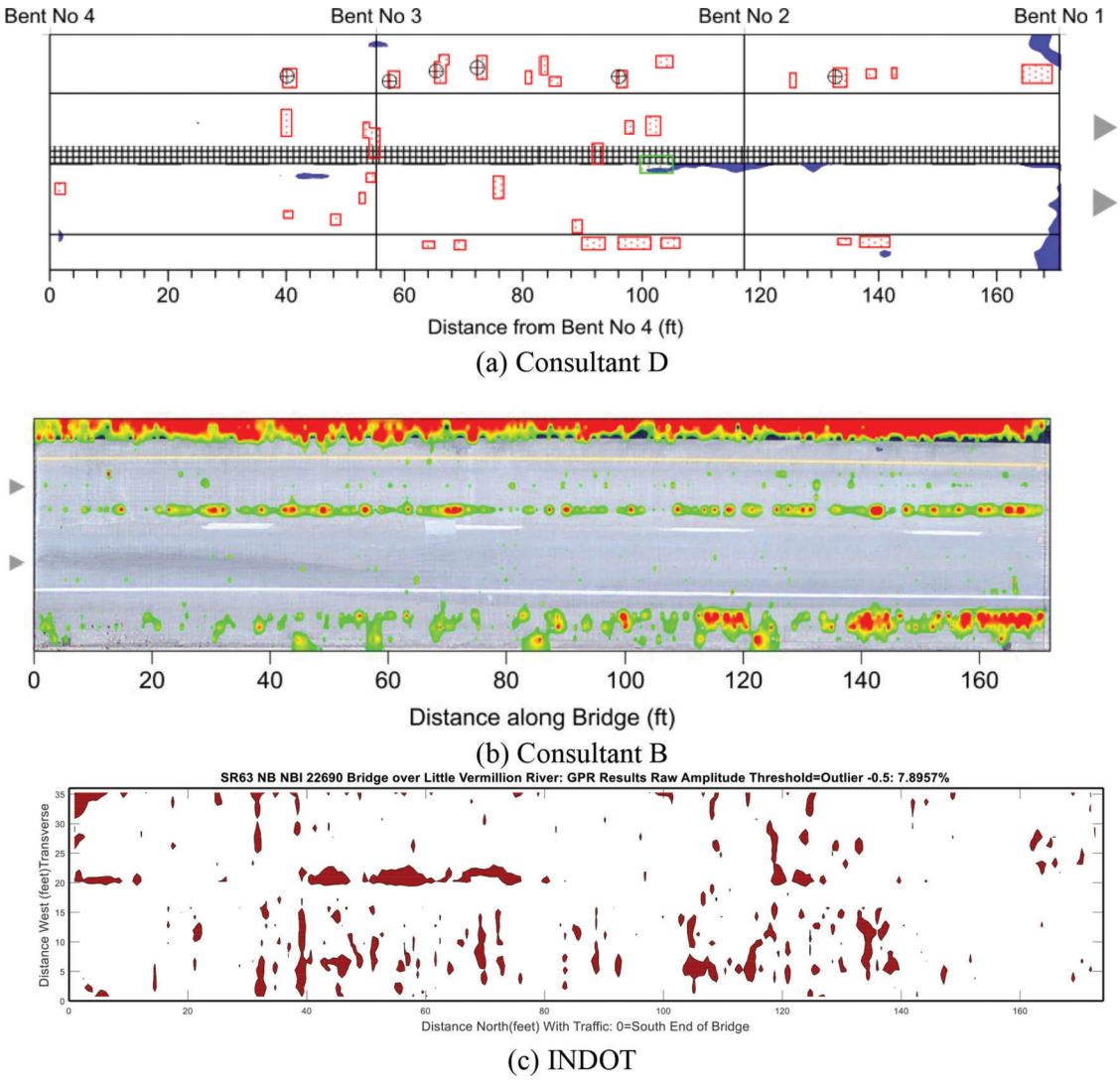

Figure 4.6 Ground-coupled GPR result maps for Bridge 22690 (used with permission from consultant).

deck. The result map provided by Consultant F for Bridge 01347 is presented in Figure 4.10b. The map includes a distance scale in 5-ft increments throughout the length and width of the bridge deck. Similarly, Figure 4.11 shows result maps for Bridge 41810 from the two entities.

The locations of delamination compare well between the result maps from INDOT and Consultant F for both bridges. INDOT and Consultant F used the same manufacturer model of IE, so it is not surprising that the results are very similar. All five bridges provide good comparisons, and this gives evidence that the IE test is fairly repeatable. Result maps for other bridges can be found in Appendix C.

Overall, based upon the results for all bridges listed in Table 4.4, good comparison was observed for the delamination percentage of area surveyed and the result maps from INDOT and Consultant F. Therefore, the IE test is believed to be reliable and repeatable for detecting delamination in a bridge deck.

4.2.4 Infrared Thermography Results

In the first round of testing, Consultant D and Consultant E used their vehicle-mounted IRT equipment to assess 20 bridges. Consultant B tested ten of these bridges with their drone-mounted IRT equipment. Consultant I surveyed two bridges with their pole-mounted IRT equipment. Lastly, aerial IRT was used by Consultant D to scan 38 bridges along I-65. In the second round of testing, Consultant E used their vehicle-mounted IRT equipment to test ten bridges, and Consultant C used drone-mounted IRT to test the same bridges. Four of these bridges were evaluated by Consultant I using their pole-mounted IRT equipment. Consultant D also scanned 37 bridges using the aerial IRT method along I-69 and SR 18. All entities provided the delamination percentage of the area surveyed as a single value. In the result maps of the vehicle-mounted IRT from Consultant D, the delamination and patched areas are highlighted in red and green, respectively, and the legend is provided in Figure 4.12a. The aerial IRT

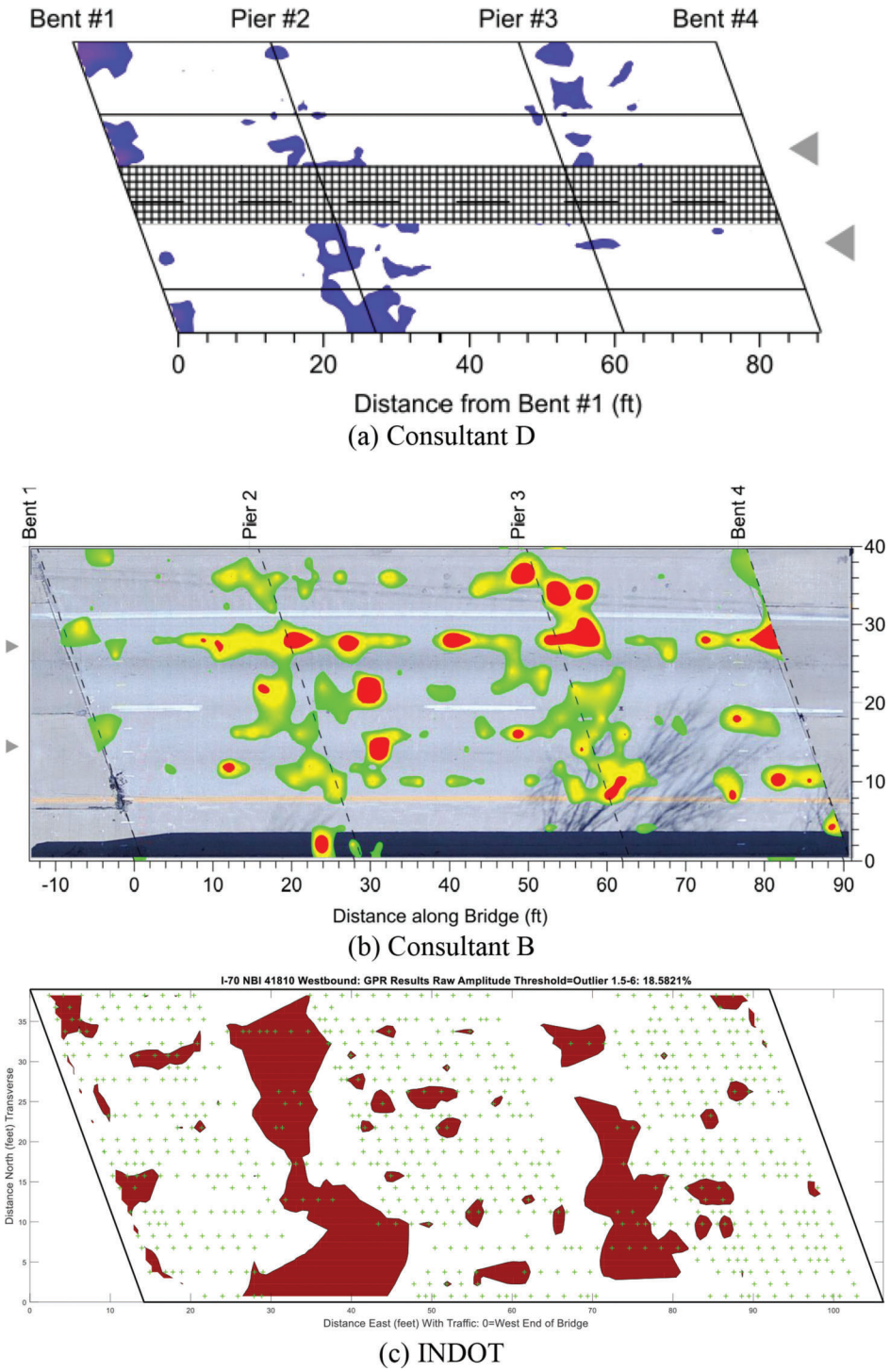

Figure 4.7 Ground-coupled GPR result maps for Bridge 41810 (used with permission from consultant).

result maps used red boxes to mark the delamination areas. In Figure 4.12b, Consultant E used colored boxes with different outline colors to represent delamination and patch areas. The legend for Consultant B is shown in Figure 4.12c, and the areas with spalling, patching, and delamination are marked by different hatched boxes. Consultant I used red to indicate deep defects in the deck and yellow marks to indicate shallow defects. Consultant C highlighted the delamination areas in blue. The delamination percentage values detected by the five entities are summarized in Table 4.5. Detailed results can be found in Appendix B.

For the first round of testing, the aerial IRT by Consultant D and drone-mounted IRT by Consultant

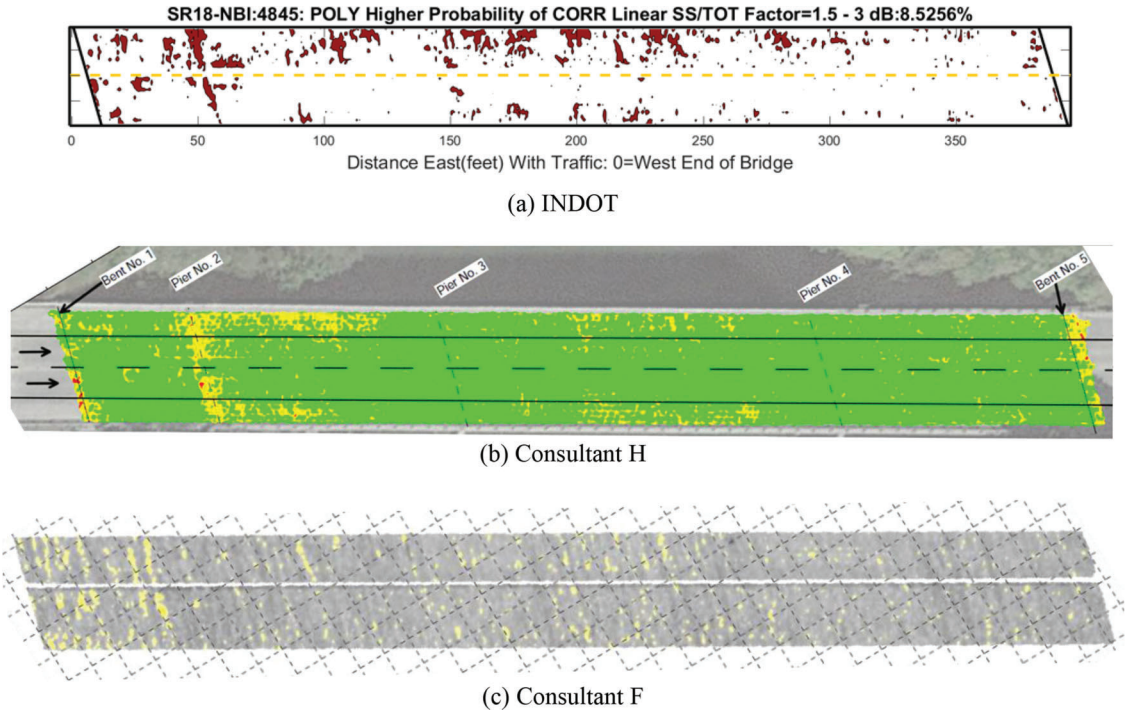

Figure 4.8 Ground-coupled GPR result maps for Bridge 04845 (used with permission from consultant).

Grey	Dark Red and Purple	Orange	Yellow	Cyan	Light Blue	Dark Blue
Sound Condition Concrete	Near Surface Delamination	Likely Top Delamination or Thickened Concrete	Possible Top Delamination or Thickened Concrete	Possible Bottom Delamination or Thin Concrete	Possible Bottom Delamination or Internal Cracking	Deep Top Delamination or Internal Cracking

Figure 4.9 Legend for IE result maps from Consultant F (used with permission from consultant).

B found a slightly lower amount of delamination than other methods, except pole-mounted IRT. For the aerial IRT, the results may be somewhat influence by the data collection period since the time involved in collecting the aerial IRT data is much shorter than other IRT methods due to the speed of the airplane and the height of the airplane above the bridge decks. Moreover, it is not surprising that a large number of bridges tested by aerial IRT may be in good condition since an entire corridor is flown in one trip and the bridges along the interstates often receive aggressive maintenance to keep them in good condition.

The drone-mounted IRT data provided by Consultant B also may have some related issues. The drones are not allowed to fly directly above the bridges due to possible conflicts with traffic on the bridge. Hence, they fly adjacent to the bridge and not directly over the bridge deck. However, their data collection period is greater than that of an airplane or even a truck with IRT equipment attached.

The vehicle-mounted IRT results between Consultant D and Consultant E match for some bridges but others do not compare well because the results can be affected by many conditions, including shaded areas, moisture, and small temperature differences. Data were collected at different times by each entity, and variables that could affect results such as moisture were not carefully controlled during the first round of testing.

For the second round of testing, some bridges, such as Bridge 49200 and Bridge 08630, have good comparisons in percentage values, while others show different values. As explained in Section 2.4, the accuracy of the IRT results can be affected by the type of IRT methods. Aerial IRT scans are collected quickly and from far above the deck, which may provide slightly less accurate results. The pole-mounted IRT has a longer testing period than any other IRT method; the system processes IRT images collected over a two-day period. Hence, it is believed that it may deliver the most accurate results. Vehicle-mounted IRT can collect data close to the surface of the deck at highway speeds, and drone-mounted IRT can slowly scan the deck but at farther distances from the surface of the deck.

TABLE 4.4
Summary table of IE results

	INDOT		Consultant F			
			Delamination (% of Area Surveyed)			
	Delamination (% of Area Surveyed)		Second Round			
Structure Number	First Round	Second Round	Sum of Three Categories	Near Surface Delamination	Likely Top Delamination or Thickened Concrete	Deep Top Delamination or Internal Cracking
01310	–	16.0	20.4	2.9	3.4	14.1
01347	–	5.1	3.5	1.8	1.3	0.4
04845	–	7.9	1.8	0.3	1.3	0.2
04930	–	35.0	29.5	17.4	10.8	1.3
08630	–	12.0	–	–	–	–
16500	0.7	–	–	–	–	–
17940	–	4.8	–	–	–	–
18770	–	–	–	–	–	–
19640	–	–	–	–	–	–
20610	–	13.1	–	–	–	–
22690	9.6	–	–	–	–	–
24220	–	–	38.0	20.5	8.2	9.3
31080	–	–	–	–	–	–
35520	0	–	–	–	–	–
37070	3.8	–	–	–	–	–
37100	13.5	–	–	–	–	–
37150	7.5	–	–	–	–	–
41810	8.2	–	–	–	–	–
41870	3.8	–	–	–	–	–
49180	–	8.2	–	–	–	–

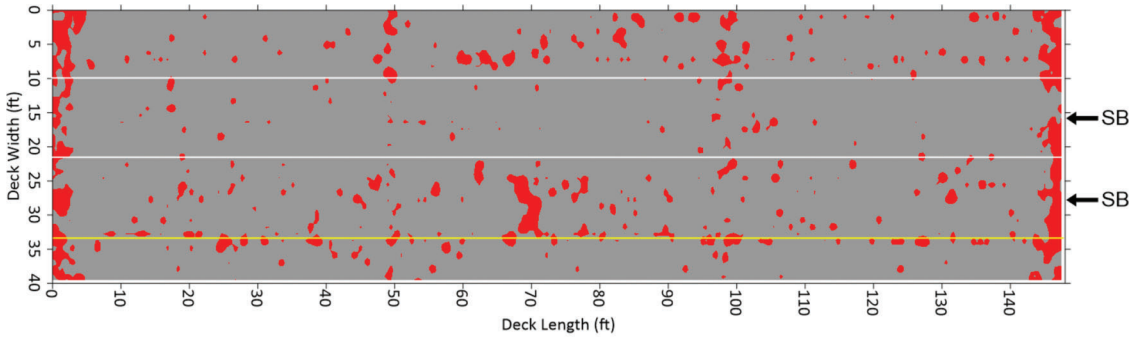

(a) INDOT

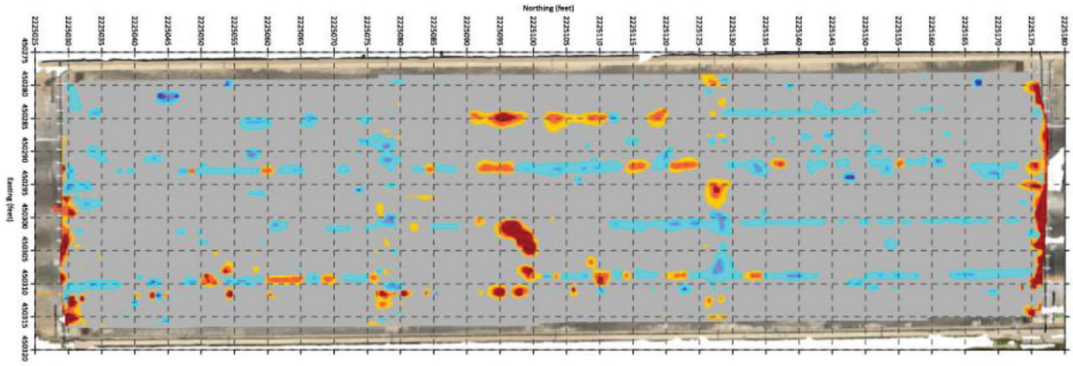
(b) Consultant F

Figure 4.10 IE result maps for Bridge 01347 (used with permission from consultant).

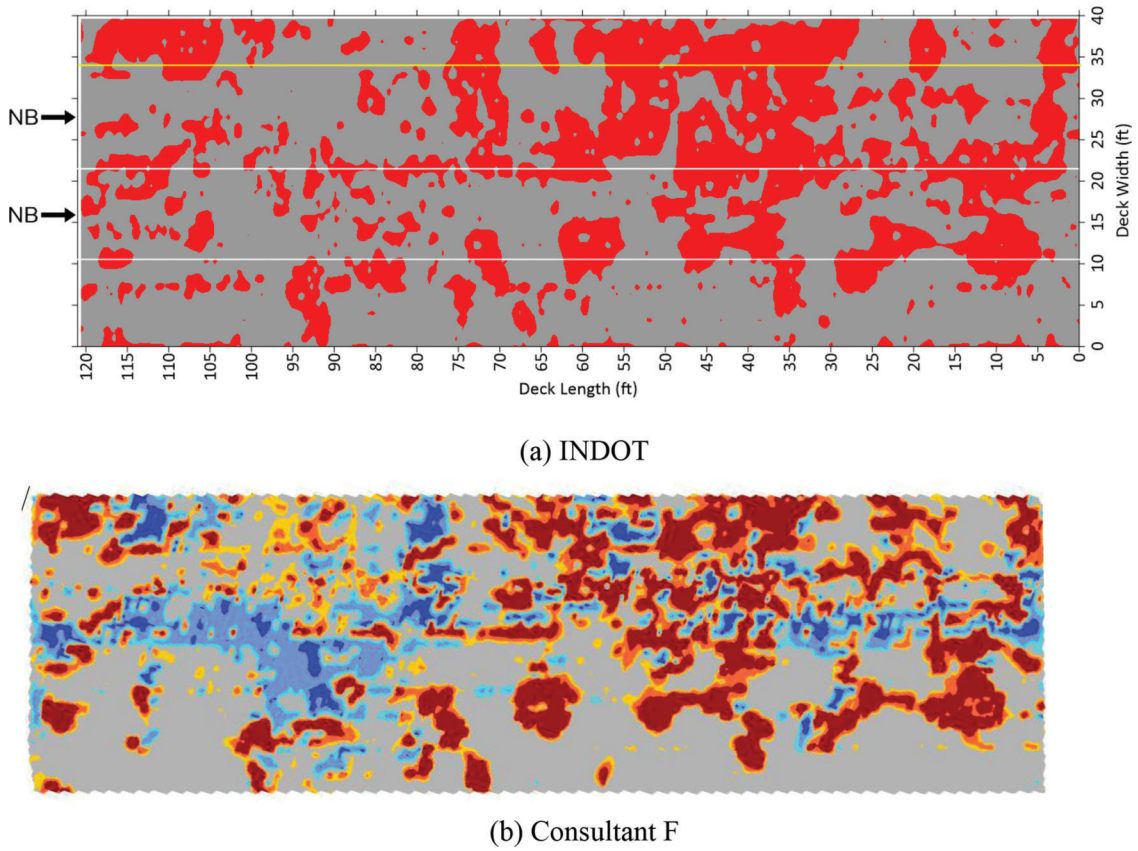

Figure 4.11 IE result maps for Bridge 24220 (used with permission from consultant).

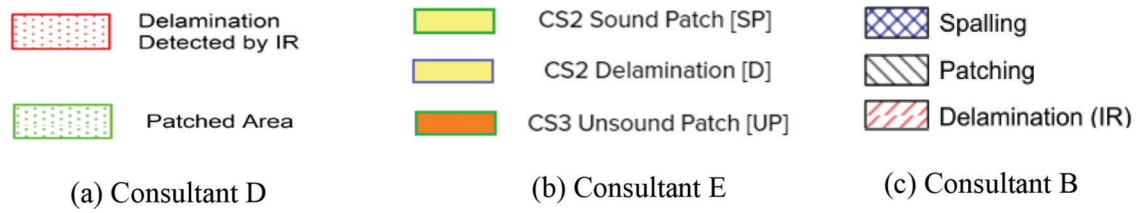

Figure 4.12 Legends for IRT result maps (used with permission from consultant).

Therefore, differences in the accuracy of the IRT methods are expected.

The first six bridges listed in Table 4.5 can be compared between the first round and the second round of testing. Consultant E provided significantly different results for the same bridges in different rounds of testing because they revised their judgment used during the analysis of the data in the second round of testing. Most entities agree that Bridge 01347 is in good condition, and Bridge 20610 has more delamination than the other five bridges. Minor delamination (less than 5%) was detected by Consultant D and Consultant E in the first round of testing indicating that most of the bridges are in good condition. However, the pole-mounted IRT used by Consultant I identified significantly more delamination than other entities for Bridge 01310, which has a latex overly. Furthermore, the delamination reported by Consultant I agreed well with that found by both entities using IE.

The delamination percentages of the area surveyed listed in Table 4.5 are generally lower for most bridges compared to the IE method. The finding may indicate that the IRT test only detected delamination at a relatively shallow depth and that deep delamination at the bottom reinforcement layer in decks cannot be easily found using this method, except perhaps for the pole-mounted IRT. Ground-truth testing (i.e., concrete coring) could help to confirm this conclusion.

For the map comparison, Bridge 31080 is selected as an example from the first round of testing. Figure 4.13a shows the result map from Consultant D. The location of bridge deck delamination can be observed on the plan view map. The map has a 4-ft increment distance scale along the length of the bridge deck. Figure 4.13b shows the result map provided by Consultant E. The map includes a distance scale with 10-ft increments throughout the length and width of the bridge deck.

TABLE 4.5
Summary table of IRT results

First Round						Second Round					
	Consultant D Delam. (% of Area Surveyed)		Consultant E Delam. (% of Area Surveyed)	Consultant B Delam. (% of Area Surveyed)	Consultant I Delam. (% of Area Surveyed)		Consultant D Delam. (% of Area Surveyed)	Consultant E Delam. (% of Area Surveyed)	Consultant C Delam. (% of Area Surveyed)	Consultant I Delam. (% of Area Surveyed)
Structure Number	Aerial IRT	Vehicle-Mounted IRT	Vehicle-Mounted IRT	Drone-Mounted IRT	Pole-Mounted IRT	Structure Number	Aerial IRT	Vehicle-Mounted IRT	Drone-Mounted IRT	Pole-Mounted IRT
01310	–	1.3	0.2	–	–	01310	–	1.0	5.5	24.0
01347	–	1.5	0.2	–	–	01347	–	4.3	<0.1	2.0
17940	–	0.7	0.2	–	–	17940	–	7.6	2.2	–
19640	–	1.4	3.3	–	–	19640	–	8.6	5.0	–
20610	–	6.3	4.5	–	–	20610	–	4.7	2.9	–
49200	–	1.6	1.1	–	–	49200	–	4.5	5.1	5.0
37070	0.0	0.7	0.1	0.0	6.0	04845	8.0	3.2	<0.1	–
37100	0.0	0.0	0.4	0.0	–	04930	4.0	2.0	7.1	–
42190	–	–	–	–	5.0	08630	–	1.5	1.3	–
05230	–	2.3	0.9	–	–	24220	–	3.6	3.6	15.0
11940	–	1.9	0.4	–	–	04708	2.0	–	–	–
16500	–	2.9	0.8	0.0	–	04710	2.0	–	–	–
18770	–	1.3	1.3	0.0	–	04730	1.0	–	–	–
18870	–	2.3	0.0	–	–	04740	<1.0	–	–	–
22690	–	2.7	2.3	1.4	–	04750	<1.0	–	–	–
31080	–	14.4	4.0	5.7	–	04770	N/A	–	–	–
35520	–	0.0	0.1	0.0	–	04820	3.0	–	–	–
37150	–	0.2	0.3	0.0	–	04830	2.0	–	–	–
41810	–	0.0	0.2	0.4	–	04859	13.0	–	–	–
41870	–	0.4	0.3	0.2	–	04860	2.0	–	–	–
76140	–	1.1	0.0	–	–	04910	1.0	–	–	–
36070	0.0	–	–	–	–	04920	<1.0	–	–	–
36130	0.0	–	–	–	–	39620	<1.0	–	–	–
36150	0.0	–	–	–	–	39630	2.0	–	–	–
36170	1.0	–	–	–	–	39640	<1.0	–	–	–
36190	0.0	–	–	–	–	39650	<1.0	–	–	–
36210	1.0	–	–	–	–	39740	2.0	–	–	–
36230	0.0	–	–	–	–	39770	2.0	–	–	–
36250	0.0	–	–	–	–	39780	<1.0	–	–	–
36270	0.0	–	–	–	–	39850	<1.0	–	–	–
36290	1.0	–	–	–	–	39860	1.0	–	–	–
36320	4.0	–	–	–	–	39870	1.0	–	–	–
36330	1.0	–	–	–	–	39880	3.0	–	–	–
36520	3.0	–	–	–	–	39910	2.0	–	–	–
36660	2.0	–	–	–	–	39920	2.0	–	–	–
36680	0.0	–	–	–	–	40000	2.0	–	–	–

Continued on next page

TABLE 4.5
(Continued)

First Round						Second Round					
	Consultant D Delam. (% of Area Surveyed)		Consultant E Delam. (% of Area Surveyed)	Consultant B Delam. (% of Area Surveyed)	Consultant I Delam. (% of Area Surveyed)		Consultant D Delam. (% of Area Surveyed)	Consultant E Delam. (% of Area Surveyed)	Consultant C Delam. (% of Area Surveyed)	Consultant I Delam. (% of Area Surveyed)
Structure Number	Aerial IRT	Vehicle-Mounted IRT	Vehicle-Mounted IRT	Drone-Mounted IRT	Pole-Mounted IRT	Structure Number	Aerial IRT	Vehicle-Mounted IRT	Drone-Mounted IRT	Pole-Mounted IRT
36690	0.0	–	–	–	–	40010	1.0	–	–	–
36700	1.0	–	–	–	–	40130	2.0	–	–	–
36720	0.0	–	–	–	–	40140	<1.0	–	–	–
36730	0.0	–	–	–	–	40220	2.0	–	–	–
36740	0.0	–	–	–	–	40230	1.0	–	–	–
36750	1.0	–	–	–	–	40330	<1.0	–	–	–
36760	0.0	–	–	–	–	40340	2.0	–	–	–
36770	0.0	–	–	–	–	40350	1.0	–	–	–
36780	0.0	–	–	–	–	40360	1.0	–	–	–
36790	0.0	–	–	–	–	–	–	–	–	–
36800	0.0	–	–	–	–	–	–	–	–	–
36850	1.0	–	–	–	–	–	–	–	–	–
36880	0.0	–	–	–	–	–	–	–	–	–
36900	0.0	–	–	–	–	–	–	–	–	–
36920	0.0	–	–	–	–	–	–	–	–	–
36950	1.0	–	–	–	–	–	–	–	–	–
36980	0.0	–	–	–	–	–	–	–	–	–
37030	2.0	–	–	–	–	–	–	–	–	–
37060	2.0	–	–	–	–	–	–	–	–	–
37120	0.0	–	–	–	–	–	–	–	–	–
50720	1.0	–	–	–	–	–	–	–	–	–

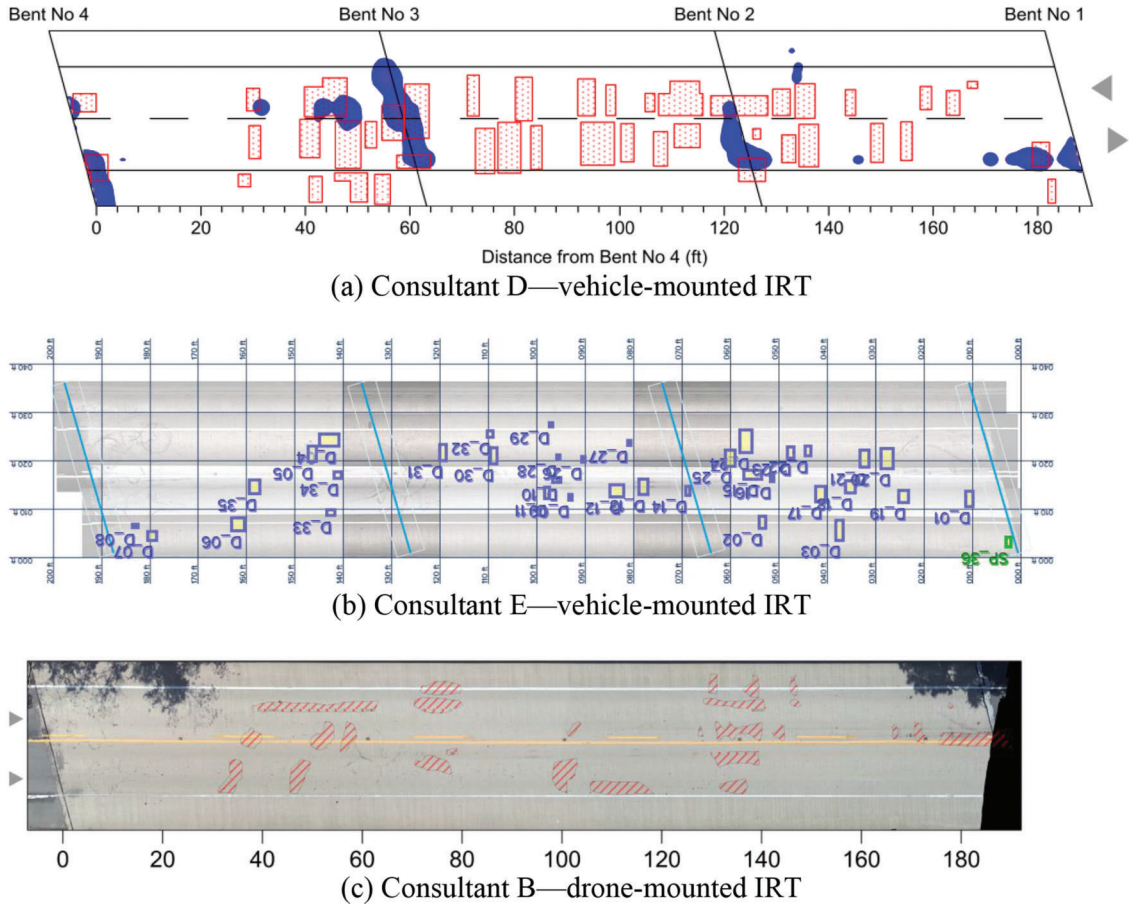

Figure 4.13 IRT result maps for Bridge 31080 for the comparison of the first round of testing (used with permission from consultant).

The third result map provided in Figure 4.13c is from Consultant B. The plan view map shows the location of bridge deck concrete deterioration and a 20-ft increment distance scale along the length of the bridge deck. For the second round of testing, Consultant E, Consultant C, and Consultant D are chosen, and the results maps for Bridge 04930 are shown in Figure 4.14. The result maps from Consultant C are shown with a 5-ft grid. Bridge 19640 is chosen for the comparison between the first round and the second round, and the result maps from Consultant E (both rounds), Consultant C (second round), and Consultant D (first round) are presented in Figure 4.15.

In general, Bridge 31080 result maps show agreement for the majority of the delaminated locations. There is a good comparison between the location of the delamination indications, even though the delamination percentages of the area surveyed are different. For Bridge 04930, the shaded areas on the bridge deck affect the IRT results for the result maps from Consultant E and Consultant D because these areas will experience less temperature change. It is difficult for both aerial IRT and vehicle-mounted IRT to measure accurate delamination results when shading is present. Other areas in the result maps are roughly comparable, but Consultant E shows less delaminated area than the other two entities. For Bridge 19640, a fairly good comparison is made between the result maps from Consultant E's first round, Consultant E's second round, and Consultant C. Consultant D indicated the least delaminated area, but most of the delaminated areas that Consultant D found are also shown by Consultant E and Consultant C. All bridges are compared, and result maps can be found in Appendix C.

Overall, considering the delamination percentage of the area surveyed and the result maps for all bridges listed in Table 4.5, the results are somewhat comparable, but there is some disagreement among the various types of IRT methods. Parameters, such as distance from the deck, testing duration, temperature difference, presence of moisture, and overlay presence likely affected the IRT results. Choosing proper IRT methods for the different goals of testing is important. Hence, aerial IRT may be ideal for network-level scanning as an initial screening of bridge condition, while pole-mounted IRT is likely a good choice for project-level scanning.

4.2.5 Automated Sounding Results

Consultant B used their automated sounding system to evaluate 10 bridges in the first round of testing and

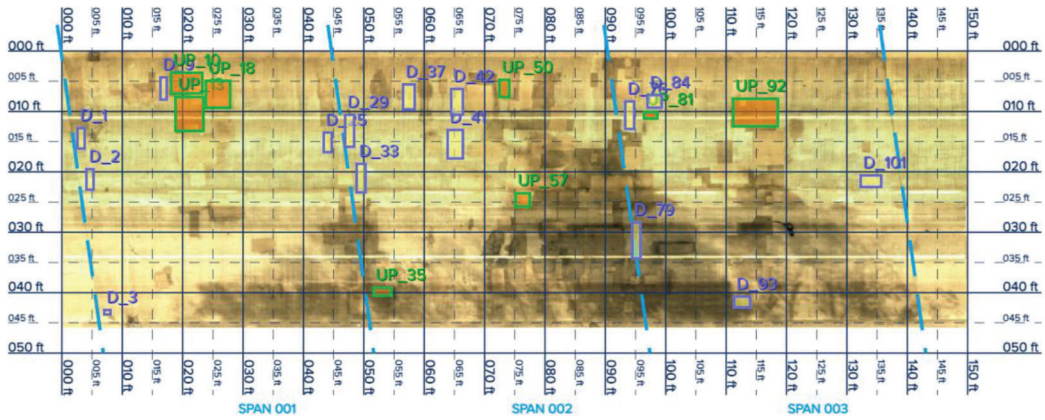

(a) Consultant E—vehicle-mounted IRT

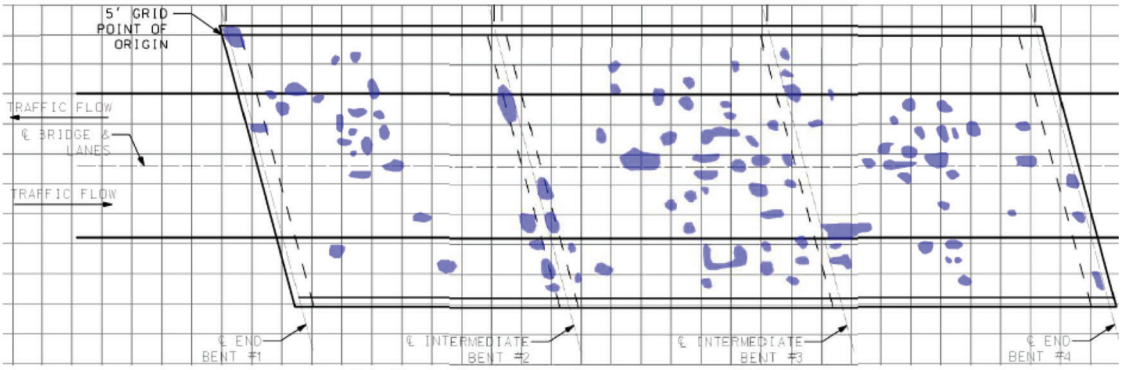

(b) Consultant C—drone-mounted IRT

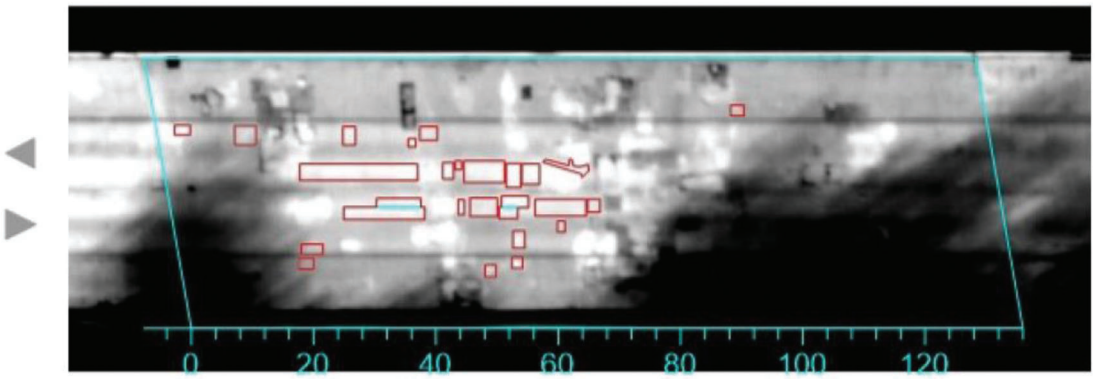

(c) Consultant D—aerial IRT

Figure 4.14 IRT result maps for Bridge 04930 for the comparison of the second round of testing (used with permission from consultant).

provided the percentage of delamination in four levels: intact, fair, poor, and severe. As indicated in Figure 4.16a, each severity level is defined by various colors. In the second round of testing, Bridge 31080 was under construction, so Consultant A tested 19 bridges with their automated sounding equipment, and 9 of these 19 bridges can be compared with the results from Consultant B. The legend used by Consultant A is provided in Figure 4.16b. The delamination percentage values detected by the two entities are summarized in Table 4.6. This study only considered the poor and severe levels indicated by Consultant B. Detailed results can be found in Appendix B.

By comparing results between Consultant B and Consultant A, it is found that both entities indicate a low amount of delamination for the bridges tested. They agree that Bridge 16500, Bridge 18770, and Bridge 37070 are in good condition. However, the percentage values between the results from the two entities have a larger difference for Bridge 22690 and Bridge 37150. Because Consultant B divided the delamination results into four levels, which levels to

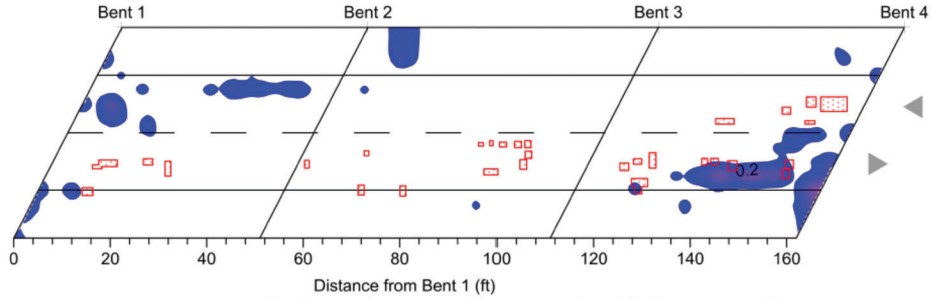

(a) Consultant D—first round vehicle-mounted IRT

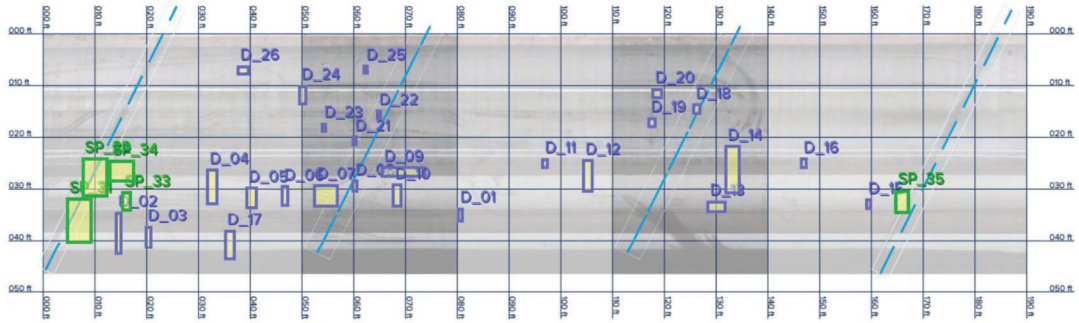

(b) Consultant E—first round vehicle-mounted IRT

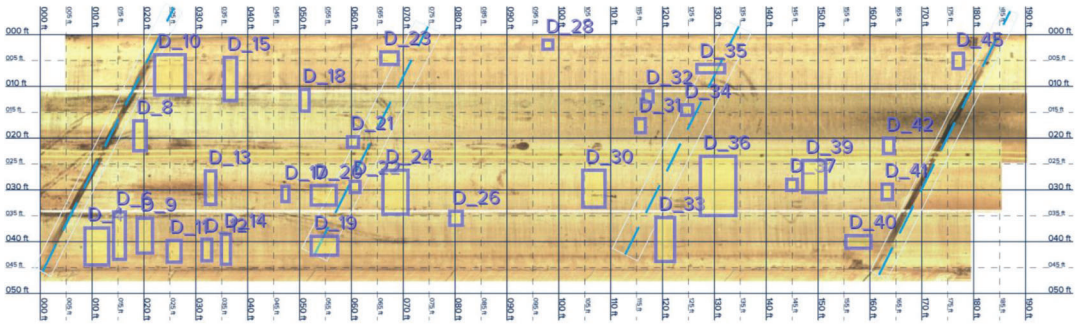

(c) Consultant E—second round vehicle-mounted IRT

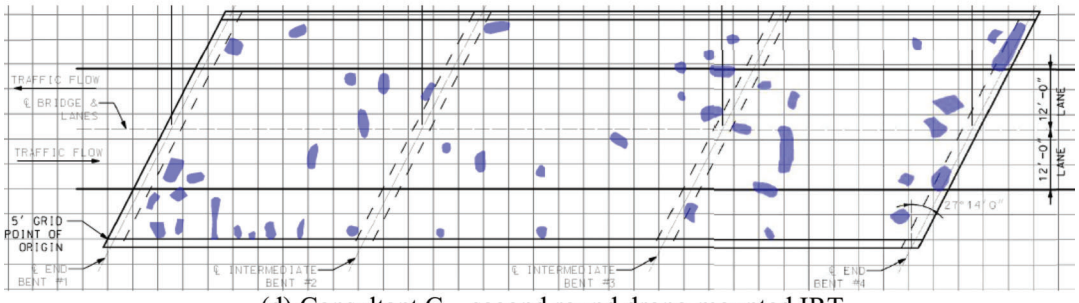

(d) Consultant C—second round drone-mounted IRT

Figure 4.15 IRT result maps for Bridge 19640 for the comparison between rounds (used with permission from consultant).

(a) Consultant B (b) Consultant A

Figure 4.16 Legends for automated sounding result maps (used with permission from consultant).

TABLE 4.6
Summary table of automated sounding results

	Consultant B			Consultant A
	Delamination (% of Area Surveyed)			Delamination (% of Area Surveyed)
	First Round			Second Round
Structure Number	Poor	Severe	Poor & Severe	
01310	–	–	–	0.4
01347	–	–	–	0.1
04845	–	–	–	0.2
04930	–	–	–	0.6
08630	–	–	–	0.0
16500	0.2	0.1	0.3	0.0
17940	–	–	–	0.0
18770	0.2	0.1	0.3	0.0
19640	–	–	–	3.9
20610	–	–	–	3.4
22690	0.3	0.1	0.4	2.9
24220	–	–	–	5.4
31080	1.1	0.4	1.5	–
35520	0.2	0.2	0.4	0.0
37070	0.1	0.1	0.2	0.0
37100	0.1	0.1	0.2	1.3
37150	0.3	0.1	0.4	1.8
41810	0.8	0.7	1.5	0.9
41870	0.1	0.0	0.1	1.2
49180	–	–	–	1.1

consider for comparison with the results from Consultant A was difficult to identify. The percentage results and the result maps should both be compared to make a better judgment.

For the map comparison, Bridge 41810 and Bridge 16500 are selected as examples. The result map from Consultant B for Bridge 41810 is provided in Figure 4.17a. The location of delamination can be observed on the plan view map. The map has a distance scale with 2-ft increments along the length and width of the bridge deck. The result map from Consultant A for Bridge 41810 is presented in Figure 4.17b. Similarly, Figure 4.18 shows result maps for Bridge 16500 from the two entities.

The locations of delamination are only comparable within the first span of Bridge 41810. Other locations for Bridge 41810, and the entire bridge for Bridge 16500, are not comparable between the result maps for the two entities. Consultant B and Consultant A used different automated sounding equipment, so the results may vary. Comparisons for other bridges are presented in Appendix C, and poor comparisons are observed for these bridges.

Overall, considering the results for all bridges listed in Table 4.6, relatively small delamination values were detected by both entities, with larger delamination values usually detected by Consultant A compared to Consultant B. However, the comparison of delamination percentage detected, and the areas indicated on the result maps from Consultant B and Consultant A is generally poor. Therefore, there are some concerns about the reliability and repeatability of the automated sounding test based on the comparisons between the results from the two consultants.

4.2.6 Reinforcing Bar Cover Depth Results

Concrete cover depth for the top reinforcement layer is an important parameter when evaluating the quality of the bridge deck construction. Therefore, in the first round of testing, Consultant D, Consultant B, and Consultant G were asked to assess ten bridges for concrete cover thickness to the top reinforcement using either ground-coupled or air-launched GPR equipment. Additionally, ten newer bridge decks were selected to check the concrete cover thickness by Consultant D. Six concrete cores were drilled by INDOT to verify the concrete cover depth for Bridge 13321 and Bridge 16171. In the second round of testing, Consultant H used their multichannel GPR equipment to measure cover depth for ten bridges. The four entities used color bars to identify the concrete cover thickness at various locations on a bridge deck. Consultant G and Consultant H used various ranges of color bars for different bridges depending on the highest cover thickness interval, and examples of the color bars are shown in Figure 4.19c and Figure 4.19d. Consultant D and Consultant B used the same color bar for all bridges (Figure 4.19a and Figure 4.19b). Average concrete cover thicknesses are presented in Table 4.7 for the bridges tested. Detailed results can be found in Appendix B.

For the first round of testing, concrete cover thicknesses compared well between the three entities.

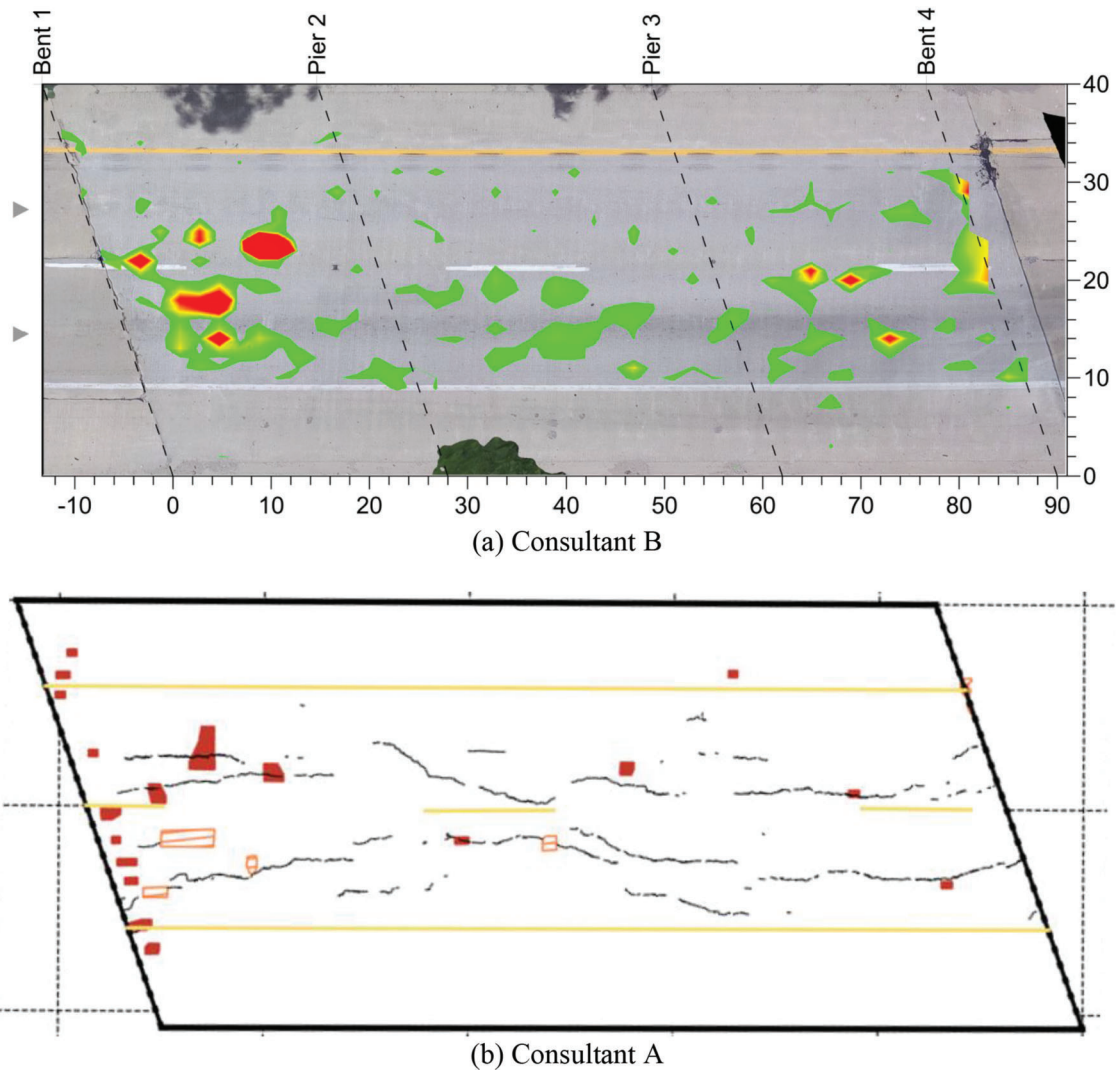

Figure 4.17 Automated sounding result maps for Bridge 41810 (used with permission from consultant).

Bridge 16500, Bridge 37100, and Bridge 41810 are slab bridges, so the concrete cover thickness is somewhat greater than other bridges. Moreover, Bridge 22690 and Bridge 35520 have a latex concrete overlay on the deck; therefore, these decks have a thicker cover thickness. The concrete cover thickness of other bridges is approximately the typical concrete cover thickness, which is 2.5 in. The average concrete cover thickness for newer bridges was measured to be greater than 2.5 in., which meets the top cover thickness requirement (2.5 in.). In the second round of testing, reasonable concrete cover thicknesses were measured by Consultant H. Bridge 01310 is a slab bridge, and Bridge 24220, Bridge 04930, and Bridge 20610 have a latex concrete overlay. Therefore, greater concrete cover thicknesses were measured. Overall, the average concrete cover thicknesses for tested bridges are acceptable.

Bridge 37100 and Bridge 41810 are used as examples to compare the result maps from Consultant B and Consultant G. Consultant D did not provide concrete cover thickness result maps. Figure 4.20a shows the result map from Consultant B for Bridge 37100. Variations in the concrete cover thickness can be observed on the plan view map. The map has a 20-ft increment distance scale along the length of the bridge deck. The result map from Consultant G for Bridge 37100 is shown in Figure 4.20b. The map includes a distance scale with 1-ft increments throughout the length and width of the bridge deck. Because Consultant G only scanned the traffic lanes, the area in the red box on Consultant B's map should be used to compare with result map from Consultant G. Similarly, Figure 4.21 shows result maps for Bridge 41810 from the two entities.

Because Consultant B used the same color bars for all bridges, the cover thickness range for the color scale is quite large. Colors have low contrast between areas with small differences in cover thicknesses. However, the result maps from Consultant B and Consultant G are comparable based on the trend of the color changes. Both entities agree that the concrete cover thickness increases to 9 in. in the third span of Bridge 37100, and

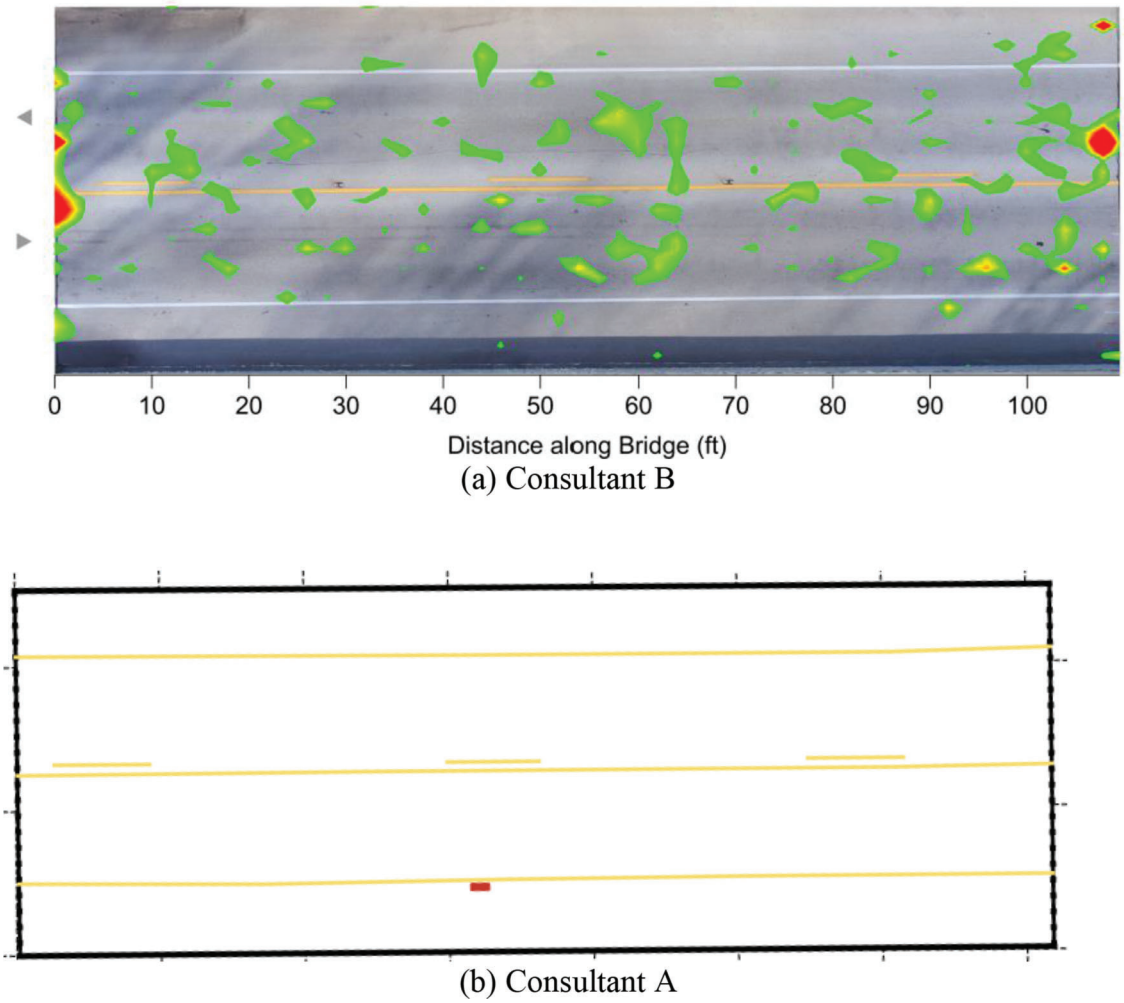

Figure 4.18 Automated sounding result maps for Bridge 16500.

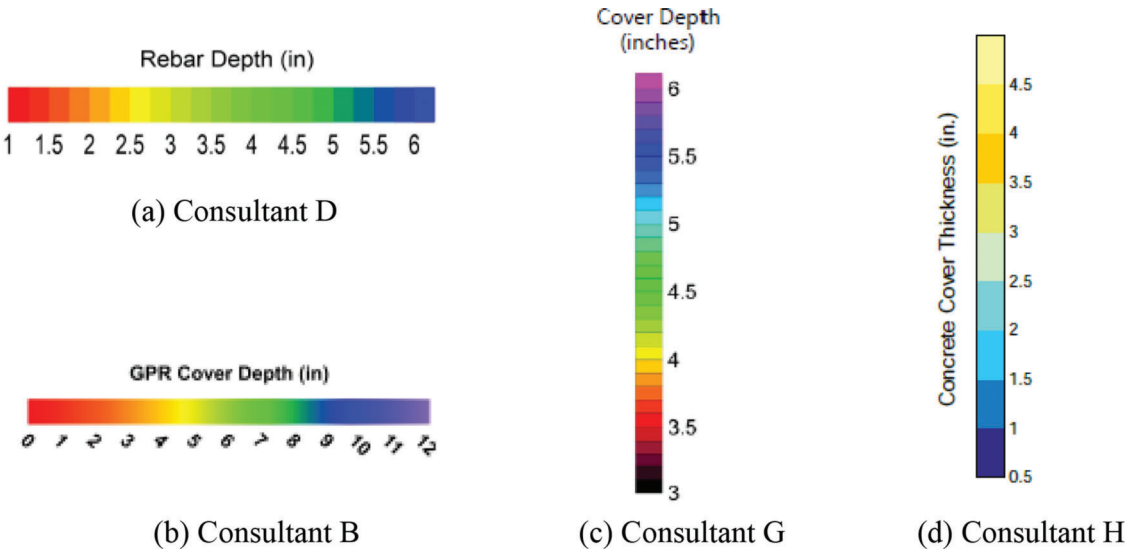

Figure 4.19 Legends for concrete cover thickness result maps (used with permission from consultant).

TABLE 4.7
Summary table of average concrete cover thickness results

Structure Number	Consultant D	Consultant B	Consultant G	Consultant H
	Avg. Concrete Cover Thickness (in.)	Avg. Concrete Cover Thickness (in.)	Avg. Concrete Cover Thickness (in.)	Avg. Concrete Cover Thickness (in.)
	First Round	First Round	First Round	Second Round
01310[1]	–	–	–	5.0
01347	–	–	–	3.1
04845	–	–	–	2.3
04930	–	–	–	3.4
08630	–	–	–	2.0
16500[1]	3.8	4.3	4.9	–
17940	–	–	–	1.9
18770	2.8	3.0	3.3	–
19640	–	–	–	1.5
20610	–	–	–	3.3
22690	4.5	4.8	4.7	–
24220	–	–	–	4.1
31080	3.6	4.1	4.0	–
35520	3.1	4.2	4.1	–
37070	2.5	2.8	2.9	–
37100[1]	6.3	7.6	6.0	–
37150	2.3	2.8	2.8	–
41810[1]	3.5	4.4	3.3	–
41870	2.5	2.9	2.9	–
49180	–	–	–	2.7
13321[2]	2.7	–	–	–
16171[2]	3.1	–	–	–
16811[2]	3.5	–	–	–
17051[2]	2.9	–	–	–
28326[2]	2.5	–	–	–
28430[2]	3.4	–	–	–
32675[2]	3.2	–	–	–
33500[2]	2.7	–	–	–
44090[2]	2.9	–	–	–
44120[2]	3.1	–	–	–

[1]Slab bridge.
[2]Bridge is a newer girder/beam bridge.

other areas of thick cover are indicated on both result maps. For Bridge 41810, both result maps show thin concrete cover thickness at the left end of the bridge and thick cover thickness at the right end of the bridge. Comparisons for other bridges can be found in Appendix C.

Consultant D used air-launched GPR to evaluate 10 newer bridge decks for the concrete cover depth of the reinforcement. For two of the bridges, concrete cores were extracted to verify the cover depth. Figure 4.22a shows the location of the three concrete cores that were drilled on the deck of Bridge 13321. For the best comparison, the three locations are also presented on the result map from Consultant D in Figure 4.22b. Three cores were also extracted from Bridge 16171, and the locations of the cores are shown in Figure 4.23.

By measuring the height of each concrete core above the top layer of reinforcement, the concrete cover depth can be determined. For Bridge 13321, the height of the core at location C1 is 2.875 in., C2 is 2.25 in., and C3 is 2.5 in. The concrete cover depth at these three locations can be observed from Consultant D's air-launched GPR result map. On the map, the depth is in a range of 2.25 in. to 2.5 in. at location C1, around 2.5 in. at location C2, and 2.5 in. to 2.75 in. at location C3. For Bridge 16171, the height of the core at location C1 is 2.5 in., C2 is 2.875 in., and C3 is 2.625 in. The concrete cover depths that are read from Consultant D's result map are in the range of 2.75 in. to 3 in. at location C1, 3 in. to 3.25 in. at location C2, and 2.75 in. to 3 in. at location C3. The comparison between the results from concrete cores and air-lauched GPR is good for the two bridges. The error is less than 0.375 in. between the two methods. As a result, air-launched GPR, which is verified by concrete cores, appears to be a very reliable and accurate method to measure the concrete cover depth.

Overall, comparing average concrete cover depth and result maps for all bridges listed in Table 4.7, a good comparison is observed for the first round of testing between the results from Consultant D, Consultant B,

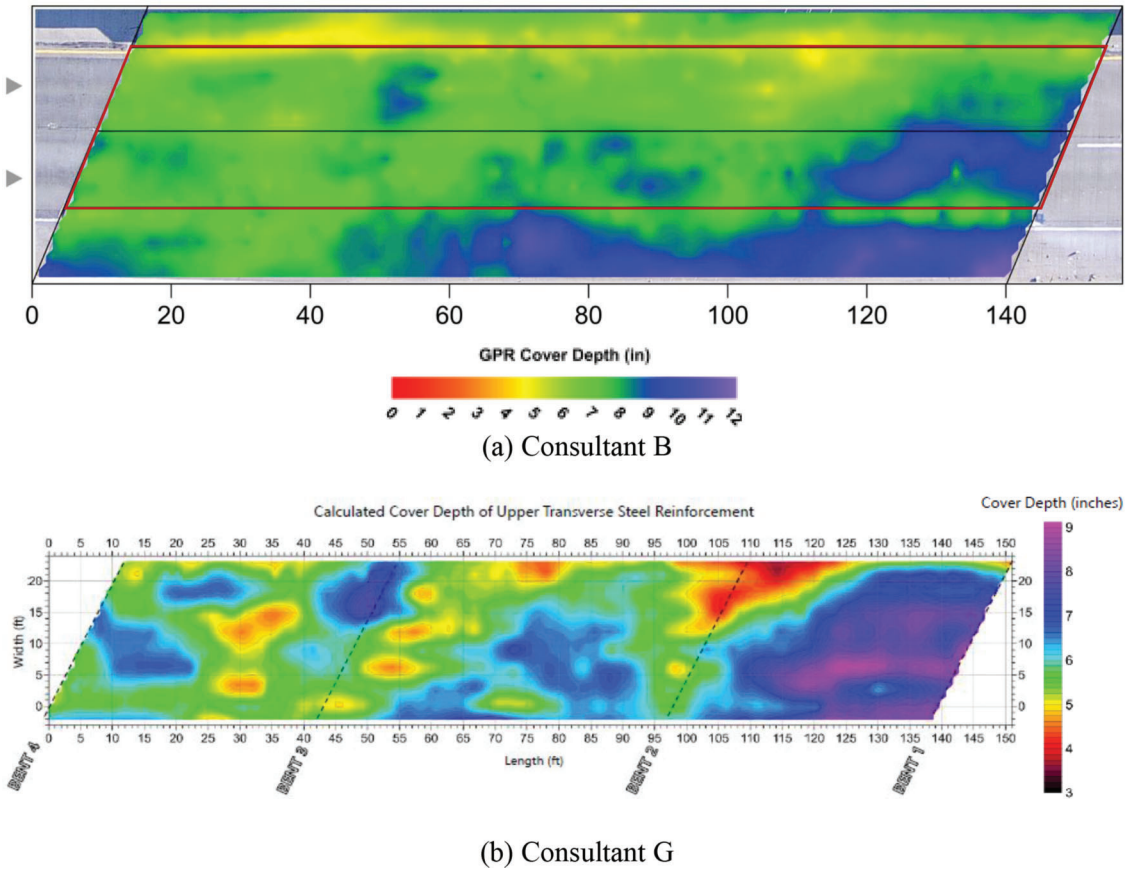

Figure 4.20 Concrete cover thickness result maps for Bridge 37100 (used with permission from consultant).

and Consultant G. The height of concrete cores above the top layer of reinforcement also matches the air-launched GPR results for two newer bridge decks. As a result, the GPR method appears to work well to measure the concrete cover depth above the top reinforcement.

4.3 Result Comparison for Different NDT Methods

In this section, test results are compared between air-launched GPR and ground-coupled GPR, air-launched GPR and IRT, IE and IRT, IE and concrete cores, and IRT and automated sounding. The reason why results between different NDT methods were compared is to determine if the various NDT methods can produce somewhat comparable results to detect delamination or deterioration. Obviously, different NDT methods measure different quantities, and some variations in results are expected.

4.3.1 Air-launched GPR vs. Ground-coupled GPR Results

Consultant B, Consultant D, Consultant F, Consultant G, Consultant H, and INDOT used air-launched or ground-coupled GPR methods to evaluate selected bridges in the two rounds of testing. Results from Consultant J are also used to compare with other GPR results. Table 4.8 summarizes the GPR results. The summation of the two most severe levels is shown in the table for the entities that divided their results into several levels of deterioration. Results from Consultant F are not shown in the table since they provided plan view maps for three different deterioration levels rather than a single distinct value.

Ground-coupled GPR is performed slower and closer to the surface of the bridge deck than air-launched GPR, so ground-coupled GPR may detect more deterioration than air-launched GPR. However, the results did not always confirm this behavior. The results for eight bridges are consistent with this expectation, but for other bridges, air-launched GPR results indicate greater percentages of deteriorated areas than ground-coupled GPR results. One of the reasons is that no standard frequency threshold for the GPR methods is used, so variations in the results may occur. Moreover, the frequency of antennas is different for air-launched GPR and ground-coupled GPR. These two factors undoubtedly affected the results.

For the map comparison, Bridge 20610 and Bridge 37100 are selected as examples to compare the results for air-launched GPR and ground-coupled GPR. Consultant D provided both a regular air-launched GPR result map and a 3D air-launched GPR result map for Bridge 20610. Consultant J used air-launched

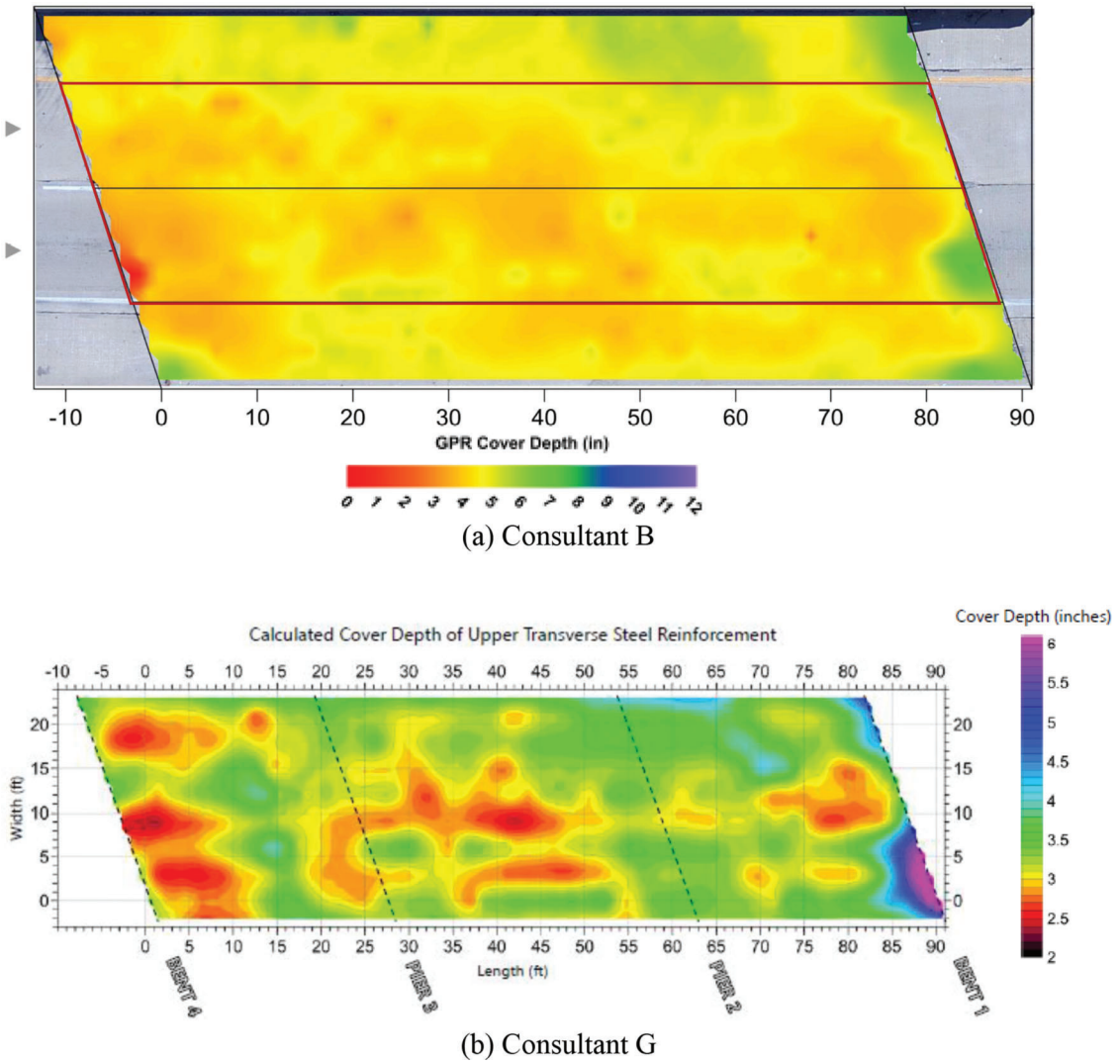

Figure 4.21 Concrete cover thickness result maps for Bridge 41810 (used with permission from consultant).

GPR to evaluate the bridge, and Consultant H and INDOT also tested this bridge by using ground-coupled GPR. Figure 4.24 shows the result maps for Bridge 20610. Similarly, Figure 4.25 shows five result maps for Bridge 37100 from Consultant D, Consultant G, Consultant J, and Consultant B.

For Bridge 20610, ground-coupled GPR result maps from Consultant H and INDOT show a large amount of deterioration that is evenly distributed over the entire bridge deck. However, air-launched GPR result maps do not indicate deterioration to the same extent. Locations of deterioration do not match between the result maps of Consultants D and J and the maps for other entities. For Bridge 37100, the result maps from each entity show different results. It is difficult to find agreement between locations and the amount of deterioration indicated by the various result maps.

Overall, the deterioration percentage of the area surveyed and the result maps for bridges listed in Table 4.8 compare poorly between entities. As a result, the GPR method was generally not found to be repeatable or reliable.

4.3.2 Air-launched GPR vs. Vehicle-mounted Infrared Thermography Results

Air-launched GPR results are compared with vehicle-mounted IRT results in this section because the equipment for both methods is truck-mounted, and the results are collected at highway speed. The air-launched GPR results are from Consultant D, Consultant G, and Consultant J. Consultant D also completed vehicle-mounted IRT testing in the first round of scanning, and Consultant E used their vehicle-mounted IRT equipment to test selected bridges in both rounds of scanning. Table 4.9 summarizes air-launched GPR results and vehicle-mounted IRT results. The summation of the two most severe levels is shown in the table for the results from Consultant G and Consultant J.

By comparing the percentage values listed in Table 4.9, the air-launched GPR results compare

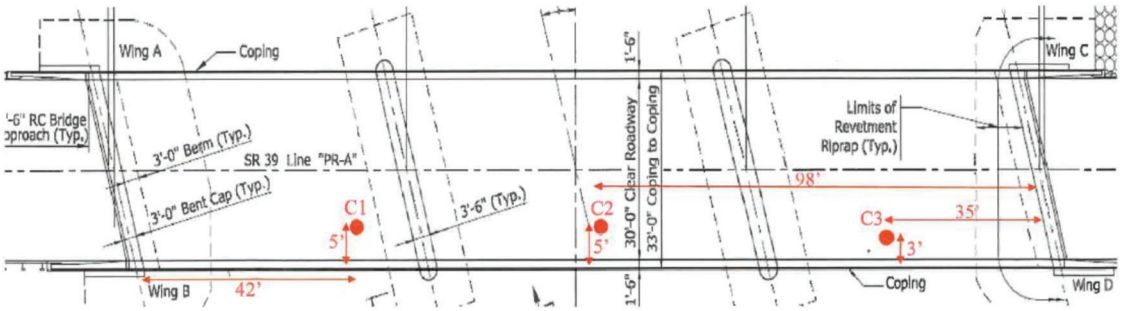

(a) Location of concrete cores

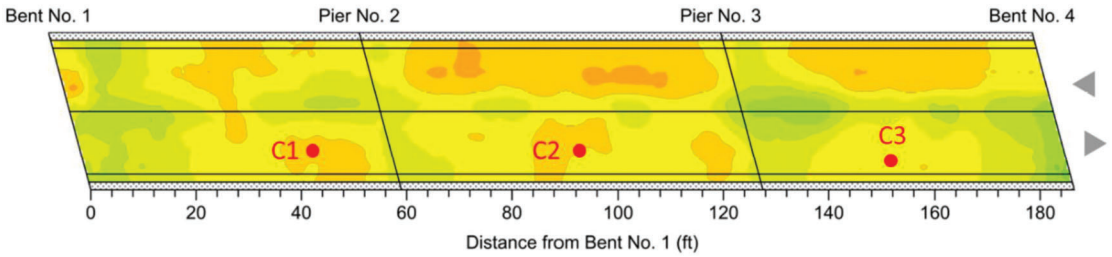

(b) Result map from Consultant D

Figure 4.22 Concrete core locations and concrete cover depth result map for Bridge 13321.

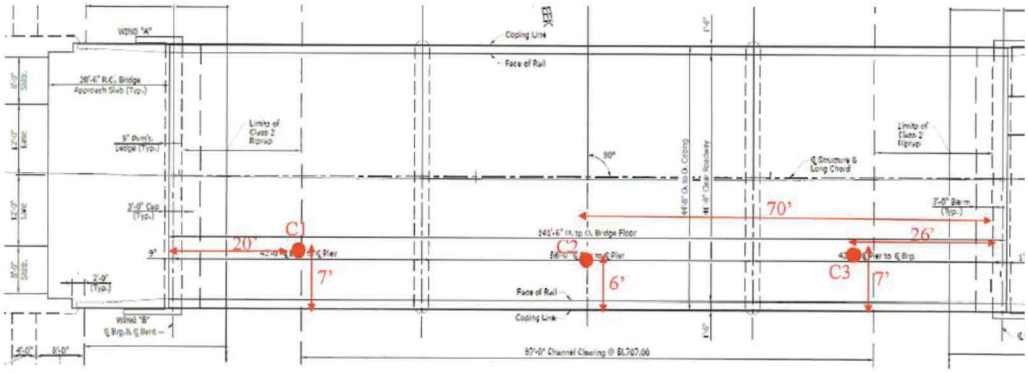

(a) Location of concrete cores

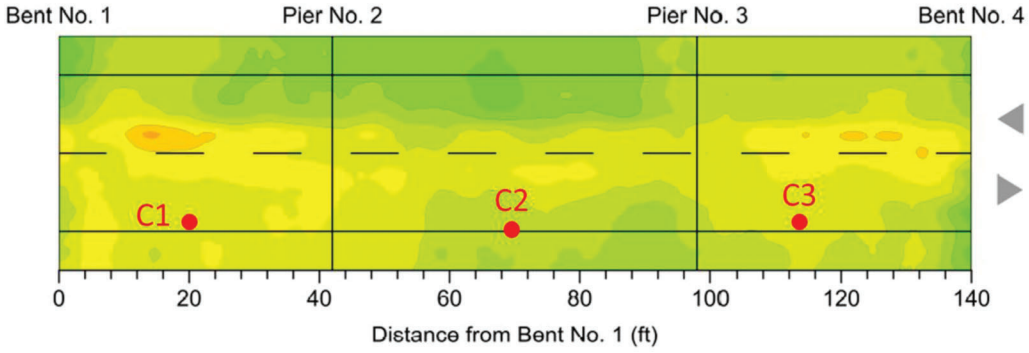

(b) Result map from Consultant D

Figure 4.23 Concrete core locations and concrete cover depth result map for Bridge 16171.

TABLE 4.8
Summary table of air-launched GPR results vs. ground-coupled GPR results

	Air-Launched GPR Deterioration (% of Area Surveyed)				Ground-Coupled GPR Deterioration (% of Area Surveyed)			
	Consultant D		Consultant G	Consultant J	Consultant D	Consultant B	Consultant H	INDOT
Structure Number	Two Antenna	3D	One Antenna	One Antenna	One Antenna	One Antenna	Multichannel	One Antenna
01310	3.1	4.7	–	–	–	–	62.0	–
01347	2.3	3.5	–	–	–	–	9.0	–
17940	9.6	16.3	–	–	–	–	10.0	–
19640	6.5	8.7	–	–	–	–	16.0	–
20610	6.5	9.1	–	2.1	–	–	66.0	44.9
49200	13.5	11.9	–	–	–	–	–	–
04845	–	10.7	–	–	–	–	13.0	–
04930	–	9.6	–	–	–	–	33.0	–
05230	2.6	–	–	–	–	–	–	–
08630	–	5.5	–	–	–	–	6.0	–
11940	3.0	–	–	–	–	–	–	–
16500	10.1	–	19.3	–	8.9	6.1	–	–
18770	1.7	–	15.8	5.6	7.2	6.3	–	–
18870	10.4	–	–	–	–	–	–	–
22690	2.0	–	22.5	2.7	1.3	5.7	–	7.9
24220	–	18.0	–	–	–	–	40.0	–
31080	5.1	–	17.7	6.6	3.0	3.8	–	–
35520	12.1	–	17.7	2.0	9.6	3.6	–	–
37070	6.8	–	13.9	1.0	9.8	21.6	–	–
37100	1.5	–	15.8	3.5	7.6	25.0	–	–
37150	3.5	–	17.9	4.7	3.2	2.6	–	–
41810	9.1	–	16.5	–	4.9	5.5	–	18.5
41870	5.9	–	13.0	3.9	5.9	7.3	–	9.0
76140	3.7	–	–	–	–	–	–	–

poorly with the vehicle-mounted IRT results. This finding is to be expected because the GPR method measures the probability of corrosion in a bridge deck, while the IRT method detects delamination. Therefore, the results from the two NDT methods are not directly comparable. However, together they provide an important picture of the behavior in the bridge deck. The GPR value and location indicates the likelihood of corrosion development, while the IRT regions indicate those areas where delamination cracking and/or separation has already occurred. The map comparisons can provide more evidence.

For the map comparison, Bridge 19640 and Bridge 31080 are selected as examples to compare the result maps for air-launched GPR and vehicle-mounted IRT. Consultant D provided air-launched GPR results and vehicle-mounted IRT results together on the same map for the first round. Blue areas show GPR results and red boxes indicate IRT results. Note that the regions of distress do not necessarily need to match. For Bridge 19640, four result maps are presented in Figure 4.26 from Consultant D and Consultant E (both rounds). Similarly, Figure 4.27 shows five result maps for Bridge 31080 from Consultant D, Consultant G, Consultant J, and Consultant E.

For both bridges, some areas do match between the GPR and the IRT results because corrosion can cause delamination in a bridge deck. A large amount of reinforcement corrosion could be present at the matching areas that led to delamination. Other areas do not match well between the result maps from different methods, which simply indicates that the two methods detect different types of deck distress in a bridge deck.

Overall, the percentage of the area surveyed and the result maps do not compare well between air-launched GPR and vehicle-mounted IRT. Therefore, other means of collecting IRT data, such as drone-mounted IRT and pole-mounted IRT, should also not be comparable with GPR results since they were found to provide comparable or greater delamination values than vehicle-mounted IRT.

4.3.3 Impact Echo vs. Infrared Thermography Results

IE results are compared with IRT results in this section. INDOT and Consultant F collected IE data, while Consultant B (drone-mounted IRT), Consultant C (drone-mounted IRT), Consultant I (pole-mounted IRT), Consultant D (vehicle-mounted IRT), and Consultant E (vehicle-mounted IRT) collected IRT data. Table 4.10 summarizes the IE

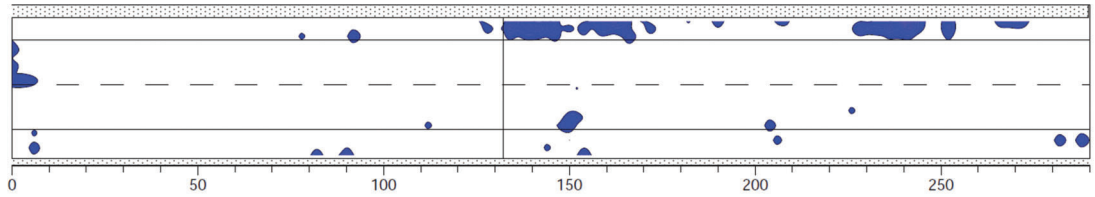

(a) Consultant D (regular air-launched GPR)

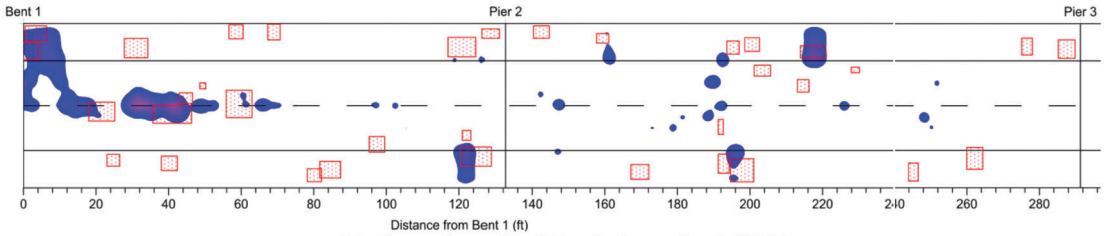

(b) Consultant D (3D air-launched GPR)

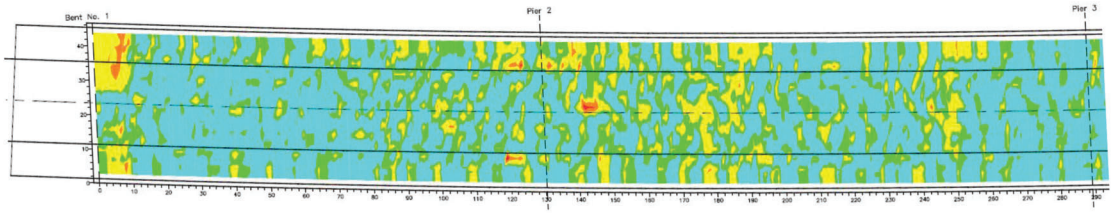

(c) Consultant J (air-launched GPR)

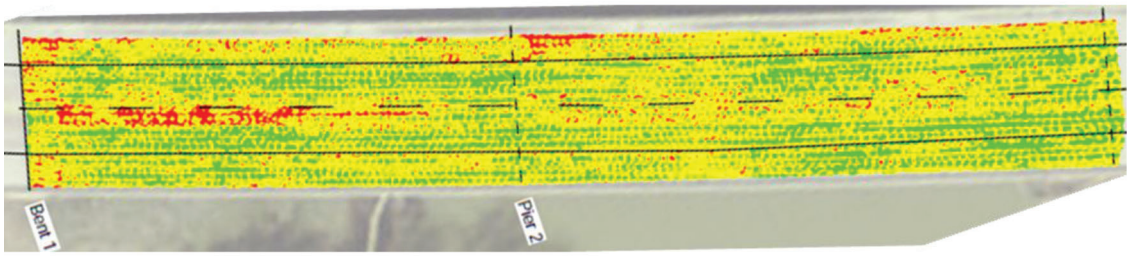

(d) Consultant H (ground-coupled MCGPR)

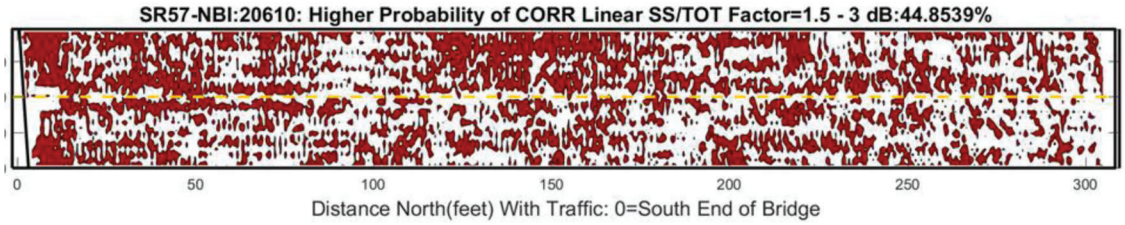

(e) INDOT (ground-coupled GPR)

Figure 4.24 GPR result maps for Bridge 20610 (used with permission from consultant).

and IRT results. A summation of the three most severe categories is shown in the table for the results from Consultant F.

By comparing the percentage values listed in Table 4.10, the IE results show a larger delamination percentage of the area surveyed than the IRT results for most bridges. The IE test is a project-level test. The equipment physically touches the surface of a bridge deck and slowly scans the deck. The vehicle-mounted IRT and drone-mounted IRT tests collect data above a bridge deck at a faster speed. The aerial IRT results are not included in this comparison because the aerial IRT detects even less delamination than other IRT methods. Therefore, more delaminated areas are detected by the IE method than by the vehicle and drone-mounted IRT methods. The pole-mounted IRT

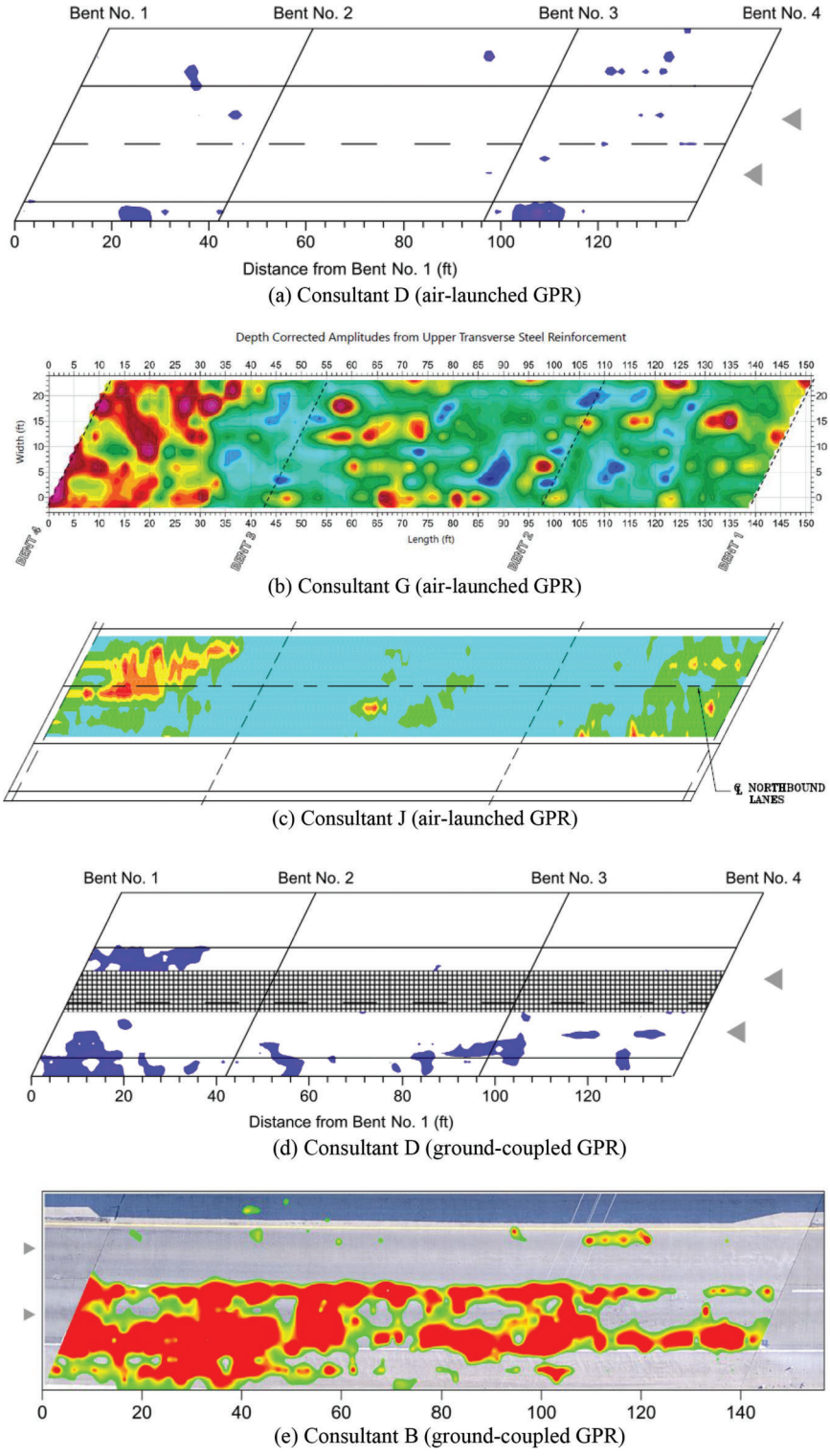

Figure 4.25 GPR result maps for Bridge 37100 (used with permission from consultant).

values were greater than the IE values for Bridge 01310 and Bridge 37070, likely because the equipment stays on the bridge deck much longer compared to other IRT methods.

For the map comparison, Bridge 19640 and Bridge 24220 are selected as examples to compare the result maps for the IE and IRT methods. For Bridge 19640, five result maps are presented in Figure 4.28 from INDOT, Consultant C, Consultant D, and Consultant E. Similarly, Figure 4.29 shows five result maps for Bridge 24220 from INDOT, Consultant F, Consultant C, Consultant I, and Consultant E.

TABLE 4.9
Summary of air-launched GPR results vs. vehicle-mounted IRT results

	Air-Launched GPR Deterioration (% of Area Surveyed)				Vehicle-Mounted IRT Delamination (% of Area Surveyed)		
	Consultant D		Consultant G	Consultant J	Consultant D	Consultant E	
Structure Number	First Round	Second Round[1]	First Round	Previous Testing	First Round	First Round	Second Round
01310	3.1	4.7	–	–	1.3	0.2	1.0
01347	2.3	3.5	–	–	1.5	0.2	4.3
17940	9.6	16.3	–	–	0.7	0.2	7.6
19640	6.5	8.7	–	–	1.4	3.3	8.6
20610	6.5	9.1	–	2.1	6.3	4.5	4.7
49200	13.5	11.9	–	–	1.6	1.1	4.5
04845	–	10.7	–	–	–	–	3.2
04930	–	9.6	–	–	–	–	2.0
05230	2.6	–	–	–	2.3	0.9	–
08630	–	5.5	–	–	–	–	1.5
11940	3.0	–	–	–	1.9	0.4	–
16500	10.1	–	19.3	–	2.9	0.8	–
18770	1.7	–	15.8	5.6	1.3	1.3	–
18870	10.4	–	–	–	2.3	0.0	–
22690	2.0	–	22.5	2.7	2.7	2.3	–
24220	–	18	–	–	–	–	3.6
31080	5.1	–	17.7	6.6	14.4	4.0	–
35520	12.1	–	17.7	2.0	0.0	0.1	–
37070	6.8	–	13.9	1.0	0.7	0.1	–
37100	1.5	–	15.8	3.5	0.0	0.4	–
37150	3.5	–	17.9	4.7	0.2	0.3	–
41810	9.1	–	16.5	–	0.0	0.2	–
41870	5.9	–	13.0	3.9	0.4	0.3	–
76140	3.7	–	–	–	1.1	0.0	–

[1]3D air-launched GPR.

By comparing the result maps, locations of delamination that are shown on IRT result maps can generally be located on result maps for the IE method. However, result maps for the IE test show much more delamination than the IRT result maps. Other comparisons between IE and IRT present the same results. Clearly, IE and IRT can both detect delamination, but IE generally provides greater detection results than the IRT methods. Hence, IRT tests, such as aerial IRT and vehicle-mounted IRT, can be used to quickly scan bridge decks to gain delamination information about a deck, but a more thorough evaluation using IE may yield a more complete picture of the delamination condition.

Overall, the percentages of the area surveyed are not comparable between the two methods, but the result maps show similarities in terms of the locations of delamination. The principles and setups of the two methods are distinct, so the results are often different. The IE method can be used to collect precise delamination results with fewer interferences, and IRT is good for rapid testing.

4.3.4 Infrared Thermography vs. Automated Sounding Results

IRT results are compared with automated sounding results in this section. Consultant A and Consultant B collected the automated sounding data, while Consultant B (drone-mounted IRT), Consultant C (drone-mounted IRT), Consultant I (pole-mounted IRT), Consultant D (vehicle-mounted IRT), and Consultant E (vehicle-mounted IRT) collected the IRT data. Table 4.11 summarizes the automated sounding and IRT results. The summation of the two most severe levels is shown in the table for the results from Consultant B.

By comparing the percentage values listed in Table 4.11, the automated sounding results show a lower delamination percentage of the area surveyed than the IRT results for 15 bridges. Another five bridges have minor delamination indicated by both methods. They all agree that Bridge 24220 is in the most severe condition compared to other bridges.

For the map comparison, Bridge 22690 and Bridge 41810 are selected as examples to compare the result maps for the automated sounding and IRT methods. For Bridge 22690, five result maps are presented in Figure 4.30 from Consultant B, Consultant A, Consultant D, and Consultant E. Similarly, Figure 4.31 shows five result maps for Bridge 41810 from the same entities.

For Bridge 22690, a few locations of delamination that are shown on the automated sounding result maps can also be located on result maps from the

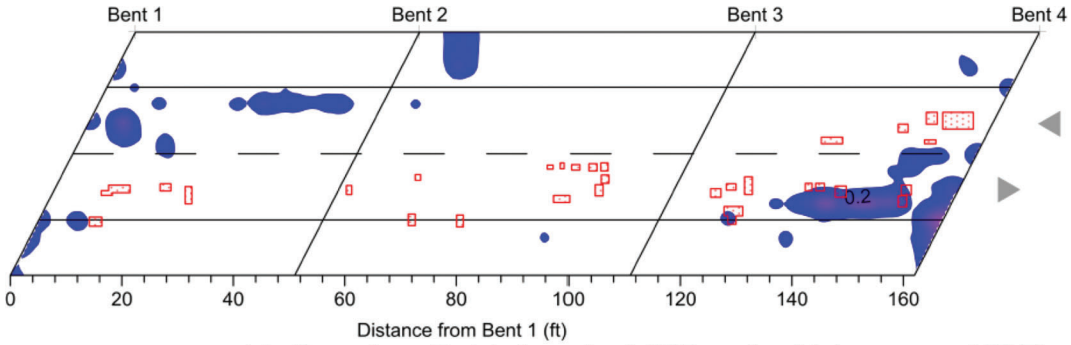

(a) Consultant D (air-launched GPR and vehicle-mounted IRT)

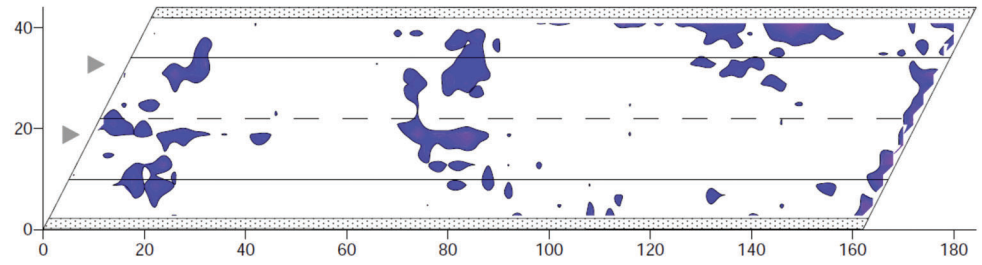

(b) Consultant D (3D air-launched GPR)

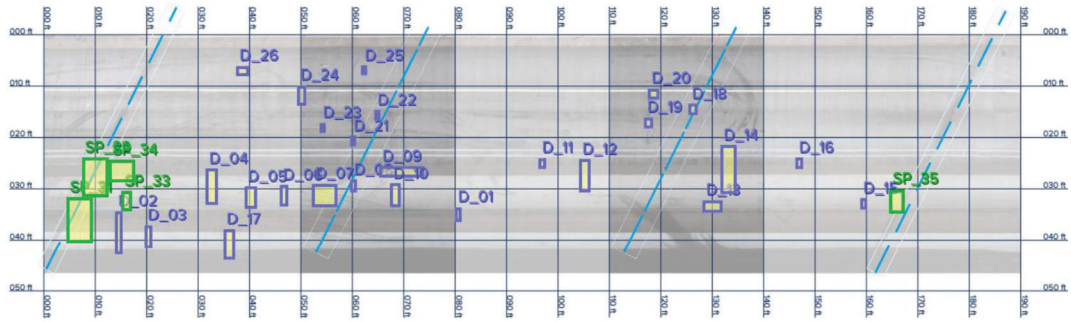

(c) Consultant E (first round vehicle-mounted IRT)

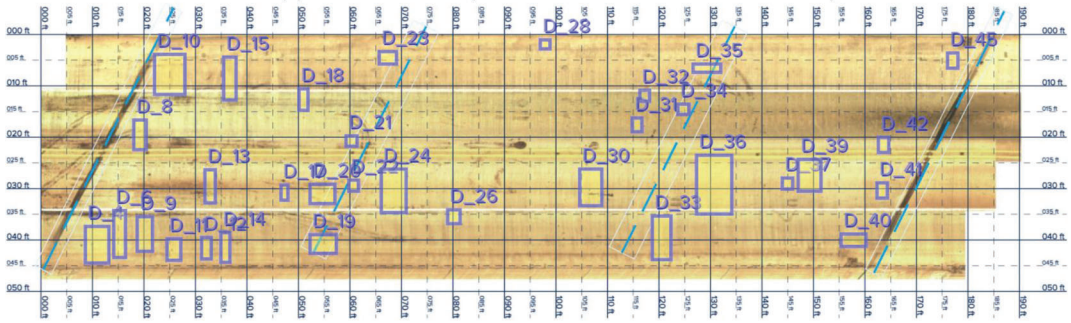

(d) Consultant E (second round vehicle-mounted IRT)

Figure 4.26 Air-launched GPR and vehicle-mounted IRT result maps for Bridge 19640 (used with permission from consultant).

IRT method, but most of the delaminated areas do not match. For Bridge 41810, result maps from automated sounding show more delamination than IRT result maps, but both methods indicate that there is little delamination present in the deck. Other comparisons between automated sounding and IRT present similar results, except with IRT results sometimes indicating more delamination than automated sounding results. It should be noted that results from Consultant A generally compare more favorably with the IRT results than results from Consultant B.

Overall, the automated sounding test usually results in lower detected delamination percentage values than

TABLE 4.10
Summary table of IE results vs. vehicle-mounted IRT results

	IE Delamination (% of Area Surveyed)			IRT Delamination (% of Area Surveyed)					
	INDOT			Consultant F	Consultant B	Consultant C	Consultant I	Consultant D	Consultant E
Structure Number	First Round	Second Round	Second Round	Drone-Mounted IRT	Drone-Mounted IRT	Pole-Mounted IRT	Vehicle-Mounted IRT	Vehicle-Mounted IRT[1]	Vehicle-Mounted IRT[2]
01310	–	16.0	20.4	–	5.5	24.0	1.3	0.2	1.0
01347	–	5.1	3.5	–	<0.1	2.0	1.5	0.2	4.3
04845	–	7.9	1.8	–	<0.1	–	–	–	3.2
04930	–	35.0	29.5	–	7.1	–	–	–	2.0
08630	–	12.0	–	–	1.3	–	–	–	1.5
16500	0.7	–	–	0.0	–	–	2.9	0.8	–
17940	–	4.8	–	–	2.2	–	0.7	0.2	7.6
18770	2.2	–	–	0.0	–	–	1.3	1.3	–
19640	–	14.0	–	–	5.0	–	1.4	3.3	8.6
20610	–	13.1	–	–	2.9	–	6.3	6.3	4.7
22690	9.6	–	–	1.4	–	–	2.7	2.3	–
24220	–	36.0	38.0	–	3.6	15.0	–	–	3.6
31080	19.5	–	–	5.7	–	–	14.4	4.0	–
35520	0	–	–	0.0	–	–	0.0	0.1	–
37070	3.8	–	–	0.0	–	6.0	0.7	0.1	–
37100	13.5	–	–	0.0	–	–	0.0	0.4	–
37150	7.5	–	–	0.0	–	–	0.2	0.3	–
41810	8.2	–	–	0.4	–	–	0.0	0.2	–
41870	3.8	–	–	0.2	–	–	0.4	0.3	–

[1]First round of testing.
[2]Second round of testing.

the IRT test. Furthermore, the map comparisons between the two methods generally do not compare well.

4.3.5 Impact Echo vs. Automated Sounding Results

Comparisons made in Section 4.3.3 and 4.3.4 show that the IE method detects greater delamination levels than the IRT method, and the IRT method usually detects more than the automated sounding method. Therefore, if comparing the results from IE and automated sounding, the automated sounding method would usually detect far less delamination than IE. The comparison of the results provide evidence that the automated sounding method is not as sensitive as the other two methods for detecting delamination.

4.3.6 Impact Echo vs. Concrete Coring Results

Concrete cores were extracted from four bridges to confirm the IE results. In the first round of testing, Bridge 22690 and Bridge 41870 were selected for concrete core testing. Four random locations were chosen on each bridge. The diameter of the cores was 3 in. For Bridge 22690, the four locations are shown in Figure 4.32, with the cores taken to an average depth of 7 in. The four concrete cores were found to be in good condition, which matches the IE results. Figure 4.33 shows the core locations for Bridge 41870, with the cores taken to an average depth of 6 in. Concrete core C1 had a vertical crack that extended from the top of the core, and the other three cores were in good condition. According to the IE results for Bridge 41870, no delamination was expected at the four locations. It should be noted that the IE test is not expected to detect vertical cracks. Photos of the concrete cores are provided in Appendix B.

For the second round of testing, Bridge 20610 and Bridge 24220 were selected for concrete core testing. Rather than selecting random core locations, the three concrete cores were extracted from each deck at the location of a delamination indicated by IE results. The diameter of the concrete cores was 4 in., and the cores were taken to an average depth of 6.5 in. Figure 4.34 and Figure 4.35 show the locations of concrete cores on the IE result maps for Bridge 20610 and Bridge 24220, respectively. For Bridge 20610, an overlay was added on the deck 26 years ago, and debonding was found on core DS2 and DS3. DS1 shows delamination close to the overlay. For Bridge 24220, the three cores revealed delamination at the top reinforcing bar level. All cores proved that there was delamination or debonding at the locations that were indicated on the IE result map. Photographs of the concrete cores are shown in Appendix B.

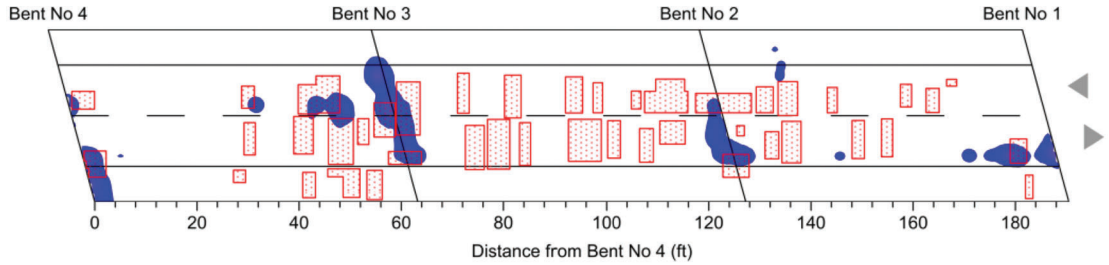

(a) Consultant D (air-launched GPR and vehicle-mounted IRT)

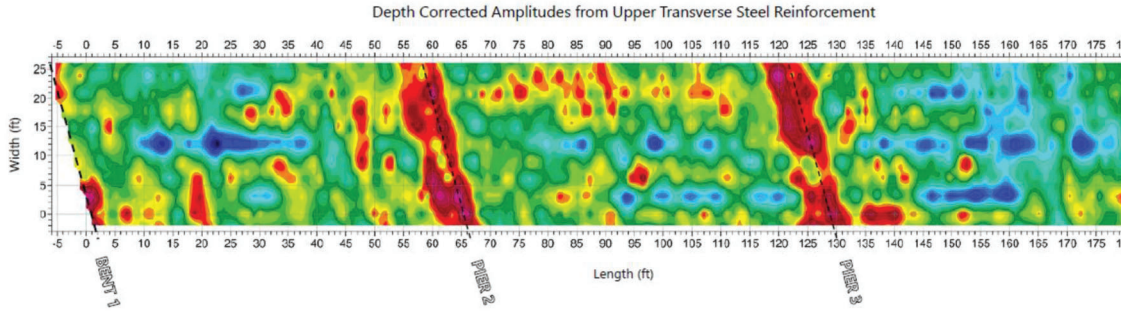

(b) Consultant G (air-launched GPR)

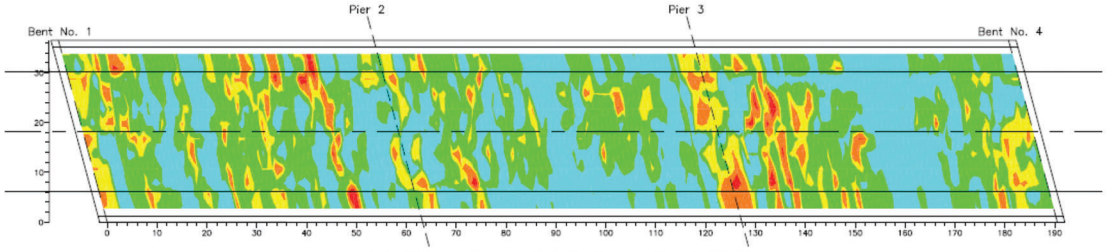

(c) Consultant J (air-launched GPR)

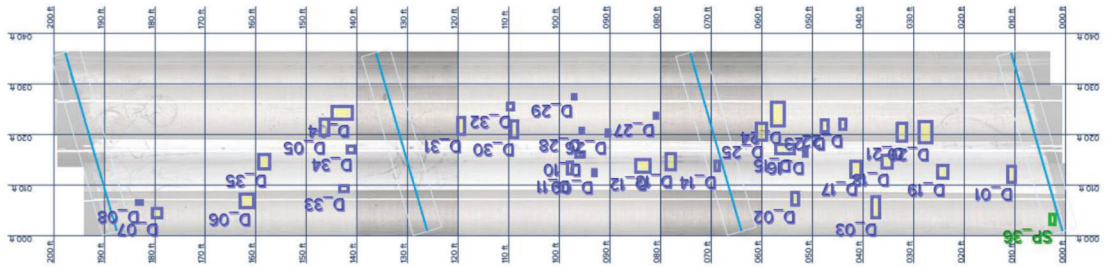

(d) Consultant E (first round vehicle-mounted IRT)

Figure 4.27 Air-launched GPR and vehicle-mounted IRT result maps for Bridge 31080 (used with permission from consultant).

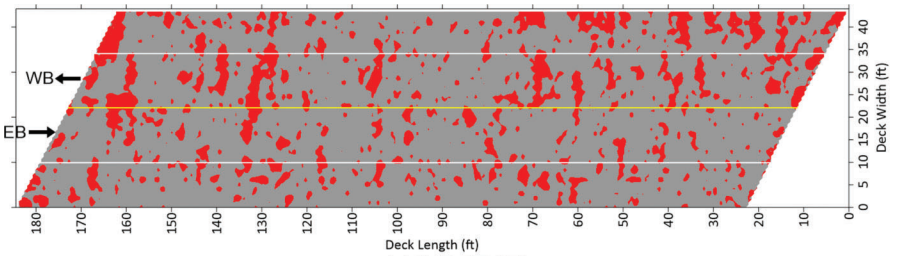

(a) INDOT (IE)

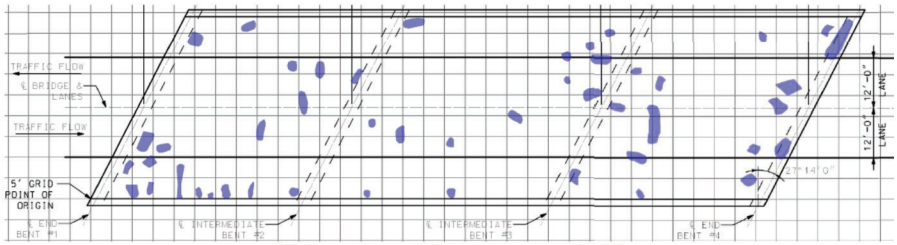

(b) Consultant C (drone-mounted IRT)

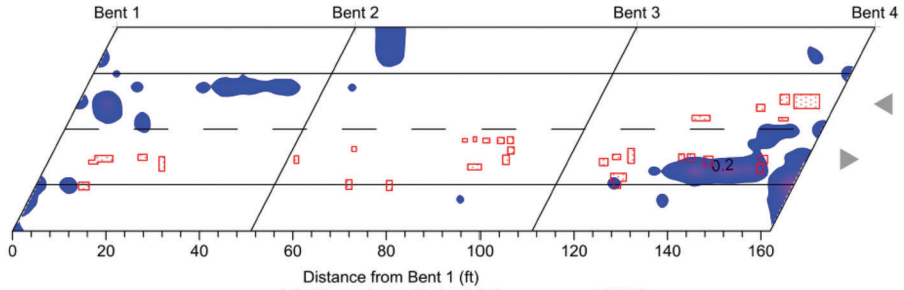

(c) Consultant D (vehicle-mounted IRT)

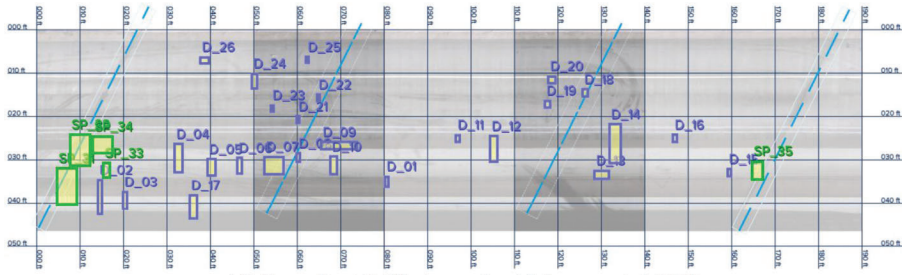

(d) Consultant E (first round vehicle-mounted IRT)

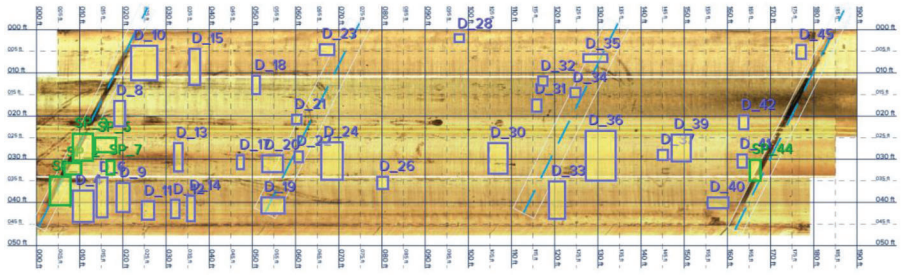

(e) Consultant E (second round vehicle-mounted IRT)

Figure 4.28 IE and IRT result maps for Bridge 19640.

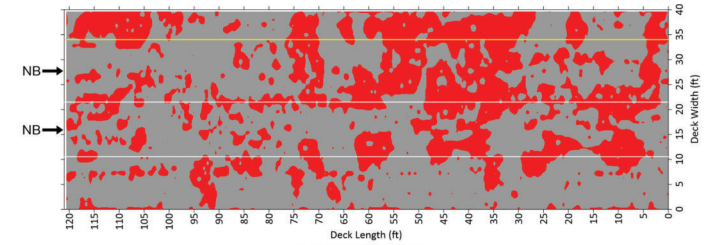

(a) INDOT (IE)

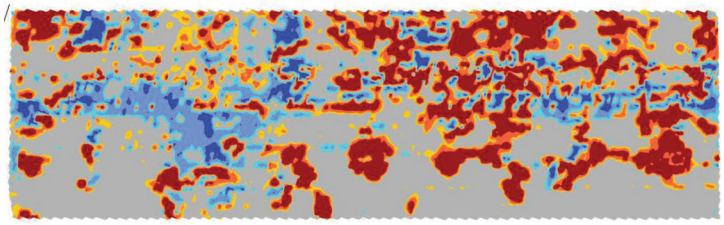

(b) Consultant F (IE)

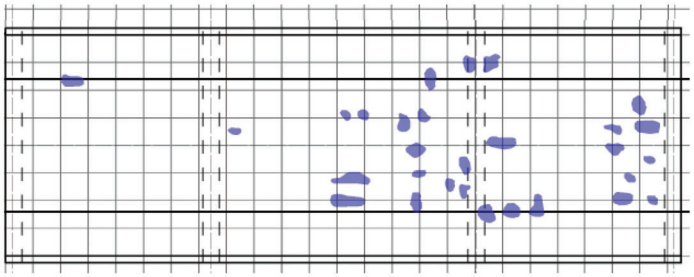

(c) Consultant C (drone-mounted IRT)

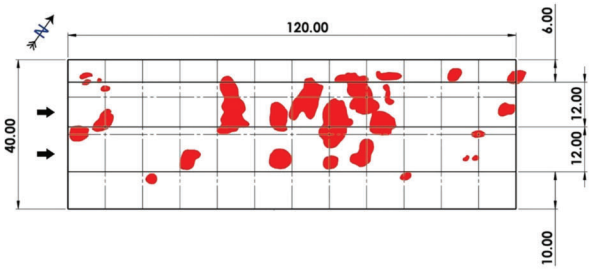

(d) Consultant I (pole-mounted IRT)

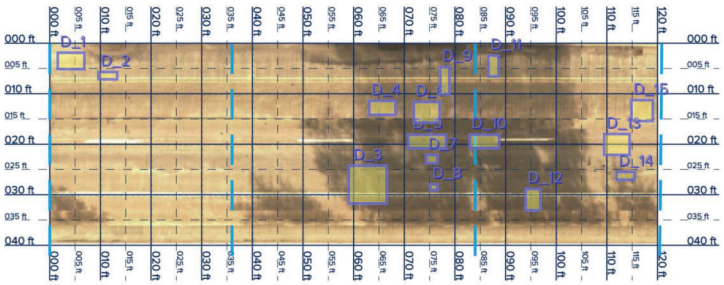

(e) Consultant E (second round vehicle-mounted IRT)

Figure 4.29 IE and IRT result maps for Bridge 24220 (used with permission from consultant).

TABLE 4.11
Summary table of automated sounding results vs. vehicle-mounted IRT results

	Automated Sounding Delamination (% of Area Surveyed)		IRT Delamination (% of Area Surveyed)					
	Consultant B	Consultant A	Consultant B	Consultant C	Consultant I	Consultant D	Consultant E	
Structure Number	First Round	Second Round	Drone-Mounted IRT	Drone-Mounted IRT	Pole-Mounted IRT	Vehicle-Mounted IRT	Vehicle-Mounted IRT[1]	Vehicle-Mounted IRT[2]
01310	–	0.4	–	5.5	24.0	1.3	0.2	1.0
01347	–	0.1	–	<0.1	2.0	1.5	0.2	4.3
04845	–	0.2	–	<0.1	–	–	–	3.2
04930	–	0.6	–	7.1	–	–	–	2.0
08630	–	0.0	–	1.3	–	–	–	1.5
16500	0.3	0.0	0.0	–	–	2.9	0.8	–
17940	–	0.0	–	2.2	–	0.7	0.2	7.6
18770	0.3	0.0	0.0	–	–	1.3	1.3	–
19640	–	3.9	–	5.0	–	1.4	3.3	8.6
20610	–	3.4	–	2.9	–	6.3	6.3	4.7
22690	0.4	2.9	1.4	–	–	2.7	2.3	–
24220	–	5.4	–	3.6	15.0	–	–	3.6
31080	1.5	–	5.7	–	–	14.4	4.0	–
35520	0.4	0.0	0.0	–	–	0.0	0.1	–
37070	0.2	0.0	0.0	–	6.0	0.7	0.1	–
37100	0.2	1.3	0.0	–	–	0.0	0.4	–
37150	0.4	1.8	0.0	–	–	0.2	0.3	–
41810	1.5	0.9	0.4	–	–	0.0	0.2	–
41870	0.1	1.2	0.2	–	–	0.4	0.3	–
49200	–	1.1	–	5.1	5.0	1.6	1.1	4.5

[1]First round of testing.
[2]Second round of testing.

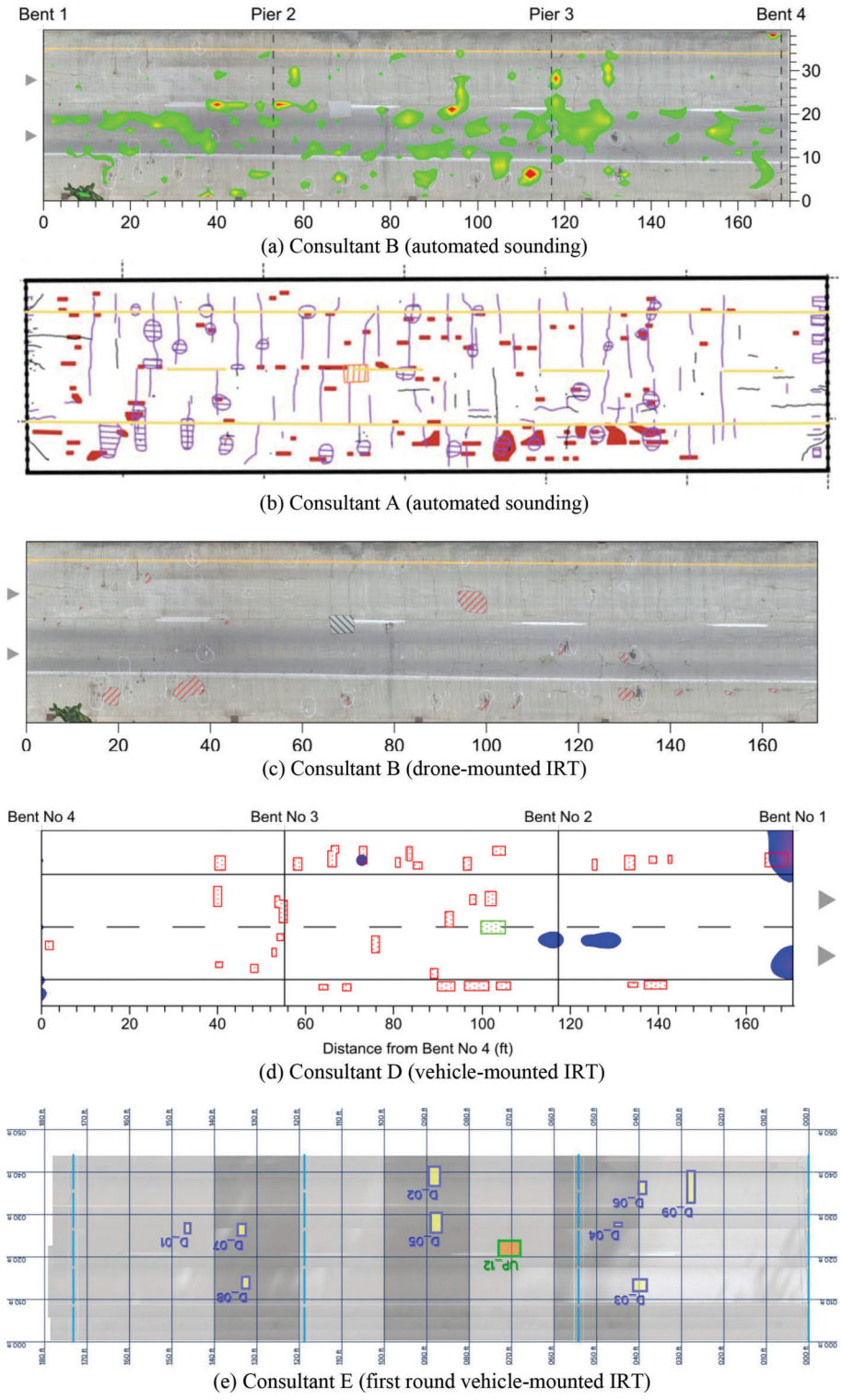

Figure 4.30 Automated sounding and IRT result maps for Bridge 22690 (used with permission from consultant).

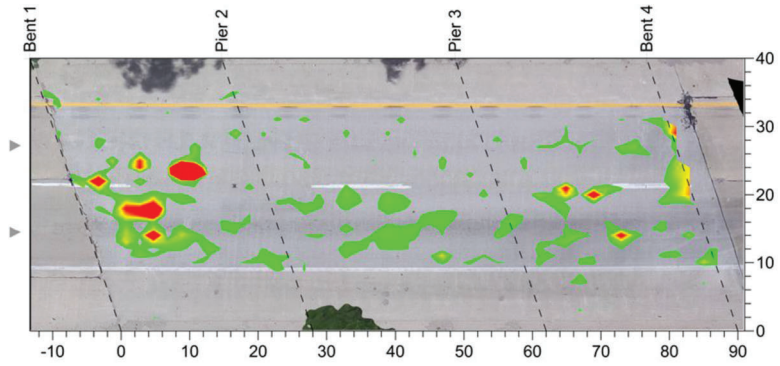

(a) Consultant B (automated sounding)

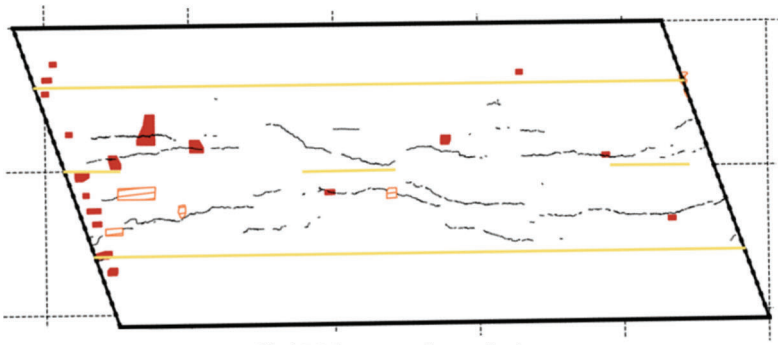
(b) ADI (automated sounding)

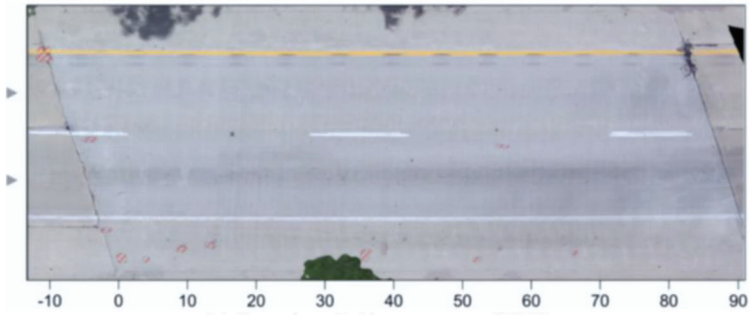

(c) Consultant B (drone-mounted IRT)

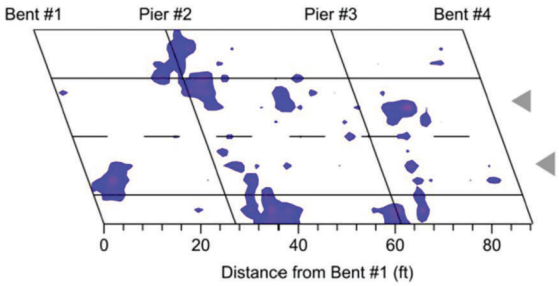

(d) Consultant D (vehicle-mounted IRT)

Figure 4.31 Continued on next page.

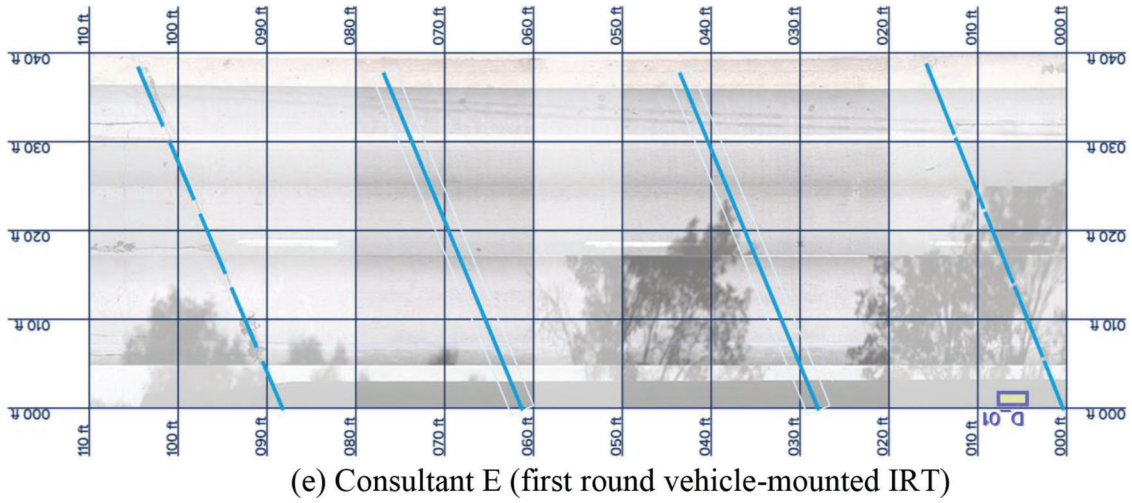

Figure 4.31 (Continued) Automated sounding and IRT result maps for Bridge 41810 (used with permission from consultant).

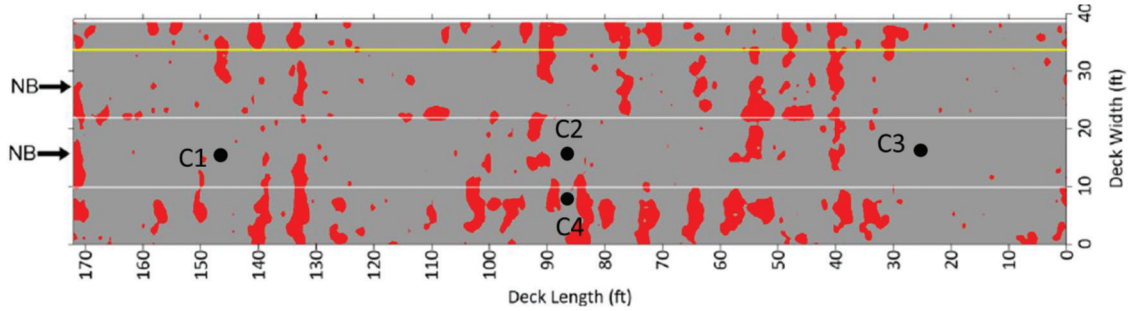

Figure 4.32 Concrete core locations on IE result map for Bridge 22690.

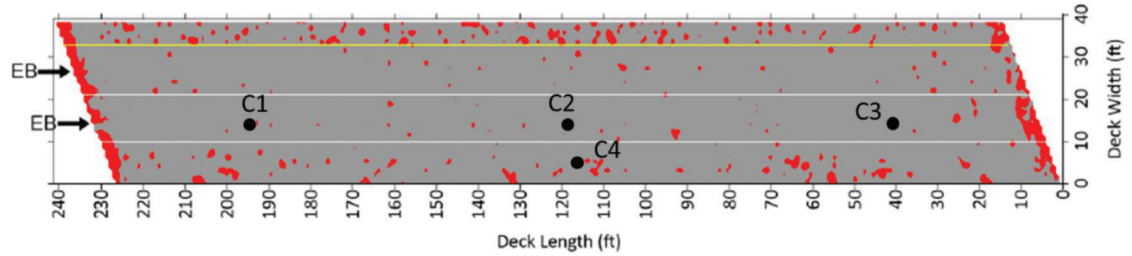

Figure 4.33 Concrete core locations on IE result map for Bridge 41870.

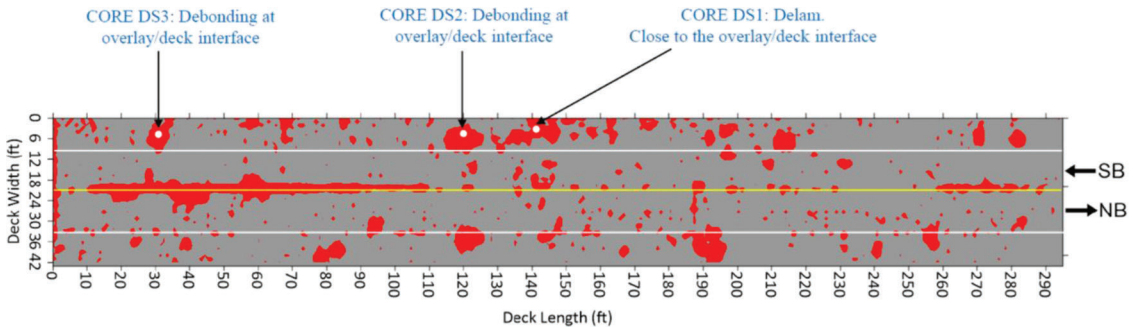

Figure 4.34 Concrete core locations on IE result map for Bridge 20610.

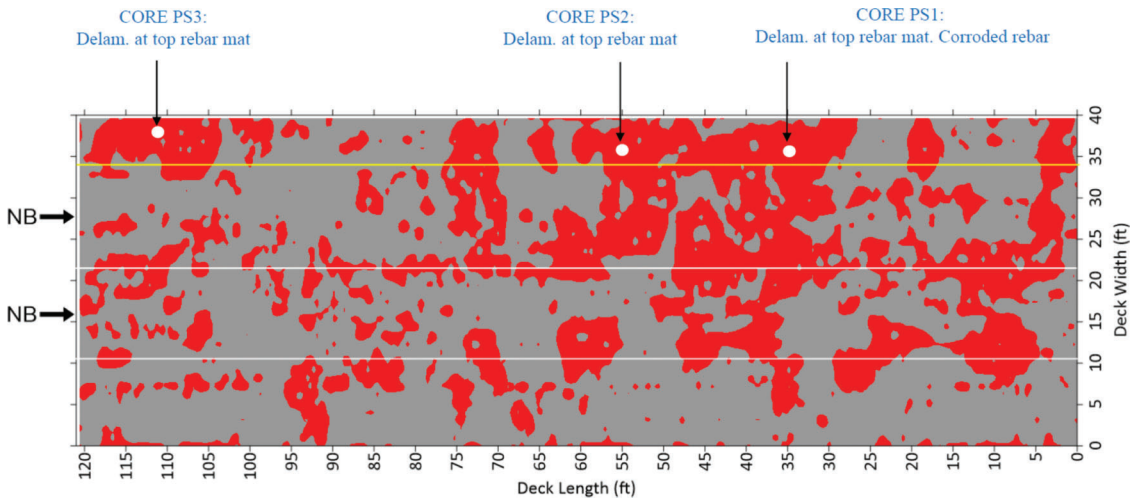

Figure 4.35 Concrete core locations on IE result map for Bridge 24220.

5. SUMMARY AND RECOMMENDED NDT BRIDGE DECK INSPECTION PROCEDURES

In this chapter, a summary of the findings on NDT effectiveness and recommendations on future network-level and project-level NDT testing are provided. The findings and recommendations are limited to the NDT methods that were considered during this research. Other NDT methods may be valuable, but they are not included in this evaluation.

5.1 Evaluation of NDT Methods

A total of ten different entities were involved in this research to provide NDT test results for 106 bridges. GPR, IRT, IE, and automated sounding methods were performed, and the results were compared between different entities and methods. A general summary of the findings of those comparisons is provided below.

- Impact echo (IE) results compare reasonably well, and the method was found to be repeatable. Selective concrete cores extracted from some of the bridge decks uniformly confirmed the IE results. IE is recommended as a project-level test for future NDT testing to detect delamination discontinuities in bridge decks.
- Infrared Thermography (IRT) results for delamination detection were found to be somewhat comparable between entities. However, it was also determined that the IRT method can be affected by shaded deck areas, moisture, and small temperature differences. Percentage delamination values detected by IRT were routinely less than those found by IE, but they were greater than the values from automated sounding for most bridges. Vehicle-mounted or aerial IRT is recommended for network-level testing, and pole-mounted IRT is recommended for project-level testing for bridges with high traffic.
- Ground-penetrating radar (GPR) was used to both detect the concrete cover thickness above the top reinforcement and assess the condition of the bridge deck.
  - Both air-launched GPR and ground-coupled GPR were found to be very effective in detecting the location of the top layer of reinforcement and determining the amount of concrete cover for the top reinforcement layer. Either method is suitable for verifying the concrete cover of a bridge deck.
  - Bridge deck deterioration results detected by both air-launched and ground-coupled GPR were found to have significant variations in both values and locations. Therefore, the method is not believed to be consistently repeatable, and is not recommended as a sole method to evaluate bridge deck condition. Nevertheless, it is believed that it can provide valuable information about the possible likelihood of corrosion activity in a bridge deck and is useful when combined with other NDT information such as IRT or IE.
- Automated sounding results were found to provide low delamination detection values compared to other methods. Only two entities were used for the testing, and the areas of delamination indicated by one of the entities were usually greater than the values indicated by the other.

5.2 Network-Level Testing

In this research, air-launched GPR, vehicle-mounted IRT, drone-mounted IRT, aerial IRT, and automated sounding methods are considered for network-level testing. Based on the comparisons in Chapter 4, aerial IRT, vehicle-mounted IRT, and air-launched GPR are recommended for future testing.

Aerial IRT is a good method to scan a large number of bridges in a short period of time. By flying over the bridges along a selected route or corridor, information on the bridge deck condition with respect to delamination can be gathered rather quickly. If significant delamination activity as a percentage of the deck area, such as greater than 5% to 8%, is detected for a particular bridge based upon this initial aerial IRT screening, then follow-up scanning using a vehicle-mounted IRT camera together with an air-launched

GPR unit will provide additional information on the delamination percentage and the probability of future corrosion activity.

Vehicle-mounted IRT is recommended for follow-up, as needed, since it can detect more delamination than aerial IRT and automated sounding based on the comparisons in Chapter 4. Vehicle-mounted IRT data are collected at highway speeds without traffic control, so the cost and time efficiency are better than using drone-mounted IRT. Air-launched GPR can be used with the vehicle-mounted IRT because the GPR method is able to detect the probability of corrosion, and a significant amount of corrosion will cause delamination. Using two NDT methods together helps to identify delamination at the top reinforcing bar level.

This information will provide bridge inspectors additional input on the bridge deck condition to consider in future inspections and data for the asset engineers that will be useful for possible future programming of work actions. If a large amount (greater than 20%) of delamination is detected by aerial IRT, or by follow-up inspection, then more sensitive project-level NDT tests, such as IE, can be considered for collecting detailed delamination data.

Lastly, the cost per bridge for aerial IRT testing is much less than other network-level testing methods explored herein. As a result, aerial IRT is recommended for the initial network-level NDT scanning, with follow-up network-level vehicle-mounted scanning by IRT and air-launched GPR on selected bridges. It is also recommended, however, that a follow-up study be conducted to directly compare aerial IRT and truck-mounted IRT. At least 50 bridges should be scanned to further assess the sensitivity of both methods and their ability to detect bridge deck delaminations. The current study, unfortunately, only had a few such comparisons and additional data would be useful.

5.3 Project-Level Testing

In this study, project-level NDT testing was carried out using ground-coupled GPR, pole-mounted IRT, and IE methods. To confirm the delamination that the IE method identified, concrete cores were also extracted. The following NDT methods are recommended for assessing bridge decks with various testing requirements for future project-level testing.

IE was found to be a reliable method to detect bridge deck delamination. IE was found to be able to detect greater delamination deterioration than IRT and automated sounding methods. IE results from different entities matched well; therefore, the method was found to be repeatable. Concrete cores also were found to verify the IE results, further indicating that the IE method is reliable. Consequently, IE is recommended as the preferred project-level test for delamination detection in bridge decks. It is recommended that selected cores be used in subsequent testing to confirm the IE findings.

Another method that can produce good delamination detection results is the use of the pole-mounted IRT system. Compared to other IRT methods, more data can be collected when using the pole-mounted IRT equipment since it monitors the bridge deck over a much longer time period. It can be set up on a bridge deck with minimal disruption to traffic, and it can gather data for extended periods of time without the need for traffic control. Therefore, the pole-mounted IRT method is believed to be ideal for monitoring bridge decks that carry very high-traffic volumes.

6. CONCLUSIONS

The goal of this research was to assess the reliability of NDT test results, evaluate their applicability in determining the condition of bridge decks, and provide recommendations for network- and project-level inspections. Based upon the NDT results, the following are the conclusions regarding NDT inspection and INDOT Strategic Goals.

- For network-level bridge deck inspection, it is recommended that a stepped screening process be used. The first step would be to use aerial IRT to monitor a number of bridges along a given corridor, such as an interstate or US Highway. The scanning can be completed rather quickly and will provide initial information on delamination content that will indicate if a problem exists or not for some of the bridges along the corridor. If a large delamination content is detected in a particular bridge, such as great than 5% to 8%, then the second step would be to conduct a follow-up NDT inspection using vehicle-mounted scanning of only the problematic bridges at highway speeds using IRT and air-launched GPR. This scan will provide information about both the delamination content and the potential for corrosion based on the chloride penetration, which affects the GPR signal. A possible third step would be to recommend a more thorough NDT inspection of selected bridges using IE if the delamination content from the vehicle-mounted scan indicates a delamination content above 20%.
- For project-level bridge deck inspection, it is recommended that the primary bridge deck inspection be conducted using IE to determine the delamination content in the deck. The IE method was found to be the most sensitive and accurate of the NDT methods explored in the study. It is reliable and repeatable. Additional verification can be obtained by using concrete cores to check on the delaminated regions that were detected by IE. A secondary project-level NDT test that can be employed would be the use of pole-mounted IRT equipment. The pole-mounted IRT system is a good choice for collecting NDT data from bridges where a very high traffic volume is carried by the bridge. The pole-mounted IRT system can be installed in about one hour and is then left in-place and collects NDT data over the span of about two days. It should be mentioned that other monitoring of a bridge deck may also be chosen to complement the above two NDT methods. These additional tests could include concrete cores along with a chloride-ion penetration test, manual chain dragging, or hammer sounding.

- The research in this study impacts the INDOT Strategic Goals related to *Innovation & Technology* and *Asset Sustainability*. INDOT (2019) indicates that Innovation and Technology involves methods that, "harness technology and innovation to develop more effective transportation solutions," while Asset Sustainability involves methods that can, "enhance ability to manage and maintain assets throughout their life cycle." Nondestructive testing is used to evaluate the condition of bridge decks. This information is used to complement other information that bridge inspectors and asset engineers have traditionally used such as the wearing surface condition and the age of the bridge deck. Nondestructive testing uses the latest in the state-of-the-art of inspection technology to look inside the decks to help assess their condition and assist in future planning of work actions. By developing strategies for both network-level and project-level NDT testing, the product of this research is able to help preserve the valuable asset of bridge decks and plan for future work in a cost-effective fashion.

REFERENCES

ASTM. (2008). *Standard test method for evaluating asphalt-covered concrete bridge decks using ground penetrating radar* (ASTM D6087). ASTM International.

Gucunski, N., Imani, A., Romero, F., Nazarian, S., Yuan, D., Wiggenhauser, H., Shokouhi, P., Taffe, A., & Kutrubes, D. (2013). *Nondestructive testing to identify concrete bridge deck deterioration* (SHRP 2 Report S2-R06A-RR-1). Transportation Research Board.

Harris, D. (2021). *Bridge deck GPR testing report NBI #4845 SR-18* [Unpublished manuscript]. Indiana Department of Transportation.

INDOT. (2019). *Indiana Department of Transportation 2019 strategic plan*. https://www.in.gov/indot/files/INDOT StrategicPlan.pdf

Maierhofer, C., Arndt, R. W., Röllig, M., Rieck, C., Walther, A., Scheel, H., & Hillemeier, B. (2006). Application of impulse-thermography for non-destructive assessment of concrete structures. *Cement and Concrete Composites*, *28*(2006), 393–401.

Maierhofer, C., Brink, A., Röllig, M., & Wiggenhauser, H. (2002, June). Transient thermography for structural investigation of concrete and composites in the surface near region. *Infrared Physics and Technology*, *43*(3–5), 271–278. https://doi.org/10.1016/S1350-4495(02)00151-2

Maierhofer, C., Krause, M., Mielentz, F., Streicher, D., Milmann, B., Gardei, A., Kohl, C., Wiggenhauser, H. (2004). Complementary application of radar, impact-echo, and ultrasonics for testing concrete structures and metallic tendon ducts. *Transportation Research Record: Journal of the Transportation Research Board*, *1892*(1), 170–177.

Maser, K., & Bernhardt, M. (2000). *Statewide bridge deck survey using ground penetrating radar* (pp. 31–37). Structural Materials Technology Conference IV, Atlantic, New Jersey.

Romero, F. A., & Roberts, R. L. (2002). The evolution in high-resolution ground penetrating radar surveys from ground-coupled to high-speed, air-coupled evaluations. *Proceedings of the Structural Materials Technology V: An NDT Conference*.

Sansalone, M., & Carino, N. J. (1989). Detecting delaminations in concrete slabs with and without overlays using the impact-echo method. *ACI Materials Journal*, *86*(2), 175–184.

Taylor, B. R., Qiao, Y., Bowman, M. D., & Labi, S. (2016). *The economic impact of implementing nondestructive testing of reinforced concrete bridge decks in Indiana* (Joint Transportation Research Program, Publication No. FHWA/IN/JTRP-2016/20). West Lafayette, IN: Purdue University. https://doi.org/10.5703/1288284316343

Taylor, B., Qiao, Y., Bowman, M., & Labi, S. (2018). Feasibility of long-term NDT programme for system-wide monitoring of bridge deck condition. *Infrastructure Asset Management*, *5*(3), 105–117. https://doi.org/10.1680/jinam.17.00034

APPENDICES

Appendix A. Bridge Information

Appendix B. Percentage Results of Testing

Appendix C. Result Maps of Testing

APPENDIX A. BRIDGE INFORMATION

Appendix A contains detailed bridge information corresponding to NL and PL testing, aerial IRT testing, and new bridges for measuring concrete cover thickness above the top layer of reinforcement.

Table A.1 Detailed Bridge Information for NL and PL Testing Bridges

Structure Number	Bridge Number	District	Latitude	Longitude	Superstructure Type	Number of Spans
1310	003-02-04023 ASBL	Fort Wayne	41.2372	-85.167297	Concrete continuous	3
1347	003-57-02566 SBL	Fort Wayne	41.35623	-85.22149	Prestressed concrete continuous	3
4845	018-27-05803 EBL	Fort Wayne	40.55676	-85.64712	Steel continuous	3
4930	018-38-05997 A	Fort Wayne	40.54409	-84.99772	Prestressed concrete	3
5230	020-64-01010 B	LaPorte	41.59126	-87.196327	Steel continuous	5
8630	030-92-03776 BEBL	Fort Wayne	41.17771	-85.59359	Prestressed concrete continuous	3
11940	(50)37-47-06615 AWBL	Vincennes	38.82589	-86.51313	Steel continuous	10
16500	044-70-06635 A	Greenfield	39.61502	-85.38899	Concrete continuous	3
17940	049-37-01938 C	LaPorte	41.25413	-87.03349	Steel	1
18770	050-15-03159 B	Seymour	39.05924	-84.901474	Steel continuous	5
18870	(6)51-45-01943 B	LaPorte	41.57052	-87.239746	Concrete continuous	16
19640	054-28-02538 B	Vincennes	39.02764	-86.9282	Steel continuous	3
20610	057-63-06013 A	Vincennes	38.53915	-87.223068	Steel continuous	6
22690	063-83-03561 CNBL	Crawfordsville	39.89257	-87.428093	Steel continuous	3
24220	067-18-05460 BNBL	Greenfield	40.14288	-85.37598	Concrete continuous	3
31080	262-58-06070	Seymour	38.97038	-85.00817	Prestressed concrete continuous	3
35520	I65-068-07910	Seymour	39.20036	-85.958069	Steel	1
37070	I65-125-04287 CNBL	Greenfield	39.88763	-86.30137	Steel continuous	5
37100	I65-126-04289 BNBL	Greenfield	39.90252	-86.31388	Concrete continuous	3
37150	I65-128-04292 CNBL	Greenfield	39.92519	-86.3342	Steel continuous	4
41810	I70-061-05181 CWBL	Crawfordsville	39.63091	-86.44582	Concrete continuous	3
41870	I70-065-05183 BEBL	Crawfordsville	39.66028	-86.38762	Steel continuous	3
49180	I94-30-02250 CEB	LaPorte	41.62437	-87.05616	Steel continuous	3
49200	I94-31-02251 CEBL	LaPorte	41.6249	-87.03363	Steel continuous	3
76140	I469-19-07224 SB	Fort Wayne	41.06327	-84.98966	Steel continuous	2

Table A.1 Detailed Bridge Information for NL and PL Testing Bridges (Continue)

Structure Number	Type of Design/Constr	Deck	Wearing Surface	Deck Membrane	Deck Protection
1310	Slab	Concrete Cast-in-Place	Latex Concrete	None	None
1347	Stringer/Multibeam or Girder	Concrete Cast-in-Place	Monolithic Concrete	None	Epoxy Coated Reinforcing
4845	Stringer/Multibeam or Girder	Concrete Cast-in-Place	Monolithic Concrete	None	Epoxy Coated Reinforcing
4930	Stringer/Multibeam or Girder	Concrete Cast-in-Place	Latex Concrete	None	None
5230	Stringer/Multibeam or Girder	Concrete Cast-in-Place	Monolithic Concrete	Built-up	Epoxy Coated Reinforcing
8630	Stringer/Multibeam or Girder	Concrete Cast-in-Place	Latex Concrete	None	Epoxy Coated Reinforcing
11940	Stringer/Multibeam or Girder	Concrete Cast-in-Place	Latex Concrete	None	Epoxy Coated Reinforcing
16500	Slab	Concrete Cast-in-Place	Epoxy Overlay	None	Epoxy Coated Reinforcing
17940	Truss - Thru	Concrete Cast-in-Place	Epoxy Overlay	None	Epoxy Coated Reinforcing
18770	Stringer/Multibeam or Girder	Concrete Cast-in-Place	Latex Concrete	None	Epoxy Coated Reinforcing
18870	Slab	Concrete Cast-in-Place	Latex Concrete	None	Epoxy Coated Reinforcing
19640	Stringer/Multibeam or Girder	Concrete Cast-in-Place	Latex Concrete	None	Epoxy Coated Reinforcing
20610	Stringer/Multibeam or Girder	Concrete Cast-in-Place	Latex Concrete	None	None
22690	Stringer/Multibeam or Girder	Concrete Cast-in-Place	Latex Concrete	None	None
24220	Stringer/Multibeam or Girder	Concrete Cast-in-Place	Latex Concrete	None	None
31080	Stringer/Multibeam or Girder	Concrete Cast-in-Place	Monolithic Concrete	None	None
35520	Arch - Thru	Concrete Cast-in-Place	Monolithic Concrete	None	Epoxy Coated Reinforcing
37070	Stringer/Multibeam or Girder	Concrete Cast-in-Place	Monolithic Concrete	None	Epoxy Coated Reinforcing
37100	Slab	Concrete Cast-in-Place	Latex Concrete	None	None
37150	Stringer/Multibeam or Girder	Concrete Cast-in-Place	Epoxy Overlay	None	Epoxy Coated Reinforcing
41810	Slab	Concrete Cast-in-Place	Monolithic Concrete	None	Epoxy Coated Reinforcing
41870	Stringer/Multibeam or Girder	Concrete Cast-in-Place	Monolithic Concrete	None	Epoxy Coated Reinforcing
49180	Stringer/Multibeam or Girder	Concrete Cast-in-Place	Monolithic Concrete	None	Epoxy Coated Reinforcing
49200	Stringer/Multibeam or Girder	Concrete Cast-in-Place	Latex Concrete	None	None
76140	Stringer/Multibeam or Girder	Concrete Cast-in-Place	Epoxy Overlay	None	Epoxy Coated Reinforcing

Table A.1 Detailed Bridge Information for NL and PL Testing Bridges (Continue)

Structure Number	Year	Age	Year of Overlay	Age of Overlay	Year of Replacement	Age of Replacement	Facility Carried	Type of road carried by bridge
1310	1959	63	1987	35			SR 3 SB	State Road
1347	1990	32					SR 3 SB	State Road
4845	1983	39					SR 18 EB	State Road
4930	1972	50	1998	24			SR 18	State Road
5230	1931	91			2019	3	US 20	US Highway
8630	1948	74	1994	28	1979	43	US 30 EB	US Highway
11940	1984	38	2002	20			US 50 WB	US Highway
16500	1982	40	2017	5			SR 44	State Road
17940	2014	8	2014	8			SR 49	State Road
18770	1952	70	2020	2	1992	30	US 50	US Highway
18870	1941	81	2003	19	1984	38	US 6	US Highway
19640	1982	40	2007	15			SR 54	State Road
20610	1972	50	1995	27			SR 57	State Road
22690	1954	68	1990	32	1968	54	SR 63 NB	State Road
24220	1973	49	2003	19			SR 67 NB	State Road
31080	1976	46					SR 262	State Road
35520	1996	26					I-65	Interstate
37070	1960	62			1994	28	I-65 NB	Interstate
37100	1960	62	1995	27			I-65 NB	Interstate
37150	1959	63	1994	28			I-65 NB	Interstate
41810	1966	56			2018	4	I-70 WB	Interstate
41870	1966	56			1995	27	I-70 EB	Interstate
49180	1969	53			2015	7	I-94 EB	Interstate
49200	1969	53	2017	5			I-94 EB	Interstate
76140	1990	32	2014	8			I-469 SB	Interstate

Table A.1 Detailed Bridge Information for NL and PL Testing Bridges (Continue)

Structure Number	Features Intersected	Average Daily Traffic	% Average Daily Truck Traffic	Length of Max Span [ft]	Structure Length [ft]	Deck Width, Out-to-Out [ft]	BRDG RDWY Width Curb TO- Curb [ft]
1310	WILLOW CREEK	14759	4	29	77	43	40
1347	CSX RR	13551	7	49.2	150	43.3	40.3
4845	MISSISSINEWA RIVER	4641	10	142	382	46.5	44
4930	BEAR CREEK	1868	33	45.5	136.3	46.5	43.5
5230	CSX RR	11225	5	66	252	57.3	54
8630	SCHUMAN DITCH	12032	27	40	129	42.5	40
11940	EAST FORK WHITE RIVER	22557	10	100.1	935	42.5	39.5
16500	RANCH FLATROCK RIVE	5236	9	42	109.5	46.5	37.5
17940	KANKAKEE RIVER	4069	10	200.1	326	30	28
18770	HOGAN CREEK	27888	5	68	405	81	68
18870	MUCK POCKET	13764	5	19.7	289	47	39
19640	INDIANA RR CO	4381	5	60	162	47.3	44
20610	EAST FORK WHITE RIVER	3264	10	158.7	900	46.5	43.5
22690	ITTLE VERMILLION RIVE	6938	3	64	172	42.5	39.4
24220	BUCK CREEK	5244	5	48	120.5	42.5	39.5
31080	S FORK LAUGHERY CREE	584	10	64	192	36.6	34
35520	SR 46	46416	5	197.5	292	96.7	81.4
37070	BIG EAGLE CREEK	50741	5	70	327.5	43.6	40.6
37100	WEST 82ND STREET	50741	5	54.5	140.1	42.8	39.8
37150	LAFAYETTE ROAD	50741	10	78	296	43.7	40.7
41810	RANCH MCCRACKEN CR	46614	10	34	91	42.5	39.6
41870	WHITE LICK CREEK	46614	36	83.5	227	42.5	39.8
49180	AMTRAK	28677	5	98	262	65.5	62.5
49200	CSX RR	54962	5	92.5	254	65.3	62.3
76140	US 30/SR 930	20035	28	120.3	247	60.5	57.6

Table A.1 Detailed Bridge Information for NL and PL Testing Bridges (Continue)

Structure Number	Surface Area [sf]	Testing Area [sf]	Number of Lanes	Skew [deg]	Deck Rating	Wearing Surface Rating
1310	3080	3080	2	6	5	5
1347	6045	6045	2	0	7	6
4845	16808	6248	2	15	5	5
4930	5929	5929	2	10	4	5
5230	13608	13608	4	45	5	6
8630	5160	5160	2	0	5	4
11940	36933	5610	2	0	7	7
16500	4106	4106	2	0	6	8
17940	9128	9128	2	0	6	7
18770	27540	9720	5	10	5	5
18870	11271	11271	2	0	5	6
19640	7128	7128	2	27	6	6
20610	39150	10800	2	0	6	5
22690	6777	6777	2	0	6	6
24220	4760	4760	2	0	6	6
31080	6528	6528	2	15	5	5
35520	23769	7008	4	0	7	6
37070	13297	13297	2	30	7	7
37100	5576	5576	2	26	5	5
37150	12047	12047	2	61	7	8
41810	3604	3604	2	20	6	6
41870	9035	9035	2	20	6	6
49180	16375	16375	3	55	7	7
49200	15824	3048	3	56	5	6
76140	14227	2964	3	19	7	8

Table A.1 Detailed Bridge Information for NL and PL Testing Bridges (Continue)

Structure Number	Note
1310	Testing Area is the entire bridge.
1347	Testing Area is the entire bridge.
4845	The testing area is the longest spans (142') across the full width of the structure.
4930	Testing Area is the entire bridge.
5230	Testing Area is the entire bridge.
8630	Testing Area is the entire bridge.
11940	The testing area is the right traffic lane along the first five spans of the structure. The structure carried WB of US 50.
16500	Testing Area is the entire bridge.
17940	Testing Area is the entire bridge.
18770	The testing area is the right two northbound (easternmost) traffic lanes along the entire length of the structure.
18870	Testing Area is the entire bridge.
19640	Testing Area is the entire bridge.
20610	The testing area is the right northbound (easternmost) traffic lane along the entire length of the structure.
22690	Testing Area is the entire bridge.
24220	Testing Area is the entire bridge.
31080	Testing Area is the entire bridge.
35520	The testing area is the right two northbound (easternmost) traffic lanes along the entire length of the structure.
37070	Testing Area is the entire bridge.
37100	Testing Area is the entire bridge.
37150	Testing Area is the entire bridge.
41810	Testing Area is the entire bridge.
41870	Testing Area is the entire bridge.
49180	Testing Area is the entire bridge.
49200	The testing area is the right traffic lane along the entire length of the structure. The structure carried EB of I-94.
76140	The testing area is the right traffic lane along the entire length of the structure. The structure carried SB of I-469.

Table A.2 Detailed Bridge Information for Aerial IRT Testing Bridges on I-65

Structure Number	Bridge Number	District	Latitude	Longitude	Superstructure Type	Type of Design/Constr
36070	I65-106-04797 CNBL	Greenfield	39.70614	-86.10883	Steel continuous	Stringer/Multibeam or Girder
36130	I65-108-05691 ANBL	Greenfield	39.72304	-86.13266	Steel continuous	Stringer/Multibeam or Girder
36150	I65-108-05622 ANBL	Greenfield	39.72868	-86.13533	Steel continuous	Stringer/Multibeam or Girder
36170	I65-108-05692 ANBL	Greenfield	39.73034	-86.13613	Steel continuous	Stringer/Multibeam or Girder
36190	I65-108-05693 ANBL	Greenfield	39.73415	-86.13702	Steel continuous	Stringer/Multibeam or Girder
36210	I65-109-05694 BNBL	Greenfield	39.73762	-86.13722	Steel continuous	Stringer/Multibeam or Girder
36230	I65-109-02422 ANBL	Greenfield	39.74138	-86.13738	Steel continuous	Stringer/Multibeam or Girder
36250	I65-109-05695 ANBL	Greenfield	39.74255	-86.13749	Steel continuous	Stringer/Multibeam or Girder
36270	I65-109-05623 BNBL	Greenfield	39.74567	-86.13847	Steel continuous	Stringer/Multibeam or Girder
36290	I65-109-05696 JANB	Greenfield	39.74694	-86.13979	Steel continuous	Stringer/Multibeam or Girder
36320	I65-110-05713 ANBL	Greenfield	39.75157	-86.14415	Steel continuous	Stringer/Multibeam or Girder
36330	I65-110-05715 B	Greenfield	39.75154	-86.14435	Steel continuous	Stringer/Multibeam or Girder
36520	I65-111-05734 ANBL	Greenfield	39.77457	-86.14235	Steel continuous	Stringer/Multibeam or Girder
36660	I65-112-02419 C	Greenfield	39.78282	-86.158	Steel continuous	Stringer/Multibeam or Girder
36680	I65-113-05670 B	Greenfield	39.78374	-86.16609	Steel continuous	Stringer/Multibeam or Girder
36690	I65-113-05671 BNBL	Greenfield	39.78457	-86.16586	Steel continuous	Stringer/Multibeam or Girder
36700	I65-113-05673 D	Greenfield	39.78835	-86.16651	Steel continuous	Stringer/Multibeam or Girder
36720	I65-114-05367 C	Greenfield	39.79498	-86.1647	Steel continuous	Stringer/Multibeam or Girder
36730	I65-114-05368 D	Greenfield	39.79691	-86.16523	Steel continuous	Stringer/Multibeam or Girder

Table A.2 Detailed Bridge Information for Aerial IRT Testing Bridges on I-65 (Continue)

Structure Number	Deck	Wearing Surface	Deck Membrane	Deck Protection	Year	Age
36070	Concrete Cast-in-Place	Monolithic Concrete	None	Epoxy Coated Reinforcing	1963	59
36130	Concrete Cast-in-Place	Monolithic Concrete	None	Epoxy Coated Reinforcing	1973	49
36150	Concrete Cast-in-Place	Monolithic Concrete	None	Epoxy Coated Reinforcing	1973	49
36170	Concrete Cast-in-Place	Monolithic Concrete	None	Epoxy Coated Reinforcing	1973	49
36190	Concrete Cast-in-Place	Monolithic Concrete	None	Epoxy Coated Reinforcing	1973	49
36210	Concrete Cast-in-Place	Monolithic Concrete	None	Epoxy Coated Reinforcing	1973	49
36230	Concrete Cast-in-Place	Monolithic Concrete	None	Epoxy Coated Reinforcing	1973	49
36250	Concrete Cast-in-Place	Monolithic Concrete	None	Epoxy Coated Reinforcing	1973	49
36270	Concrete Cast-in-Place	Monolithic Concrete	None	Epoxy Coated Reinforcing	1973	49
36290	Concrete Cast-in-Place	Monolithic Concrete	None	Epoxy Coated Reinforcing	1973	49
36320	Concrete Cast-in-Place	Monolithic Concrete	None	Epoxy Coated Reinforcing	1973	49
36330	Concrete Cast-in-Place	Monolithic Concrete	None	Epoxy Coated Reinforcing	1973	49
36520	Concrete Cast-in-Place	Latex Concrete	None	None	1974	48
36660	Concrete Cast-in-Place	Latex Concrete	None	None	1972	50
36680	Concrete Cast-in-Place	Latex Concrete	None	None	1970	52
36690	Concrete Cast-in-Place	Latex Concrete	None	None	1970	52
36700	Concrete Cast-in-Place	Latex Concrete	None	None	1969	53
36720	Concrete Cast-in-Place	Monolithic Concrete	None	Epoxy Coated Reinforcing	1968	54
36730	Concrete Cast-in-Place	Monolithic Concrete	None	Epoxy Coated Reinforcing	1968	54

Table A.2 Detailed Bridge Information for Aerial IRT Testing Bridges on I-65 (Continue)

Structure Number	Year of Overlay	Age of Overlay	Year of Replacement	Age of Replacement	Facility Carried	Type of road carried by bridge
36070			2017	5	I-65 NB	Interstate
36130			1997	25	I-65 NB	Interstate
36150			1997	25	I-65 NB	Interstate
36170			1997	25	I-65 NB	Interstate
36190			1997	25	I-65 NB	Interstate
36210			1997	25	I-65 NB	Interstate
36230			1997	25	I-65 NB	Interstate
36250			1997	25	I-65 NB	Interstate
36270			1997	25	I-65 NB	Interstate
36290			1997	25	I-65 NB	Interstate
36320			2019	3	I-65 NB	Interstate
36330			2015	7	RAMP I-65 NB, I-70 WB	Interstate
36520	2003	19			I-65 NB	Interstate
36660	2020	2			I-65	Interstate
36680	2019	3			I-65 ON/OFF RAMPS	Interstate
36690	2019	3			I-65 NB	Interstate
36700	2019	3			I-65	Interstate
36720			2005	17	I-65	Interstate
36730			2005	17	I-65	Interstate

Table A.2 Detailed Bridge Information for Aerial IRT Testing Bridges on I-65 (Continue)

Structure Number	Features Intersected	Average Daily Traffic	% Average Daily Truck Traffic	Length of Max Span [ft]	Structure Length [ft]
36070	LICK CREEK	121671	19	70	173
36130	TROY AVENUE & PATH	90845	5	76.5	156.2
36150	NELSON ST, BEAN CREEK	90845	5	69	299.2
36170	SOUTHERN AVENUE	90845	5	62.2	133.1
36190	BRADBURY AVENUE	90845	5	45.2	118.7
36210	RAYMOND STREET	90845	5	75.5	149.2
36230	CSX RR	33713	5	82.2	190.7
36250	NAOMI STREET	33713	5	54	144.5
36270	PLEASANT RUN, PARKWAYS	33713	5	76.9	398.8
36290	SHELBY STREET	33713	5	71.5	246.3
36320	MORRIS ST, PROSPECT ST	33713	5	97.4	162.1
36330	MORRIS ST, PROSPECT ST	14378	29	80	160.5
36520	I-65 RAMP NB	60912	5	82.5	176.3
36660	7 STS ACCESS RD, MONORAIL	137635	5	93	3507
36680	WEST ST ON RAMP TO I-65N	13599	4	61.5	166.1
36690	WEST ST ON RAMP	137635	10	81	211.7
36700	16TH STREET	124245	9	86	161.3
36720	21ST STREET	124245	5	89.3	171.3
36730	FALL CR, PARKWAY N DR	96283	9	85.7	546

Table A.2 Detailed Bridge Information for Aerial IRT Testing Bridges on I-65 (Continue)

Structure Number	Deck Width, Out-to-Out [ft]	BRDG RDWY Width Curb TO- Curb [ft]	Surface Area [sf]	Number of Spans	Number of Lanes	Skew [deg]	Deck Rating	Wearing Surface Rating
36070	87.8	85	14705	3	4	12	8	8
36130	67.2	64.4	10059	2	3	19	7	7
36150	67.2	64.5	19298	5	3	20	7	7
36170	67.5	64.8	8625	3	3	18	7	7
36190	93.3	90.5	10742	3	4	3	7	7
36210	81.8	79	11787	2	4	1	6	6
36230	79.2	76.5	14589	3	3	0	7	7
36250	67.2	64.5	9320	3	3	0	7	7
36270	67.2	64.5	25723	7	3	99	7	6
36290	79.2	76.5	18842	4	3	43	7	7
36320	49.2	46.2	7489	1	2	2	6	6
36330	42.5	39.5	6340	3	2	6	7	7
36520	66.5	63.5	11195	3	4	99	6	5
36660	107.6	102.4	359117	65	6	99	6	6
36680	60.5	55.2	9169	3	2	99	6	8
36690	54.7	51.7	10945	3	3	44	5	8
36700	124.5	118.8	19162	3	8	3	6	8
36720	133	127.3	21806	3	7	9	7	7
36730	133	127.2	69451	8	7	99	7	7

Table A.2 Detailed Bridge Information for Aerial IRT Testing Bridges on I-65 (Continue)

Structure Number	Bridge Number	District	Latitude	Longitude	Superstructure Type	Type of Design/Constr
36740	I65-114-05368 DRC	Greenfield	39.79686	-86.1664	Steel continuous	Stringer/Multibeam or Girder
36750	I65-114-05974 C	Greenfield	39.80094	-86.16592	Concrete continuous	Slab
36760	I65-114-05369 C	Greenfield	39.80429	-86.16602	Steel continuous	Stringer/Multibeam or Girder
36770	I65-115-05370 C	Greenfield	39.80832	-86.1663	Steel continuous	Stringer/Multibeam or Girder
36780	I65-115-05371 C	Greenfield	39.81013	-86.16712	Steel continuous	Stringer/Multibeam or Girder
36790	I65-115-04913 C	Greenfield	39.81186	-86.17468	Steel continuous	Stringer/Multibeam or Girder
36800	I65-116-04914 C	Greenfield	39.81254	-86.1805	Steel continuous	Stringer/Multibeam or Girder
36850	I65-117-04838 CNBL	Greenfield	39.82418	-86.2047	Steel continuous	Stringer/Multibeam or Girder
36880	I65-118-02313 CNBL	Greenfield	39.82415	-86.22593	Steel continuous	Stringer/Multibeam or Girder
36900	I65-118-04840 BNBL	Greenfield	39.8248	-86.22824	Steel continuous	Stringer/Multibeam or Girder
36920	I65-119-04841 BNBL	Greenfield	39.82803	-86.23211	Steel continuous	Stringer/Multibeam or Girder
36950	I65-120-04842 CNBL	Greenfield	39.84154	-86.25206	Steel continuous	Stringer/Multibeam or Girder
36980	I65-122-04844 BNBL	Greenfield	39.85299	-86.26489	Steel continuous	Stringer/Multibeam or Girder
37030	I65-124-04285 ENBL	Greenfield	39.88019	-86.2924	Steel continuous	Stringer/Multibeam or Girder
37060	I65-124-04285 CNBR	Greenfield	39.88049	-86.29203	Concrete	Stringer/Multibeam or Girder
37070	I65-125-04287 CNBL	Greenfield	39.88763	-86.30137	Steel continuous	Stringer/Multibeam or Girder
37100	I65-126-04289 BNBL	Greenfield	39.90252	-86.31388	Concrete continuous	Slab
37120	I65-126-04290 CNBL	Greenfield	39.90647	-86.31705	Concrete continuous	Stringer/Multibeam or Girder
50720	(I65)I465-145-04566 B	Greenfield	39.86182	-86.27647	Steel continuous	Stringer/Multibeam or Girder

Table A.2 Detailed Bridge Information for Aerial IRT Testing Bridges on I-65 (Continue)

Structure Number	Deck	Wearing Surface	Deck Membrane	Deck Protection	Year	Age
36740	Concrete Cast-in-Place	Monolithic Concrete	None	Epoxy Coated Reinforcing	1968	54
36750	Concrete Cast-in-Place	Monolithic Concrete	None	Epoxy Coated Reinforcing	1969	53
36760	Concrete Cast-in-Place	Monolithic Concrete	None	Epoxy Coated Reinforcing	1968	54
36770	Concrete Cast-in-Place	Monolithic Concrete	None	Epoxy Coated Reinforcing	1968	54
36780	Concrete Cast-in-Place	Monolithic Concrete	None	Epoxy Coated Reinforcing	1968	54
36790	Concrete Cast-in-Place	Monolithic Concrete	None	Epoxy Coated Reinforcing	1968	54
36800	Concrete Cast-in-Place	Monolithic Concrete	None	Epoxy Coated Reinforcing	1968	54
36850	Concrete Cast-in-Place	Monolithic Concrete	None	Epoxy Coated Reinforcing	1964	58
36880	Concrete Cast-in-Place	Monolithic Concrete	None	Epoxy Coated Reinforcing	1964	58
36900	Concrete Cast-in-Place	Monolithic Concrete	None	Epoxy Coated Reinforcing	1964	58
36920	Concrete Cast-in-Place	Monolithic Concrete	None	Epoxy Coated Reinforcing	1963	59
36950	Concrete Cast-in-Place	Monolithic Concrete	None	Epoxy Coated Reinforcing	1963	59
36980	Concrete Cast-in-Place	Monolithic Concrete	None	Epoxy Coated Reinforcing	1963	59
37030	Concrete Cast-in-Place	Monolithic Concrete	None	Epoxy Coated Reinforcing	1960	62
37060	Concrete Cast-in-Place	Latex Concrete	None	None	1960	62
37070	Concrete Cast-in-Place	Monolithic Concrete	None	Epoxy Coated Reinforcing	1960	62
37100	Concrete Cast-in-Place	Latex Concrete	None	None	1960	62
37120	Concrete Cast-in-Place	Latex Concrete	None	None	1960	62
50720	Concrete Cast-in-Place	Monolithic Concrete	None	Epoxy Coated Reinforcing	1959	63

Table A.2 Detailed Bridge Information for Aerial IRT Testing Bridges on I-65 (Continue)

Structure Number	Year of Overlay	Age of Overlay	Year of Replacement	Age of Replacement	Facility Carried	Type of road carried by bridge
36740			2005	17	I-65 RAMP	Interstate
36750			2005	17	I-65	Interstate
36760			2005	17	I-65	Interstate
36770			2005	17	I-65	Interstate
36780			2005	17	I-65	Interstate
36790			1996	26	I-65	Interstate
36800			1996	26	I-65	Interstate
36850			1996	26	I-65 NB	Interstate
36880			2000	22	I-65 NB	Interstate
36900			2000	22	I-65 NB	Interstate
36920			2000	22	I-65 NB	Interstate
36950			2000	22	I-65 NB	Interstate
36980			2000	22	I-65 NB	Interstate
37030			1994	28	I-65 NB	Interstate
37060	1994	28			I-65 NB ON RAMP	Interstate
37070			1994	28	I-65 NB	Interstate
37100	1995	27			I-65 NB	Interstate
37120	1994	28			I-65 NB	Interstate
50720			1994	28	I-65 NB RAMP	Interstate

Table A.2 Detailed Bridge Information for Aerial IRT Testing Bridges on I-65 (Continue)

Structure Number	Features Intersected	Average Daily Traffic	% Average Daily Truck Traffic	Length of Max Span [ft]	Structure Length [ft]	Deck Width, Out-to-Out [ft]
36740	FALL CR, PARKWAY N DR	4740	10	84.5	571	29
36750	PEDESTRIAN WALK	96283	9	20	52	145.5
36760	26TH STREET	96283	5	52.5	119	154.4
36770	29TH STREET	96283	5	62.5	144	129.7
36780	WEST 30TH STREET	96283	5	83.9	187.4	129.7
36790	DR ML KING DRIVE	96283	5	54.5	179.4	132.1
36800	CLIFTON STREET	94183	5	77.9	181.9	134.4
36850	CROOKED CREEK	94183	15	73.5	199.7	65.6
36880	CSX RR, GUION ROAD	71463	15	83	258.3	74.1
36900	38TH ST INDUSTR BLVD	71463	15	67.5	237.1	63.6
36920	LITTLE EAGLE CREEK	71463	15	76	205.6	65.3
36950	LAFAYETTE ROAD	71463	15	60.8	227.6	65.3
36980	WEST 56TH STREET	15427	13	46.3	169.9	65.3
37030	WEST 71ST, BUSHS RUN	54916	5	69.5	218	43.7
37060	BUSHS RUN	1633	5	28	30	42.8
37070	BIG EAGLE CREEK	50741	5	70	327.5	43.6
37100	WEST 82ND STREET	50741	5	54.5	140.1	42.8
37120	FISHBACK CREEK	50741	5	62	156	44.6
50720	I-465 SB	4596	5	101.9	226	41.7

Table A.3 Detailed Bridge Information for Aerial IRT Testing Bridges on SR 18

Structure Number	Bridge Number	District	Latitude	Longitude	Superstructure Type	Number of Spans
4708	018-52-06631 A	Fort Wayne	40.58486	-86.12478	Concrete continuous	3
4710	018-52-06141	Fort Wayne	40.58519	-86.08688	Concrete continuous	3
4730	018-52-06889 A	Fort Wayne	40.5792	-85.95126	Concrete continuous	3
4740	018-52-06749 A	Fort Wayne	40.57937	-85.93426	Concrete continuous	3
4750	018-52-01434 B	Fort Wayne	40.57743	-85.87541	Prestressed concrete	1
4770	018-27-01432 A	Fort Wayne	40.57087	-85.82933	Steel	1
4820	018-27-04108 B	Fort Wayne	40.56313	-85.71238	Steel continuous	3
4830	018-27-02215 B	Fort Wayne	40.56301	-85.7111	Steel continuous	3
4845	018-27-05803 EBL	Fort Wayne	40.55676	-85.64712	Steel continuous	3
4859	018-27-04766 BEBL	Fort Wayne	40.55341	-85.54688	Concrete continuous	3
4860	018-27-04766 JWBL	Fort Wayne	40.55354	-85.54688	Concrete continuous	3
4910	018-38-06891 A	Fort Wayne	40.54753	-85.02666	Concrete continuous	3
4920	018-38-07159	Fort Wayne	40.54749	-85.01775	Prestressed concrete	1
4930	018-38-05997 A	Fort Wayne	40.54409	-84.99772	Prestressed concrete	3

Table A.2 Detailed Bridge Information for Aerial IRT Testing Bridges on I-65 (Continue)

Structure Number	BRDG RDWY Width Curb TO- Curb [ft]	Surface Area [sf]	Number of Spans	Number of Lanes	Skew [deg]	Deck Rating	Wearing Surface Rating
36740	26	14846	8	1	99	7	7
36750	140.5	7306	3	8	0	6	6
36760	148.6	17683	3	9	2	7	7
36770	124	17856	3	6	6	7	6
36780	124	23238	3	6	33	7	6
36790	126	22604	4	7	20	7	7
36800	128.4	23356	3	8	35	6	6
36850	62.6	12501	3	3	17	7	7
36880	71.3	18417	4	3	99	7	7
36900	60.8	14416	4	3	99	7	7
36920	60.8	12500	3	3	30	6	6
36950	60.8	13838	4	3	44	7	9
36980	60.8	10330	4	3	27	7	7
37030	40.7	8873	4	2	20	6	6
37060	40	1200	1	1	15	4	4
37070	40.6	13297	5	2	30	7	7
37100	39.8	5576	3	2	26	5	5
37120	41.6	6490	3	2	30	5	6
50720	38.7	8746	3	2	53	7	7

Table A.3 Detailed Bridge Information for Aerial IRT Testing Bridges on SR 18 (Continue)

Structure Number	Type of Design/Constr	Deck	Wearing Surface	Deck Membrane	Deck Protection
4708	Slab	Concrete Cast-in-Place	Latex Concrete	None	Epoxy Coated Reinforcing
4710	Slab	Concrete Cast-in-Place	Monolithic Concrete	None	Epoxy Coated Reinforcing
4730	Slab	Concrete Cast-in-Place	Latex Concrete	None	Epoxy Coated Reinforcing
4740	Slab	Concrete Cast-in-Place	Latex Concrete	None	Epoxy Coated Reinforcing
4750	Stringer/Multibeam or Girder	Concrete Cast-in-Place	Monolithic Concrete	None	Epoxy Coated Reinforcing
4770	Stringer/Multibeam or Girder	Concrete Cast-in-Place	Monolithic Concrete	None	Epoxy Coated Reinforcing
4820	Stringer/Multibeam or Girder	Concrete Cast-in-Place	Latex Concrete	None	Epoxy Coated Reinforcing
4830	Stringer/Multibeam or Girder	Concrete Cast-in-Place	Latex Concrete	None	Epoxy Coated Reinforcing
4845	Stringer/Multibeam or Girder	Concrete Cast-in-Place	Monolithic Concrete	None	Epoxy Coated Reinforcing
4859	Slab	Concrete Cast-in-Place	Latex Concrete	None	None
4860	Slab	Concrete Cast-in-Place	Monolithic Concrete	None	Epoxy Coated Reinforcing
4910	Slab	Concrete Cast-in-Place	Latex Concrete	None	Epoxy Coated Reinforcing
4920	Stringer/Multibeam or Girder	Concrete Cast-in-Place	Monolithic Concrete	None	Epoxy Coated Reinforcing
4930	Stringer/Multibeam or Girder	Concrete Cast-in-Place	Latex Concrete	None	None

Table A.3 Detailed Bridge Information for Aerial IRT Testing Bridges on SR 18 (Continue)

Structure Number	Year	Age	Year of Overlay	Age of Overlay	Year of Replacement	Age of Replacement	Facility Carried
4708	1981	41	2006	16			SR 18
4710	1991	31					SR 18
4730	1985	37	2016 (West Approach)	6			SR 18
4740	1984	38	2016	6			SR 18
4750	1933	89			1990	32	SR 18
4770	1937	85			1984	38	SR 18
4820	1956	66	2003	19	1976	46	SR 18
4830	1954	68	2003	19	1976	46	SR 18
4845	1983	39					SR 18 EB
4859	1964	58	1989	33			SR 18 EB
4860	1993	29					SR 18 WB
4910	1986	36	2014	8			SR 18
4920	1990	32					SR 18
4930	1972	50	1998	24			SR 18

Table A.3 Detailed Bridge Information for Aerial IRT Testing Bridges on SR 18 (Continue)

Structure Number	Type of road carried by bridge	Features Intersected	Average Daily Traffic	% Average Daily Truck Traffic	Length of Max Span [ft]
4708	State Road	RUSSELL DITCH	2205	16	29.5
4710	State Road	WISE DITCH	2125	20	22
4730	State Road	HONEY CREEK	1523	22	32
4740	State Road	SUGAR CREEK	1572	22	25
4750	State Road	LITTLE PIPE CREEK	3287	16	37.3
4770	State Road	PIPE CREEK	3994	12	50
4820	State Road	NORTH TROY RD (CR 200 W)	5971	15	48.1
4830	State Road	NS RR (GM Spur)	5971	15	57
4845	State Road	MISSISSINEWA RIVER	4641	10	142
4859	State Road	TIPPEY DITCH	2547	14	29
4860	State Road	TIPPEY DITCH	2715	12	29
4910	State Road	LOUIS DITCH	1380	44	30
4920	State Road	WOLF CREEK	1384	45	63.5
4930	State Road	BEAR CREEK	1868	33	45.5

Table A.3 Detailed Bridge Information for Aerial IRT Testing Bridges on SR 18 (Continue)

Structure Number	Structure Length [ft]	Deck Width, Out-to-Out [ft]	BRDG RDWY Width Curb TO- Curb [ft]	Surface Area [sf]	Number of Lanes	Skew [deg]	Wearing Surface Rating	Deck Rating
4708	76.3	46.5	44.5	3395	2	35	6	7
4710	58.7	48.3	45.3	2659	2	25	7	7
4730	81.6	46.5	43.5	3550	2	15	6	7
4740	64.5	46.5	43.5	2806	2	10	7	7
4750	39	48.3	45.3	1767	2	0	7	7
4770	54.5	46.5	44	2398	2	0	7	7
4820	127	35.5	32.5	4128	2	0	6	6
4830	156	35.3	32.3	5039	2	0	7	7
4845	382	46.5	44	16808	2	15	5	5
4859	79	42.2	39.4	3113	2	0	6	6
4860	79	44.1	40.7	3215	2	0	6	6
4910	77	46.5	43.5	3350	2	25	6	7
4920	67.5	44.3	41.3	2788	2	0	7	7
4930	136.3	46.5	43.5	5929	2	10	4	5

Table A.4 Detailed Bridge Information for Aerial IRT Testing Bridges on I-69

Structure Number	Bridge Number	District	Latitude	Longitude	Superstructure Type	Number of Spans	Type of Design/Constr	Deck
39620	I69-256-04760 CNB	Fort Wayne	40.45494	-85.54956	Prestressed concrete continuous	7	Stringer/Multibeam or Girder	Concrete Cast-in-Place
39630	I69-256-04760 CSB	Fort Wayne	40.45503	-85.54993	Prestressed concrete continuous	7	Stringer/Multibeam or Girder	Concrete Cast-in-Place
39640	I69-258-02306 BNB	Fort Wayne	40.47403	-85.54896	Steel continuous	3	Stringer/Multibeam or Girder	Concrete Cast-in-Place
39650	I69-258-02306 BSB	Fort Wayne	40.47404	-85.54928	Steel continuous	3	Stringer/Multibeam or Girder	Concrete Cast-in-Place
39740	I69-263-04876 CSB	Fort Wayne	40.54616	-85.55084	Concrete continuous	3	Slab	Concrete Cast-in-Place
39770	I69-264-04767 BNB	Fort Wayne	40.56901	-85.55104	Concrete continuous	3	Slab	Concrete Cast-in-Place
39780	I69-264-04767 BSB	Fort Wayne	40.569	-85.55137	Concrete continuous	3	Slab	Concrete Cast-in-Place
39850	I69-270-05043 CNB	Fort Wayne	40.6455	-85.5101	Concrete continuous	3	Slab	Concrete Cast-in-Place
39860	I69-270-05043 CSB	Fort Wayne	40.64546	-85.51051	Concrete continuous	3	Slab	Concrete Cast-in-Place
39870	I69-273-04772 BNB	Fort Wayne	40.66795	-85.49347	Steel continuous	3	Stringer/Multibeam or Girder	Concrete Cast-in-Place
39880	I69-273-04772 BSB	Fort Wayne	40.66793	-85.49383	Steel continuous	3	Stringer/Multibeam or Girder	Concrete Cast-in-Place
39910	I69-276-04775 BNB	Fort Wayne	40.70611	-85.45419	Concrete continuous	6	Stringer/Multibeam or Girder	Concrete Cast-in-Place
39920	I69-276-04775 BSB	Fort Wayne	40.70635	-85.45433	Concrete continuous	6	Stringer/Multibeam or Girder	Concrete Cast-in-Place
40000	I69-287-04781 DNB	Fort Wayne	40.81842	-85.36374	Steel continuous	6	Girder and Floorbeam System	Concrete Cast-in-Place
40010	I69-287-04781 CSB	Fort Wayne	40.81858	-85.36401	Steel continuous	6	Girder and Floorbeam System	Concrete Cast-in-Place
40130	I69-300-04966 BNB	Fort Wayne	41.00891	-85.25829	Concrete continuous	3	Slab	Concrete Cast-in-Place
40140	I69-300-04966 BSB	Fort Wayne	41.009	-85.25857	Concrete continuous	3	Slab	Concrete Cast-in-Place
40220	I69-304-04543 CNB	Fort Wayne	41.0624	-85.23659	Steel continuous	3	Stringer/Multibeam or Girder	Concrete Cast-in-Place
40230	I69-304-04543 DSB	Fort Wayne	41.06266	-85.23659	Steel continuous	3	Stringer/Multibeam or Girder	Concrete Cast-in-Place
40330	I69-310-04550 CNB	Fort Wayne	41.12902	-85.16608	Prestressed concrete continuous	3	Stringer/Multibeam or Girder	Concrete Cast-in-Place
40340	I69-310-04550 CSB	Fort Wayne	41.12923	-85.1662	Prestressed concrete continuous	3	Stringer/Multibeam or Girder	Concrete Cast-in-Place
40350	I69-311-07303 ANB	Fort Wayne	41.1326	-85.14749	Prestressed concrete continuous	2	Stringer/Multibeam or Girder	Concrete Cast-in-Place
40360	I69-311-07303 ASB	Fort Wayne	41.13256	-85.14803	Prestressed concrete continuous	2	Stringer/Multibeam or Girder	Concrete Cast-in-Place

Table A.4 Detailed Bridge Information for Aerial IRT Testing Bridges on I-69 (Continue)

Structure Number	Wearing Surface	Deck Membrane	Deck Protection	Year	Age	Year of Overlay	Age of Overlay	Year of Replacement	Age of Replacement
39620	Monolithic Concrete	None	Epoxy Coated Reinforcing	1963	59			1993	29
39630	Monolithic Concrete	None	Epoxy Coated Reinforcing	1963	59			1993	29
39640	Monolithic Concrete	None	Epoxy Coated Reinforcing	1963	59			1993	29
39650	Monolithic Concrete	None	Epoxy Coated Reinforcing	1963	59			1993	29
39740	Latex Concrete	None	None	1963	59	2016	6		
39770	Latex Concrete	None	None	1963	59	2001	21		
39780	Latex Concrete	None	None	1963	59	2001	21		
39850	Monolithic Concrete	None	Epoxy Coated Reinforcing	1963	59			2013	9
39860	Monolithic Concrete	None	Epoxy Coated Reinforcing	1963	59			2013	9
39870	Monolithic Concrete	None	Epoxy Coated Reinforcing	1963	59	1996	26		
39880	Monolithic Concrete	None	Epoxy Coated Reinforcing	1963	59			1996	26
39910	Latex Concrete	None	None	1963	59	1996	26		
39920	Latex Concrete	None	None	1963	59	1996	26		
40000	Monolithic Concrete	None	Epoxy Coated Reinforcing	1964	58			2010	12
40010	Monolithic Concrete	None	Epoxy Coated Reinforcing	1964	58			1993	29
40130	Latex Concrete	None	None	1963	59	1993	29		
40140	Latex Concrete	None	None	1963	59	1993	29		
40220	Latex Concrete	None	Epoxy Coated Reinforcing	1961	61	2004	18	1993	29
40230	Latex Concrete	None	Epoxy Coated Reinforcing	1961	61	2004	18	1993	29
40330	Latex Concrete	None	Epoxy Coated Reinforcing	1960	62	2005	17	1992	30
40340	Latex Concrete	None	Epoxy Coated Reinforcing	1960	62	2004	18	1992	30
40350	Latex Concrete	None	Epoxy Coated Reinforcing	1992	30	2003	19		
40360	Latex Concrete	None	Epoxy Coated Reinforcing	1992	30	2003	19		

Table A.4 Detailed Bridge Information for Aerial IRT Testing Bridges on I-69 (Continue)

Structure Number	Facility Carried	Type of road carried by bridge	Features Intersected	Average Daily Traffic	% Average Daily Truck Traffic	Length of Max Span [ft]	Structure Length [ft]
39620	I-69 NB	Interstate	MISSISSINEWA RIVER	15350	35	68	397
39630	I-69 SB	Interstate	MISSISSINEWA RIVER	14932	37	68	397
39640	I-69 NB	Interstate	CENTRAL RR CO OF IN	12895	37	60	158
39650	I-69 SB	Interstate	CENTRAL RR CO OF IN	13160	37	60	158
39740	I-69 SB	Interstate	TIPPEY DITCH	1069	39	33	86
39770	I-69 NB	Interstate	TIPPEY DITCH	15447	34	24	62
39780	I-69 SB	Interstate	TIPPEY DITCH	15281	35	24	62
39850	I-69 NB	Interstate	LITTLE BLACK CREEK	14276	35	28	71.8
39860	I-69 SB	Interstate	LITTLE BLACK CREEK	15281	35	28	71.8
39870	I-69 NB	Interstate	SR 5 & SR 218	14632	37	54.8	138
39880	I-69 SB	Interstate	SR 5 & SR 218	13066	31	54.8	138
39910	I-69 NB	Interstate	SALAMONIE RIVER, ROAD	14632	36	75	414
39920	I-69 SB	Interstate	SALAMONIE RIVER, ROAD	14432	38	75	414
40000	I-69 NB	Interstate	WABASH RIVER, ROAD	15570	34	97.5	548
40010	I-69 SB	Interstate	WABASH RIVER, ROAD	14084	35	97.5	551
40130	I-69 NB	Interstate	ROBINSON CREEK	18155	18	31.2	83
40140	I-69 SB	Interstate	ROBINSON CREEK	18155	18	31.2	83
40220	I-69 NB	Interstate	HADLEY ROAD	24898	12	55.1	157.5
40230	I-69 SB	Interstate	HADLEY ROAD	24898	12	55.1	157.4
40330	I-69 NB	Interstate	SPY RUN CREEK	36327	10	36	109.6
40340	I-69 SB	Interstate	SPY RUN CREEK	35732	10	36	109.6
40350	I-69 NB	Interstate	WASHINGTON CENTER ROAD	31927	10	106.6	221
40360	I-69 SB	Interstate	WASHINGTON CENTER ROAD	31404	8	106.6	221

Table A.4 Detailed Bridge Information for Aerial IRT Testing Bridges on I-69 (Continue)

Structure Number	Deck Width, Out-to-Out [ft]	BRDG RDWY Width Curb TO- Curb [ft]	Surface Area [sf]	Number of Lanes	Skew [deg]	Wearing Surface Rating	Deck Rating
39620	43.7	40.7	16158	2	0	7	7
39630	43.7	40.7	16158	2	0	6	7
39640	43.7	40.7	6431	2	4	6	7
39650	43.7	40.7	6431	2	4	6	6
39740	42.8	39.5	3397	2	30	7	6
39770	42.8	39.8	2468	2	0	6	6
39780	42.8	39.8	2468	2	0	5	6
39850	43	40	2872	2	35	6	6
39860	43	40	2872	2	35	7	7
39870	42.7	39.7	5479	2	33	6	6
39880	42.7	39.7	5479	2	33	7	7
39910	42.7	39.7	16436	2	30	7	6
39920	42.7	39.7	16436	2	30	6	6
40000	42.3	39.3	21536	2	0	7	7
40010	42.3	39.3	21654	2	0	6	6
40130	42.9	39.5	3279	2	0	5	5
40140	42.9	39.5	3279	2	0	4	5
40220	66.1	63.3	9970	3	45	6	7
40230	66.1	63.3	9963	3	46	6	7
40330	78.1	75.3	8253	4	20	7	7
40340	78.1	75.3	8253	4	20	5	6
40350	66.1	63.3	13989	3	60	6	7
40360	66.1	63.3	13989	3	60	6	7

Table A.5 Detailed Bridge Information for Newer Bridges

Structure Number	Bridge Number	District	Latitude	Longitude	Superstructure Type	Number of Spans
13321	039-06-09895	Crawfordsville	40.16167	-86.48561	Prestressed concrete continuous	3
16171	231-79-10021	Crawfordsville	40.2725	-86.90315	Steel continuous	3
16811	045-28-10003	Vincennes	38.91705	-86.91625	Concrete continuous	3
28326	068-87-01281 C	Vincennes	38.19056	-87.06364	Steel	1
32675	(443X)52-79-05783 B	Crawfordsville	40.45259	-86.90309	Steel continuous	2
33500	I64-24-05219 FEBL	Vincennes	38.16692	-87.55052	Steel continuous	4
44090	I74-34-02334 DEBL	Crawfordsville	40.07839	-86.89987	Steel continuous	3
17051	046-11-10070	Crawfordsville	39.38404	-87.02087	Prestressed concrete continuous	3
28430	163-83-05325 B	Crawfordsville	39.65649	-87.39477	Steel continuous	5
44120	I74-34-04946 CEBL	Crawfordsville	40.07615	-86.88895	Steel continuous	5

Table A.5 Detailed Bridge Information for Newer Bridges (Continue)

Structure Number	Type of Design/Constr	Deck	Wearing Surface	Deck Membrane	Deck Protection
13321	Stringer/Multibeam or Girder	Concrete Cast-in-Place	Monolithic Concrete	None	Epoxy Coated Reinforcing
16171	Stringer/Multibeam or Girder	Concrete Cast-in-Place	Monolithic Concrete	None	Epoxy Coated Reinforcing
16811	Slab	Concrete Cast-in-Place	Monolithic Concrete	Other	Epoxy Coated Reinforcing
28326	Stringer/Multibeam or Girder	Concrete Cast-in-Place	Monolithic Concrete	None	Epoxy Coated Reinforcing
32675	Stringer/Multibeam or Girder	Concrete Cast-in-Place	Monolithic Concrete	None	Epoxy Coated Reinforcing
33500	Stringer/Multibeam or Girder	Concrete Cast-in-Place	Monolithic Concrete	None	Epoxy Coated Reinforcing
44090	Stringer/Multibeam or Girder	Concrete Cast-in-Place	Monolithic Concrete	None	Epoxy Coated Reinforcing
17051	Tee Beam	Concrete Cast-in-Place	Monolithic Concrete	None	Epoxy Coated Reinforcing
28430	Stringer/Multibeam or Girder	Concrete Cast-in-Place	Monolithic Concrete	None	Epoxy Coated Reinforcing
44120	Stringer/Multibeam or Girder	Concrete Cast-in-Place	Monolithic Concrete	None	Epoxy Coated Reinforcing

Table A.5 Detailed Bridge Information for Newer Bridges (Continue)

Structure Number	Year	Age	Year of Replacement	Age of Replacement	Facility Carried	Type of road carried by bridge	Features Intersected
13321	2019	3			SR 39	State Road	SUGAR CREEK
16171	2019	3			US 231	US Highway	BIG WEA CREEK
16811	2019	3			SR 45/SR 58	State Road	DOANS CREEK
28326	1932	90	2019	3	SR 68/161	State Road	UPPER PIGEON CREEK
32675	1976	46	2018	4	SOLDIERS HOME RD	City Road	SAGAMORE PKWY(OLD US 52)
33500	1968	54	2017	5	I-64 EB	Interstate	US 41 NB/SB
44090	1964	58	2019	3	I-74 EB	Interstate	CSX RR
17051	2019	3			SR 46	State Road	EEL RIVER
28430	1964	58	2020	2	SR 163	State Road	WABASH RIVER
44120	1964	58	2018	4	I-74 EB	Interstate	SUGAR CREEK

Table A.5 Detailed Bridge Information for Newer Bridges (Continue)

Structure Number	Average Daily Traffic	% Average Daily Truck Traffic	Length of Max Span [ft]	Structure Length [ft]	Deck Width, Out-to-Out [ft]	BRDG RDWY Width Curb TO- Curb [ft]	Surface Area [sf]
13321	5060	5	68.5	188.6	33	30	5658
16171	8420	7	56	141.5	44.7	41.7	5901
16811	5570	16	42.5	111.2	40.1	37.1	4126
28326	794	16	72	74.7	31.0	28.0	2092
32675	20083	4	120	245	51.5	39.5	9678
33500	15496	35	67.3	208	48.7	45.7	9506
44090	16689	39	72	197.7	55.1	52.1	10300
17051	3240	14	151	437.4	40.3	37.3	16315
28430	6548	4	160	1073.5	36.3	34.3	36821
44120	16689	39	84	394	41	38	14972

Table A.5 Detailed Bridge Information for Newer Bridges (Continue)

Structure Number	Testing Area [sf]	Number of Lanes	Skew [deg]	Deck Rating	Wearing Surface	Notes
13321	5658	2	15	9	9	Testing Area is the entire bridge.
16171	5901	2	0	9	9	Testing Area is the entire bridge.
16811	4126	2	30	9	9	Testing Area is the entire bridge.
28326	2092	2	0	9	9	Testing Area is the entire bridge.
32675	9678	2	2	8	8	Testing Area is the entire bridge.
33500	9506	3	0	8	8	Testing Area is the entire bridge.
44090	10300	2	45	8	8	Testing Area is the entire bridge.
17051	5249	2	20	9	9	The testing area is the westbound traffic lane along the entire length of the structure.
28430	12882	2	17	8	8	The testing area is the westbound traffic lane along the entire length of the structure.
44120	14972	2	30	8	8	Testing Area is the entire bridge.

APPENDIX B. PERCENTAGE RESULTS OF TESTING

Appendix B contains percentage result data from each entity for GPR, IE, IRT, automated sounding, and concrete cover thickness tests. Photographs of concrete cores taken by INDOT are also provided.

Table B.1 Detailed Percentage Deterioration Results for Air-launched GPR

Structure Number	Wearing Surface	Age of Deck	Age of Overlay	Deck Rating	Wearing Surface Rating	Consultant D			
						First Round		Second Round	
						Deterioration (s.f)	Deterioration (% of area surveyed)	Deterioration (s.f)	Deterioration (% of area surveyed)
1310	Latex Concrete	63	35	5	5	95.3	3.1	102.0	4.7
1347	Monolithic Concrete	32	-	7	6	141.4	2.3	211.0	3.5
4845	Monolithic Concrete	39	-	5	5	-	-	1615.0	10.7
4930	Latex Concrete	50	24	4	5	-	-	453.0	9.6
5230	Monolithic Concrete	3	-	5	6	348.2	2.6	-	-
8630	Latex Concrete	43	28	5	4	-	-	252.0	5.5
11940	Latex Concrete	38	20	7	7	169.7	3.0	-	-
16500	Epoxy Overlay	40	5	6	8	412.9	10.1	-	-
17940	Epoxy Overlay	8	8	6	7	872.8	9.6	1237.0	16.3
18770	Latex Concrete	30	2	5	5	186.0	1.7	-	-
18870	Latex Concrete	38	19	5	6	900.0	10.4	-	-
19640	Latex Concrete	40	15	6	6	463.2	6.5	527.0	8.7
20610	Latex Concrete	50	27	6	5	2582.8	6.5	392.0	9.1
22690	Latex Concrete	54	32	6	6	137.4	2.0	-	-
24220	Latex Concrete	49	19	6	6	-	-	766.0	18.0
31080	Monolithic Concrete	46	-	5	5	335.3	5.1	-	-
35520	Monolithic Concrete	26	-	7	6	847.5	12.1	-	-
37070	Monolithic Concrete	28	-	7	7	898.3	6.8	-	-
37100	Latex Concrete	62	27	5	5	84.8	1.5	-	-
37150	Epoxy Overlay	63	28	7	8	425.7	3.5	-	-
41810	Monolithic Concrete	4	-	6	6	328.3	9.1	-	-
41870	Monolithic Concrete	27	-	6	6	532.8	5.9	-	-
49200	Latex Concrete	53	5	5	6	2119.6	13.5	654.0	11.9
76140	Epoxy Overlay	32	8	7	8	219.0	3.7	-	-

Table B.1 Detailed Percentage Deterioration Results for Air-launched GPR (Continue)

Structure Number	Consultant G					Consultant J											
	First Round					Previous Test											
	Deterioration (% of area surveyed)					Deterioration (s.f)						Deterioration (% of area surveyed)					
	Poor & Severe	Severe	Poor	Fair	Good	Orange+Red	Red	Orange	Yellow	Green	Blue	Orange+Red	Red	Orange	Yellow	Green	Blue
1310	-	-	-	-	-	-	-	-	-	-	-	-	-	-	-	-	-
1347	-	-	-	-	-	-	-	-	-	-	-	-	-	-	-	-	-
4845	-	-	-	-	-	-	-	-	-	-	-	-	-	-	-	-	-
4930	-	-	-	-	-	-	-	-	-	-	-	-	-	-	-	-	-
5230	-	-	-	-	-	-	-	-	-	-	-	-	-	-	-	-	-
8630	-	-	-	-	-	-	-	-	-	-	-	-	-	-	-	-	-
11940	-	-	-	-	-	-	-	-	-	-	-	-	-	-	-	-	-
16500	19.3	4.5	14.8	70.4	10.3	-	-	-	-	-	-	-	-	-	-	-	-
17940	-	-	-	-	-	-	-	-	-	-	-	-	-	-	-	-	-
18770	15.8	5.5	10.3	77.1	7.0	1243.5	175.4	1068.1	2801.2	10849	7174.2	5.6	0.8	4.8	12.7	49.2	32.5
18870	-	-	-	-	-	-	-	-	-	-	-	-	-	-	-	-	-
19640	-	-	-	-	-	-	-	-	-	-	-	-	-	-	-	-	-
20610	-	-	-	-	-	1608.7	955.0	653.7	7313.3	10107.8	18534.6	2.1	0.3	1.8	19.9	27.5	50.5
22690	22.5	7.1	15.5	67.3	10.1	160.0	23.9	136.1	958.1	2889.8	2197.1	2.7	0.4	2.3	15.4	46.6	35.4
24220	-	-	-	-	-	-	-	-	-	-	-	-	-	-	-	-	-
31080	17.7	5.6	12.1	68.9	13.4	389.7	34.5	355.2	772.7	2548.4	2194.9	6.6	0.6	6.0	13.1	43.1	37.2
35520	17.7	6.4	11.3	66.9	15.4	441.6	26.5	415.1	1528.0	6507.2	13068.6	2.0	0.1	1.9	7.1	30.2	60.7
37070	13.9	3.2	10.6	73.7	12.4	68.5	0.1	68.4	333.3	975.1	5385.0	1.0	0.0	1.0	4.9	14.4	79.7
37100	15.8	6.8	9.0	71.7	12.5	104.0	21.5	82.5	154.2	701.6	1982.5	3.5	0.7	2.8	5.2	23.9	67.4
37150	17.9	5.2	12.7	69.4	12.7	283.5	40.8	242.7	573.0	2417.4	2732.2	4.7	0.7	4.0	9.5	40.3	45.5
41810	16.5	4.6	11.9	73.8	9.8	-	-	-	-	-	-	-	-	-	-	-	-
41870	13.0	2.9	10.1	69.7	17.3	321.1	55.8	265.3	864.5	3230.1	3798.2	3.9	0.7	3.2	10.5	39.3	46.3
49200	-	-	-	-	-	-	-	-	-	-	-	-	-	-	-	-	-
76140	-	-	-	-	-	-	-	-	-	-	-	-	-	-	-	-	-

Table B.2 Detailed Percentage Deterioration Results for Ground-coupled GPR

Structure Number	Wearing Surface	Age of Deck	Age of Overlay	Deck Rating	Wearing Surface Rating	Consultant D	
						First Round	
						Deterioration (% of area surveyed)	Deterioration (s.f)
1310	Latex Concrete	63	35	5	5	-	-
1347	Monolithic Concrete	32	-	7	6	-	-
4845	Monolithic Concrete	39	-	5	5	-	-
4930	Latex Concrete	50	24	4	5	-	-
8630	Latex Concrete	43	28	5	4	-	-
16500	Epoxy Overlay	40	5	6	8	8.9	360
17940	Epoxy Overlay	8	8	6	7	-	-
18770	Latex Concrete	30	2	5	5	7.2	644
19640	Latex Concrete	40	15	6	6	-	-
20610	Latex Concrete	50	27	6	5	-	-
22690	Latex Concrete	54	32	6	6	1.3	91
24220	Latex Concrete	49	19	6	6	-	-
31080	Monolithic Concrete	46	-	5	5	3.0	230
35520	Monolithic Concrete	26	-	7	6	9.6	561
37070	Monolithic Concrete	28	-	7	7	9.8	1366
37100	Latex Concrete	62	27	5	5	7.6	323
37150	Epoxy Overlay	63	28	7	8	3.2	442
41810	Monolithic Concrete	4	-	6	6	4.9	207
41870	Monolithic Concrete	27	-	6	6	5.9	484
49180	Monolithic Concrete	7	-	7	7	-	-

Table B.2 Detailed Percentage Deterioration Results for Ground-coupled GPR (Continue)

Structure Number	Consultant B										INDOT		Consultant H			
	First Round										First Round	Second Round	Second Round			
	Deterioration (% of area surveyed)					Deterioration (s.f)					Deterioration (% of area surveyed)		Deterioration (% of area surveyed)			
	Poor & Severe	Severe	Poor	Fair	Intact	Poor & Severe	Severe	Poor	Fair	Intact			High & Medium	High	Medium	Low
1310	-	-	-	-	-	-	-	-	-	-	-	-	62	3	59	38
1347	-	-	-	-	-	-	-	-	-	-	-	-	9	<1	9	91
4845	-	-	-	-	-	-	-	-	-	-	-	8.5	13	<1	13	87
4930	-	-	-	-	-	-	-	-	-	-	-	-	33	1	31	67
8630	-	-	-	-	-	-	-	-	-	-	-	-	6	<1	6	94
16500	6.1	1.7	4.4	16.4	77.6	254	71	183	682	3229	-	-	-	-	-	-
17940	-	-	-	-	-	-	-	-	-	-	-	-	10	<1	9	90
18770	6.3	3.3	3.0	11.2	82.5	612	321	291	1089	8019	-	-	-	-	-	-
19640	-	-	-	-	-	-	-	-	-	-	-	-	16	<1	16	84
20610	-	-	-	-	-	-	-	-	-	-	-	44.9	66	4	62	34
22690	5.7	2.2	3.5	10.1	84.2	386	149	237	685	5706	7.9	-	-	-	-	-
24220	-	-	-	-	-	-	-	-	-	-	-	38.7	40	4	37	60
31080	3.8	0.7	3.1	19.5	76.7	248	46	202	1273	5007	-	-	-	-	-	-
35520	3.6	0.9	2.7	15.5	80.8	431	108	323	1856	9673	-	-	-	-	-	-
37070	21.6	17.2	4.4	9.9	68.5	2900	2310	591	1329	9198	-	-	-	-	-	-
37100	25	17.0	8.0	13.1	62.0	1401	953	448	734	3475	-	-	-	-	-	-
37150	2.6	0.6	2.0	22.1	75.4	316	73	243	2682	9151	-	-	-	-	-	-
41810	5.5	2.1	3.4	16.5	78.0	200	76	124	601	2839	18.5	-	-	-	-	-
41870	7.3	6.0	1.3	5.5	87.2	663	545	118	499	7918	9	-	-	-	-	-
49180	-	-	-	-	-	-	-	-	-	-	-	-	4	<1	3	96

Table B.3 Detailed Percentage Delamination Results for IE

Structure Number	Wearing Surface	Age of Deck	Age of Overlay	Deck Rating	Wearing Surface Rating	INDOT	
						First Round	Second Round
						Delamination (% of area surveyed)	Delamination (% of area surveyed)
1310	Latex Concrete	63	35	5	5	-	16.0
1347	Monolithic Concrete	32	-	7	6	-	5.1
4845	Monolithic Concrete	39	-	5	5	-	7.9
4930	Latex Concrete	50	24	4	5	-	35.0
8630	Latex Concrete	43	28	5	4	-	12.0
16500	Epoxy Overlay	40	5	6	8	0.7	-
17940	Epoxy Overlay	8	8	6	7	-	4.8
18770	Latex Concrete	30	2	5	5	2.2	-
19640	Latex Concrete	40	15	6	6	-	14.0
20610	Latex Concrete	50	27	6	5	-	13.1
22690	Latex Concrete	54	32	6	6	9.6	-
24220	Latex Concrete	49	19	6	6	-	36.0
31080	Monolithic Concrete	46	-	5	5	19.5	-
35520	Monolithic Concrete	26	-	7	6	0.0	-
37070	Monolithic Concrete	28	-	7	7	3.8	-
37100	Latex Concrete	62	27	5	5	13.5	-
37150	Epoxy Overlay	63	28	7	8	7.5	-
41810	Monolithic Concrete	4	-	6	6	8.2	-
41870	Monolithic Concrete	27	-	6	6	3.8	-
49180	Monolithic Concrete	7	-	7	7	-	8.2

Table B.3 Detailed Percentage Delamination Results for IE (Continue)

Structure Number	Consultant F First Round Delamination (s.f)							
	Red+Orange +Dark Bule	Near Surface Delamination	Likely Top Delamination or Thickened Concrete	Possible Top Delamination or Thickened Concrete	Possible Bottom Delamination or Thin Concrete	Possible Bottom Delamination or Internal Cracking	Deep Top Delamination or Internal Cracking	Sound Condition Concrete
1310	632	90	105	177	31	112	437	2151
1347	192	99	71	110	264	154	22	4786
4845	269	45	194	1727	729	759	30	11404
4930	1653	975	605	510	78	95	73	3272
8630	-	-	-	-	-	-	-	-
16500	-	-	-	-	-	-	-	-
17940	-	-	-	-	-	-	-	-
18770	-	-	-	-	-	-	-	-
19640	-	-	-	-	-	-	-	-
20610	-	-	-	-	-	-	-	-
22690	-	-	-	-	-	-	-	-
24220	1578	851	341	303	46	245	386	1977
31080	-	-	-	-	-	-	-	-
35520	-	-	-	-	-	-	-	-
37070	-	-	-	-	-	-	-	-
37100	-	-	-	-	-	-	-	-
37150	-	-	-	-	-	-	-	-
41810	-	-	-	-	-	-	-	-
41870	-	-	-	-	-	-	-	-
49180	-	-	-	-	-	-	-	-

Table B.3 Detailed Percentage Delamination Results for IE (Continue)

Structure Number	Consultant F First Round Delamination (% of area surveyed) Red+Orange +Dark Bule	Near Surface Delamination	Likely Top Delamination or Thickened Concrete	Possible Top Delamination or Thickened Concrete	Possible Bottom Delamination or Thin Concrete	Possible Bottom Delamination or Internal Cracking	Deep Top Delamination or Internal Cracking	Sound Condition Concrete
1310	20.4	2.9	3.4	5.7	1.0	3.6	14.1	69.4
1347	3.5	1.8	1.3	2.0	4.8	2.8	0.4	87.1
4845	1.8	0.3	1.3	11.6	4.9	5.1	0.2	76.6
4930	29.5	17.4	10.8	9.1	1.4	1.7	1.3	58.4
8630	-	-	-	-	-	-	-	-
16500	-	-	-	-	-	-	-	-
17940	-	-	-	-	-	-	-	-
18770	-	-	-	-	-	-	-	-
19640	-	-	-	-	-	-	-	-
20610	-	-	-	-	-	-	-	-
22690	-	-	-	-	-	-	-	-
24220	38.0	20.5	8.2	7.3	1.1	5.9	9.3	47.6
31080	-	-	-	-	-	-	-	-
35520	-	-	-	-	-	-	-	-
37070	-	-	-	-	-	-	-	-
37100	-	-	-	-	-	-	-	-
37150	-	-	-	-	-	-	-	-
41810	-	-	-	-	-	-	-	-
41870	-	-	-	-	-	-	-	-
49180	-	-	-	-	-	-	-	-

Table B.4 Detailed Percentage Delamination Results for IRT

	First Round														
						Consultant D				Consultant E		Consultant B		Consultant I	
Structure Number	Wearing Surface	Age of Deck	Age of Overlay	Deck Rating	Wearing Surface Rating	Aerial IRT		Vehicle IRT		Vehicle IRT		Drone IRT		Pole IRT	
						Delamination (% of area surveyed)	Delamination (s.f)	Delamination (% of area surveyed)	Delamination (s.f)	Delamination (% of area surveyed)	Delamination (s.f)	Delamination (% of area surveyed)	Delamination (s.f)	Delaminatio n (% of area surveyed)	Delamination (s.f)
01310	Latex Concrete	36	35	5	5	-	-	1.3	39	0.2	6	-	-	-	-
01347	Monolithic Concrete	32	-	7	6	-	-	1.5	90	0.2	12	-	-	-	-
17940	Epoxy Overlay	8	8	6	7	-	-	0.7	62	0.2	21	-	-	-	-
19640	Latex Concrete	40	15	6	6	-	-	1.4	101	3.3	233	-	-	-	-
20610	Latex Concrete	50	27	6	5	-	-	6.3	2512	4.5	1766	-	-	-	-
49200	Latex Concrete	53	5	5	6	-	-	1.6	260	1.1	179	-	-	-	-
37070	Monolithic Concrete	28	-	7	7	0	82	0.7	95	0.1	18	0	0	6	637
37100	Latex Concrete	62	27	5	5	0	12	0	0	0.4	24	0	0	-	-
42190	Latex Concrete	50	27	6	6	-	-	-	-	-	-	-	-	5	668
05230	Monolithic Concrete	3	-	5	6	-	-	2.3	317	0.9	119	-	-	-	-
11940	Latex Concrete	38	20	7	7	-	-	1.9	104	0.4	132	-	-	-	-
16500	Epoxy Overlay	40	5	6	8	-	-	2.9	119	0.8	32	0	0	-	-
18770	Latex Concrete	30	2	5	5	-	-	1.3	139	1.3	349	0	0	-	-
18870	Latex Concrete	38	19	5	6	-	-	2.3	260	0	0	-	-	-	-
22690	Latex Concrete	54	32	6	6	-	-	2.7	183	2.3	152	1.4	92	-	-
31080	Monolithic Concrete	46	-	5	5	-	-	14.4	941	4	258	5.7	376	-	-
35520	Monolithic Concrete	26	-	7	6	-	-	0	0	0.1	11	0	0	-	-
37150	Epoxy Overlay	63	28	7	8	-	-	0.2	25	0.3	31	0	0	-	-
41810	Monolithic Concrete	4	-	6	6	-	-	0	0	0.2	6	0.4	15	-	-

Table B.4 Detailed Percentage Delamination Results for IRT (Continue)

	First Round														
						Consultant D				Consultant E		Consultant B		Consultant I	
						Aerial IRT		Vehicle IRT		Vehicle IRT		Drone IRT		Pole IRT	
Structure Number	Wearing Surface	Age of Deck	Age of Overlay	Deck Rating	Wearing Surface Rating	Delamination (% of area surveyed)	Delamination (s.f)	Delamination (% of area surveyed)	Delamination (s.f)	Delamination (% of area surveyed)	Delamination (s.f)	Delamination (% of area surveyed)	Delamination (s.f)	Delamination (% of area surveyed)	Delamination (s.f)
41870	Monolithic Concrete	27	-	6	6	-	-	0.4	40	0.3	29	0.2	19	-	-
76140	Epoxy Overlay	32	8	7	8	-	-	1.1	67	0	0	-	-	-	-
36070	Monolithic Concrete	5		8	8	0	30	-	-	-	-	-	-	-	-
36130	Monolithic Concrete	25		7	7	0	6	-	-	-	-	-	-	-	-
36150	Monolithic Concrete	25		7	7	0	82	-	-	-	-	-	-	-	-
36170	Monolithic Concrete	25		7	7	1	74	-	-	-	-	-	-	-	-
36190	Monolithic Concrete	25		7	7	0	0	-	-	-	-	-	-	-	-
36210	Monolithic Concrete	25		6	6	1	60	-	-	-	-	-	-	-	-
36230	Monolithic Concrete	25		7	7	0	0	-	-	-	-	-	-	-	-
36250	Monolithic Concrete	25		7	7	0	36	-	-	-	-	-	-	-	-
36270	Monolithic Concrete	25		7	6	0	196	-	-	-	-	-	-	-	-
36290	Monolithic Concrete	25		7	7	1	120	-	-	-	-	-	-	-	-
36320	Monolithic Concrete	3		6	6	4	271	-	-	-	-	-	-	-	-
36330	Monolithic Concrete	7		7	7	1	46	-	-	-	-	-	-	-	-
36520	Latex Concrete	48	19	6	5	3	284	-	-	-	-	-	-	-	-
36660	Latex Concrete	50	2	6	6	2	9654	-	-	-	-	-	-	-	-
36680	Latex Concrete	52	3	6	8	0	0	-	-	-	-	-	-	-	-
36690	Latex Concrete	52	3	5	8	0	0	-	-	-	-	-	-	-	-
36700	Latex Concrete	53	3	6	8	1	104	-	-	-	-	-	-	-	-
36720	Monolithic Concrete	17		7	7	0	0	-	-	-	-	-	-	-	-
36730	Monolithic Concrete	17		7	7	0	17	-	-	-	-	-	-	-	-
36740	Monolithic Concrete	17		7	7	0	5	-	-	-	-	-	-	-	-
36750	Monolithic Concrete	17		6	6	1	78	-	-	-	-	-	-	-	-

Table B.4 Detailed Percentage Delamination Results for IRT (Continue)

	First Round														
						Consultant D				Consultant E		Consultant B		Consultant I	
						Aerial IRT		Vehicle IRT		Vehicle IRT		Drone IRT		Pole IRT	
Structure Number	Wearing Surface	Age of Deck	Age of Overlay	Deck Rating	Wearing Surface Rating	Delamination (% of area surveyed)	Delamination (s.f)	Delamination (% of area surveyed)	Delamination (s.f)	Delamination (% of area surveyed)	Delamination (s.f)	Delamination (% of area surveyed)	Delamination (s.f)	Delaminatio n (% of area surveyed)	Delamination (s.f)
36760	Monolithic Concrete	17		7	7	0	0	-	-	-	-	-	-	-	-
36770	Monolithic Concrete	17		7	6	0	41	-	-	-	-	-	-	-	-
36780	Monolithic Concrete	17		7	6	0	0	-	-	-	-	-	-	-	-
36790	Monolithic Concrete	26		7	7	0	33	-	-	-	-	-	-	-	-
36800	Monolithic Concrete	26		6	6	0	43	-	-	-	-	-	-	-	-
36850	Monolithic Concrete	26		7	7	1	97	-	-	-	-	-	-	-	-
36880	Monolithic Concrete	22		7	7	0	34	-	-	-	-	-	-	-	-
36900	Monolithic Concrete	22		7	7	0	17	-	-	-	-	-	-	-	-
36920	Monolithic Concrete	22		6	6	0	106	-	-	-	-	-	-	-	-
36950	Monolithic Concrete	22		7	9	1	113	-	-	-	-	-	-	-	-
36980	Monolithic Concrete	22		7	7	0	23	-	-	-	-	-	-	-	-
37030	Monolithic Concrete	28		6	6	2	144	-	-	-	-	-	-	-	-
37060	Latex Concrete	62	28	4	4	2	23	-	-	-	-	-	-	-	-
37120	Latex Concrete	62	28	5	6	0	30	-	-	-	-	-	-	-	-
50720	Monolithic Concrete	28		7	7	1	126	-	-	-	-	-	-	-	-

Table B.4 Detailed Percentage Delamination Results for IRT (Continue)

Structure Number	Wearing Surface	Age of Deck	Age of Overlay	Deck Rating	Wearing Surface Rating	Second Round							
						Consultant D		Consultant E		Consultant C		Consultant I	
						Aerial IRT		Vehicle IRT		Drone IRT		Pole IRT	
						Delamination (% of area surveyed)	Delamination (s.f)	Delamination (% of area surveyed)	Delamination (s.f)	Delamination (% of area surveyed)	Delamination (s.f)	Delamination (% of area surveyed)	Delamination (s.f)
01310	Latex Concrete	36	35	5	5	-	-	1	31.7	5.5	169.4	24	760
01347	Monolithic Concrete	32	-	7	6	-	-	4.3	258.9	<0.1	21.7	2	96
17940	Epoxy Overlay	8	8	6	7	-	-	7.6	740.7	2.2	206.4	-	-
19640	Latex Concrete	40	15	6	6	-	-	8.6	614.4	5	358.4	-	-
20610	Latex Concrete	50	27	6	5	-	-	4.7	651	2.9	364	-	-
49200	Latex Concrete	53	5	5	6	-	-	4.5	249.8	5.1	230.7	5	830
04845	Monolithic Concrete	39	-	5	5	8	1287	3.2	544.6	<0.1	14	-	-
04930	Latex Concrete	50	24	4	5	4	262	2	128.1	7.1	422.4	-	-
08630	Latex Concrete	43	28	5	4	-	-	1.5	81.5	1.3	66.7	-	-
24220	Latex Concrete	48	18	6	6	-	-	3.6	297.4	3.6	170.3	15	709
04708	Latex Concrete	41	16	7	6	2	53	-	-	-	-	-	-
04710	Monolithic Concrete	31	-	7	7	2	45	-	-	-	-	-	-
04730	Latex Concrete	37	6	7	6	1	49	-	-	-	-	-	-
04740	Latex Concrete	38	6	7	7	<1.0	26	-	-	-	-	-	-
04750	Monolithic Concrete	32	-	7	7	<1.0	10	-	-	-	-	-	-
04770	Monolithic Concrete	38	-	7	7	N/A	N/A	-	-	-	-	-	-
04820	Latex Concrete	46	19	6	6	3	105	-	-	-	-	-	-
04830	Latex Concrete	46	19	7	7	2	77	-	-	-	-	-	-
04859	Latex Concrete	58	33	6	6	13	417	-	-	-	-	-	-
04860	Monolithic Concrete	29	-	6	6	2	56	-	-	-	-	-	-
04910	Latex Concrete	36	8	7	6	1	37	-	-	-	-	-	-
04920	Monolithic Concrete	32	-	7	7	<1.0	9	-	-	-	-	-	-

Table B.4 Detailed Percentage Delamination Results for IRT (Continue)

Structure Number	Wearing Surface	Age of Deck	Age of Overlay	Deck Rating	Wearing Surface Rating	Second Round							
						Consultant D		Consultant E		Consultant C		Consultant I	
						Aerial IRT		Vehicle IRT		Drone IRT		Pole IRT	
						Delamination (% of area surveyed)	Delamination (s.f)	Delamination (% of area surveyed)	Delamination (s.f)	Delamination (% of area surveyed)	Delamination (s.f)	Delamination (% of area surveyed)	Delamination (s.f)
39620	Monolithic Concrete	29	-	7	7	<1.0	101	-	-	-	-	-	-
39630	Monolithic Concrete	29	-	7	6	2	267	-	-	-	-	-	-
39640	Monolithic Concrete	29	-	7	6	<1.0	27	-	-	-	-	-	-
39650	Monolithic Concrete	29	-	6	6	<1.0	40	-	-	-	-	-	-
39740	Latex Concrete	59	6	6	7	2	66	-	-	-	-	-	-
39770	Latex Concrete	59	21	6	6	2	44	-	-	-	-	-	-
39780	Latex Concrete	59	21	6	5	<1.0	11	-	-	-	-	-	-
39850	Monolithic Concrete	9	-	6	6	<1.0	25	-	-	-	-	-	-
39860	Monolithic Concrete	9	-	7	7	1	32	-	-	-	-	-	-
39870	Monolithic Concrete	59	26	6	6	1	77	-	-	-	-	-	-
39880	Monolithic Concrete	26	-	7	7	3	136	-	-	-	-	-	-
39910	Latex Concrete	59	26	6	7	2	313	-	-	-	-	-	-
39920	Latex Concrete	59	26	6	6	2	302	-	-	-	-	-	-
40000	Monolithic Concrete	12	-	7	7	2	377	-	-	-	-	-	-
40010	Monolithic Concrete	29	-	6	6	1	270	-	-	-	-	-	-
40130	Latex Concrete	59	29	5	5	2	78	-	-	-	-	-	-
40140	Latex Concrete	59	29	5	4	<1.0	7	-	-	-	-	-	-
40220	Latex Concrete	29	18	7	6	2	175	-	-	-	-	-	-
40230	Latex Concrete	29	18	7	6	1	100	-	-	-	-	-	-
40330	Latex Concrete	30	17	7	7	<1.0	55	-	-	-	-	-	-
40340	Latex Concrete	30	18	6	5	2	200	-	-	-	-	-	-
40350	Latex Concrete	30	19	7	6	1	167	-	-	-	-	-	-
40360	Latex Concrete	30	19	7	6	1	154	-	-	-	-	-	-

Table B.5 Detailed Percentage Delamination Results for AS

Structure Number	Wearing Surface	Age of Deck	Age of Overlay	Deck Rating	Wearing Surface Rating	Consultant B										Consultant A	
						First Round										Second Round	
						Delamination (s.f)					Delamination (% of area surveyed)					Delamination (s.f)	Delamination (% of area surveyed)
						Poor & Severe	Severe	Poor	Fair	Intact	Poor & Severe	Severe	Poor	Fair	Intact		
1310	Latex Concrete	63	35	5	5	-	-	-	-	-	-	-	-	-	-	12	0.4
1347	Monolithic Concrete	32	-	7	6	-	-	-	-	-	-	-	-	-	-	4	0.1
4845	Monolithic Concrete	39	-	5	5	-	-	-	-	-	-	-	-	-	-	29	0.2
4930	Latex Concrete	50	24	4	5	-	-	-	-	-	-	-	-	-	-	33	0.6
8630	Latex Concrete	43	28	5	4	-	-	-	-	-	-	-	-	-	-	1	0.0
16500	Epoxy Overlay	40	5	6	8	13	4	8	354	3791	0.3	0.1	0.2	8.5	91.1	1	0.0
17940	Epoxy Overlay	8	8	6	7	-	-	-	-	-	-	-	-	-	-	0	0.0
18770	Latex Concrete	30	2	5	5	29	10	19	622	9069	0.3	0.1	0.2	6.4	93.3	0	0.0
19640	Latex Concrete	40	15	6	6	-	-	-	-	-	-	-	-	-	-	262	3.9
20610	Latex Concrete	50	27	6	5	-	-	-	-	-	-	-	-	-	-	1322	3.4
22690	Latex Concrete	54	32	6	6	27	7	20	806	5943	0.4	0.1	0.3	11.9	87.7	192	2.9
24220	Latex Concrete	49	19	6	6	-	-	-	-	-	-	-	-	-	-	244	5.4
31080	Monolithic Concrete	46	-	5	5	98	26	72	575	5856	1.5	0.4	1.1	8.8	89.7	-	-
35520	Monolithic Concrete	26	-	7	6	48	24	24	766	11170	0.4	0.2	0.2	6.4	93.3	5	0.0
37070	Monolithic Concrete	28	-	7	7	27	13	13	712	12702	0.2	0.1	0.1	5.3	94.6	4	0.0
37100	Latex Concrete	62	27	5	5	11	6	6	656	4943	0.2	0.1	0.1	11.7	88.2	70	1.3
37150	Epoxy Overlay	63	28	7	8	49	12	36	935	11153	0.4	0.1	0.3	7.7	91.9	202	1.8
41810	Monolithic Concrete	4	-	6	6	55	26	29	328	3261	1.5	0.7	0.8	9.0	89.6	28	0.9
41870	Monolithic Concrete	27	-	6	6	9	0	9	835	8236	0.1	0.0	0.1	9.2	90.7	105	1.2
49200	Latex Concrete	53	5	5	6	-	-	-	-	-	-	-	-	-	-	65	1.1

Table B.6 Detailed Concrete Cover Thickness Results for PL and NL Bridges

Structure Number	Wearing Surface	Age of Deck	Age of Overlay	Deck Rating	Wearing Surface Rating	Consultant C	Consultant H													
						First Round	Second Round													
						Avg. Concrete Cover (in.)	Avg. Concrete Cover (in.)	Interpreted Concrete Cover Thickness Percentages												
								Concrete Cover Thickness (in.)												
								0.5-1	1-1.5	1.5-2	2-2.5	2.5-3	3-3.5	3.5-4	4-4.5	4.5-5	5-5.5	5.5-6	6-6.5	6.5-7	7-7.5
1310	Latex Concrete	63	35	5	5	-	5	-	-	-	-	-	<1	4	18	27	27	18	4	<1	<1
1347	Monolithic Concrete	32	-	7	6	-	3.1	-	-	-	3	43	42	12	1	<1	-	-	-	-	-
4845	Monolithic Concrete	39	-	5	5	-	2.3	<1	9	28	32	20	8	2	<1	-	-	-	-	-	-
4930	Latex Concrete	50	24	4	5	-	3.4		<1	<1	4	15	38	30	10	2	-	-	-	-	-
8630	Latex Concrete	43	28	5	4	-	2	<1	<1	8	44	41	6	<1	-	-	-	-	-	-	-
16500	Epoxy Overlay	40	5	6	8	3.8	-	-	-	-	-	-	-	-	-	-	-	-	-	-	-
17940	Epoxy Overlay	8	8	6	7	-	1.9	<1	1	10	51	27	9	2	-	-	-	-	-	-	-
18770	Latex Concrete	30	2	5	5	2.8	-	-	-	-	-	-	-	-	-	-	-	-	-	-	-
19640	Latex Concrete	40	15	6	6	-	1.5	<1	4	45	44	6	1	<1	-	-	-	-	-	-	-
20610	Latex Concrete	50	27	6	5	-	3.3		<1	<1	<1	19	54	24	2	<1	-	-	-	-	-
22690	Latex Concrete	54	32	6	6	4.5	-	-	-	-	-	-	-	-	-	-	-	-	-	-	-
24220	Latex Concrete	49	19	6	6	-	4.1	-	-	-	<1	1	6	34	39	17	3	<1	-	-	-
31080	Monolithic Concrete	46	-	5	5	3.6	-	-	-	-	-	-	-	-	-	-	-	-	-	-	-
35520	Monolithic Concrete	26	-	7	6	3.1	-	-	-	-	-	-	-	-	-	-	-	-	-	-	-
37070	Monolithic Concrete	28	-	7	7	2.5	-	-	-	-	-	-	-	-	-	-	-	-	-	-	-
37100	Latex Concrete	62	27	5	5	6.3	-	-	-	-	-	-	-	-	-	-	-	-	-	-	-
37150	Epoxy Overlay	63	28	7	8	2.3	-	-	-	-	-	-	-	-	-	-	-	-	-	-	-
41810	Monolithic Concrete	4	-	6	6	3.5	-	-	-	-	-	-	-	-	-	-	-	-	-	-	-
41870	Monolithic Concrete	27	-	6	6	2.5	-	-	-	-	-	-	-	-	-	-	-	-	-	-	-
49180	Monolithic Concrete	7	-	7	7	-	2.7	<1	11	9	23	24	17	12	3	<1	-	-	-	-	-

Table B.6 Detailed Concrete Cover Thickness Results for PL and NL Bridges (Continue)

Structure Number	Consultant B																			
	First Round																			
	Avg. Concrete Cover (in.)	Interpreted Concrete Cover Thickness Percentages																		
		Concrete Cover Thickness (in.)																		
		1.5-2	2-2.5	2.5-3	3-3.5	3.5-4	4-4.5	4.5-5	5-5.5	5.5-6	6-6.5	6.5-7	7-7.5	7.5-8	8-8.5	8.5-9	9-9.5	9.5-10	10-10.5	10.5-11
1310	-	-	-	-	-	-	-	-	-	-	-	-	-	-	-	-	-	-	-	-
1347	-	-	-	-	-	-	-	-	-	-	-	-	-	-	-	-	-	-	-	-
4845	-	-	-	-	-	-	-	-	-	-	-	-	-	-	-	-	-	-	-	-
4930	-	-	-	-	-	-	-	-	-	-	-	-	-	-	-	-	-	-	-	-
8630	-	-	-	-	-	-	-	-	-	-	-	-	-	-	-	-	-	-	-	-
16500	4.3	-	-	4	12	22	38	12	6	3	2	1	1	-	-	-	-	-	-	-
17940	-	-	-	-	-	-	-	-	-	-	-	-	-	-	-	-	-	-	-	-
18770	3	-	8	52	26	10	1	1	1	0	1	-	-	-	-	-	-	-	-	-
19640	-	-	-	-	-	-	-	-	-	-	-	-	-	-	-	-	-	-	-	-
20610	-	-	-	-	-	-	-	-	-	-	-	-	-	-	-	-	-	-	-	-
22690	4.8	-	-	-	-	1	24	50	22	3	-	-	-	-	-	-	-	-	-	-
24220	-	-	-	-	-	-	-	-	-	-	-	-	-	-	-	-	-	-	-	-
31080	4.1	-	-	1	3	35	43	16	2	-	-	-	-	-	-	-	-	-	-	-
35520	4.2	-	-	-	5	33	36	14	5	2	1	1	1	-	-	-	-	-	-	-
37070	2.8	5	14	48	24	8	1	-	-	-	-	-	-	-	-	-	-	-	-	-
37100	7.6	-	-	-	-	-	-	2	4	7	8	14	18	15	12	7	6	3	4	1
37150	2.8	4	28	45	18	5	1	-	-	-	-	-	-	-	-	-	-	-	-	-
41810	4.4	-	-	-	1	16	40	25	13	3	1	-	-	-	-	-	-	-	-	-
41870	2.9	1	12	53	31	3	-	-	-	-	-	-	-	-	-	-	-	-	-	-
49180	-	-	-	-	-	-	-	-	-	-	-	-	-	-	-	-	-	-	-	-

Table B.6 Detailed Concrete Cover Thickness Results for PL and NL Bridges (Continue)

Structure Number	Consultant G																					
	First Round																					
	Avg. Concrete Cover (in.)	Interpreted Concrete Cover Thickness Percentages																				
		Concrete Cover Thickness (in.)																				
		1-1.5	1.5-2	2-2.5	2.5-3	3-3.5	3.5-4	4-4.5	4.5-5	5-5.5	5.5-6	6-6.5	6.5-7	7-7.5	7.5-8	8-8.5	8.5-9	9-9.5	9.5-10	10-10.5	10.5-11	>11
1310	-	-	-	-	-	-	-	-	-	-	-	-	-	-	-	-	-	-	-	-	-	-
1347	-	-	-	-	-	-	-	-	-	-	-	-	-	-	-	-	-	-	-	-	-	-
4845	-	-	-	-	-	-	-	-	-	-	-	-	-	-	-	-	-	-	-	-	-	-
4930	-	-	-	-	-	-	-	-	-	-	-	-	-	-	-	-	-	-	-	-	-	-
8630	-	-	-	-	-	-	-	-	-	-	-	-	-	-	-	-	-	-	-	-	-	-
16500	4.9	-	-	0.1	0.4	2.2	7.7	17.9	29.0	27.4	9.7	2.9	2.4	0.3	-	-	-	-	-	-	-	-
17940	-	-	-	-	-	-	-	-	-	-	-	-	-	-	-	-	-	-	-	-	-	-
18770	3.3	-	1.9	14.2	46.5	18.4	4.1	4.1	2.2	0.8	0.8	0.5	1.1	0.5	0.9	1.2	0.6	0.6	0.6	0.5	0.4	0.1
19640	-	-	-	-	-	-	-	-	-	-	-	-	-	-	-	-	-	-	-	-	-	-
20610	-	-	-	-	-	-	-	-	-	-	-	-	-	-	-	-	-	-	-	-	-	-
22690	4.7	-	-	-	-	-	0.9	36.1	48.8	11.7	1.9	0.5	-	-	-	-	-	-	-	-	-	-
24220	-	-	-	-	-	-	-	-	-	-	-	-	-	-	-	-	-	-	-	-	-	-
31080	4	-	-	-	0.0	7.1	48.6	31.7	9.6	2.3	0.6	-	-	-	-	-	-	-	-	-	-	-
35520	4.1	-	-	-	-	6.1	46.1	35.2	7.7	2.7	2.1	0.2	-	-	-	-	-	-	-	-	-	-
37070	2.9	0.0	0.2	9.8	52.5	32.4	5.0	0.2	-	-	-	-	-	-	-	-	-	-	-	-	-	-
37100	6	-	-	-	-	-	2.0	3.7	9.7	14.1	24.0	14.6	15.6	5.5	4.6	4.6	1.3	0.1	-	-	-	-
37150	2.8	0.0	4.6	25.8	39.0	22.3	7.2	0.9	0.1	0.0	-	-	-	-	-	-	-	-	-	-	-	-
41810	3.3	-	-	1.1	25.8	48.5	19.0	3.4	1.2	0.3	0.3	0.2	0.1	-	-	-	-	-	-	-	-	-
41870	2.9	0.1	1.6	8.6	51.5	32.9	5.1	0.2	-	-	-	-	-	-	-	-	-	-	-	-	-	-
49180	-	-	-	-	-	-	-	-	-	-	-	-	-	-	-	-	-	-	-	-	-	-

Table B.7 Detailed Concrete Cover Thickness Results for Newer Bridges

Structure Number	Wearing Surface	Age of Deck	Age of Overlay	Deck Rating	Wearing Surface Rating	Consultant D First Round Avg. Concrete Cover (in.)
16171	Monolithic Concrete	3	-	9	9	3.1
16811	Monolithic Concrete	3	-	9	9	3.5
17051	Monolithic Concrete	3	-	9	9	2.9
28326	Monolithic Concrete	4	-	8	8	2.5
28430	Monolithic Concrete	5	-	8	8	3.4
32675	Monolithic Concrete	3	-	8	8	3.2
33500	Monolithic Concrete	3	-	9	9	2.7
44090	Monolithic Concrete	2	-	8	8	2.9
44120	Monolithic Concrete	4	-	8	8	3.1

C1

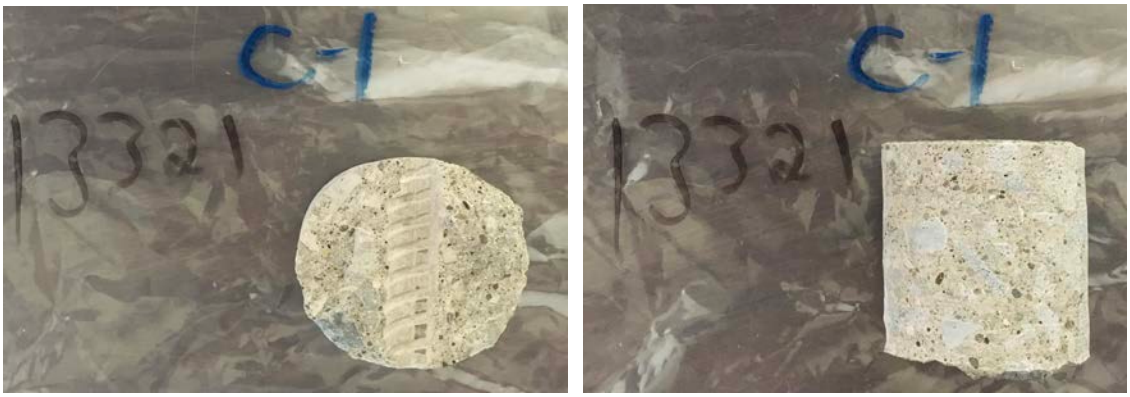

C2

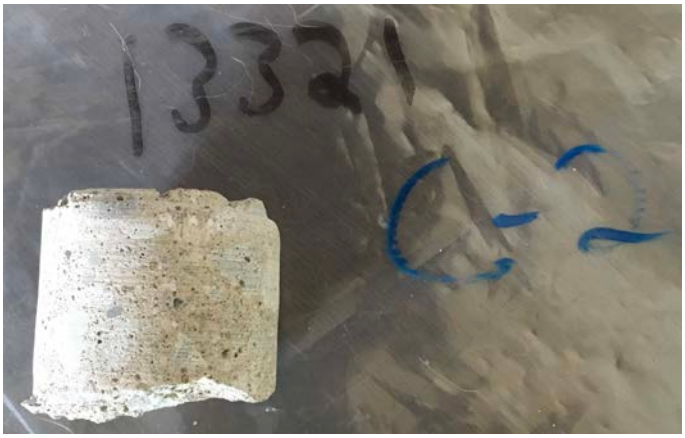

C3

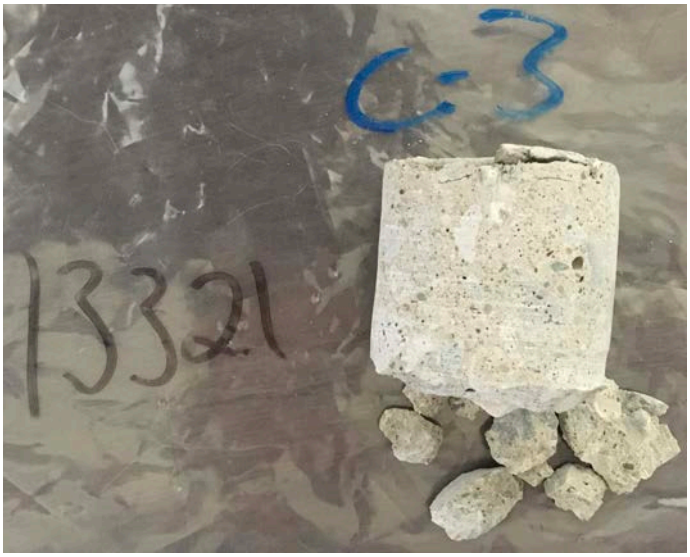

Figure B.1 Photos of the concrete cores for Bridges 13321 (Newer Bridge).

C1

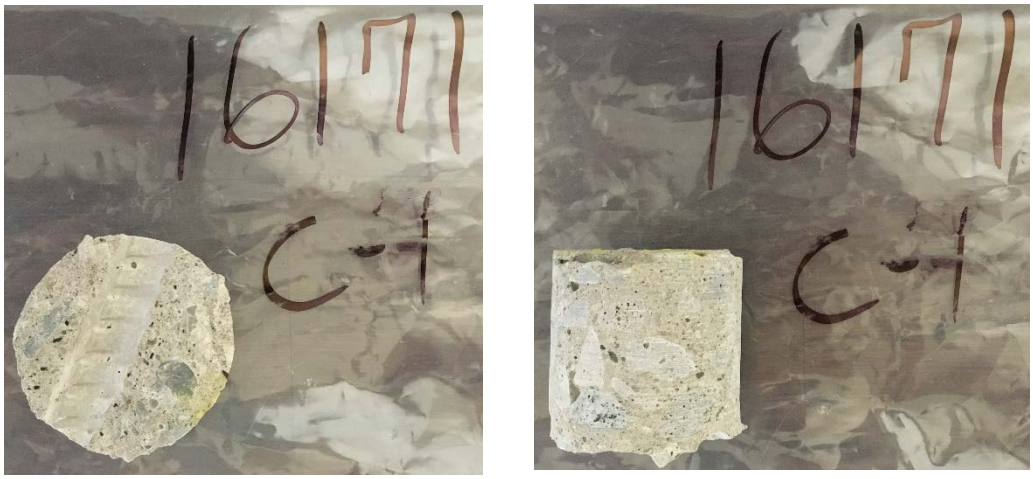

C2

C3

Figure B.2 Photos of the concrete cores for Bridges 16171 (Newer Bridge)

C1

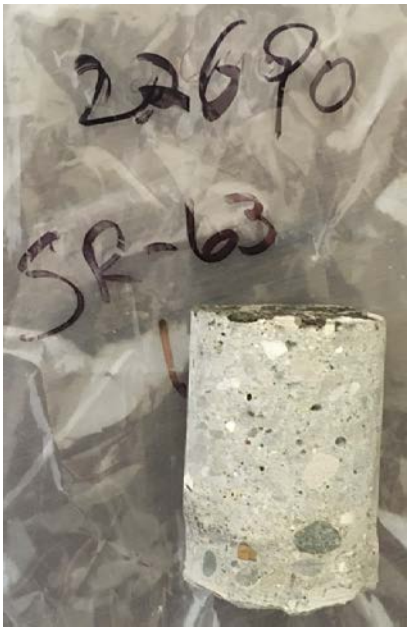

C2

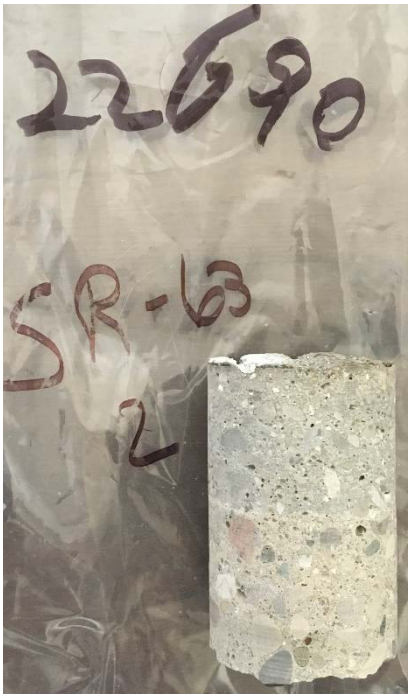

C3

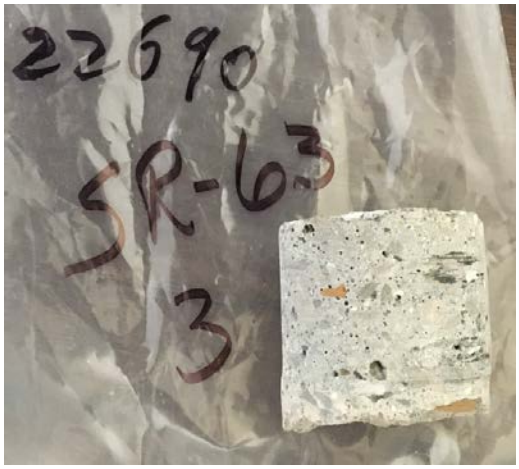

C4

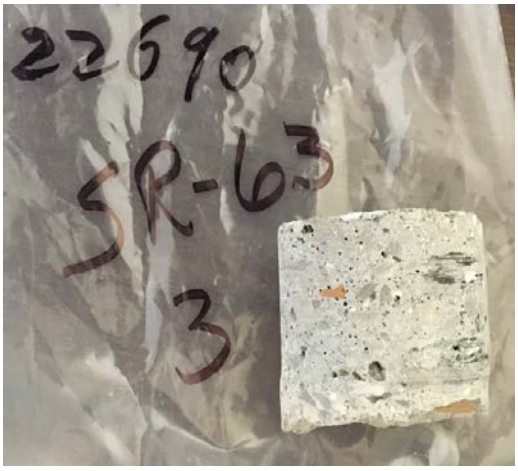

Figure B.3 Photos of the concrete cores for Bridges 22690 (First Round).

C1

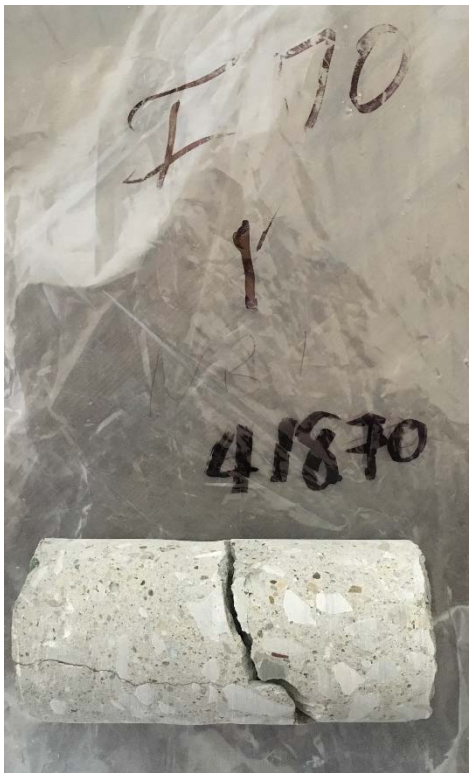

C2

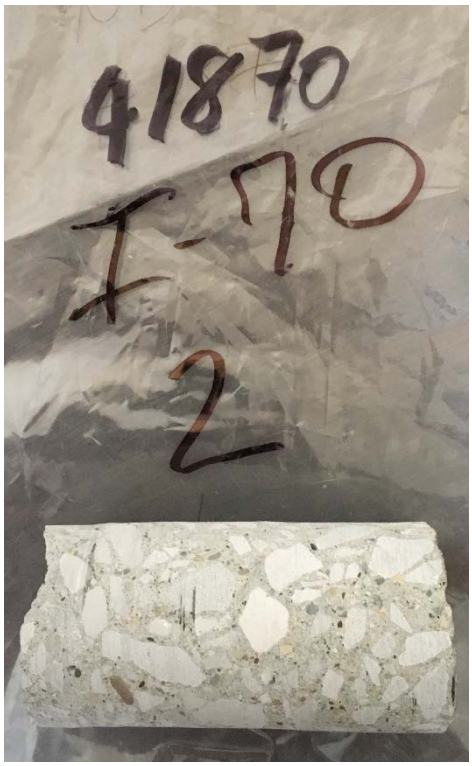

C3

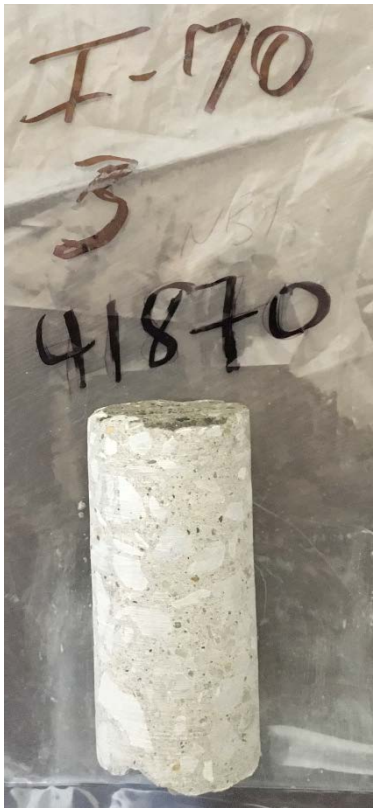

C4

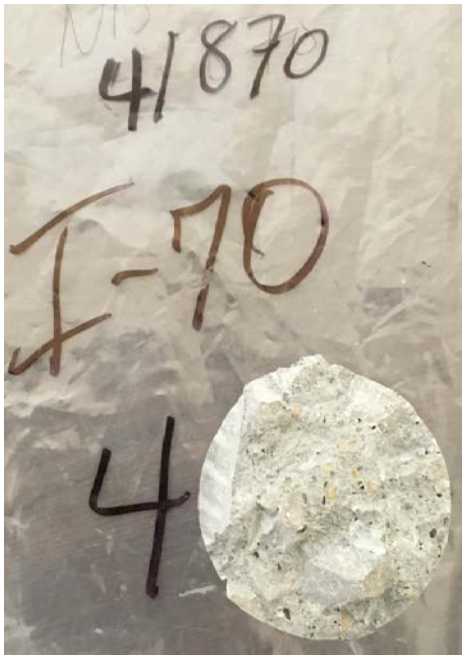

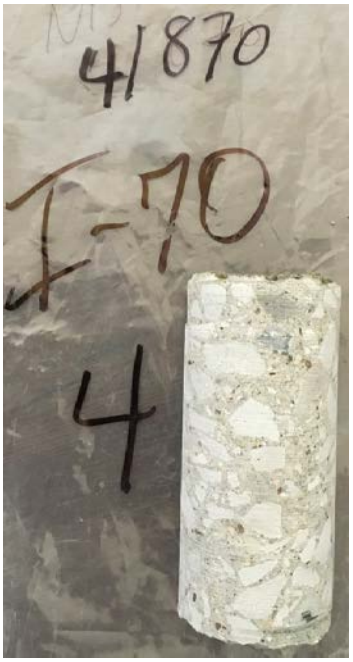

Figure B.4 Photos of the concrete cores for Bridges 41870 (First Round).

C1

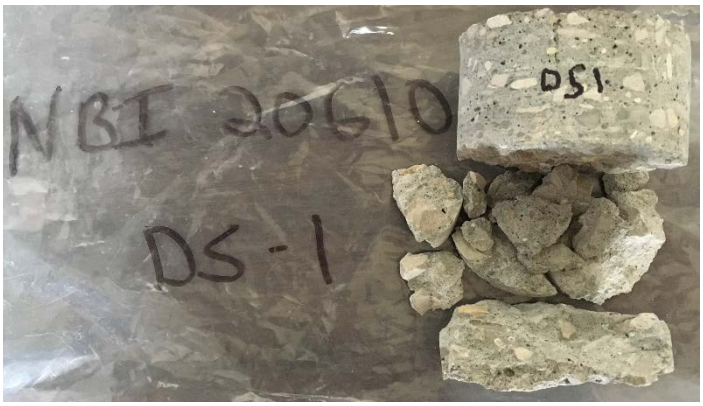

C2

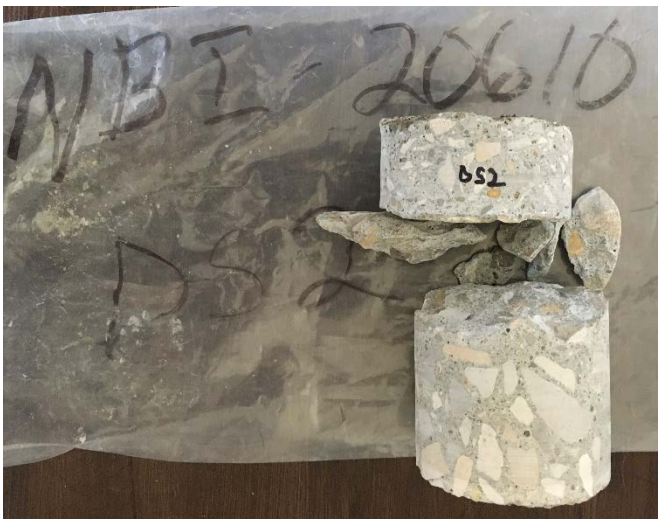

C3

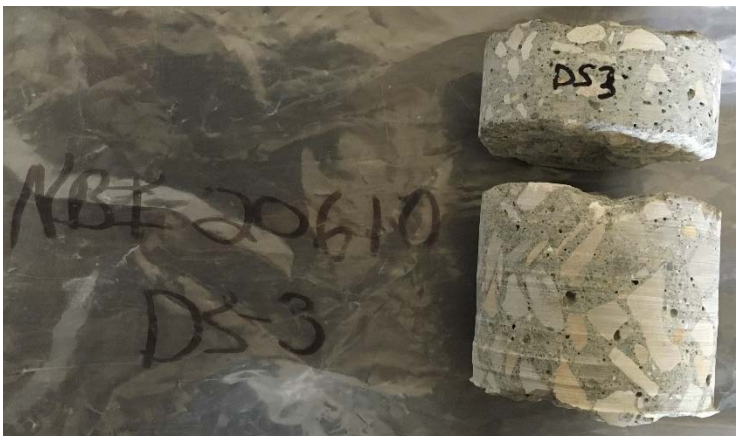

Figure B.5 Photos of the concrete cores for Bridges 20610 (Second Round).

C1

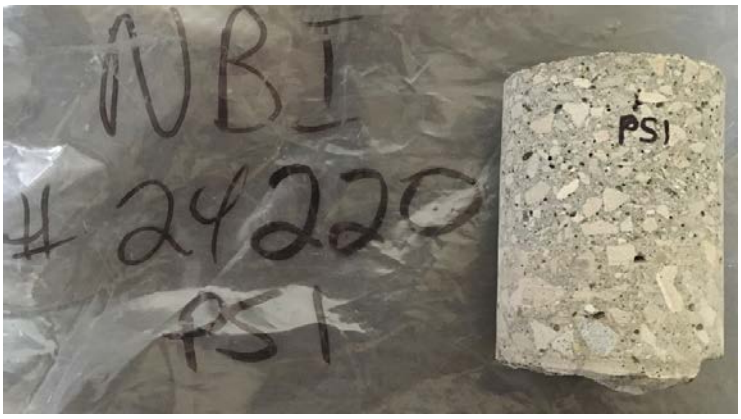

C2

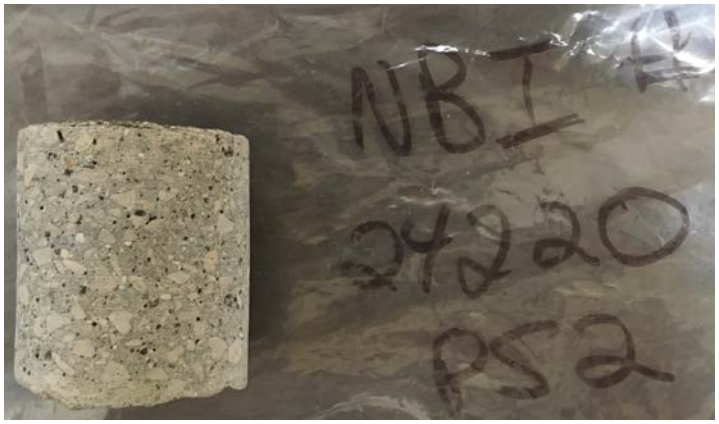

C3

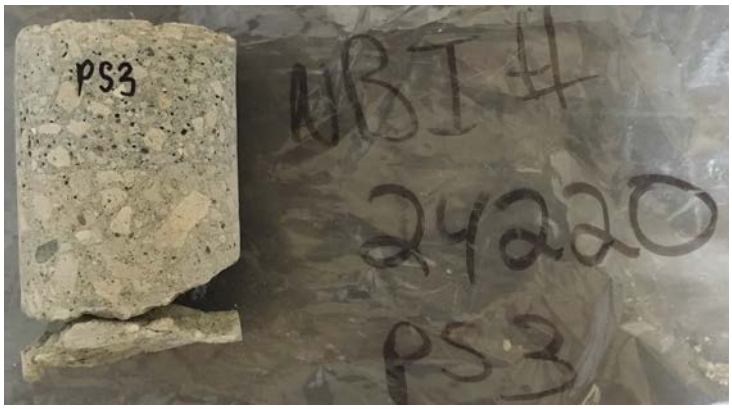

Figure B.6 Photos of the concrete cores for Bridges 24220 (Second Round).

APPENDIX C. RESULT MAPS OF TESTING

C.1 Air-Launched GPR

C.1.1 Consultant D–First Round: (Result maps contain both air-launched GPR and IRT results)

Bridge 01310

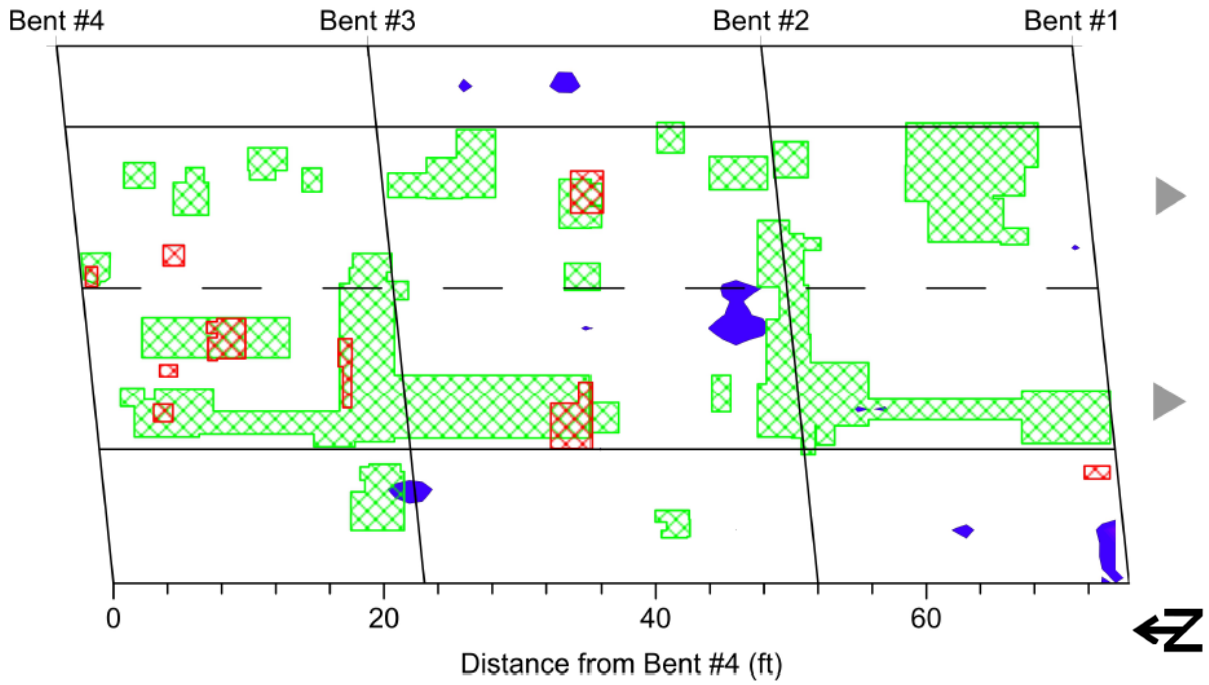

Bridge 01347

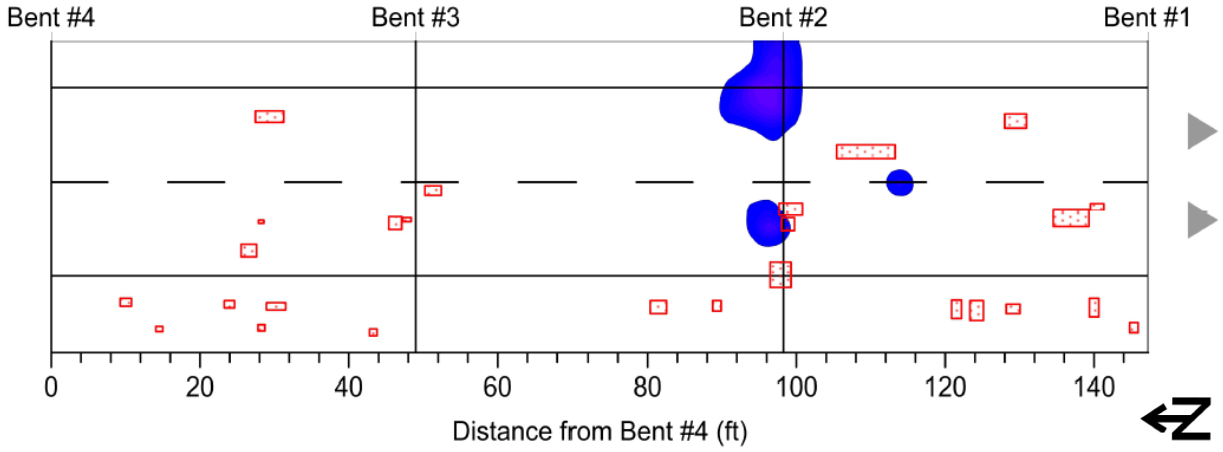

Bridge 05230

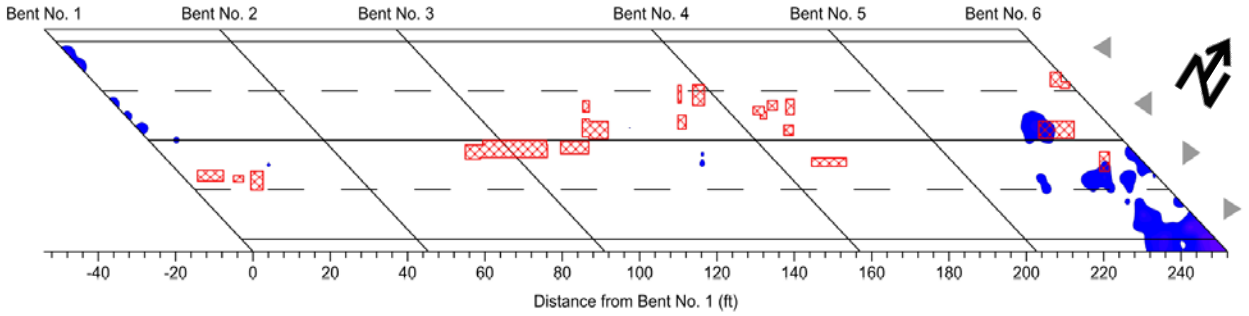

Bridge 11940

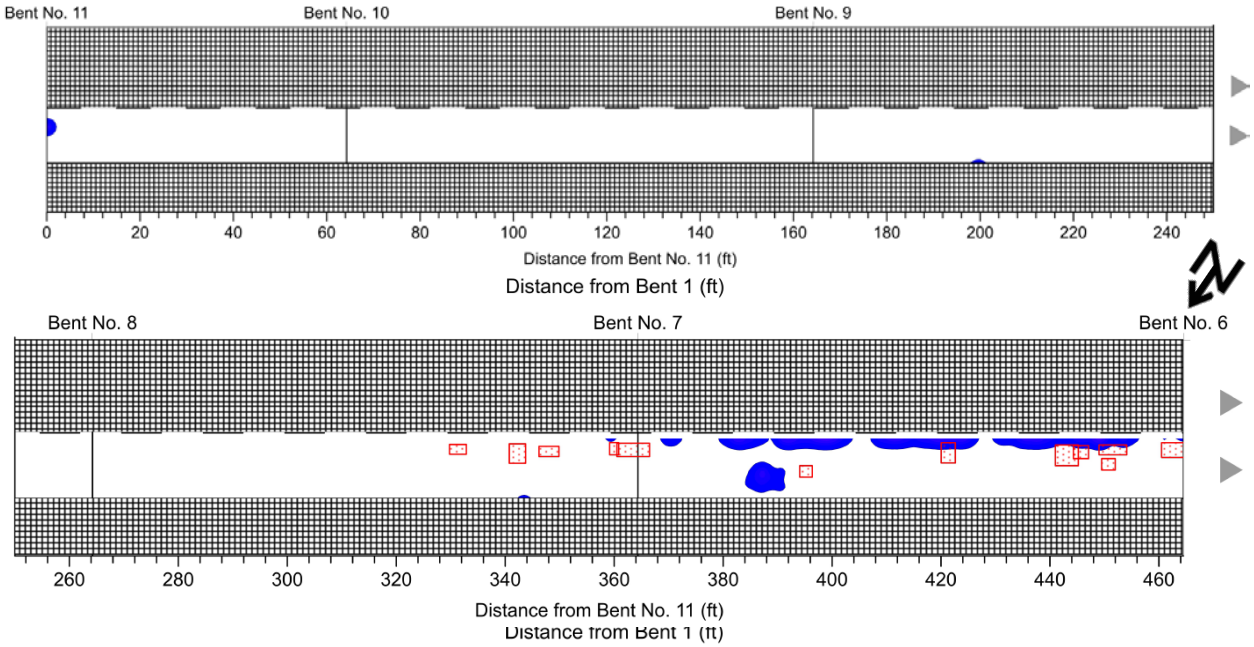

Bridge 16500

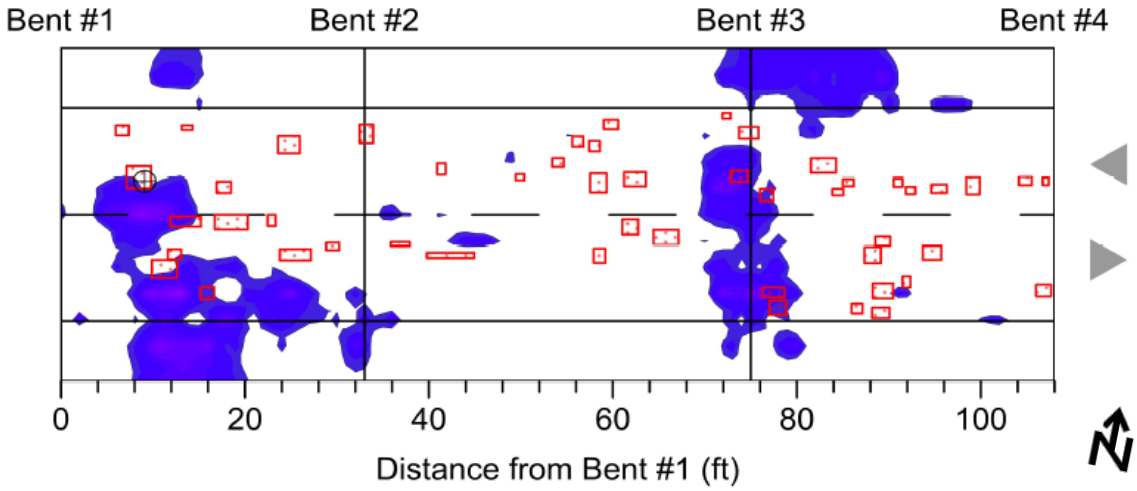

Bridge 17940

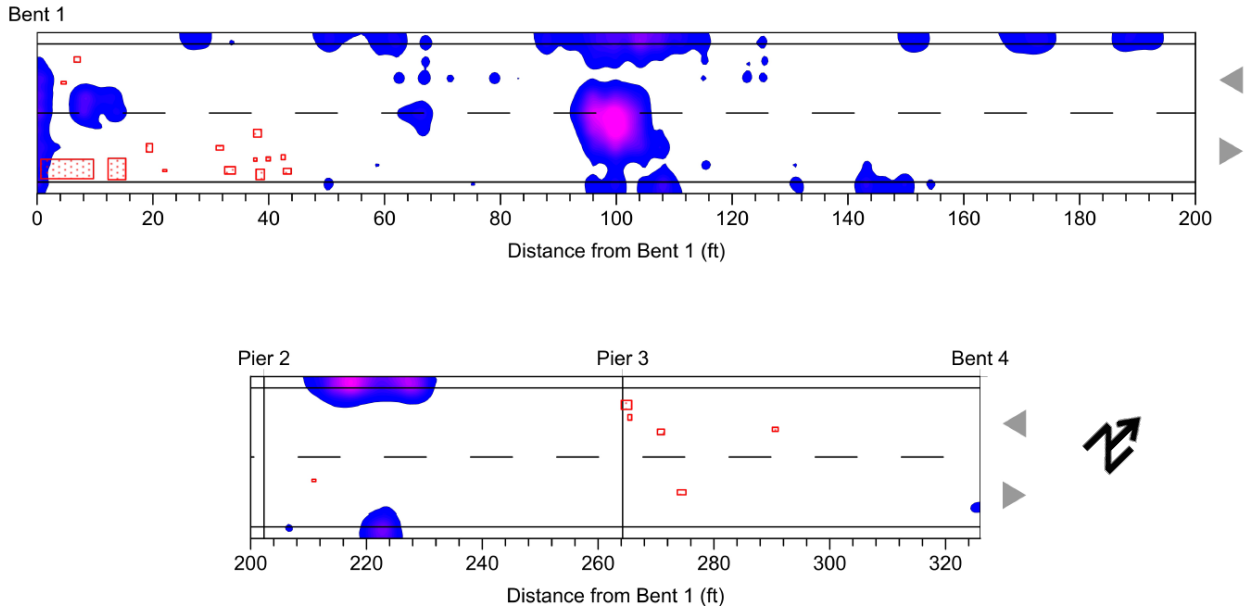

Bridge 18770

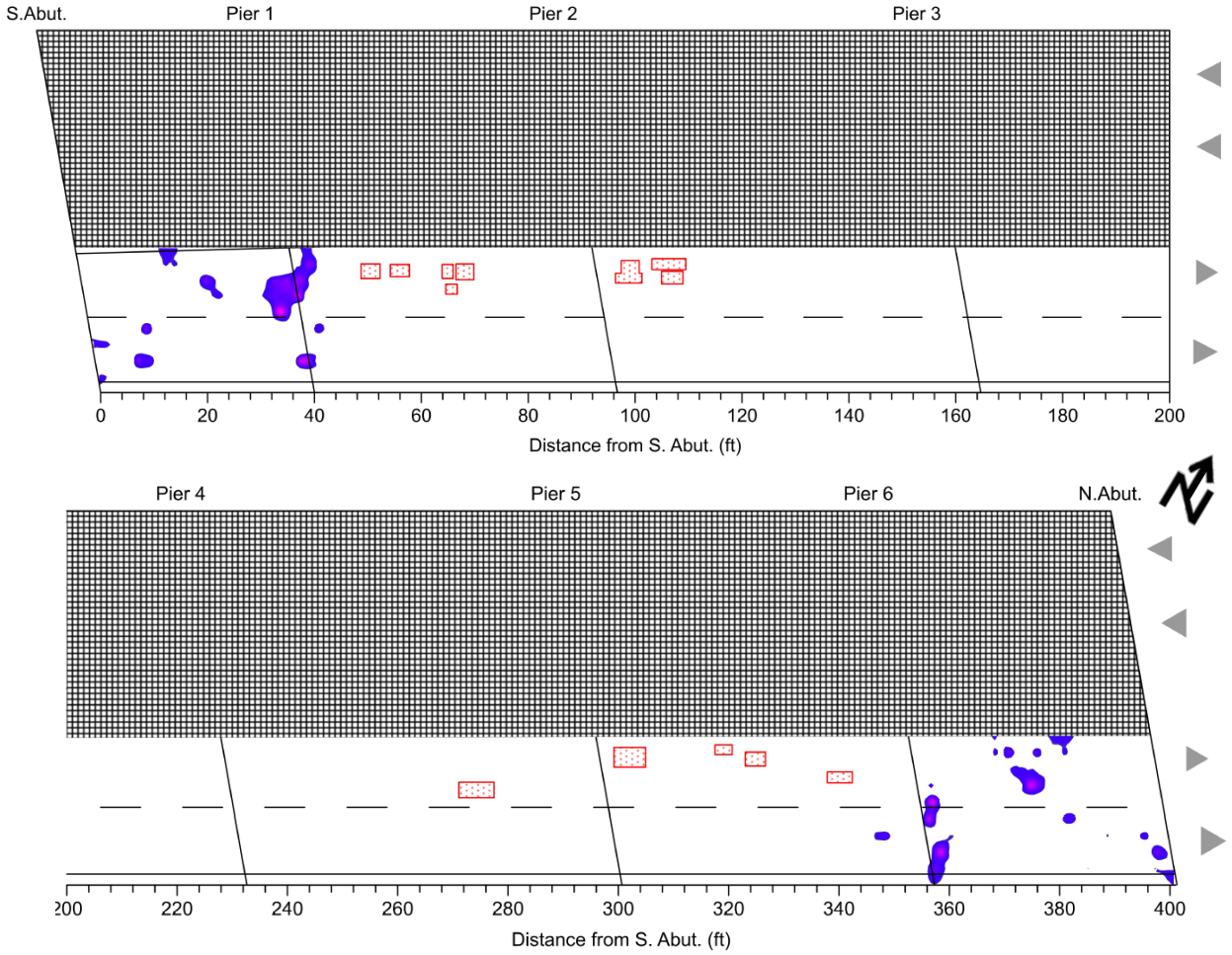

Bridge 18870

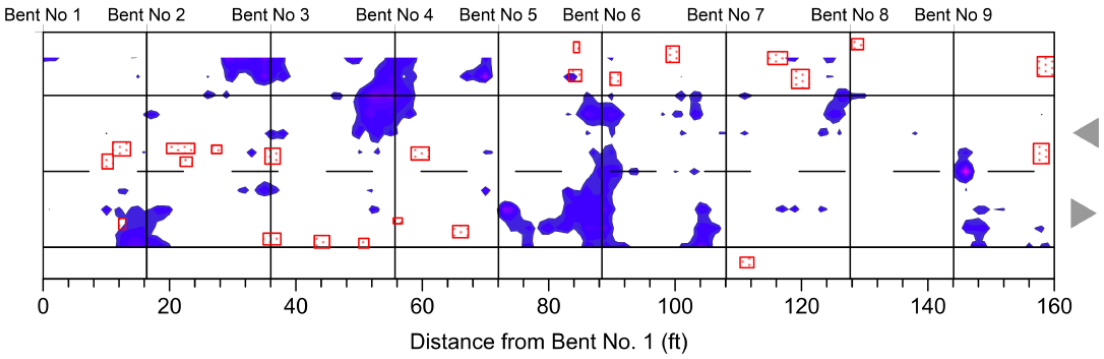

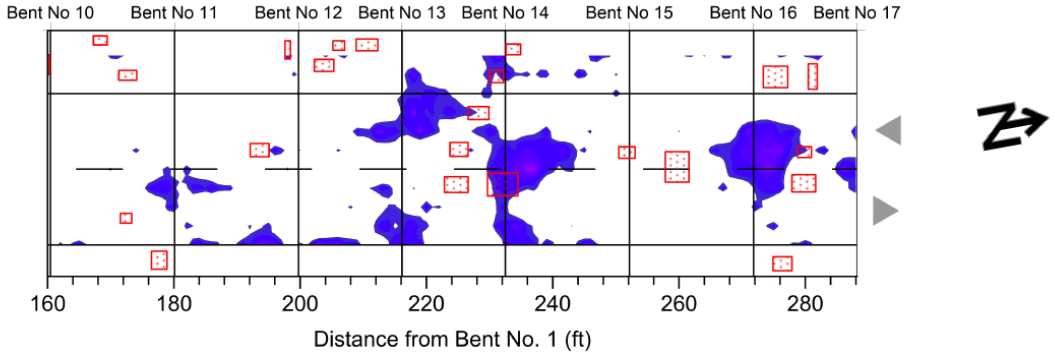

Bridge 19640

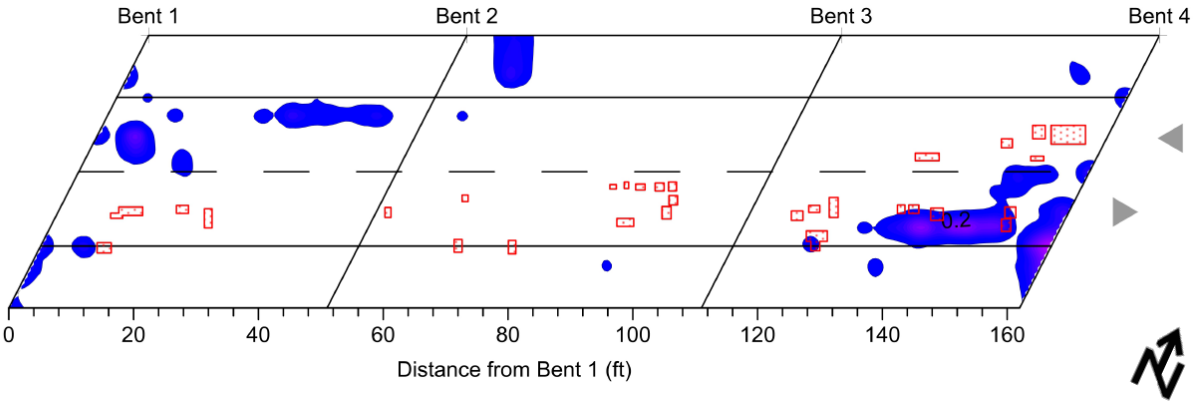

Bridge 20610

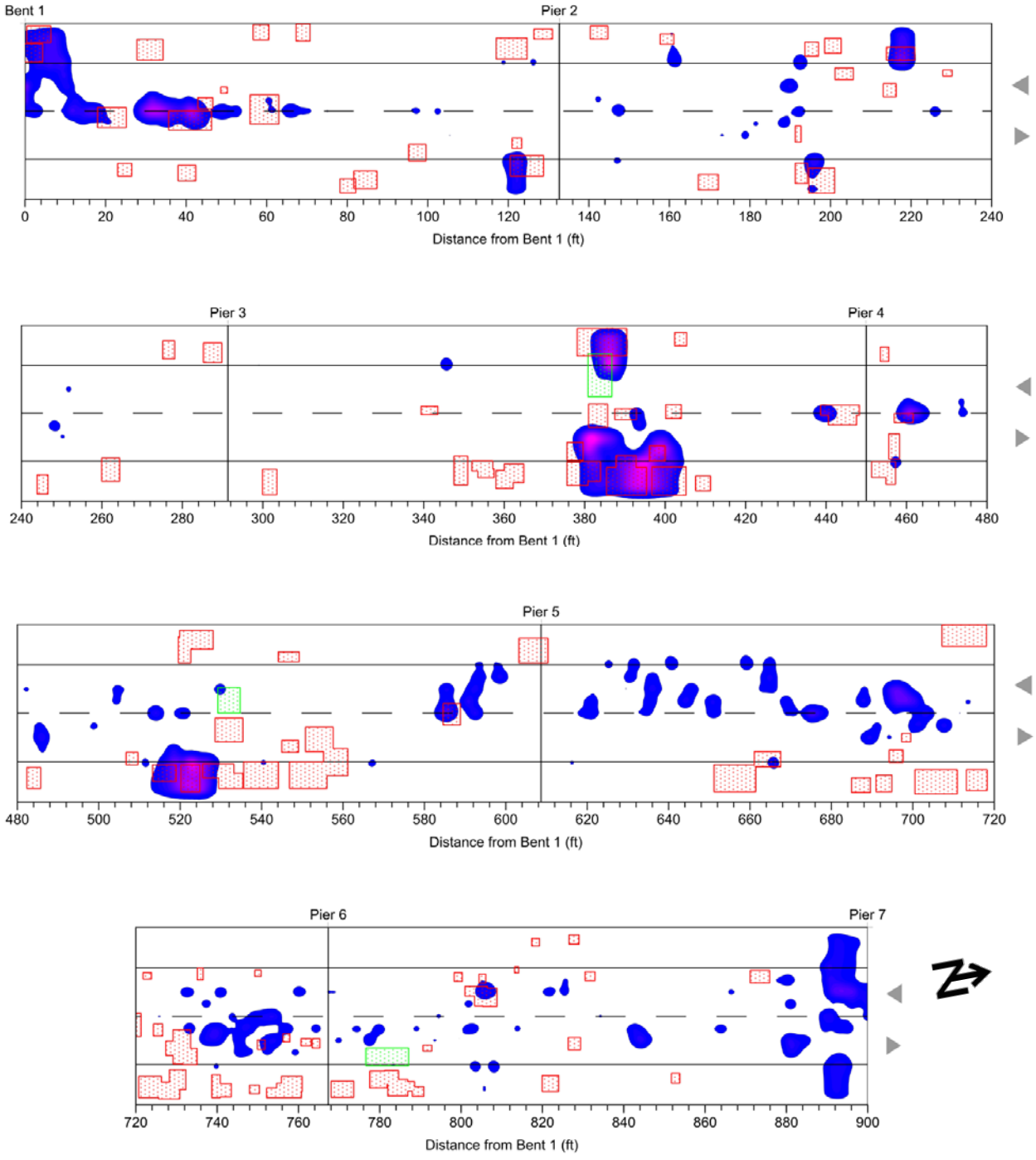

Bridge 22690

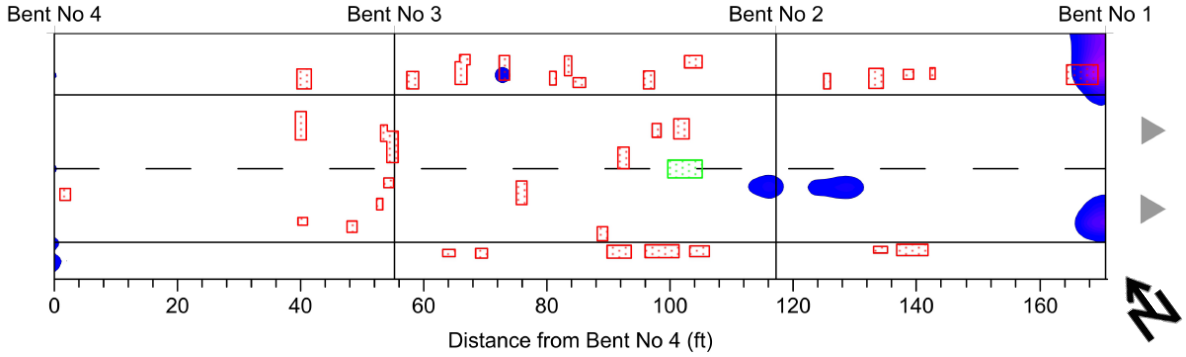

Bridge 31080

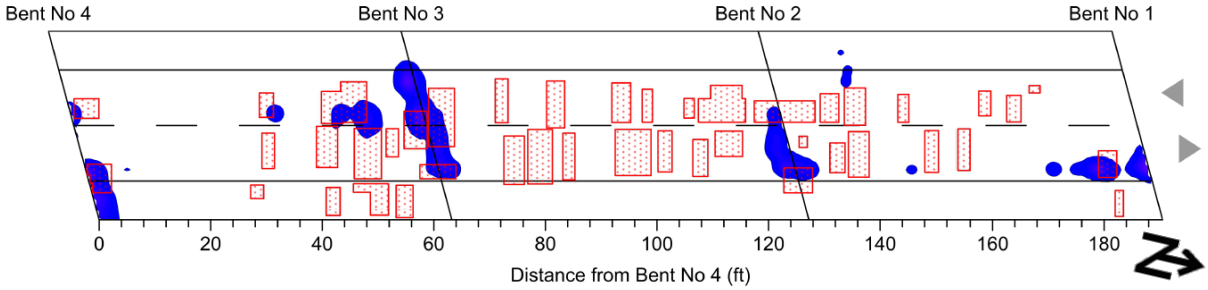

Bridge 35520

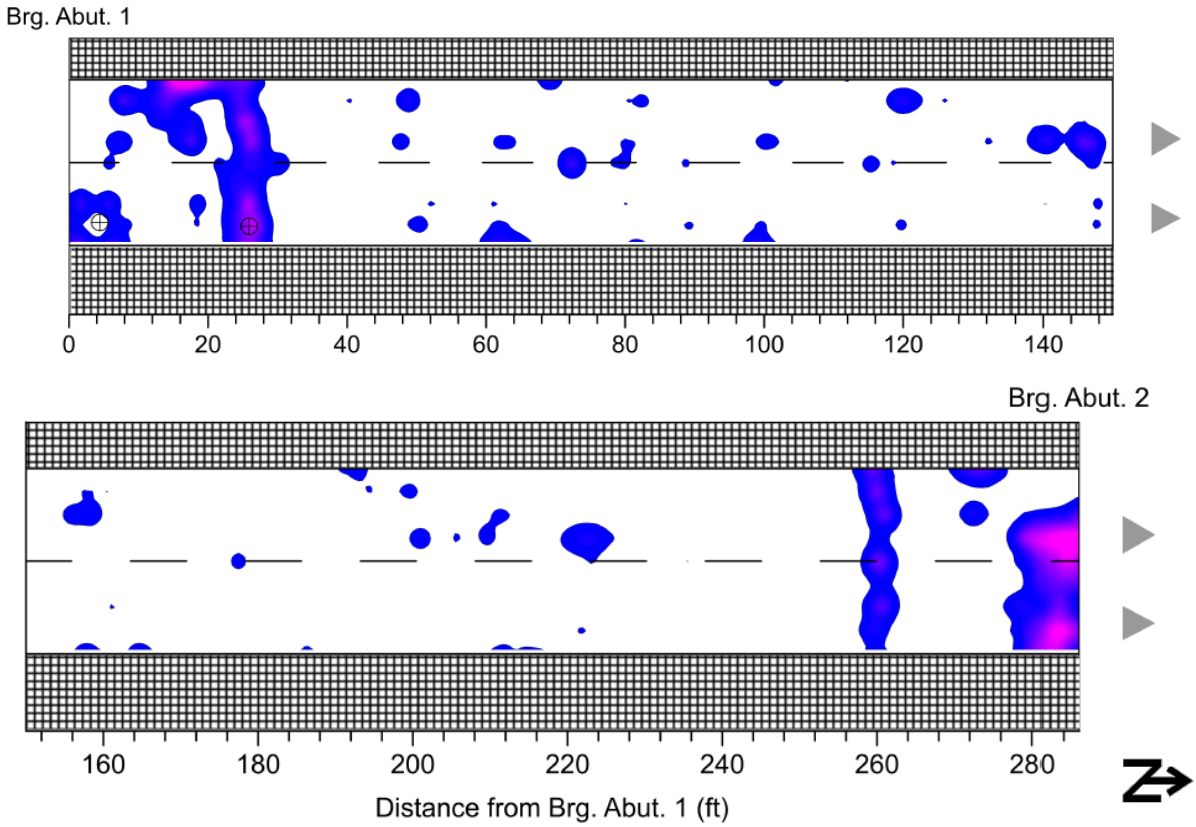

Bridge 37070

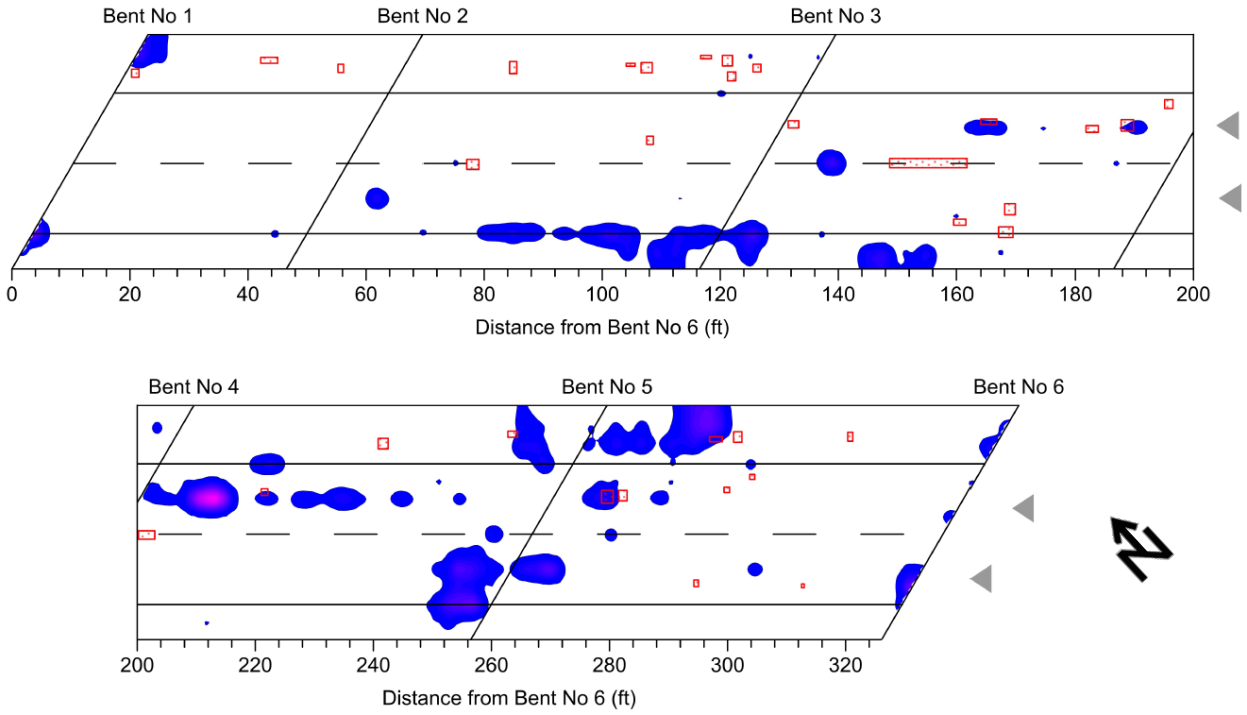

Bridge 37100

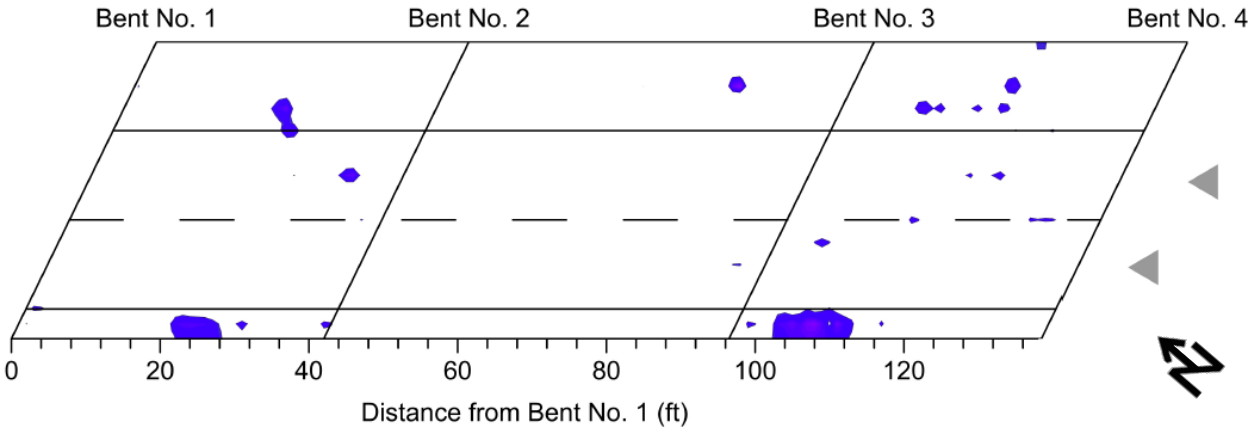

Bridge 37150

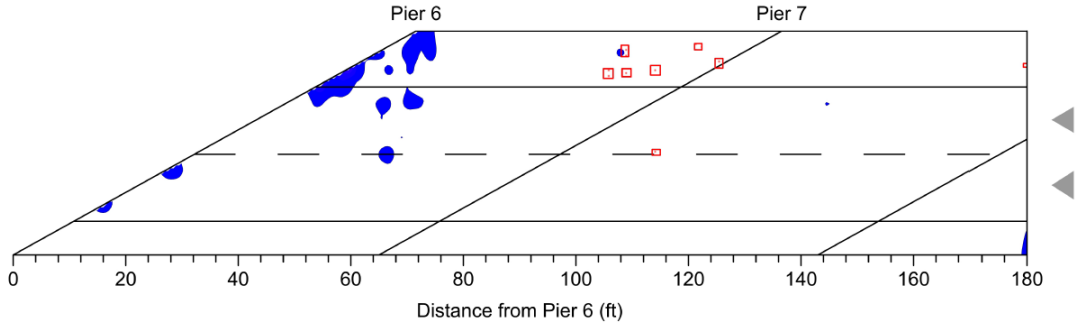

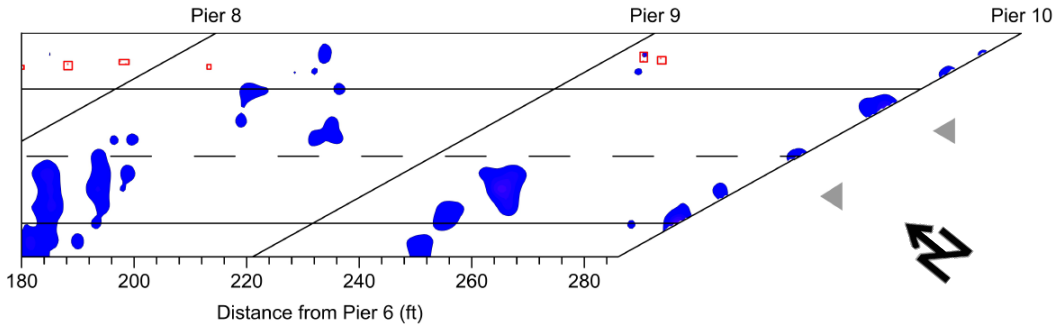

Bridge 41810

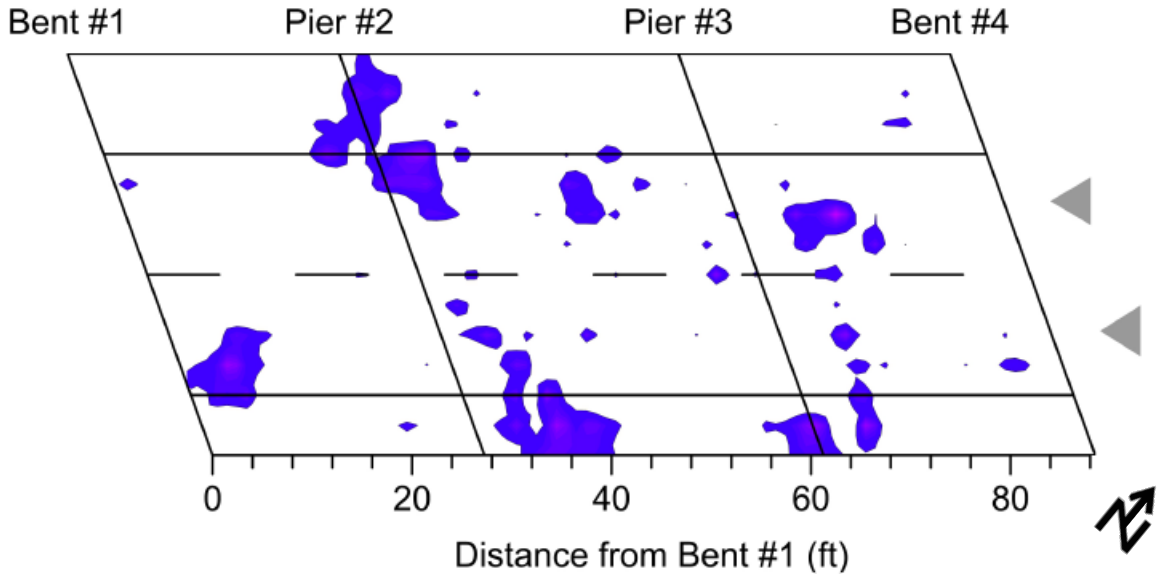

Bridge 41870

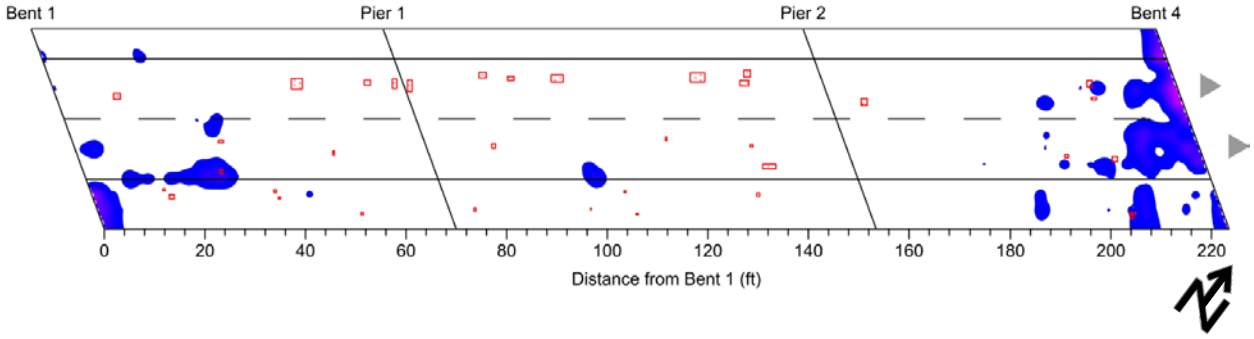

Bridge 49200

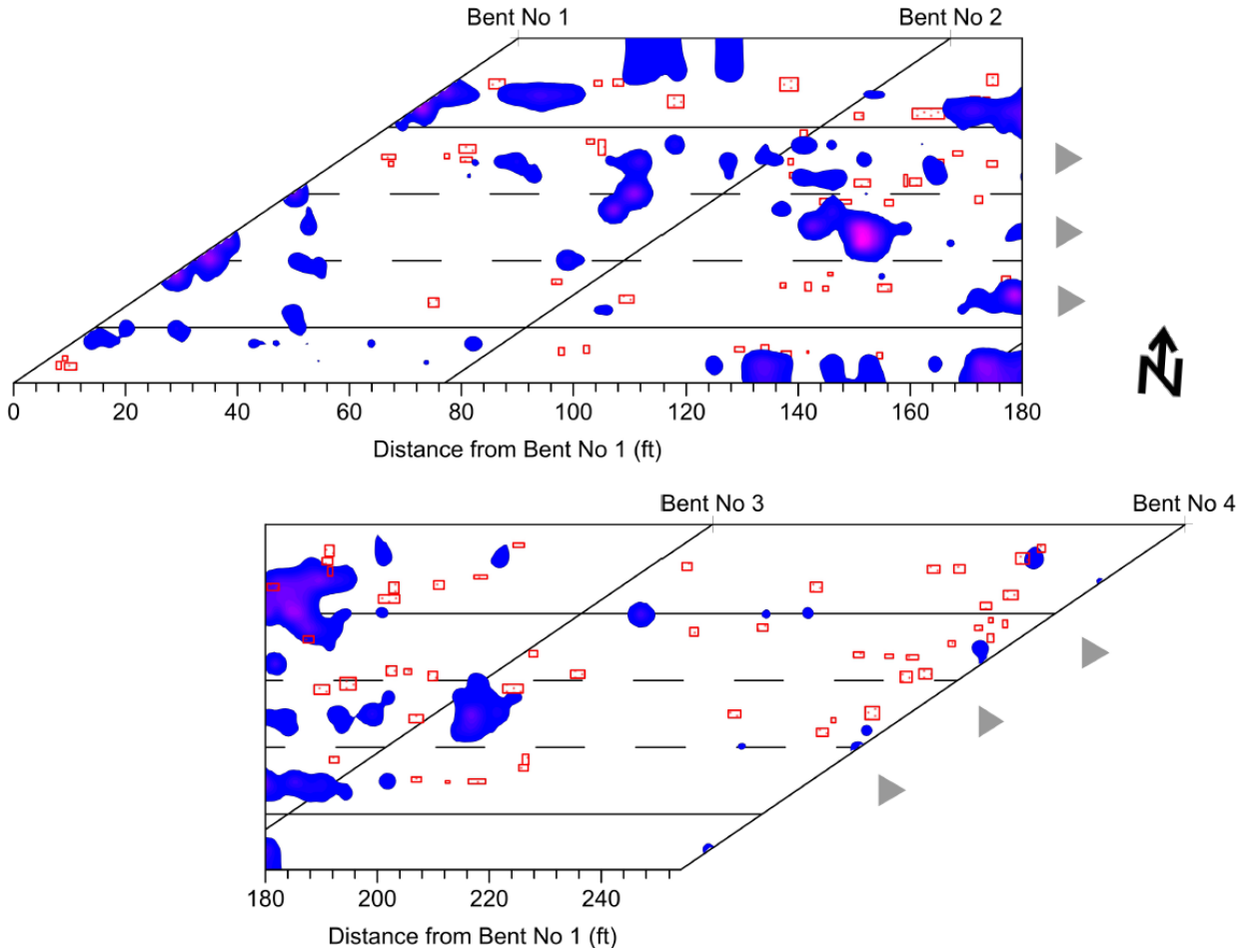

Bridge 76140

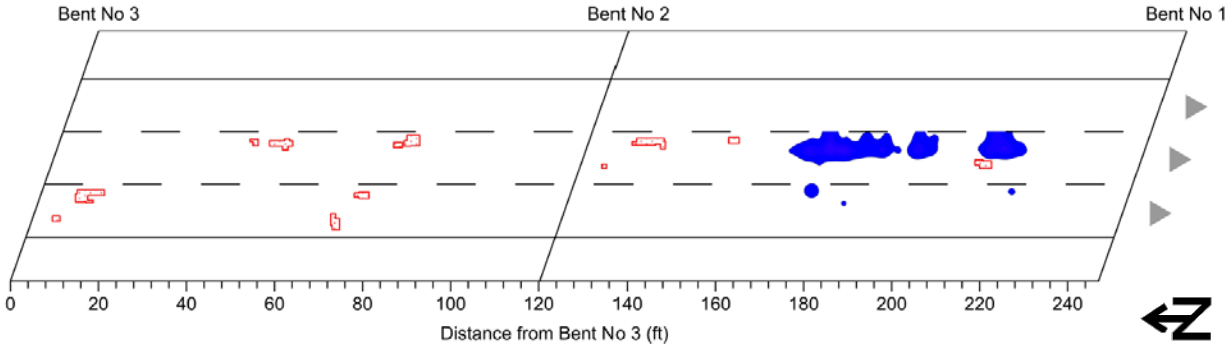

C.1.2 Consultant D–Second Round

Bridge 01310

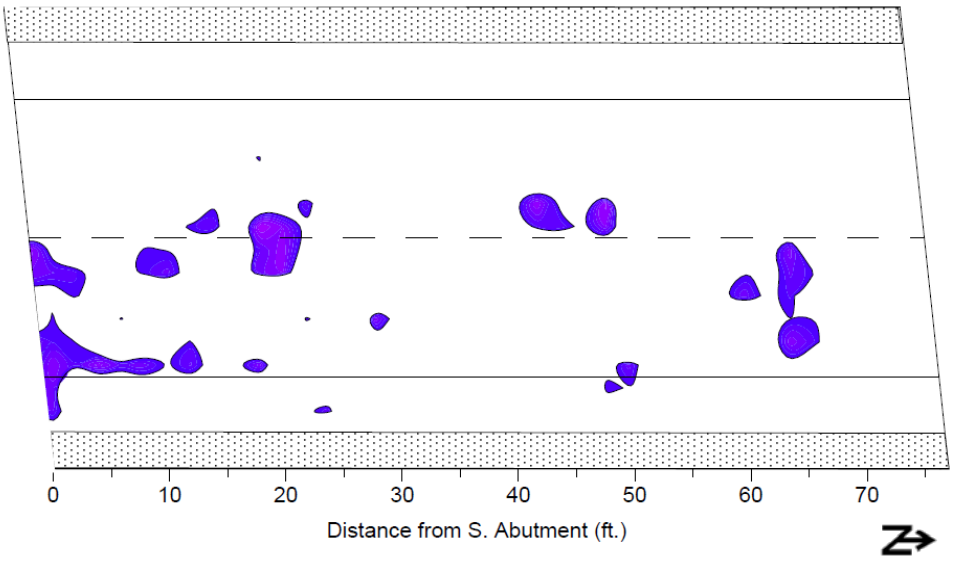

Bridge 01347

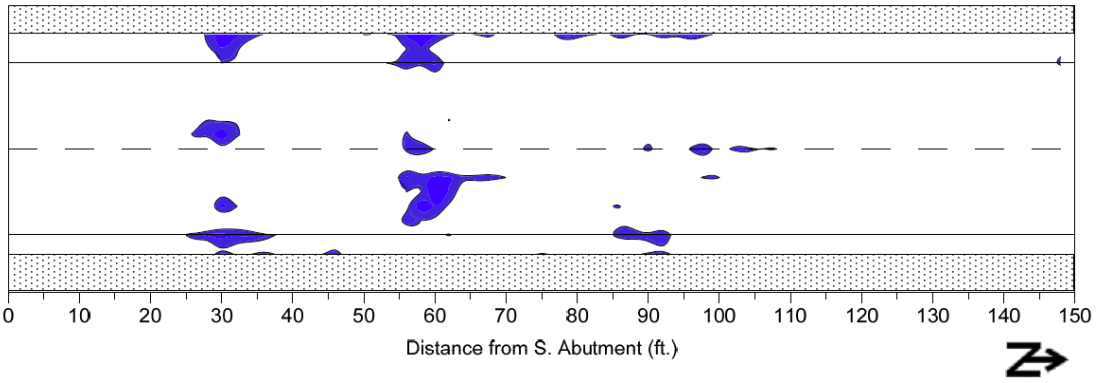

Bridge 04845

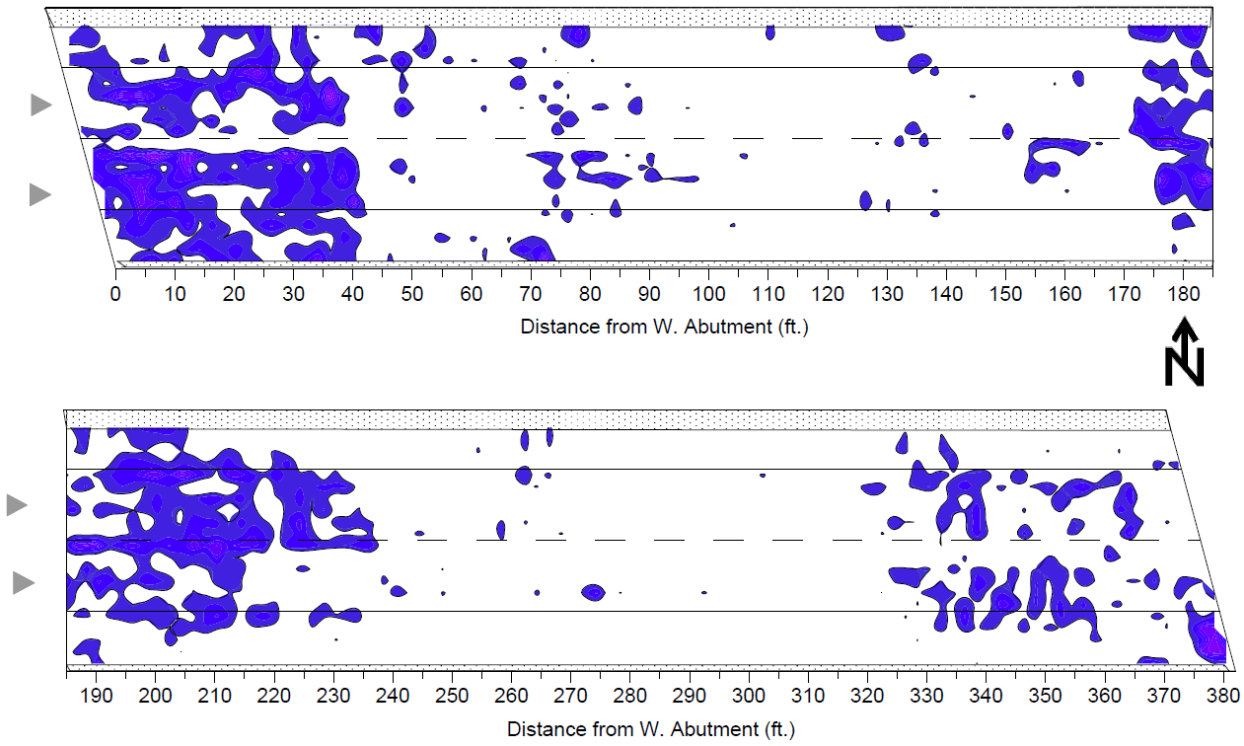

Bridge 04930

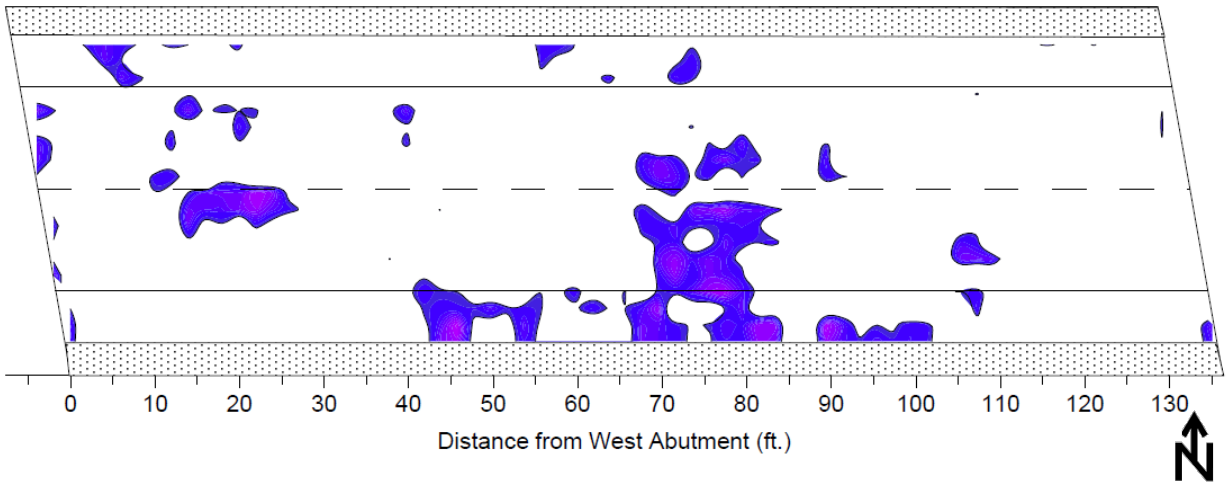

Bridge 08630

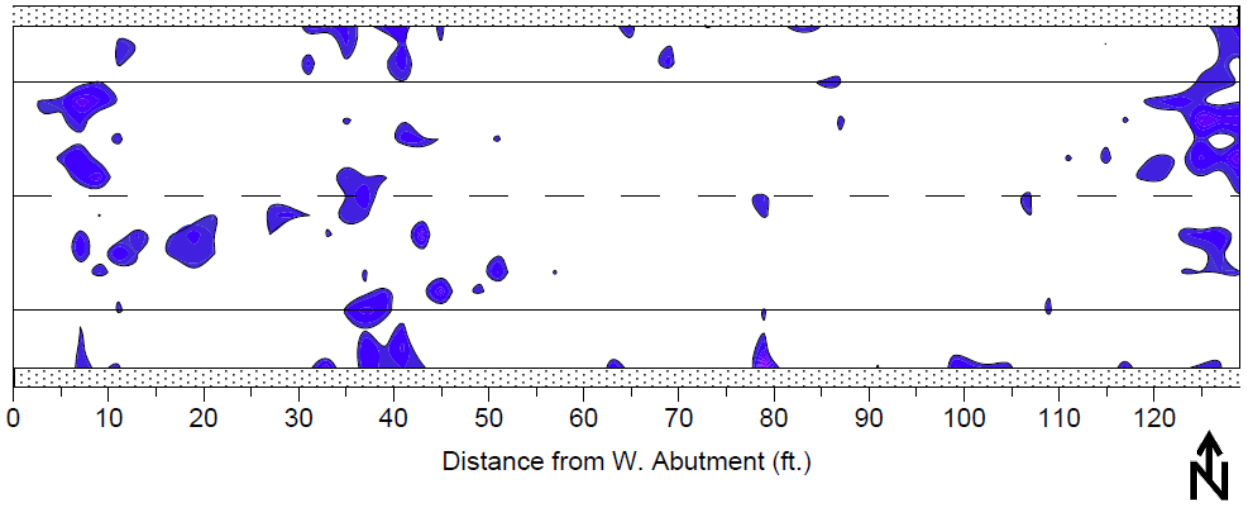

Bridge 17940

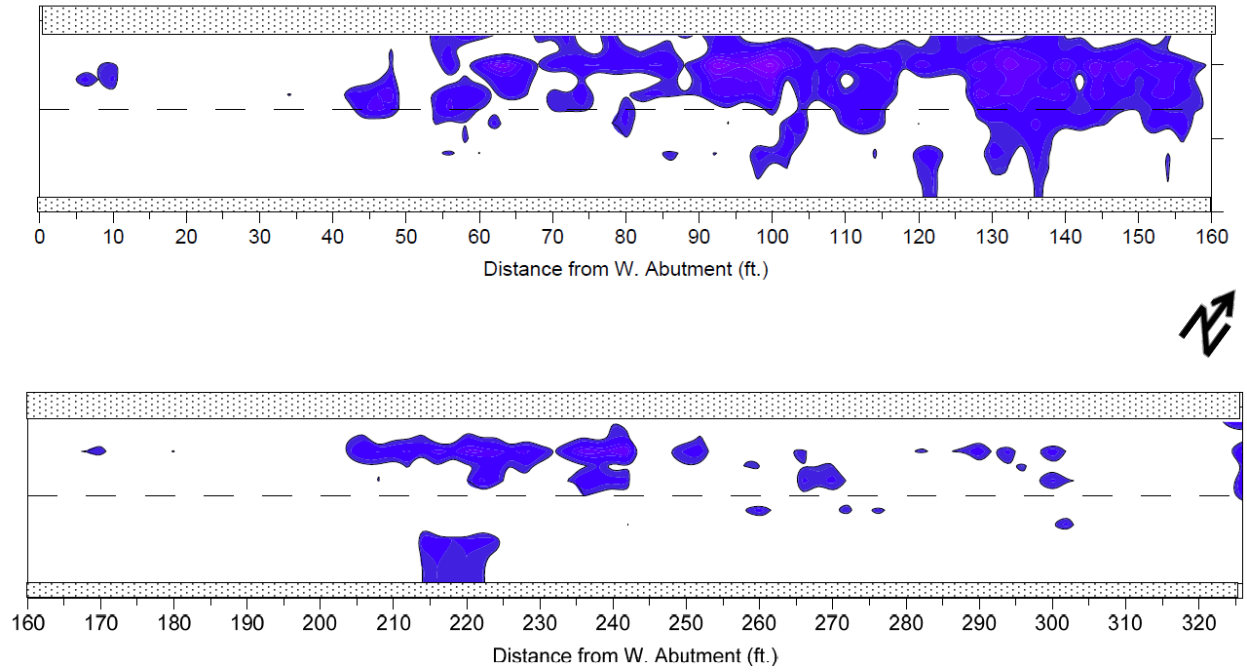

Bridge 19640

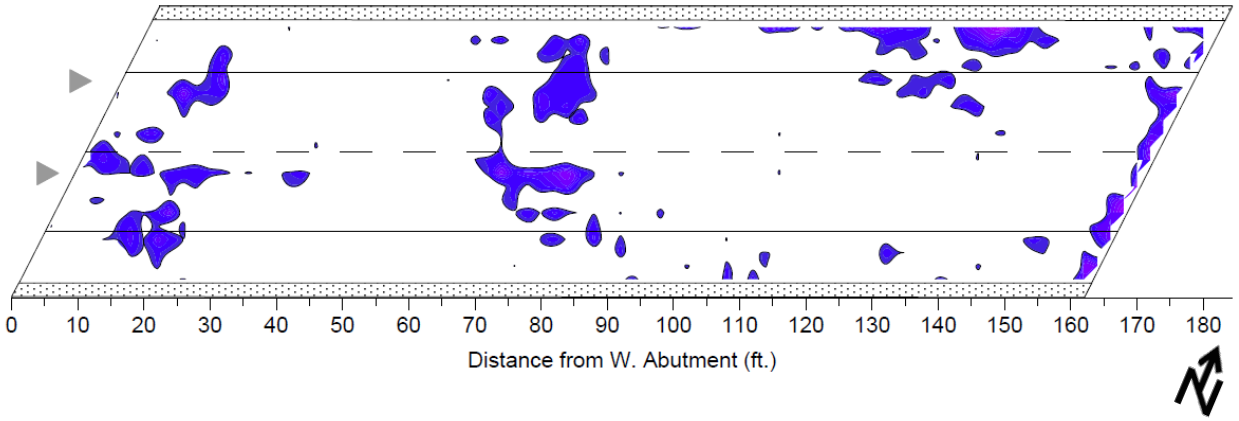

Bridge 20610

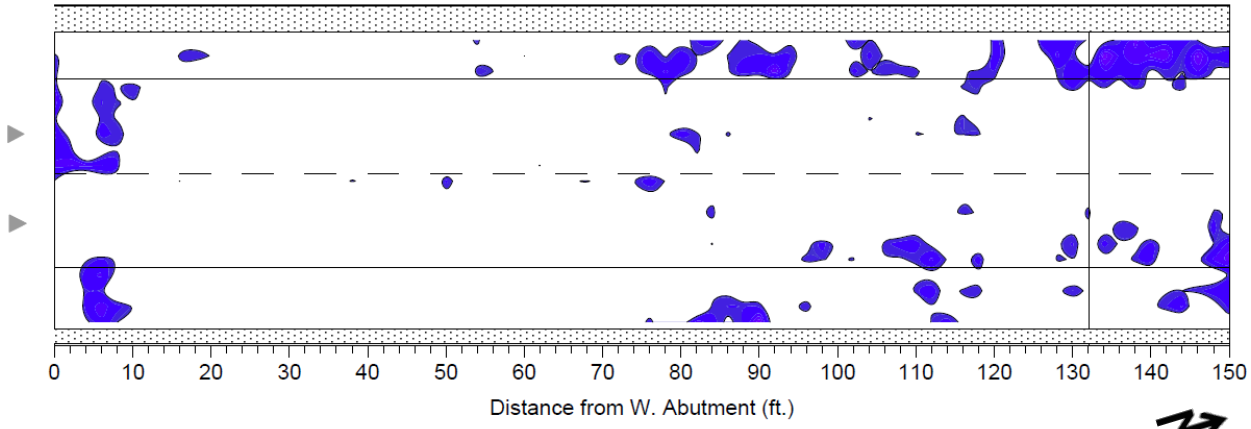

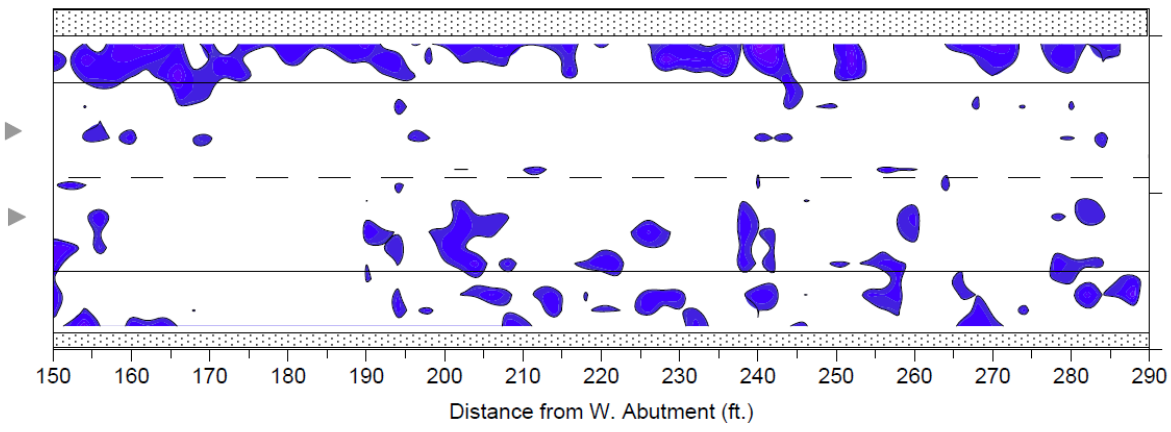

Bridge 24220

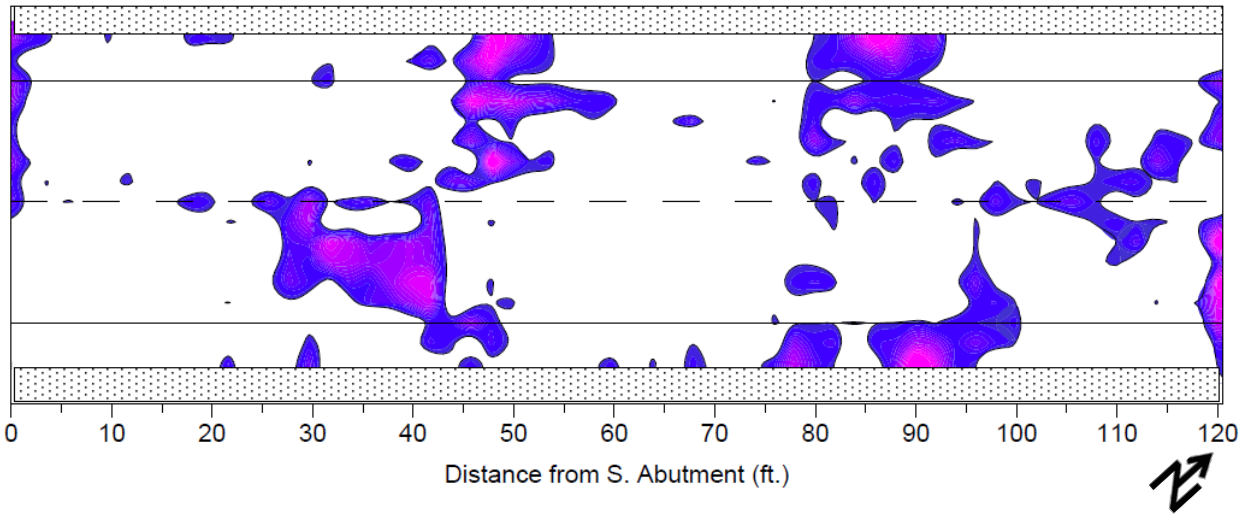

Bridge 49200

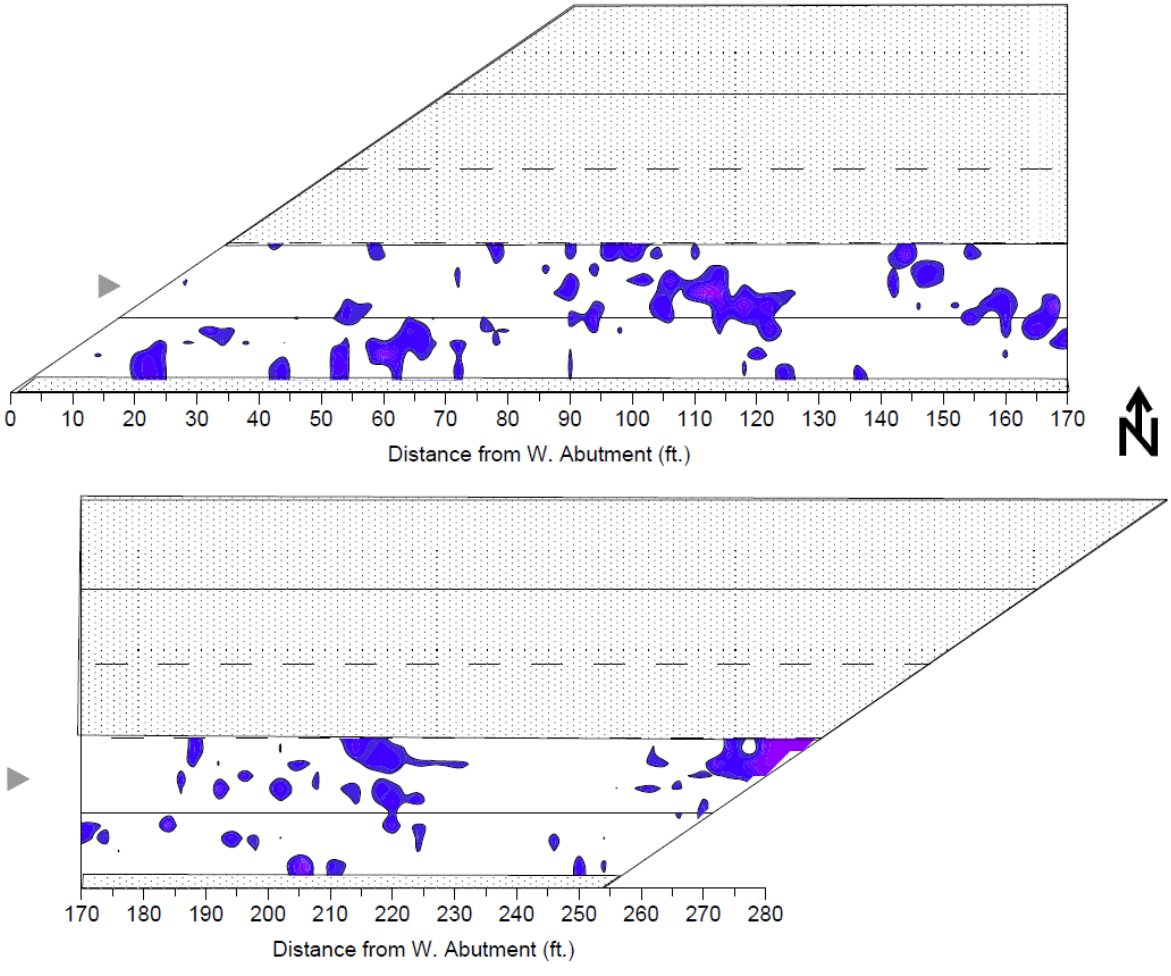

C.1.3 Consultant G

Bridge 16500

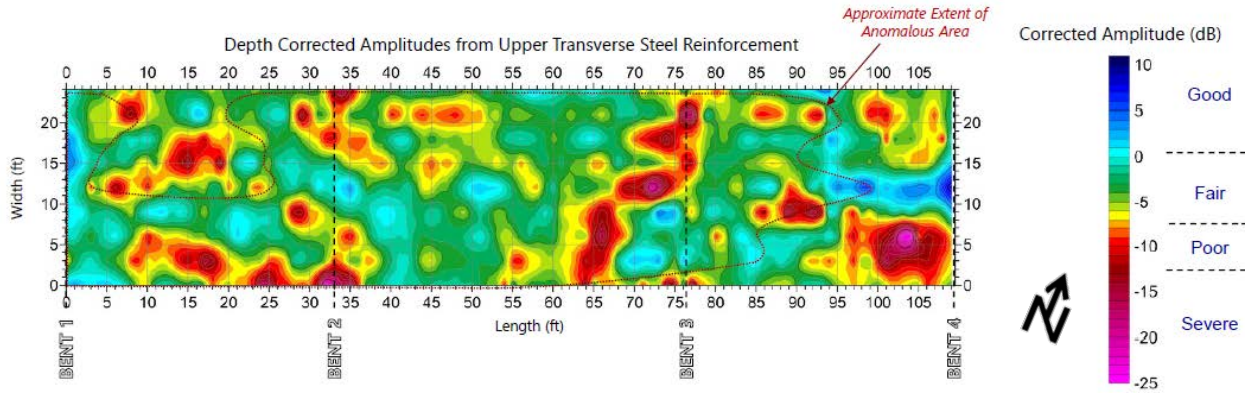

Bridge 18770

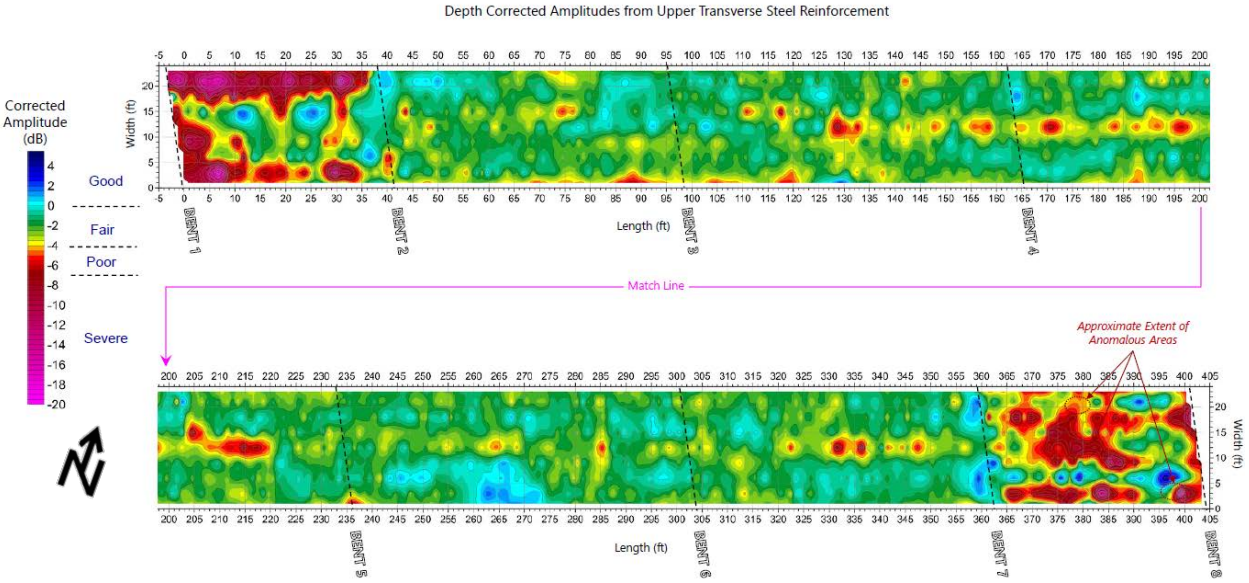

Bridge 22690

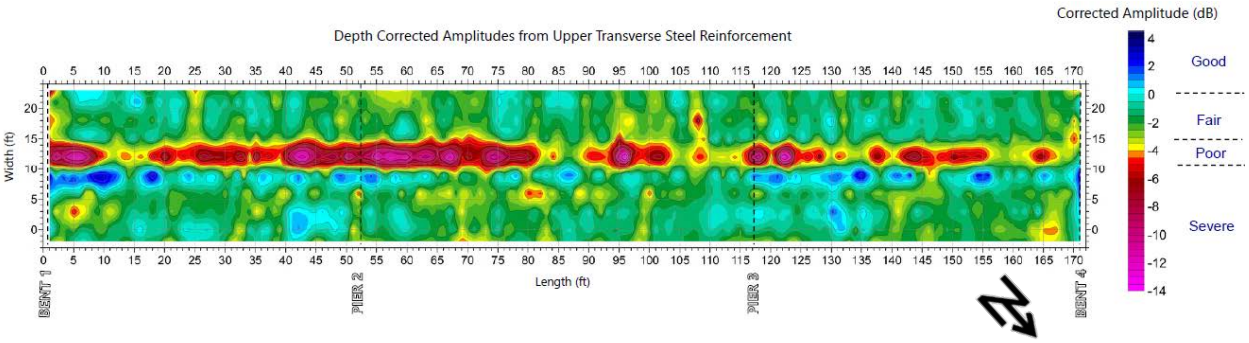

Bridge 31080

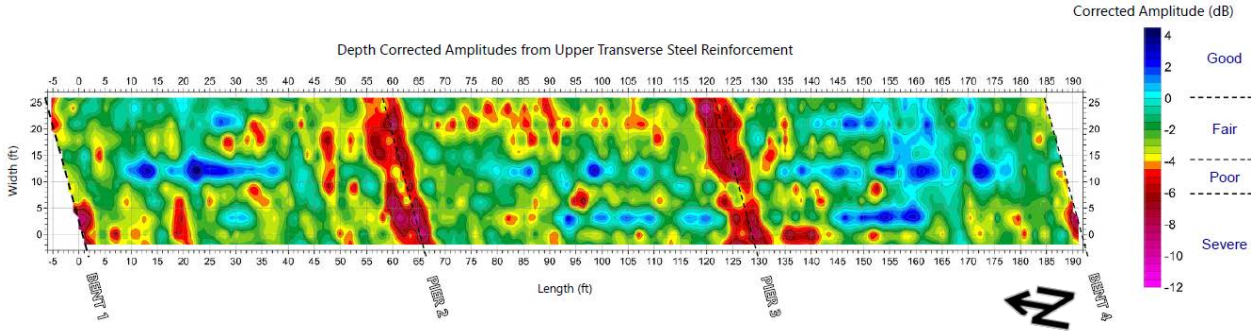

Bridge 35520

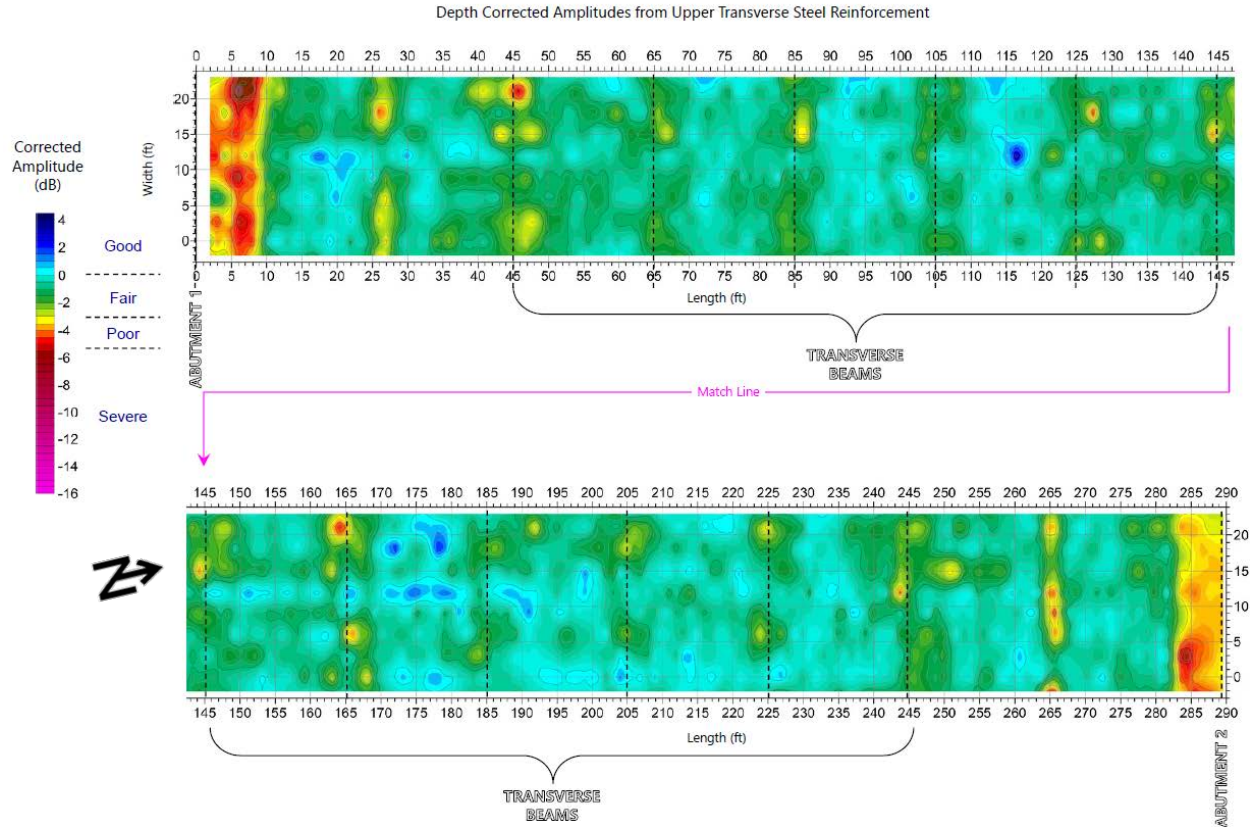

Bridge 37070

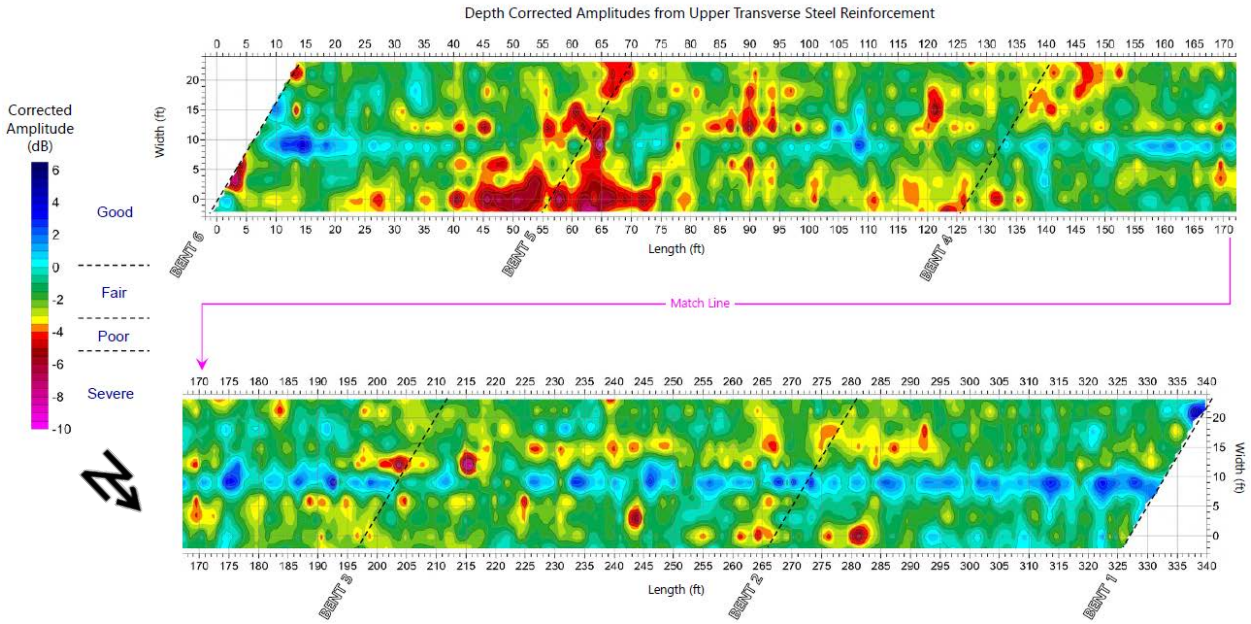

Bridge 37100

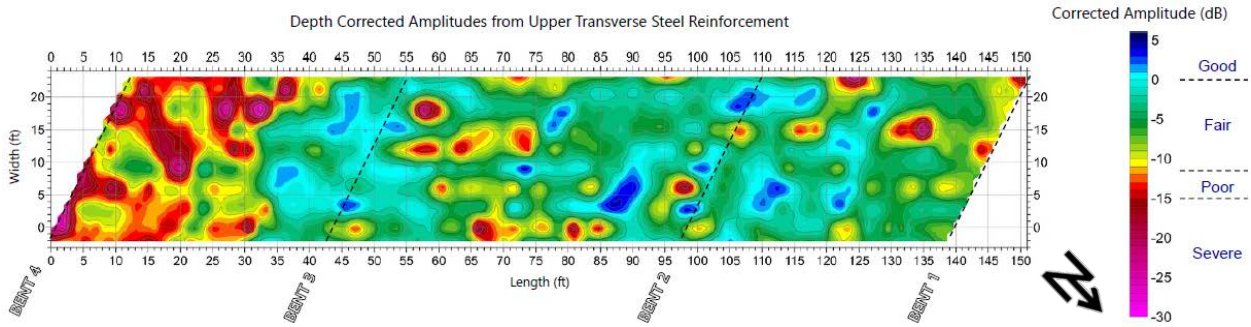

Bridge 37150

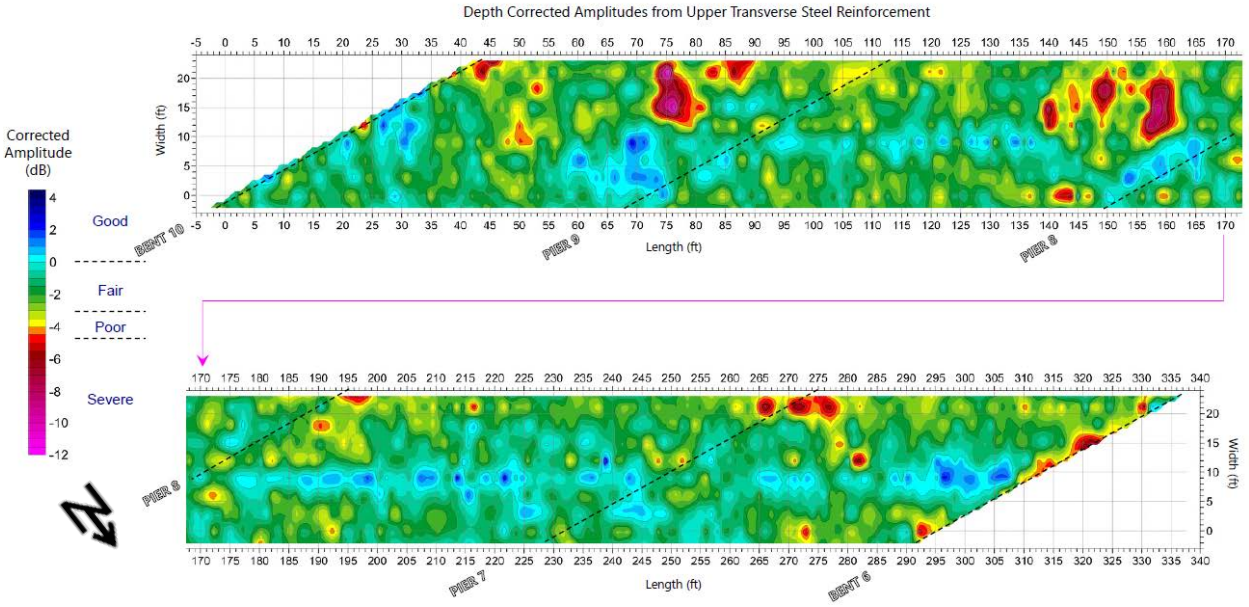

Bridge 41810

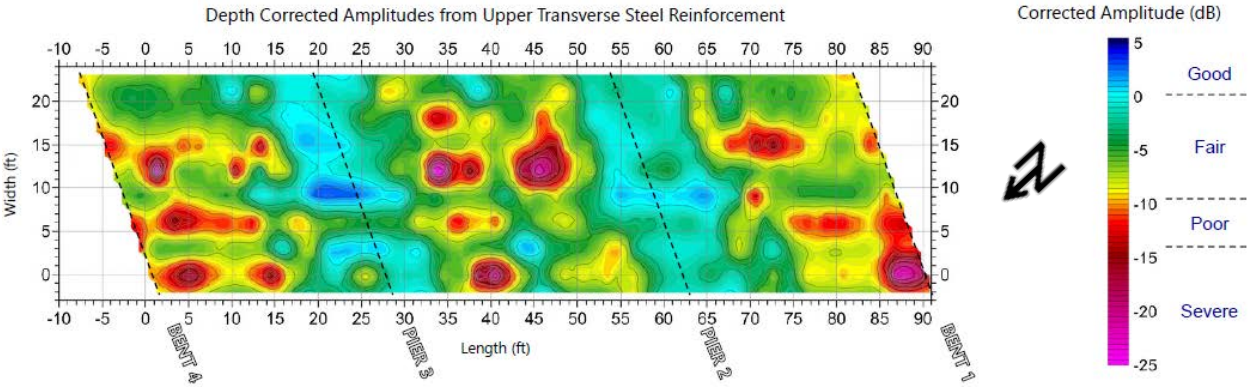

Bridge 41870

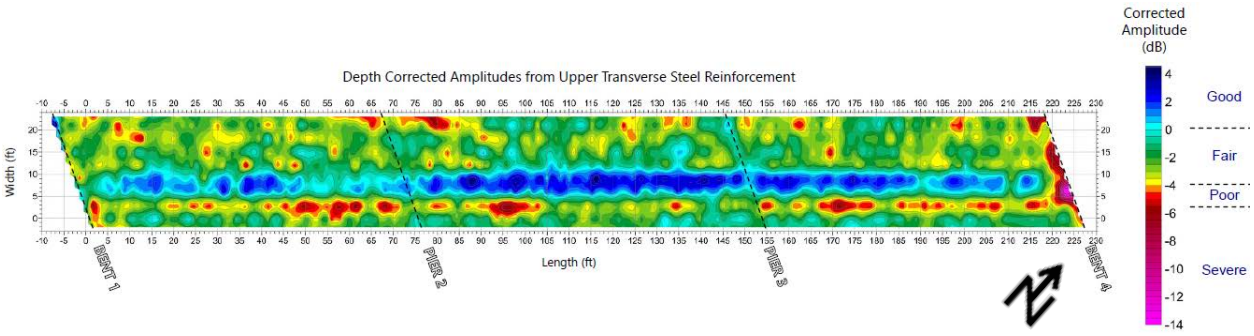

C.1.4 Consultant J

Bridge 18770

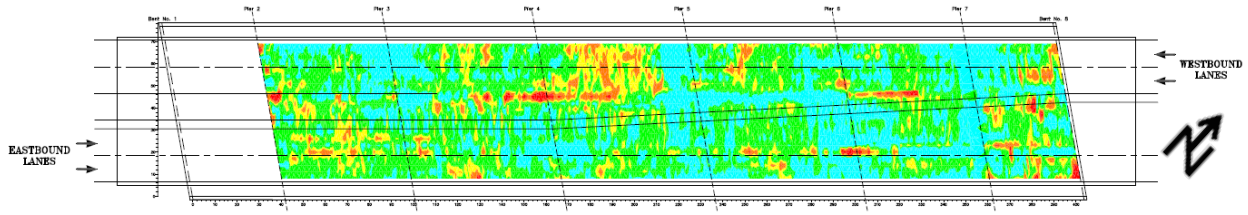

Bridge 22610

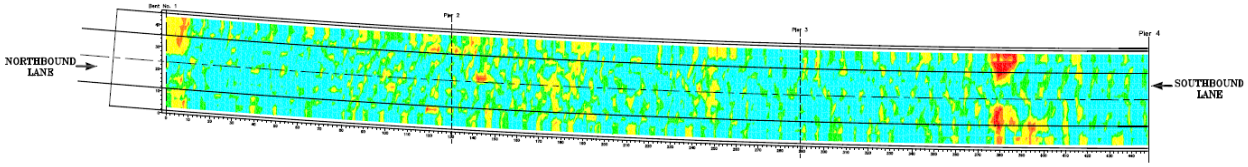

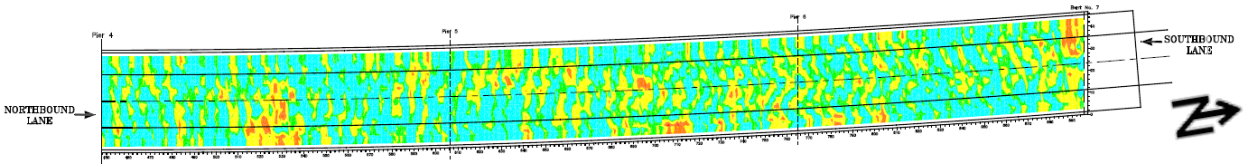

Bridge 22690

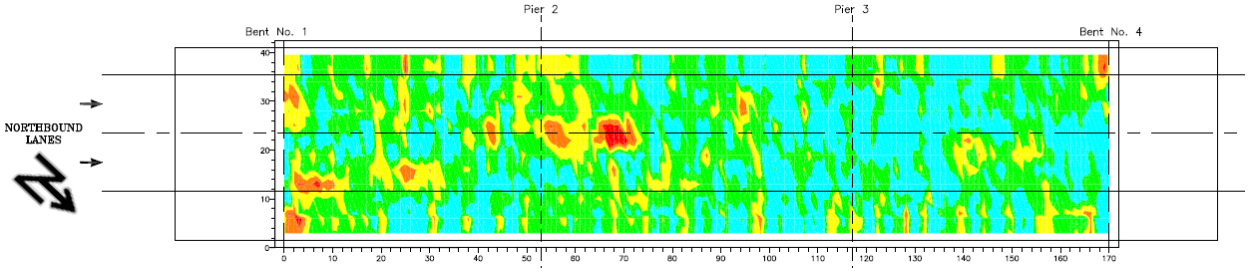

Bridge 31080

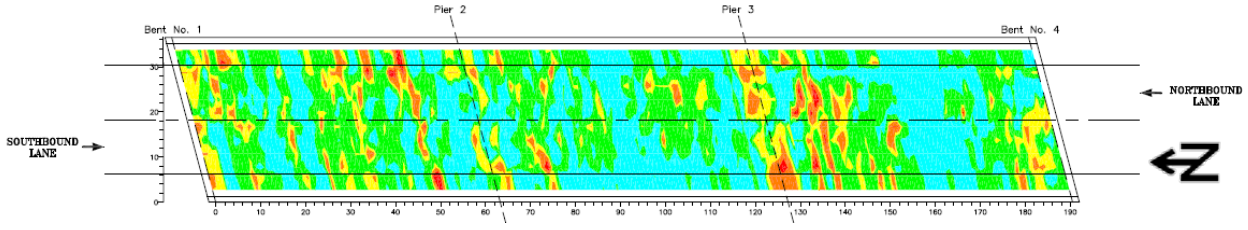

Bridge 35520

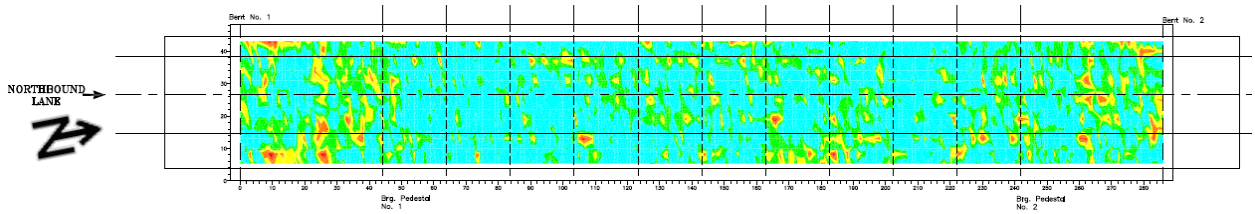

Bridge 37070

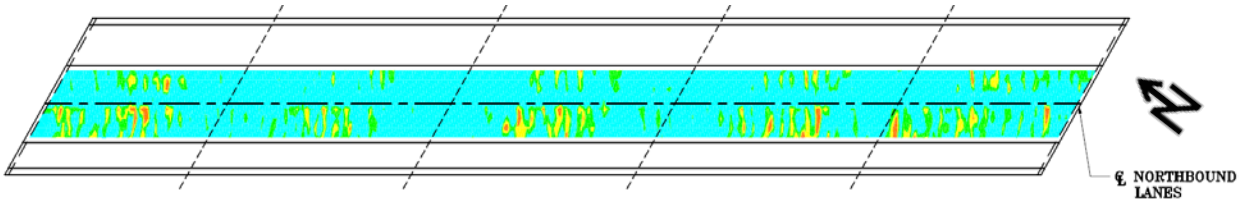

Bridge 37100

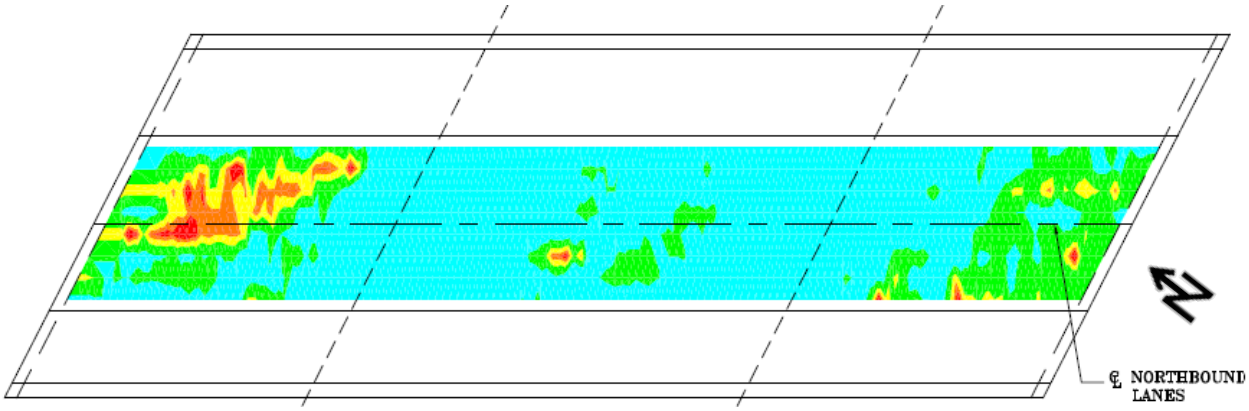

Bridge 37150

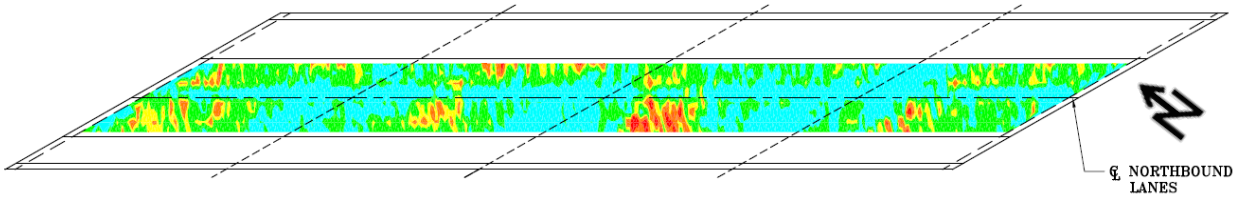

Bridge 41870

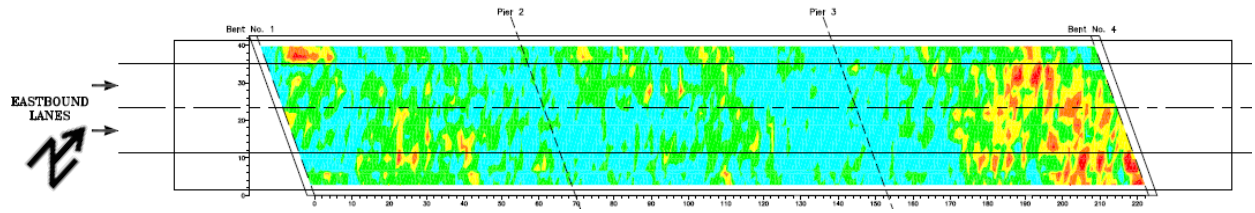

C.2 Ground-Coupled GPR

C.2.1 Consultant D

Bridge 16500

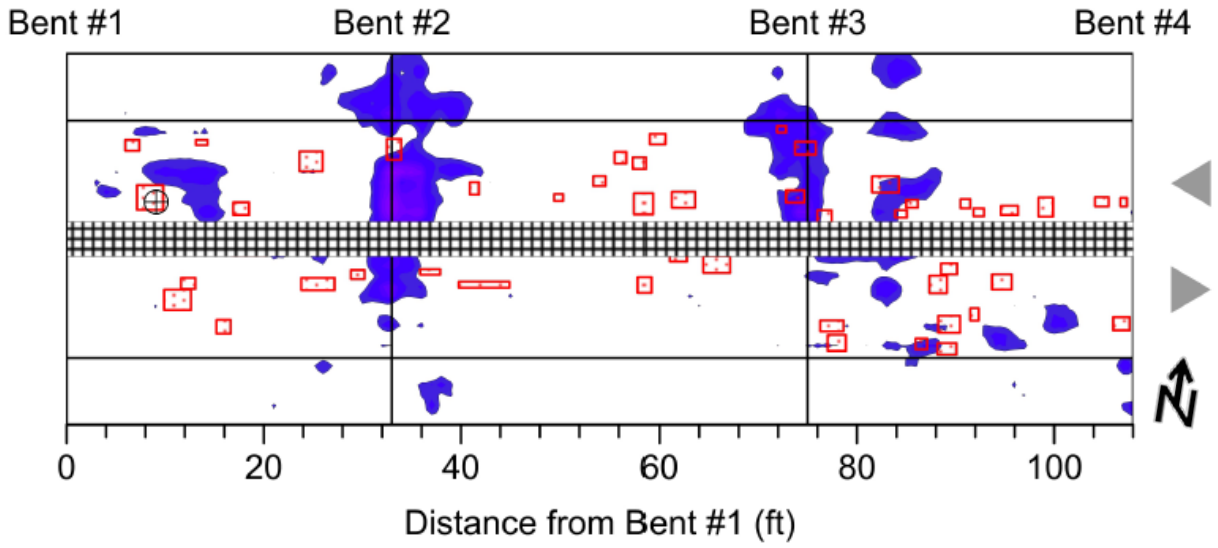

Bridge 18770

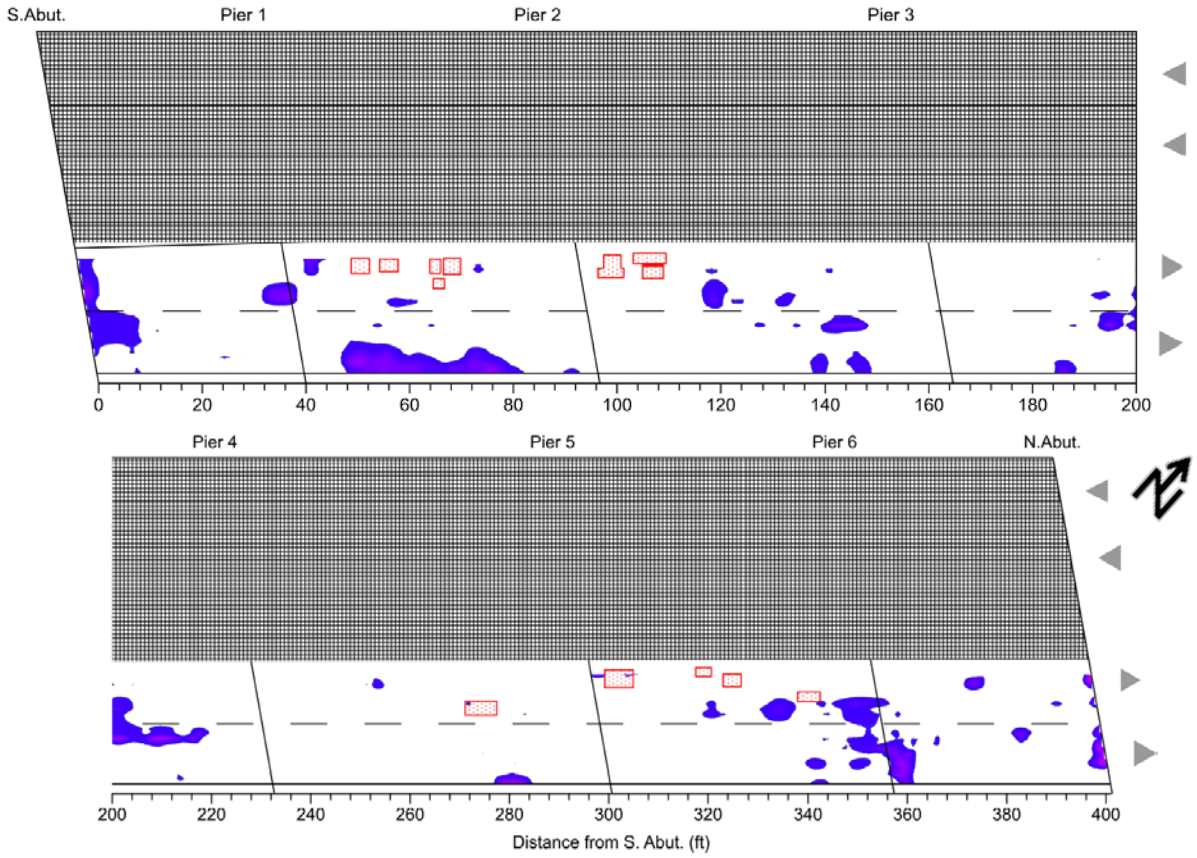

Bridge 22690

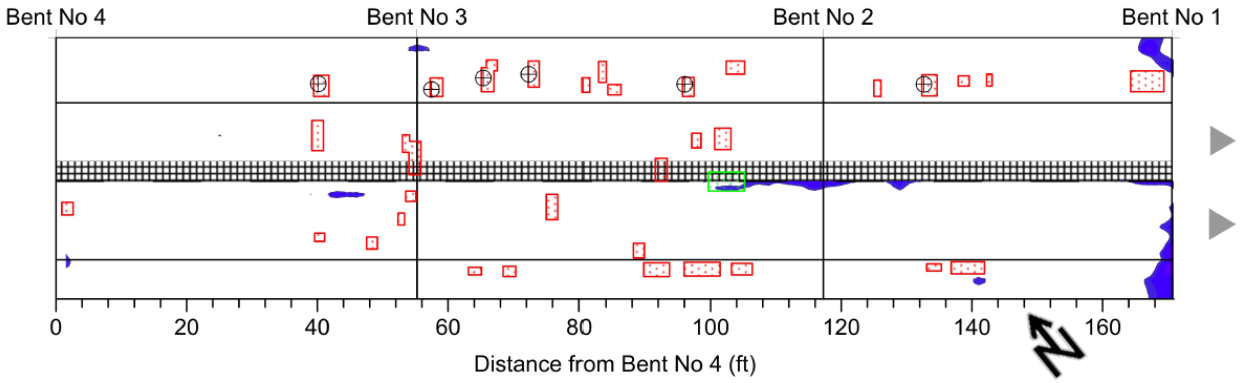

Bridge 31080

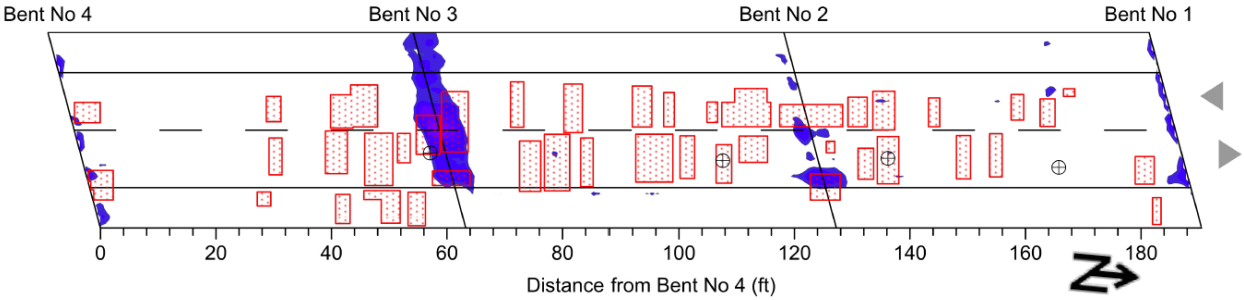

Bridge 35520

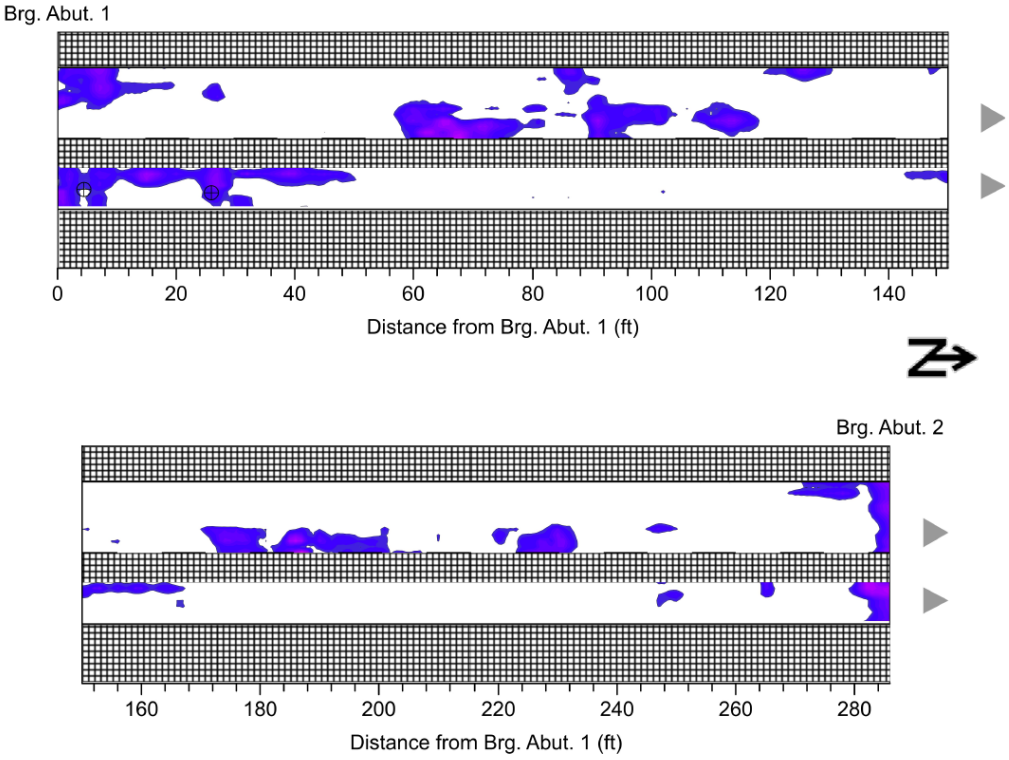

Bridge 37070

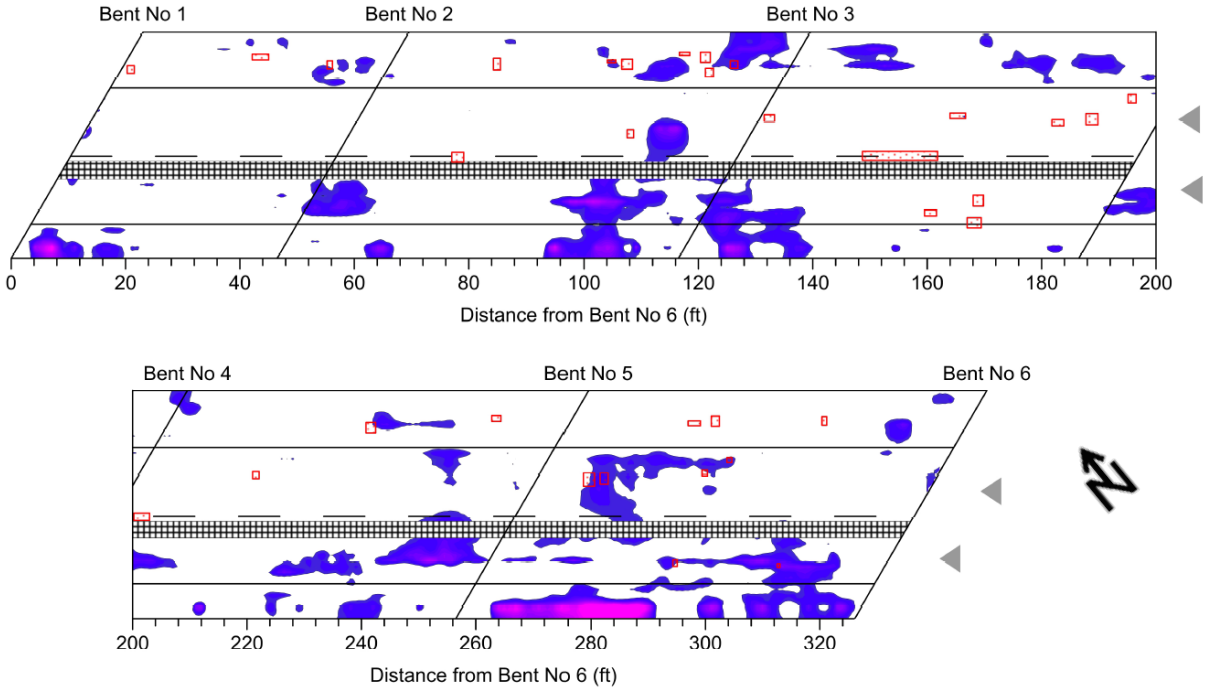

Bridge 37100

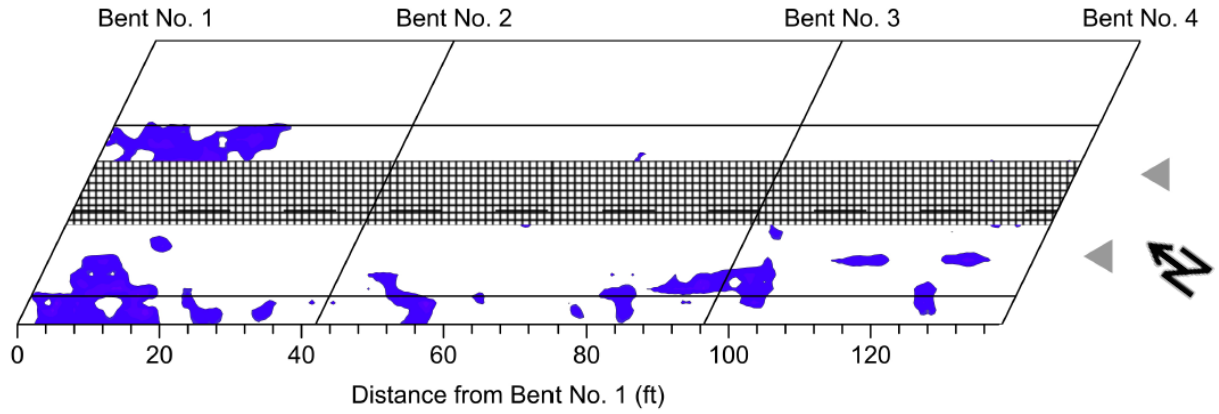

Bridge 37150

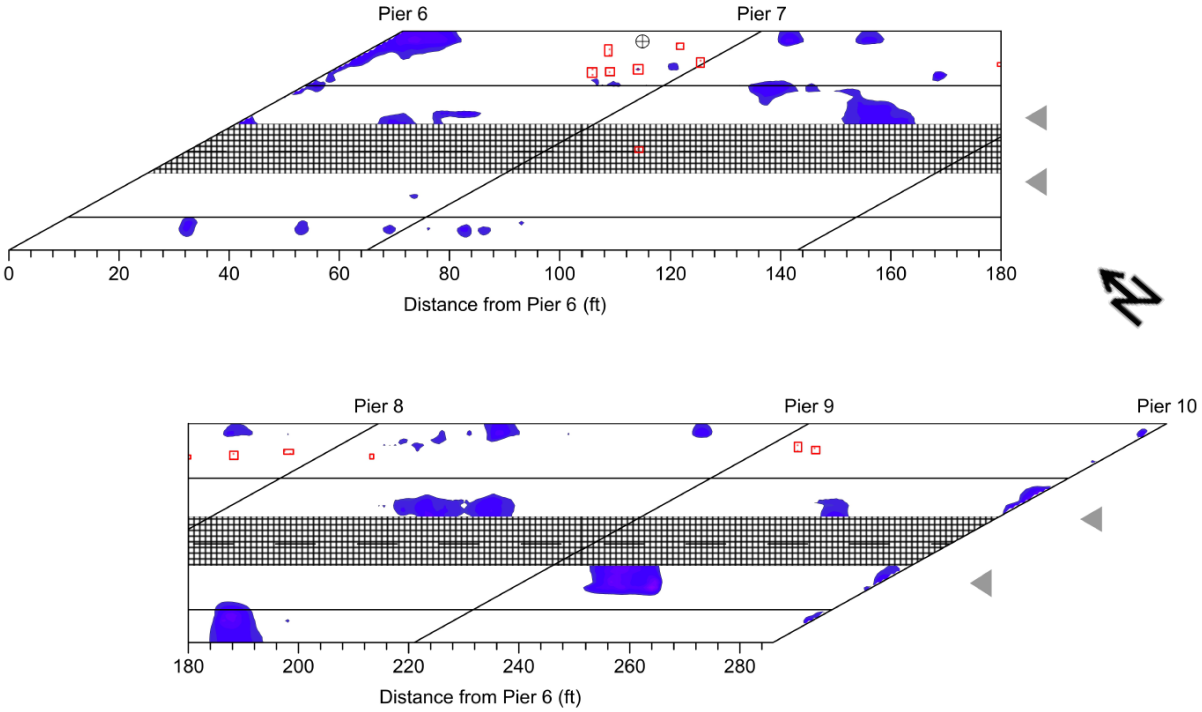

Bridge 41810

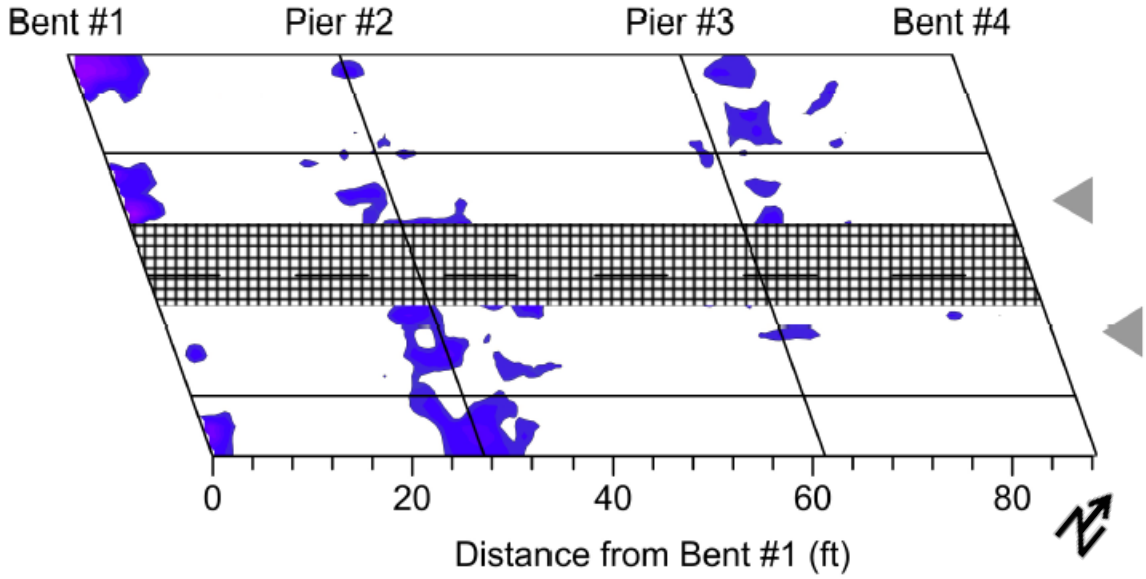

Bridge 41870

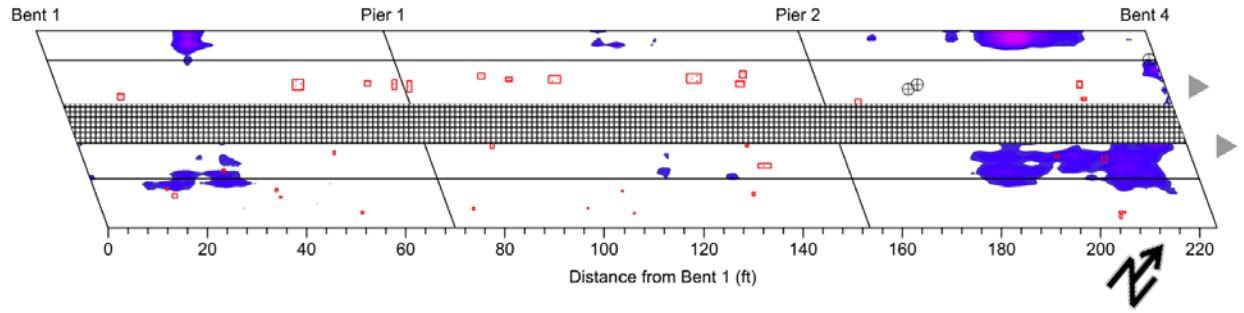

C.2.2 Consultant B

Bridge 16500

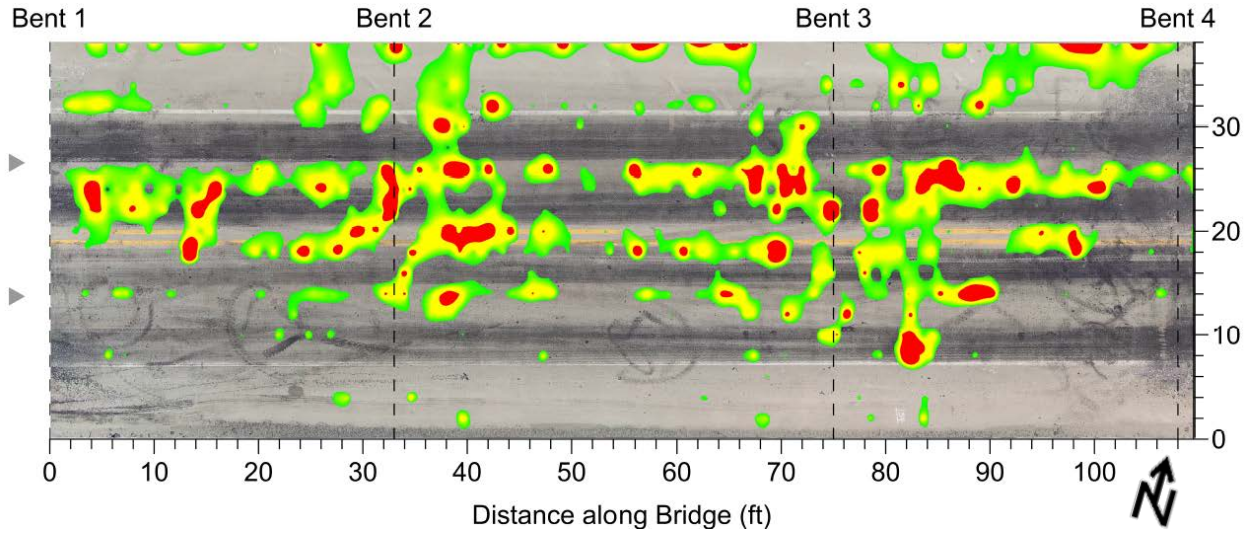

Bridge 18770

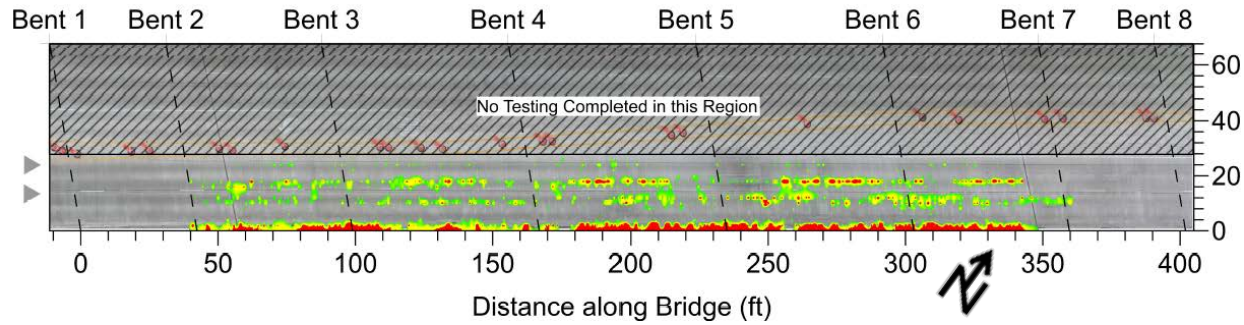

Bridge 22690

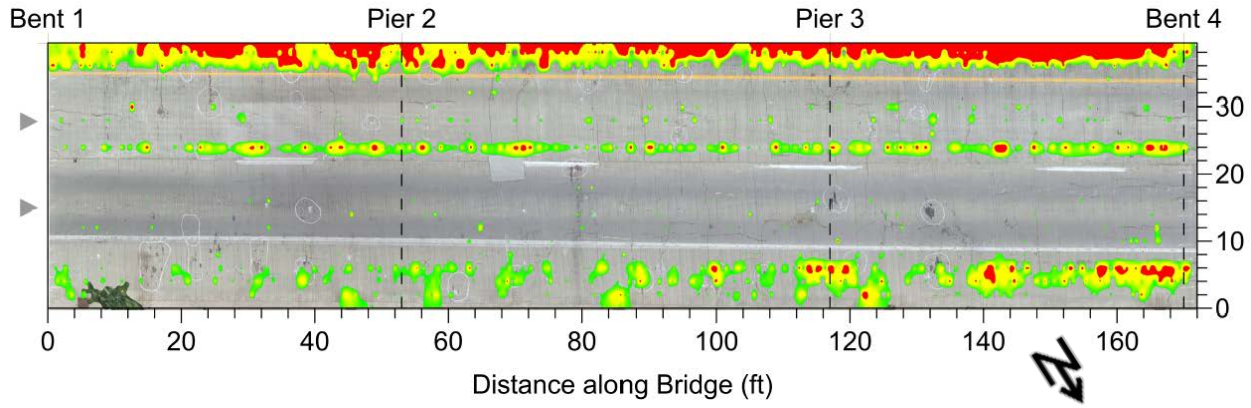

Bridge 31080

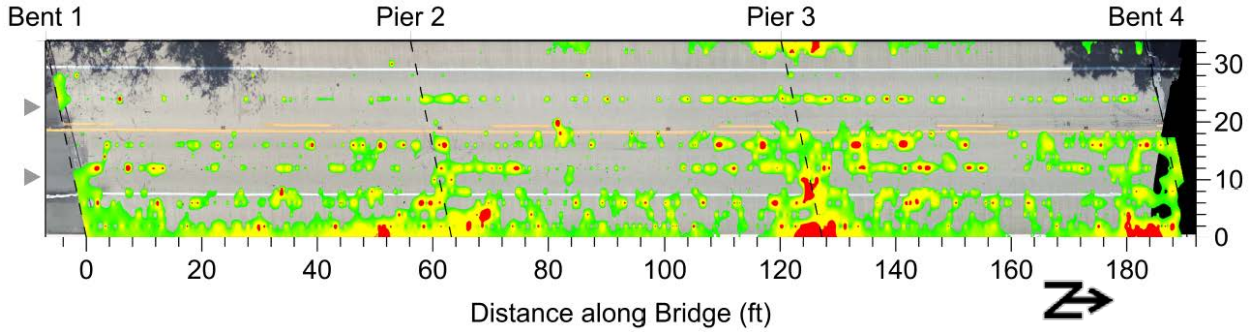

Bridge 35520

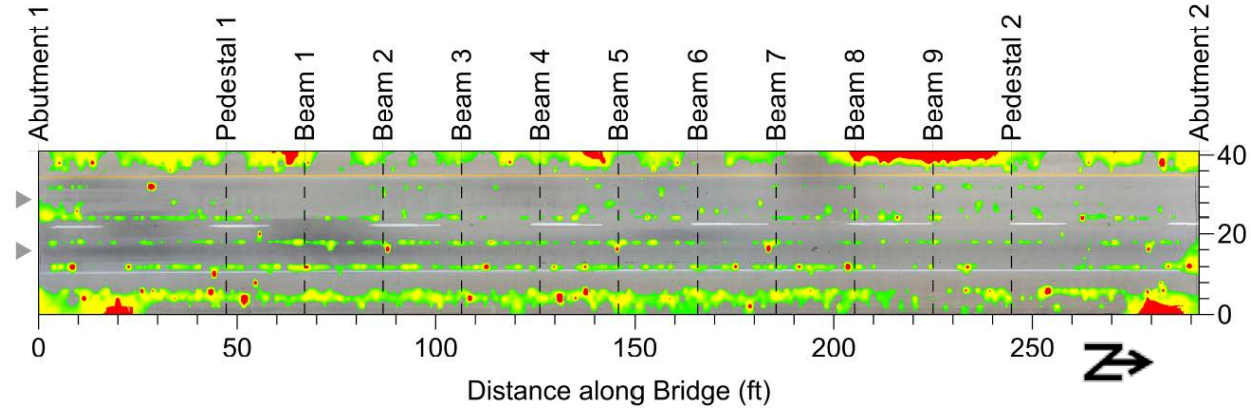

Bridge 37070

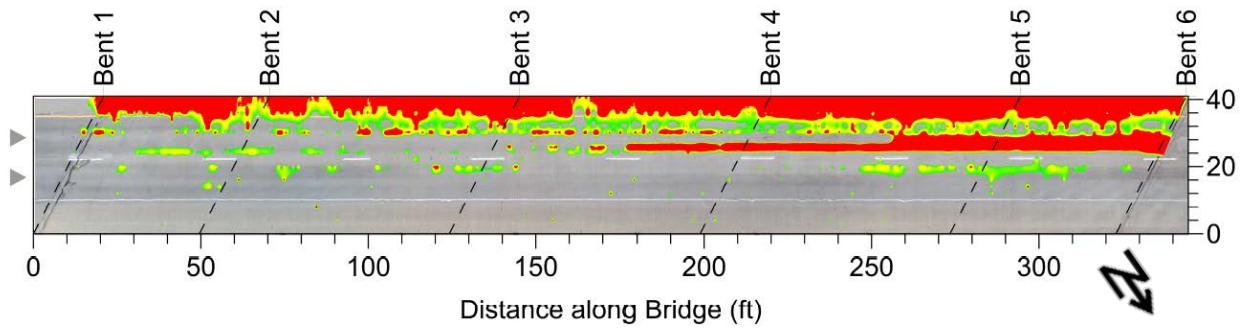

Bridge 37100

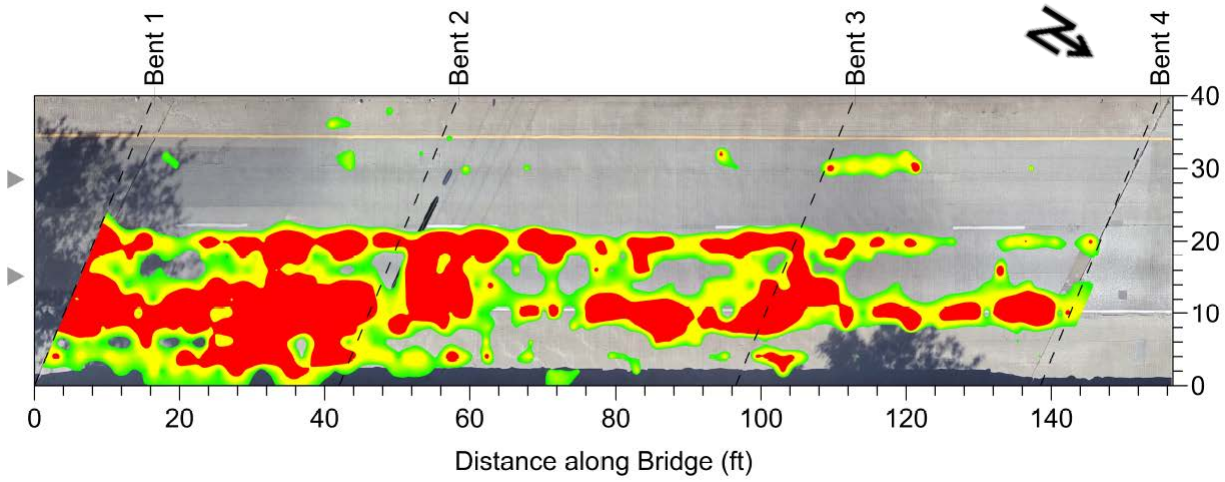

Bridge 37150

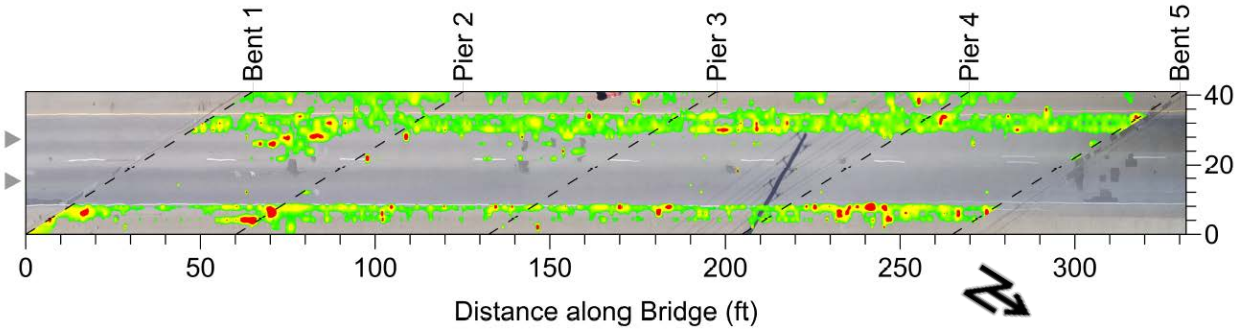

Bridge 41810

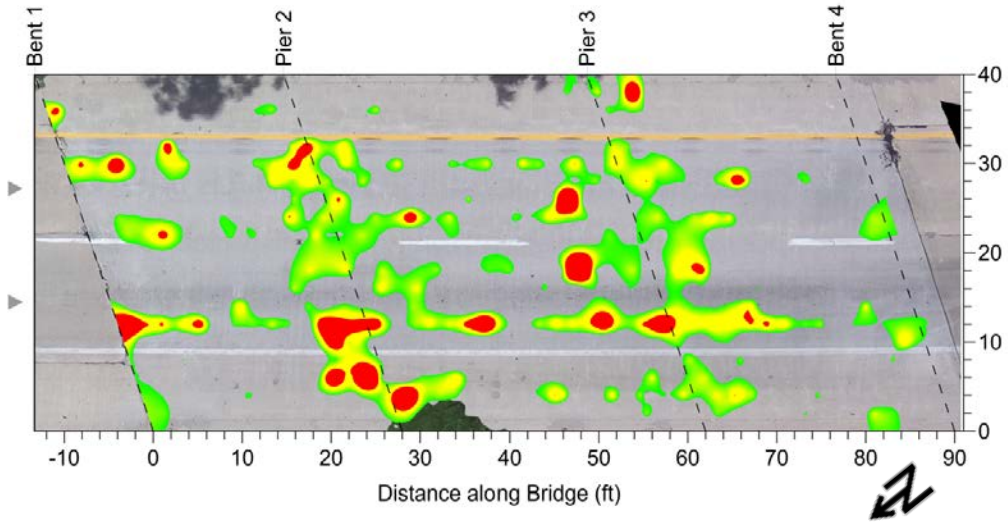

Bridge 41870

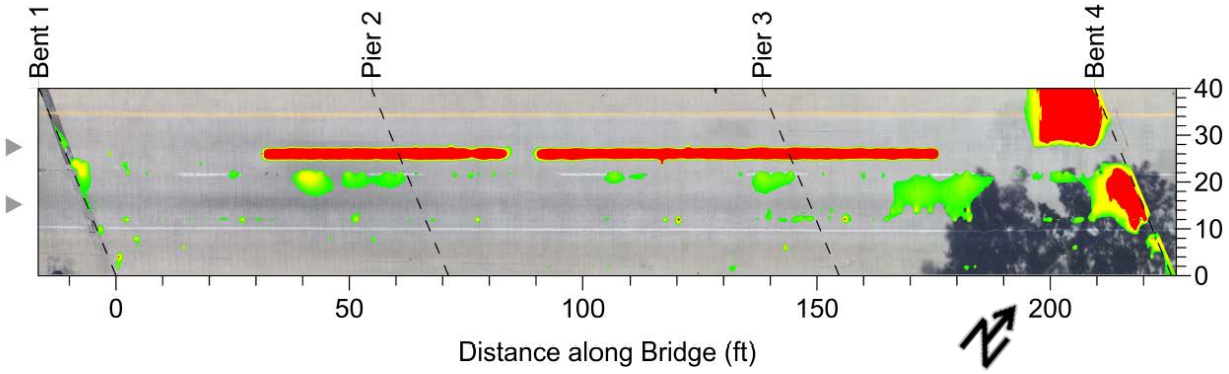

C.2.3 INDOT–First Round

Bridge 22690

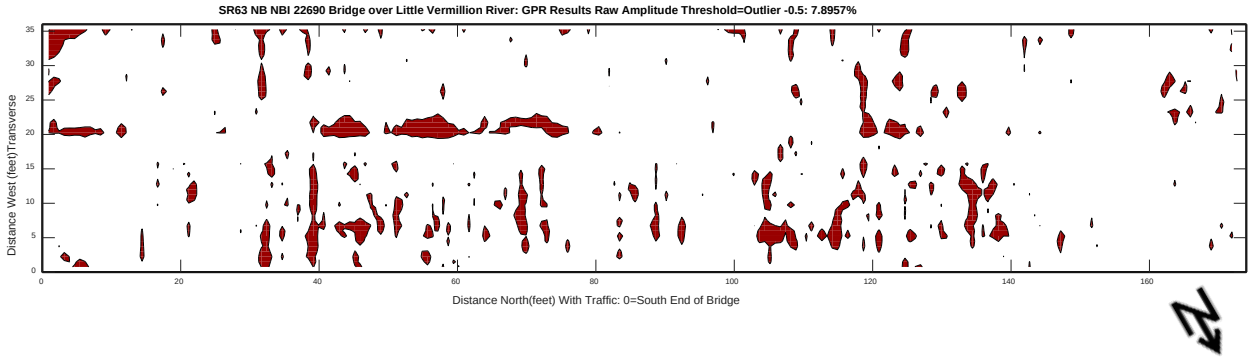

Bridge 41810

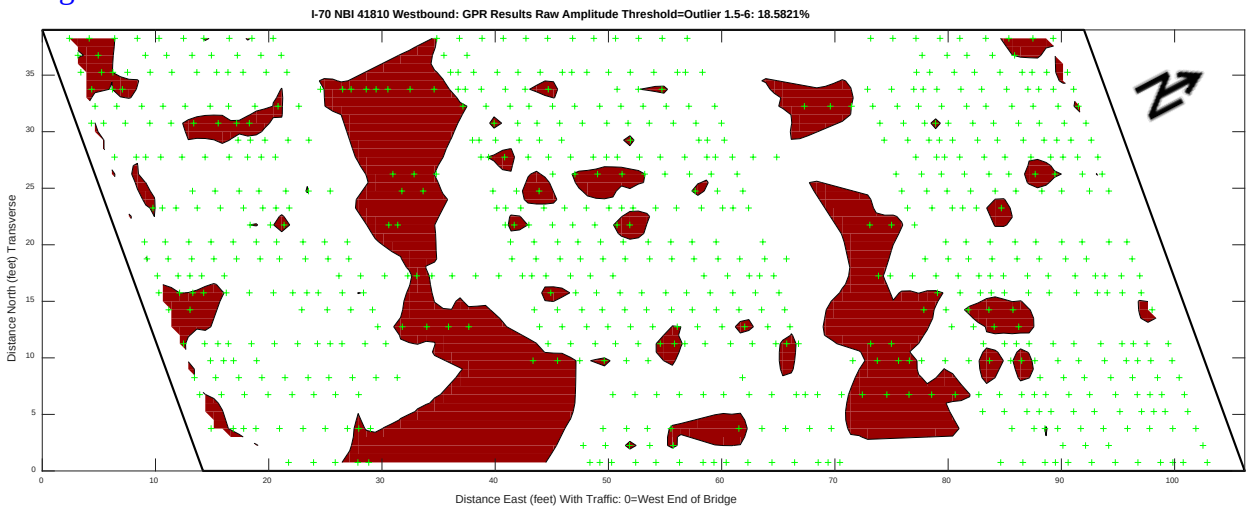

Bridge 41870

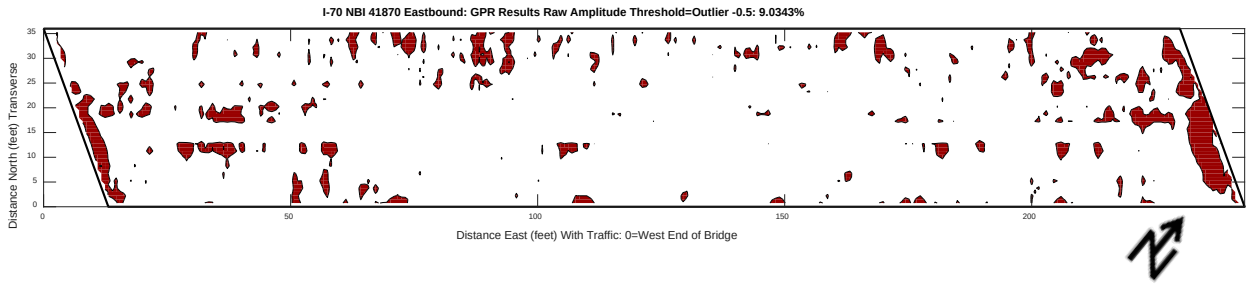

C.2.4 INDOT–Second Round

Bridge 04845

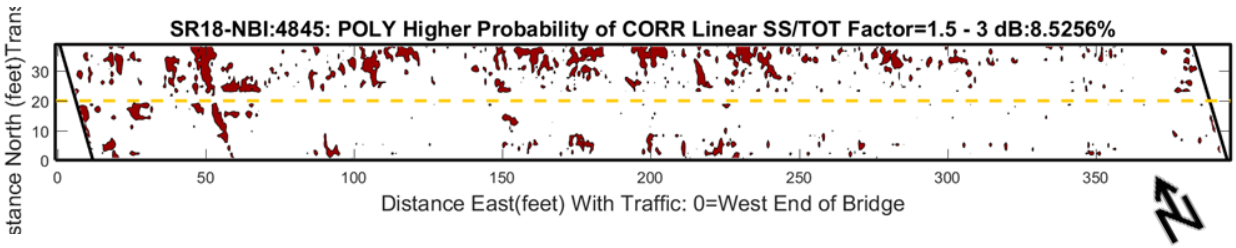

Bridge 20610

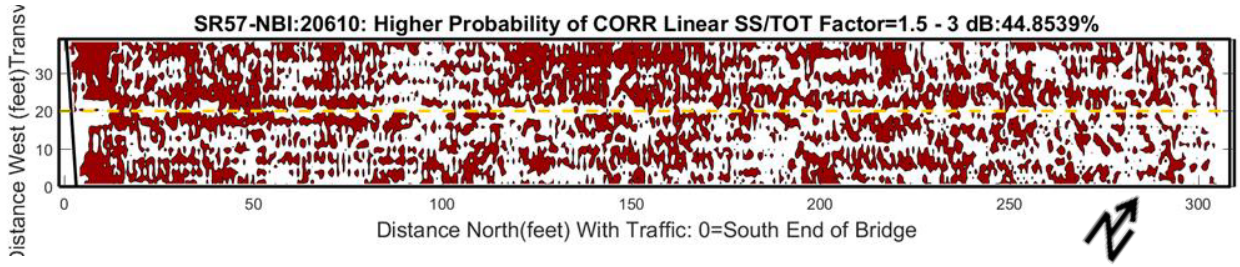

Bridge 24220

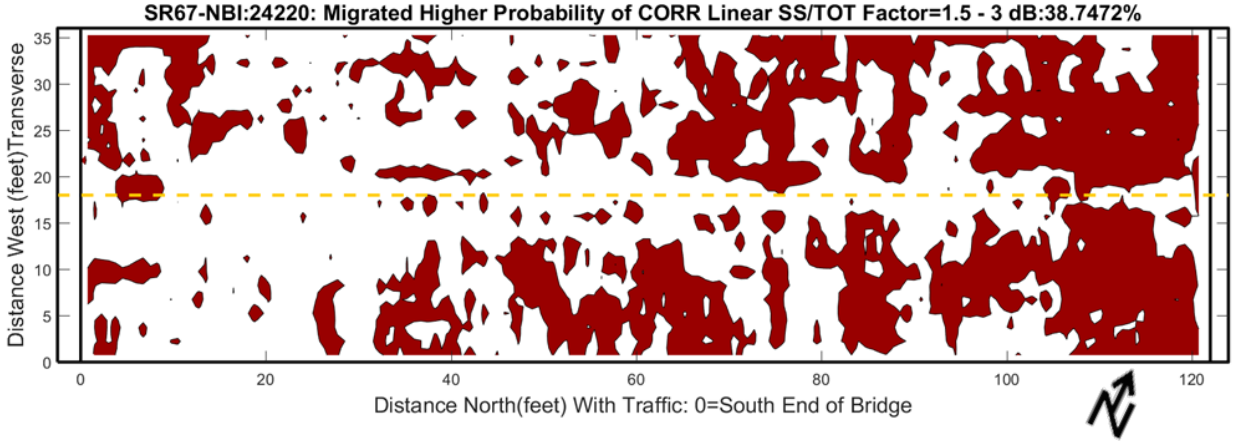

C.2.5 Consultant H

Bridge 01310

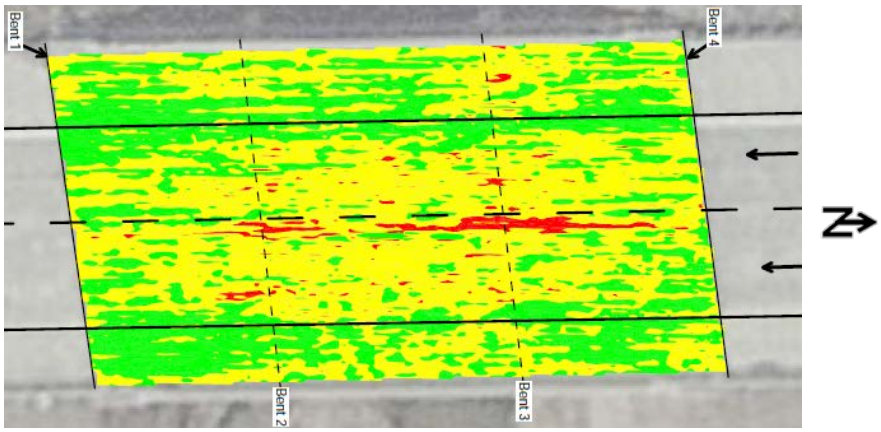

Bridge 01347

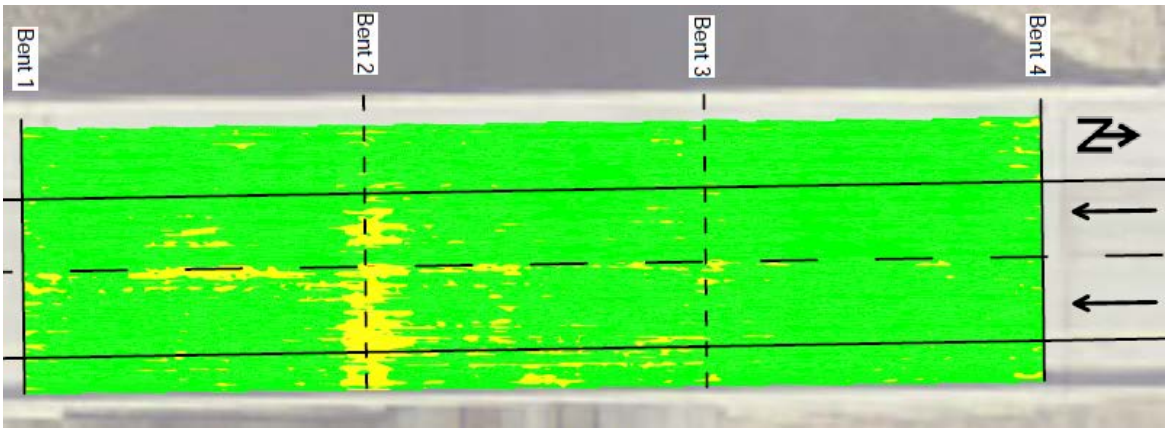

Bridge 04845

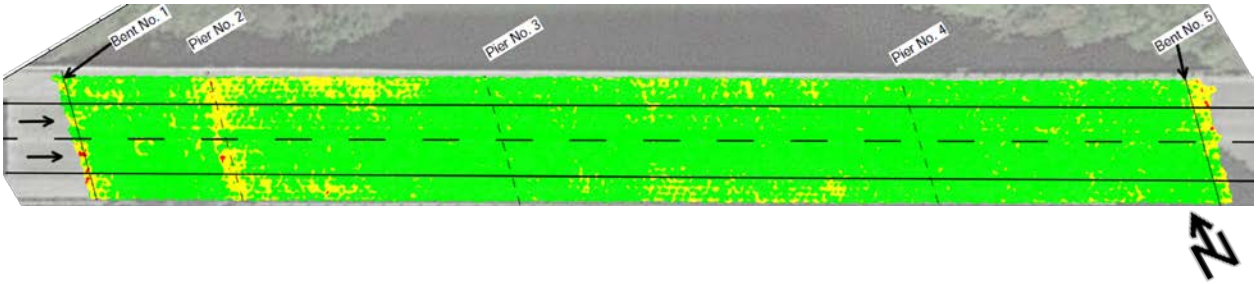

Bridge 04930

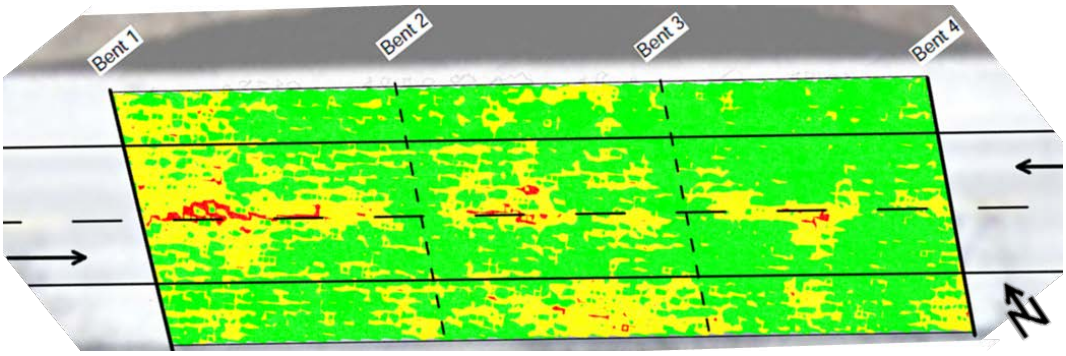

Bridge 08630

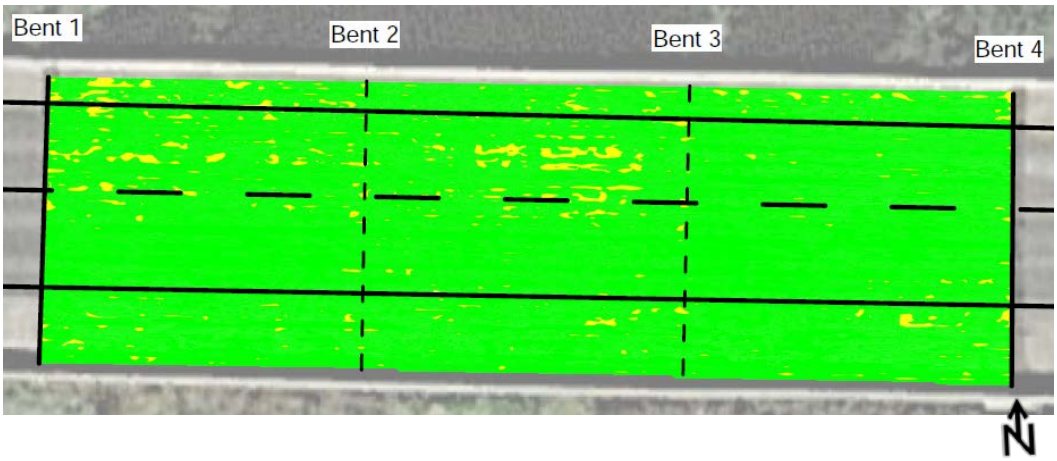

Bridge 17940

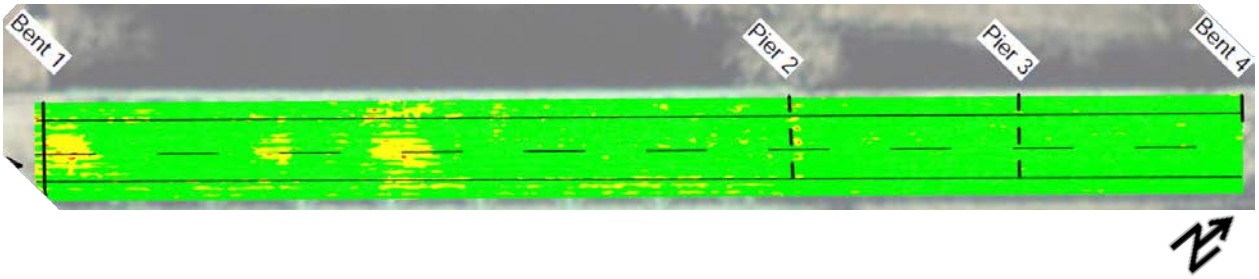

Bridge 19640

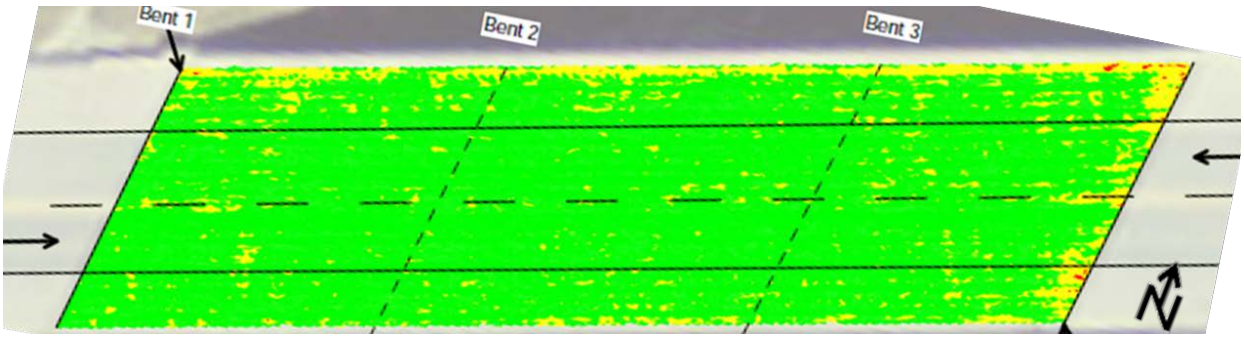

Bridge 20610

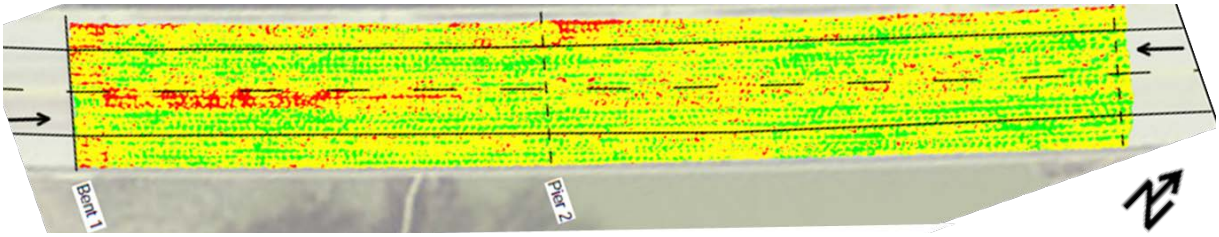

Bridge 24220

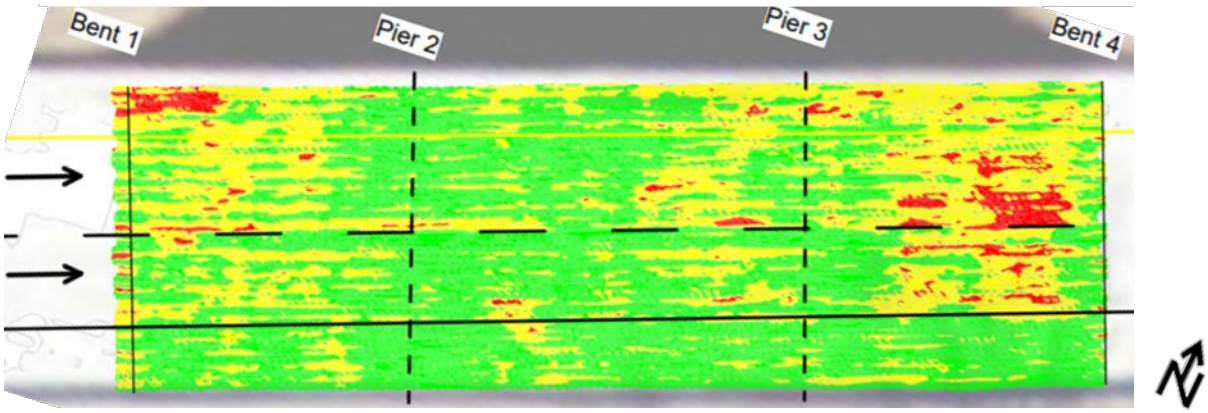

Bridge 49180

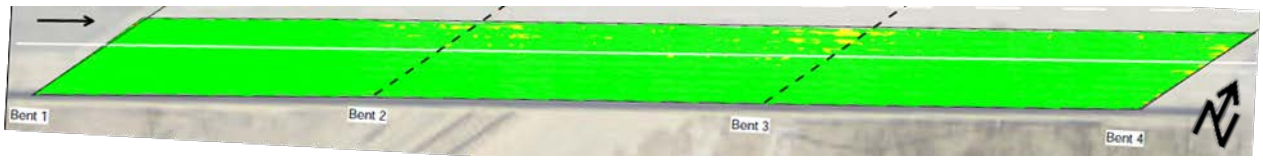

C.3 Impact Echo

C.3.1 INDOT–First Round

Bridge 16500

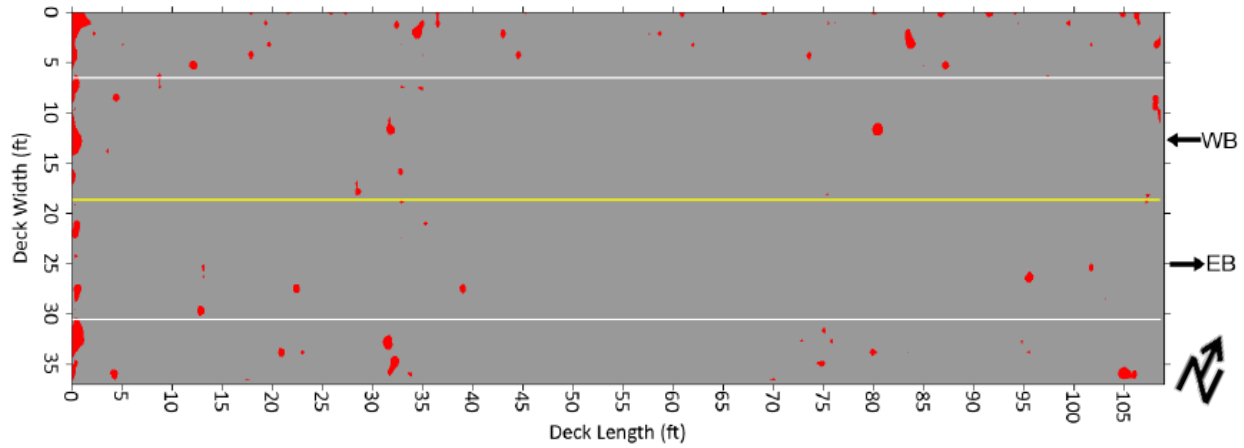

Bridge 18770

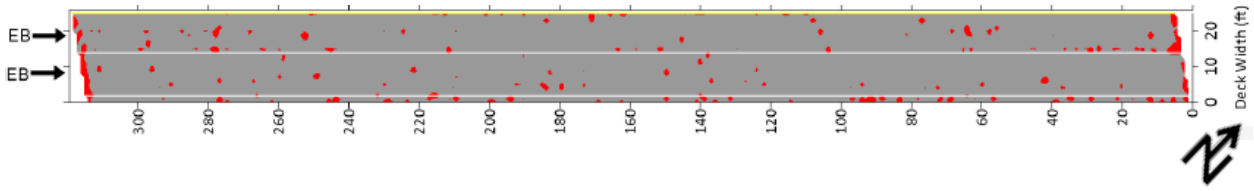

Bridge 22690

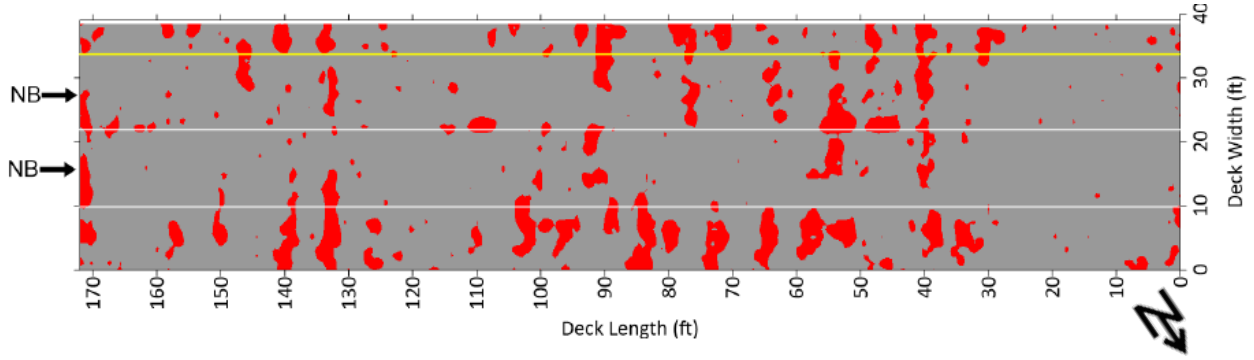

Bridge 31080

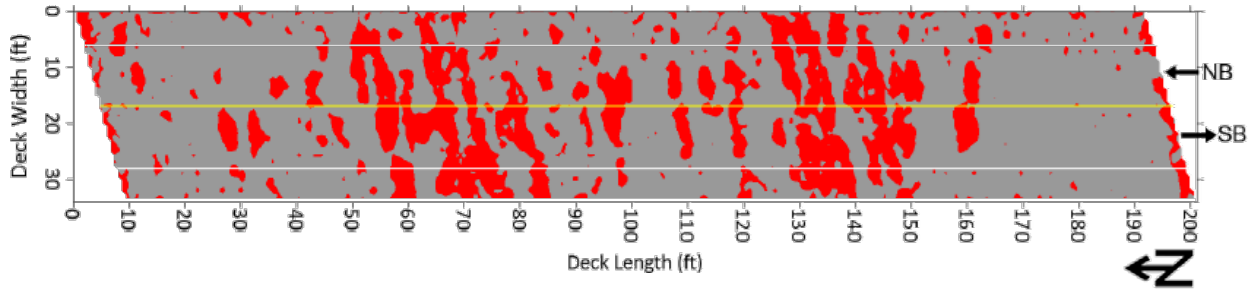

Bridge 35520

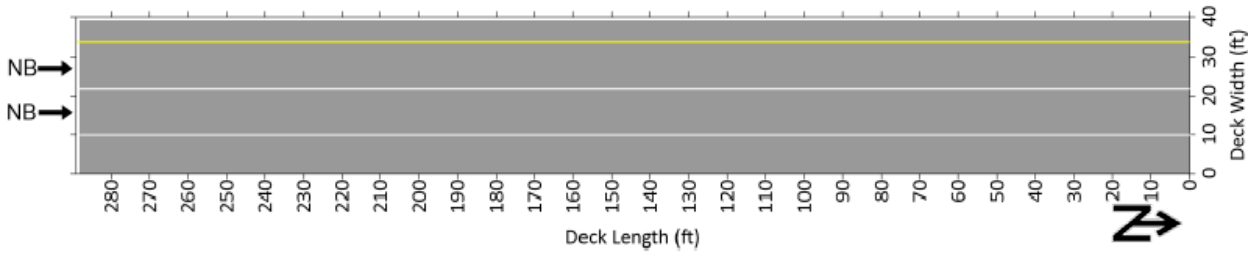

Bridge 37070

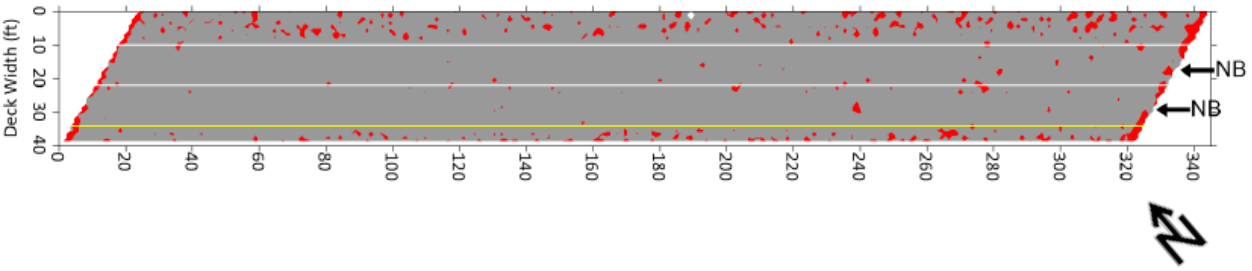

Bridge 37100

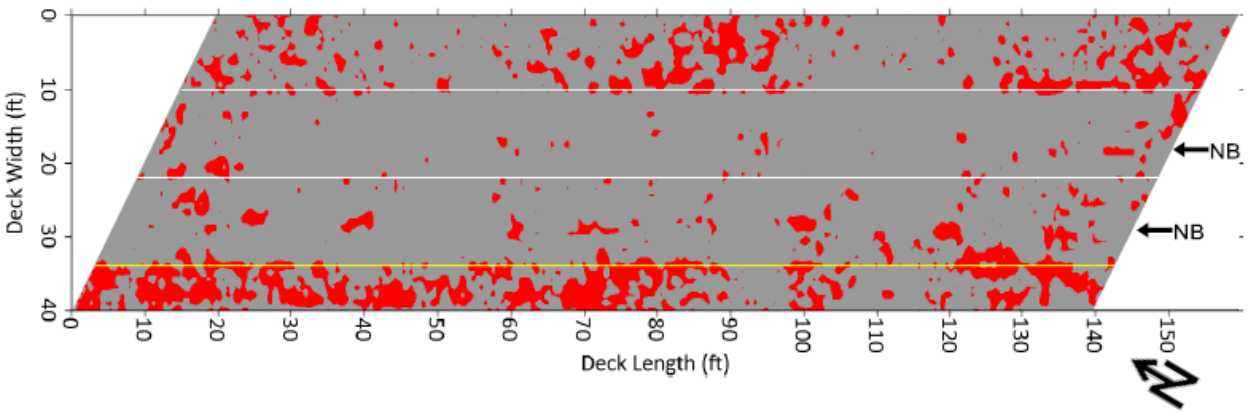

Bridge 37150

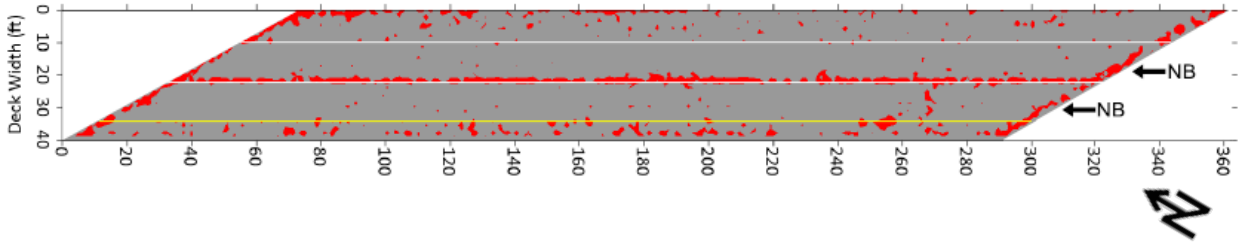

Bridge 41810

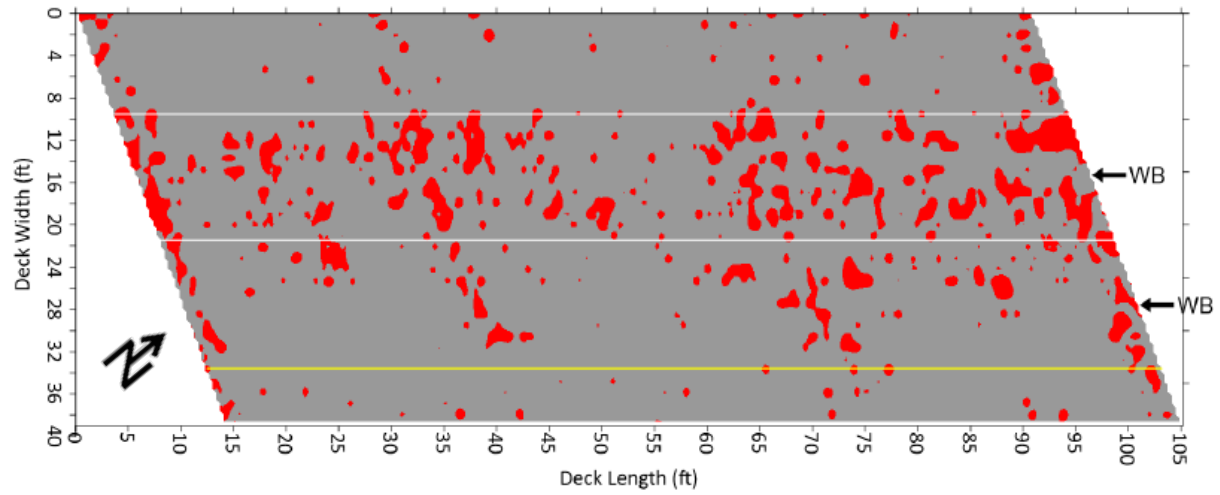

Bridge 41870

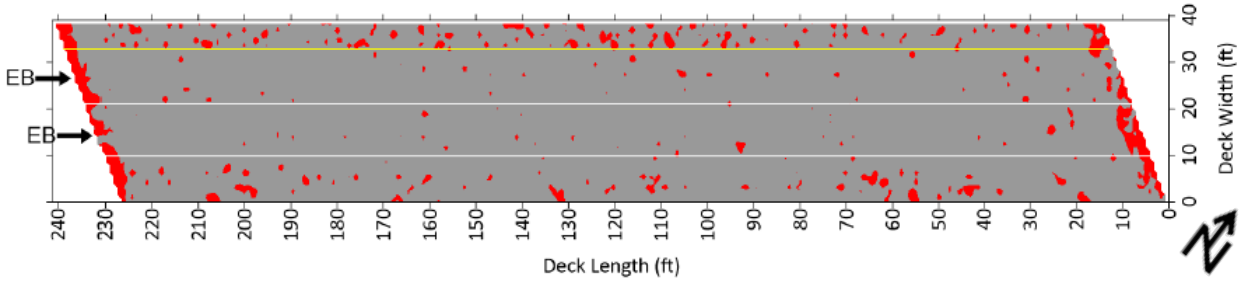

C.3.2 INDOT–Second Round

Bridge 01310

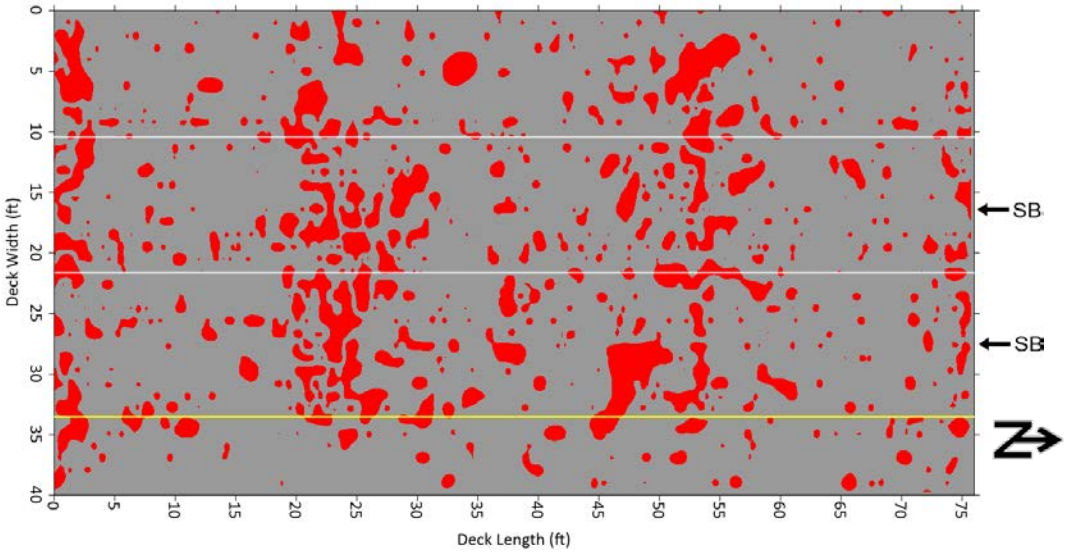

Bridge 01347

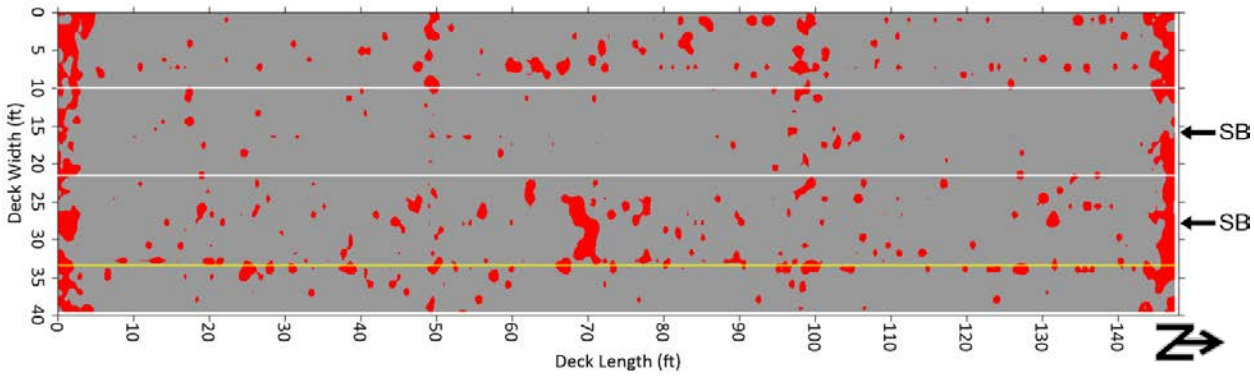

Bridge 04845

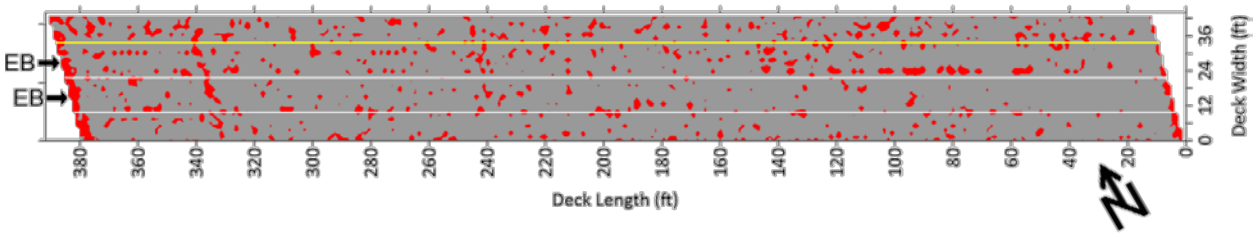

Bridge 04930

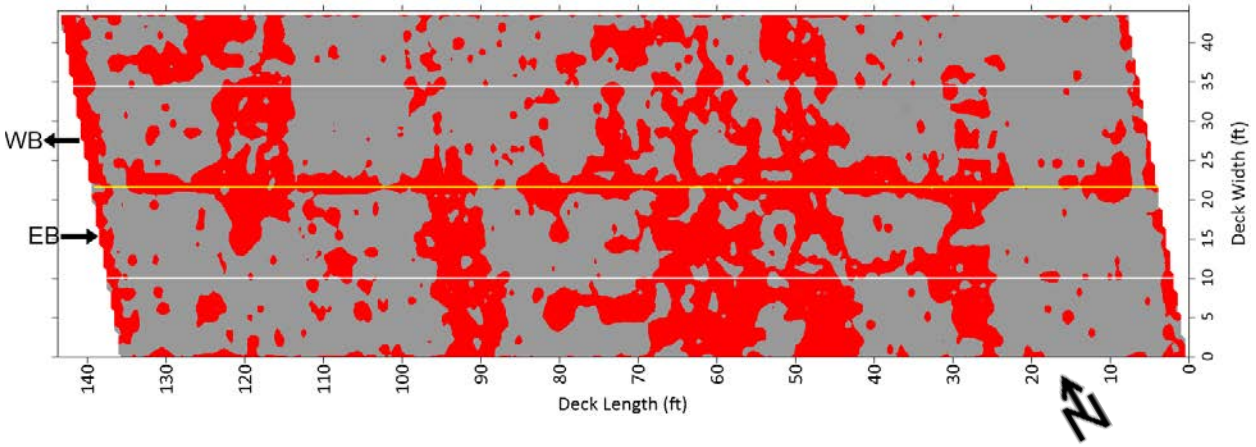

Bridge 08630

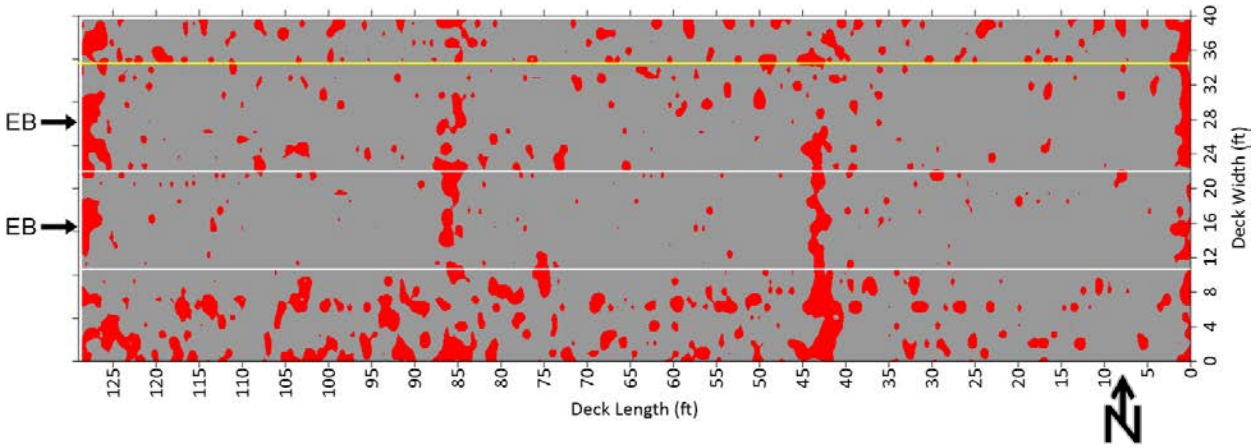

Bridge 17940

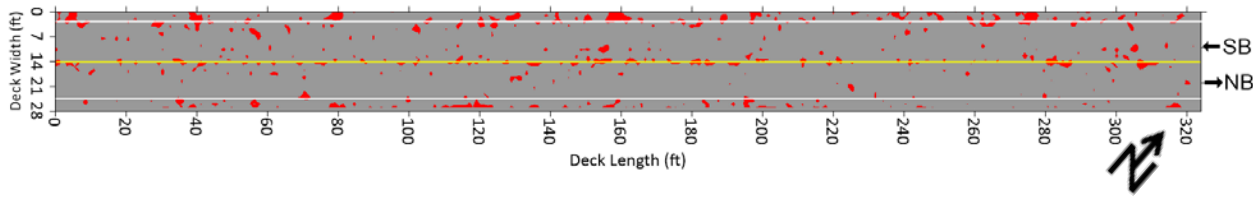

Bridge 19640

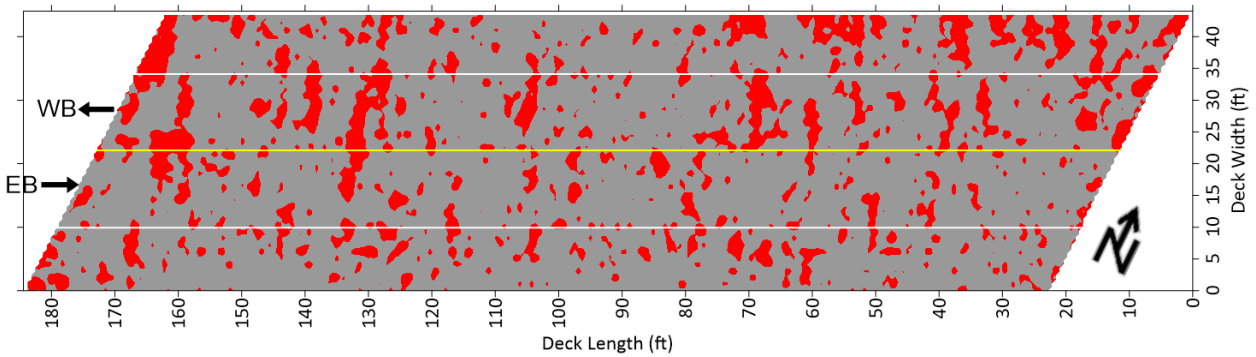

Bridge 20610

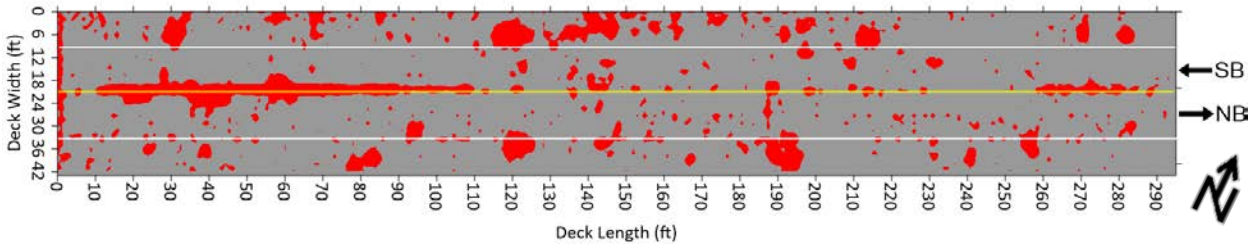

Bridge 24220

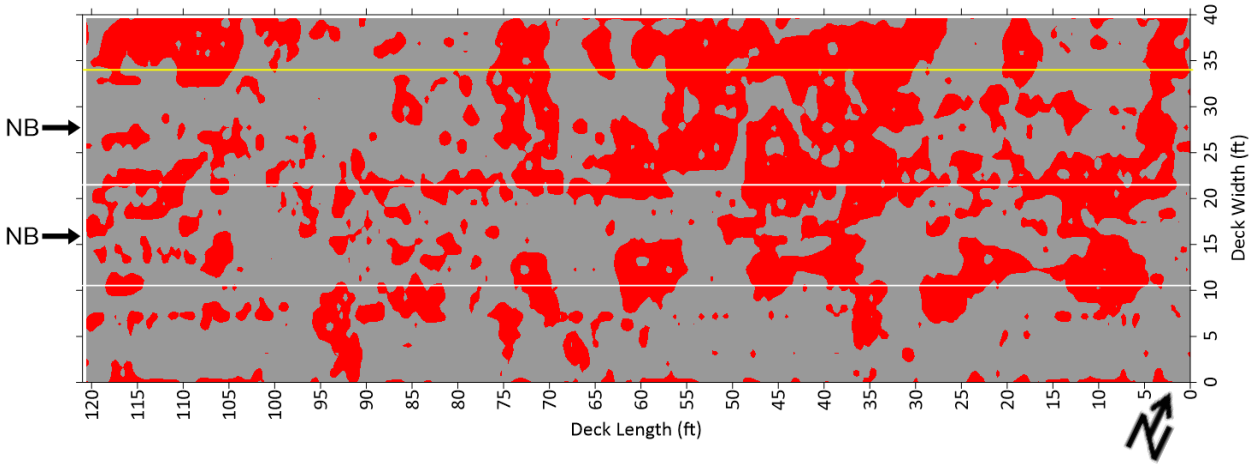

Bridge 49180

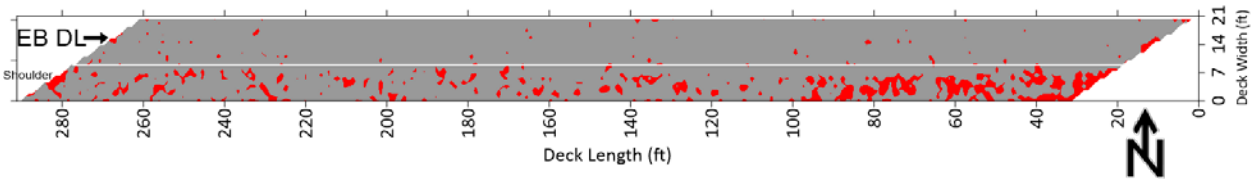

C.3.3 Consultant F

Bridge 01310

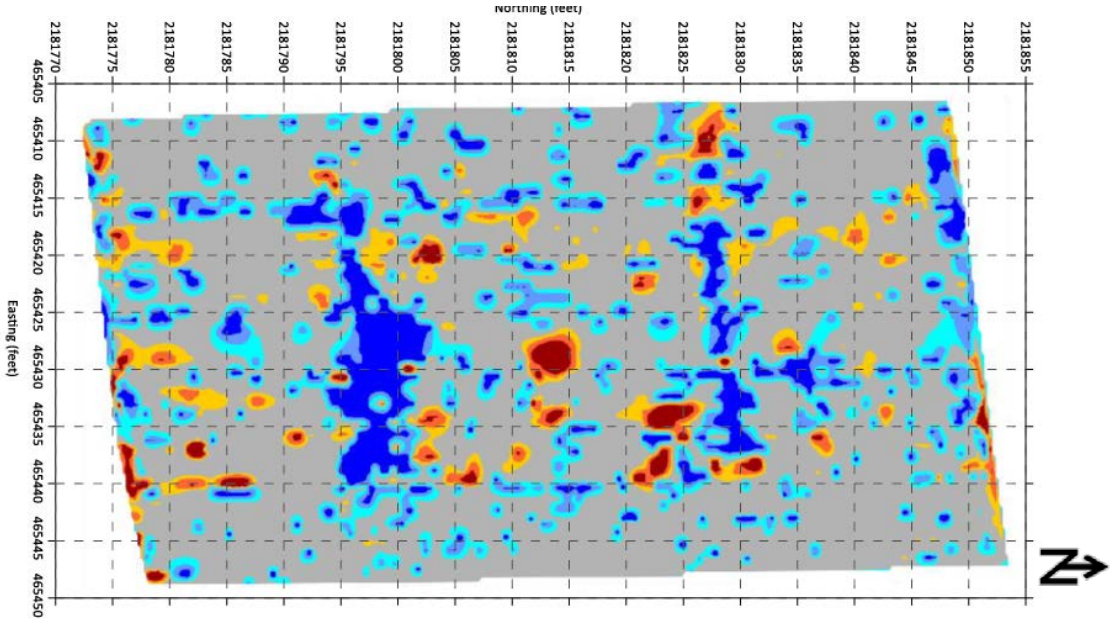

Bridge 01347

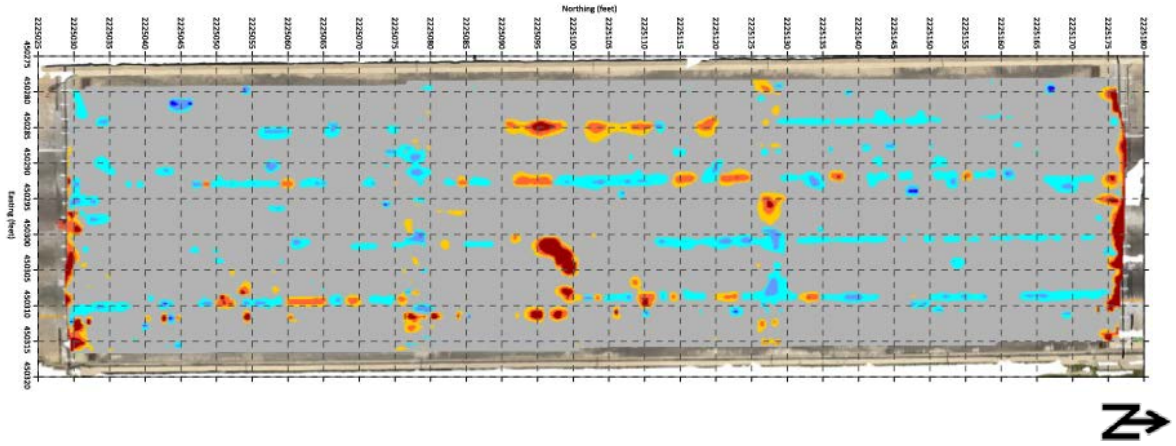

Bridge 04845

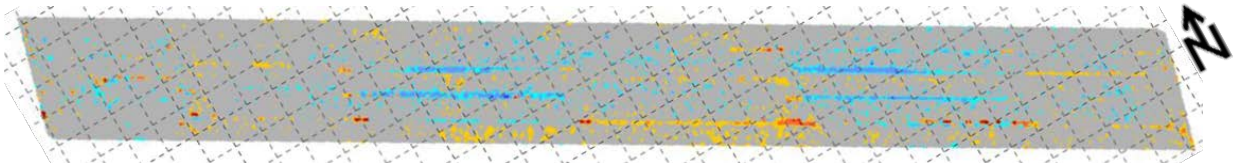

Bridge 04930

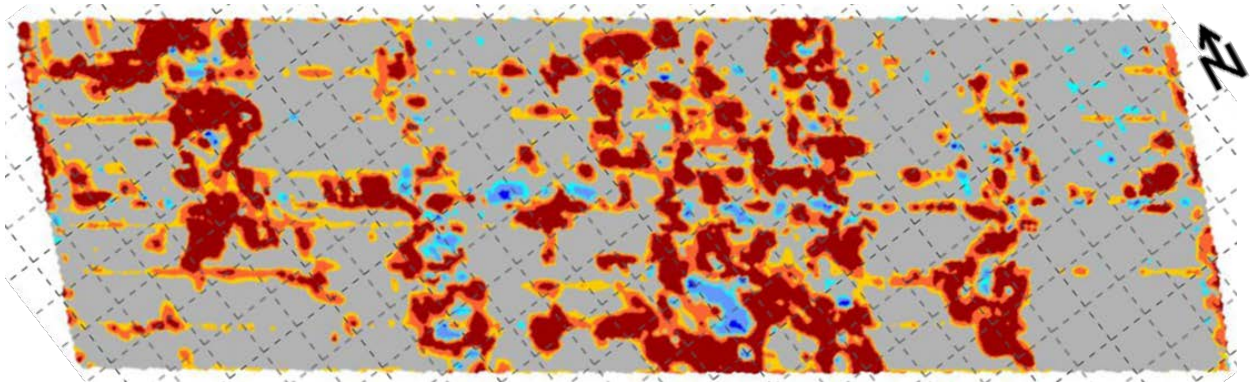

Bridge 24220

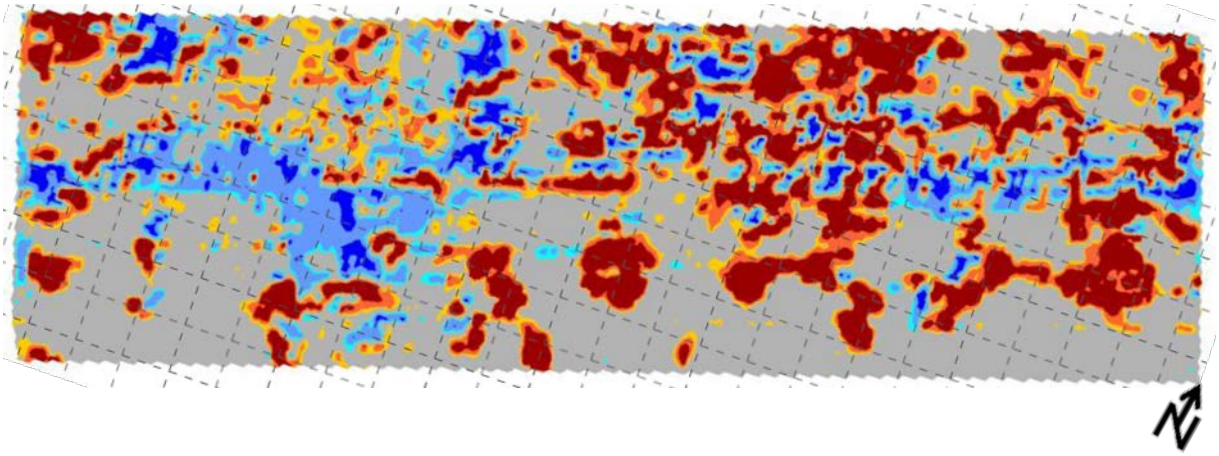

C.4 Infrared Thermography

C.4.1 Consultant D (Aerial IRT)–First Round

Bridge 36070

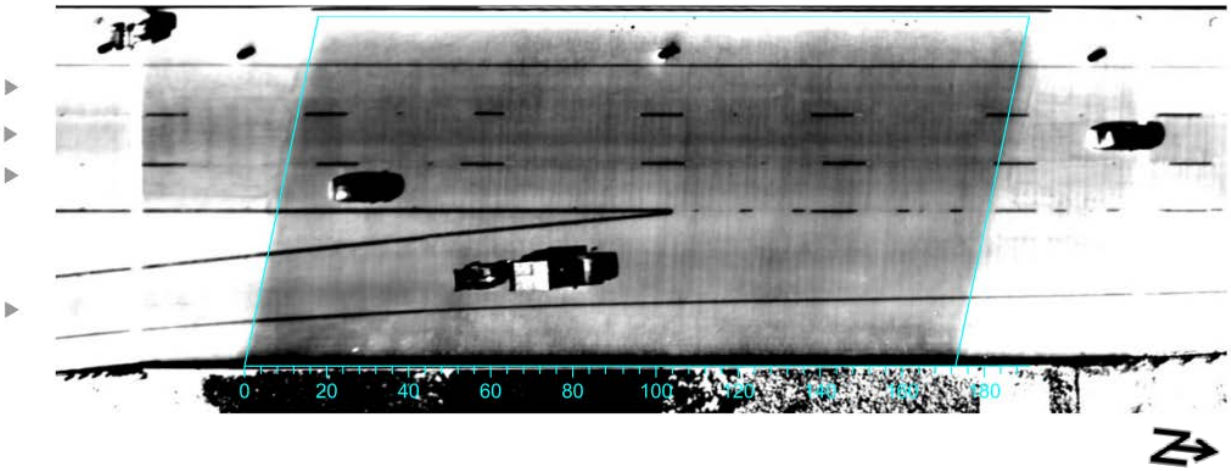

Bridge 36130

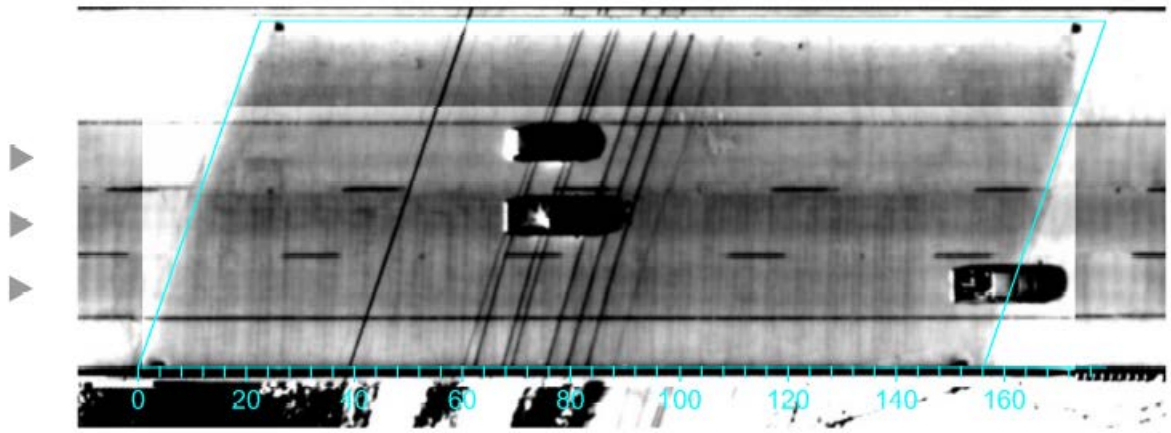

Bridge 36150

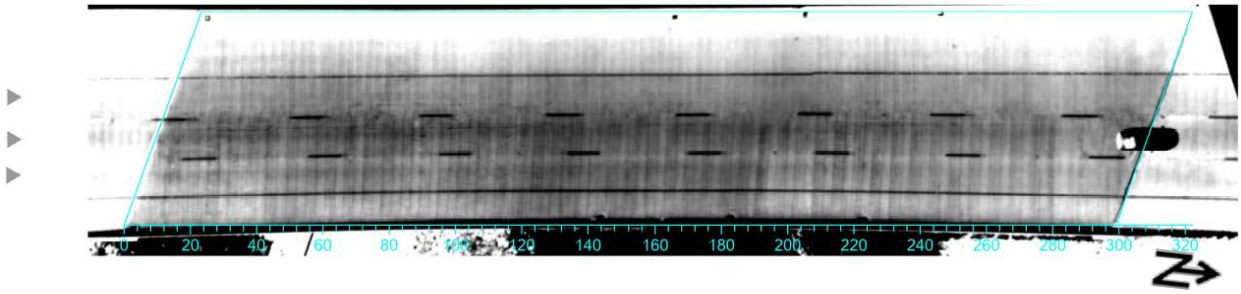

Bridge 36170

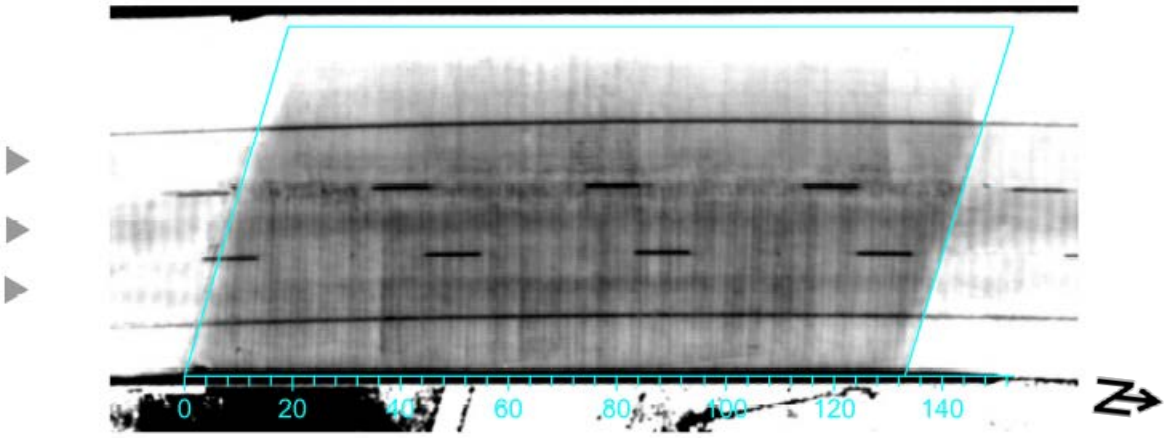

Bridge 36190

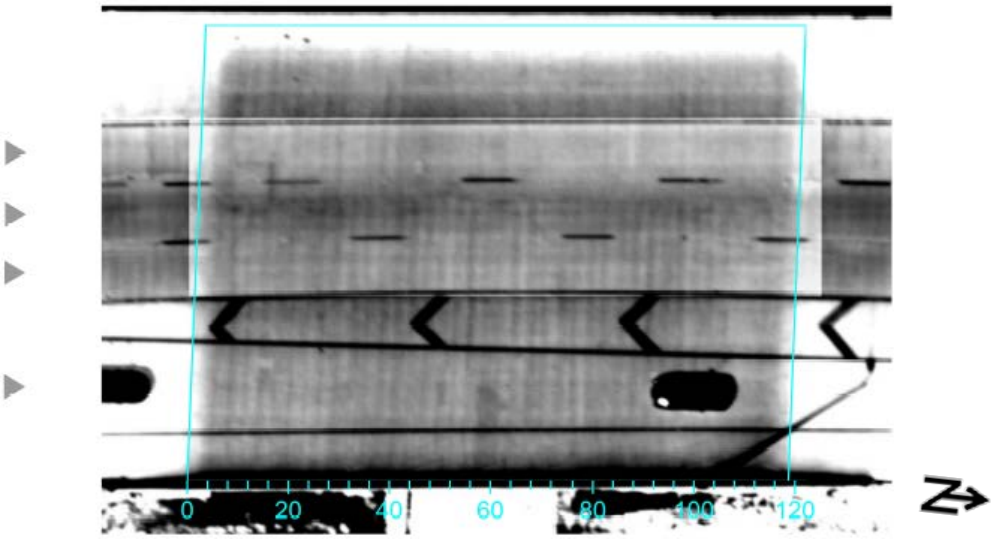

Bridge 36210

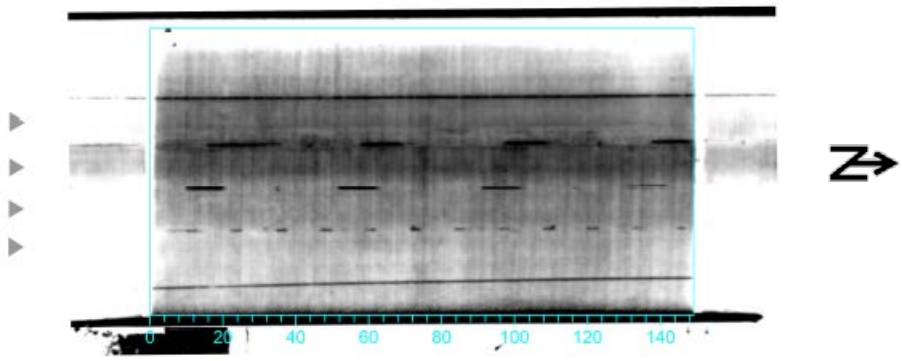

Bridge 36230

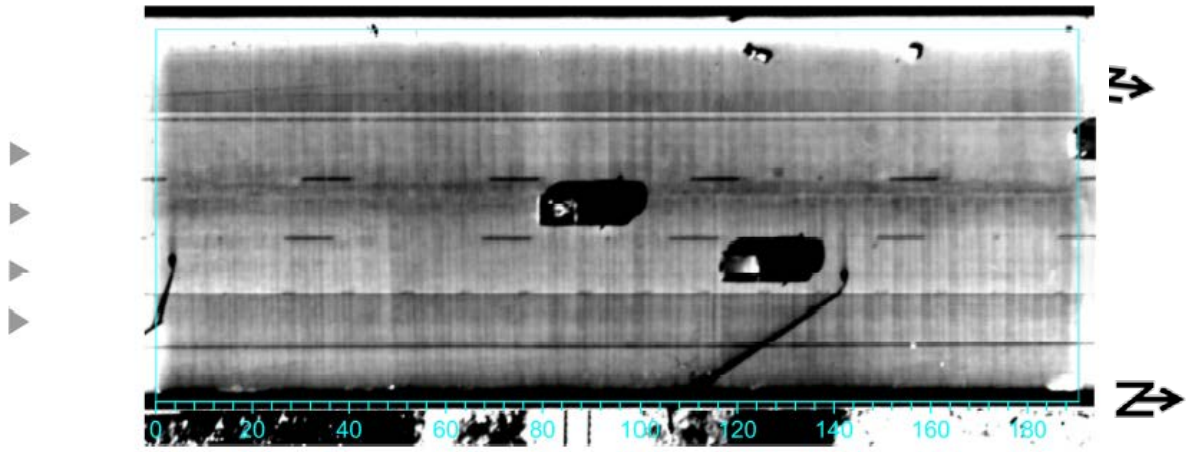

Bridge 36250

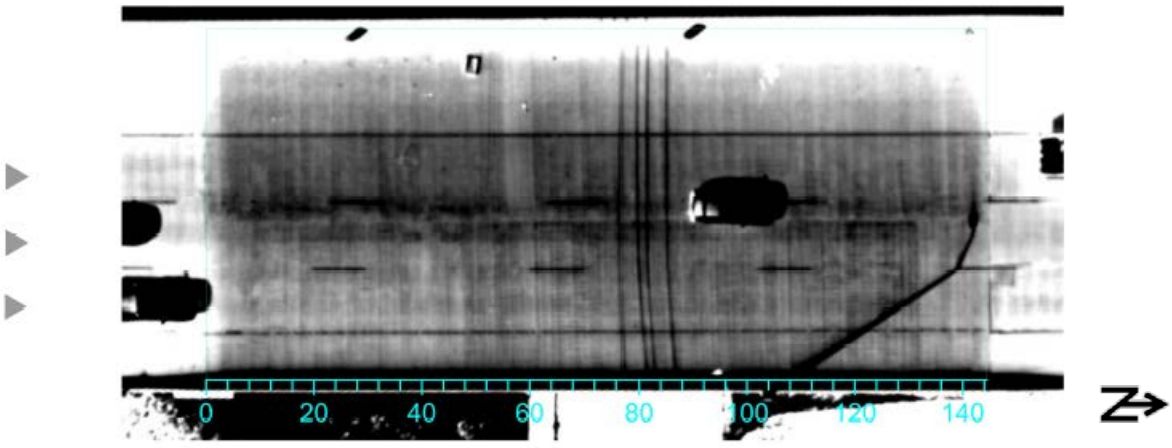

Bridge 36270

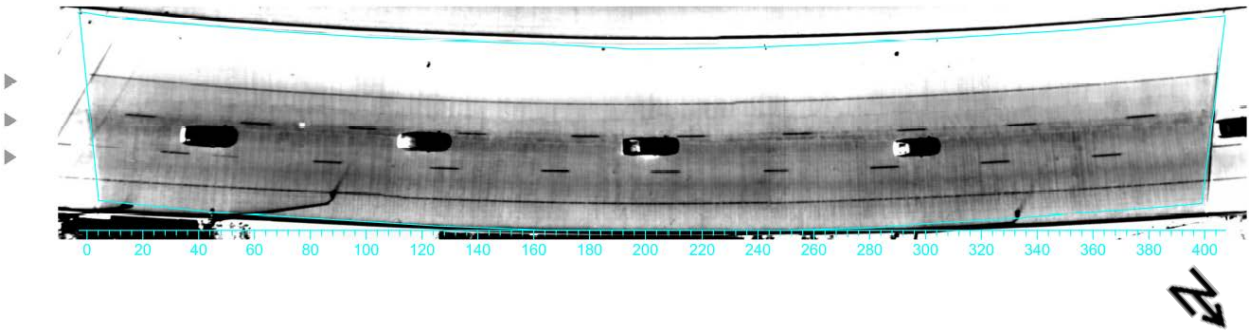

Bridge 36290

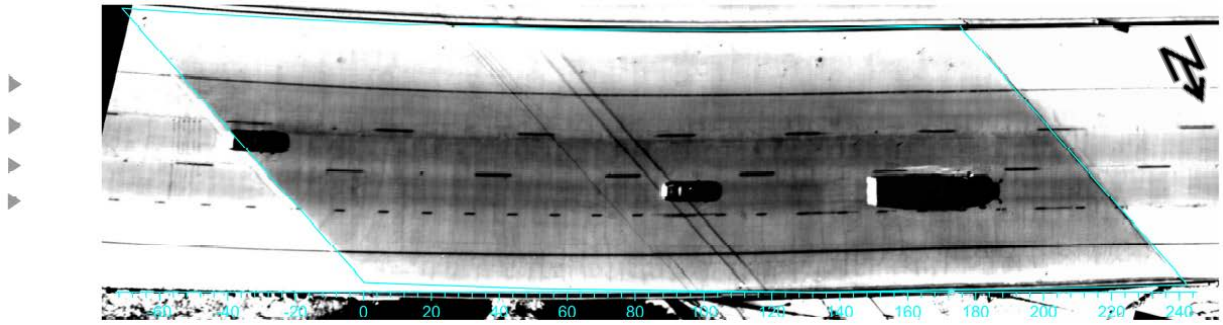

Bridge 36320

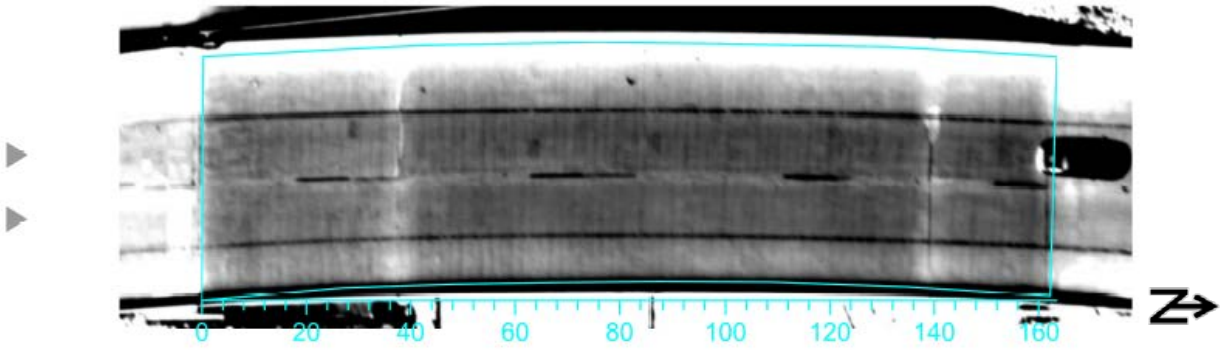

Bridge 36330

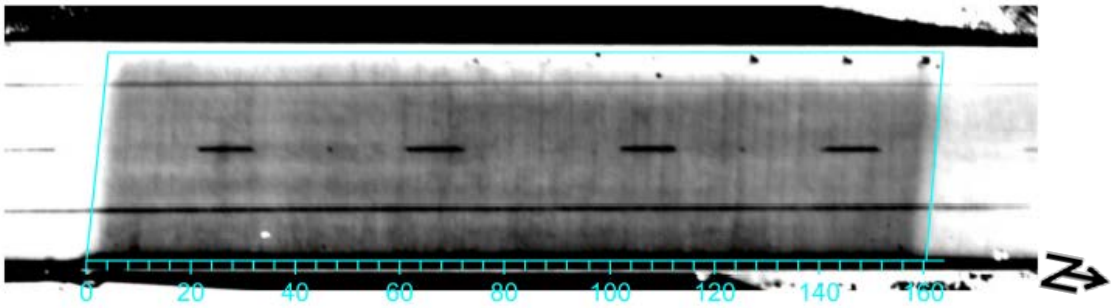

Bridge 36520

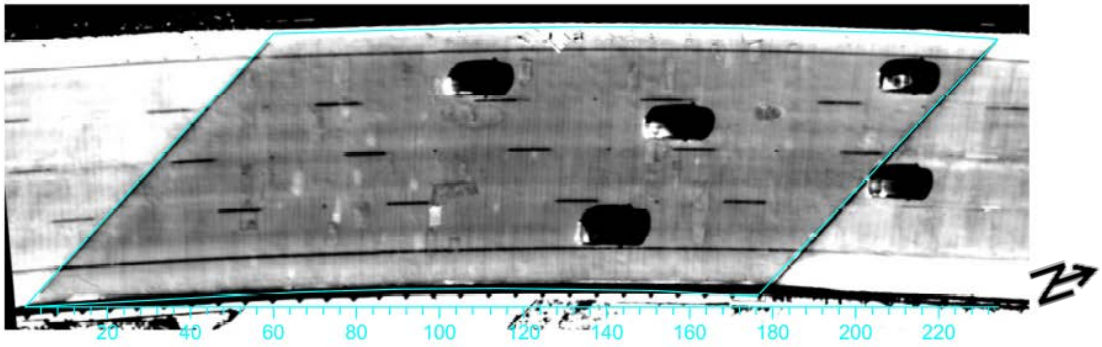

Bridge 36660

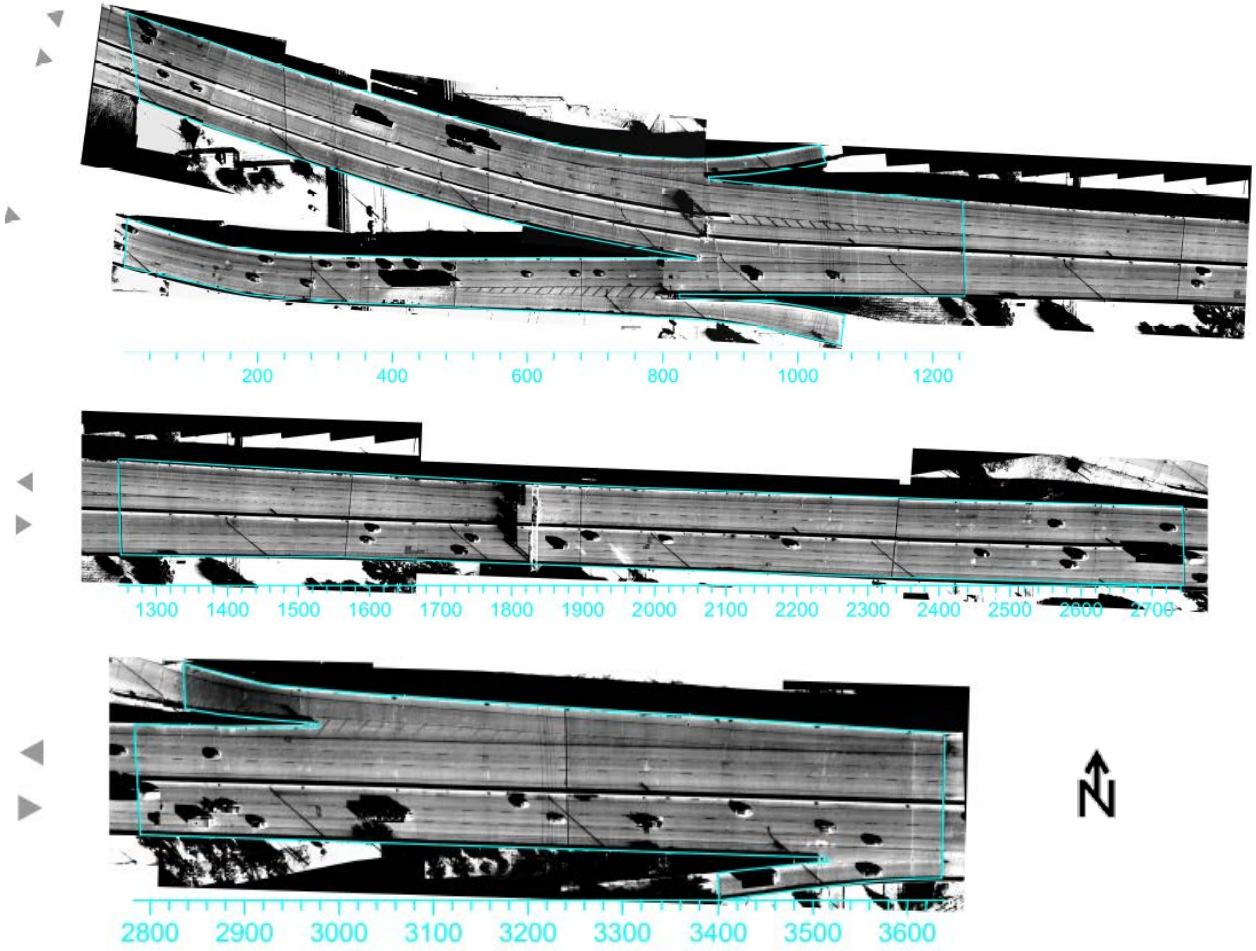

Bridge 36680

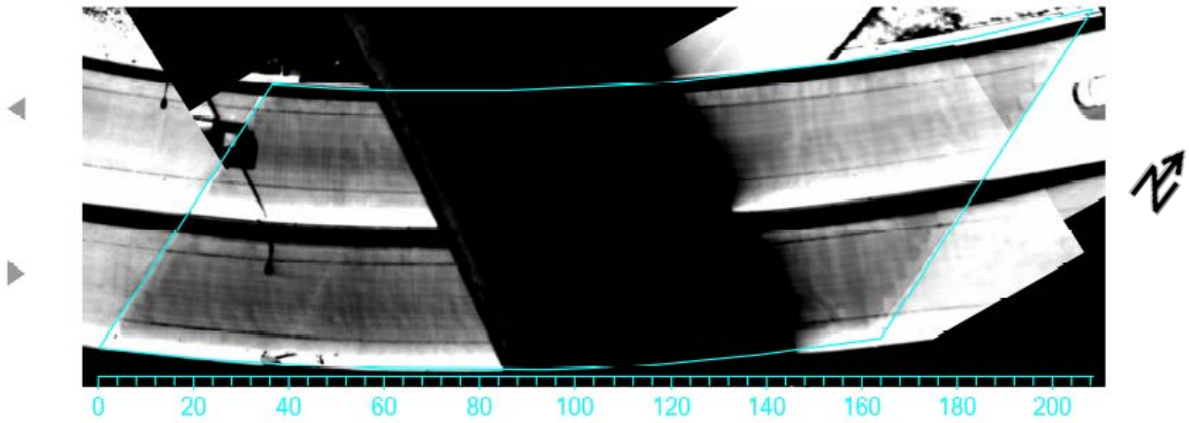

Bridge 36690

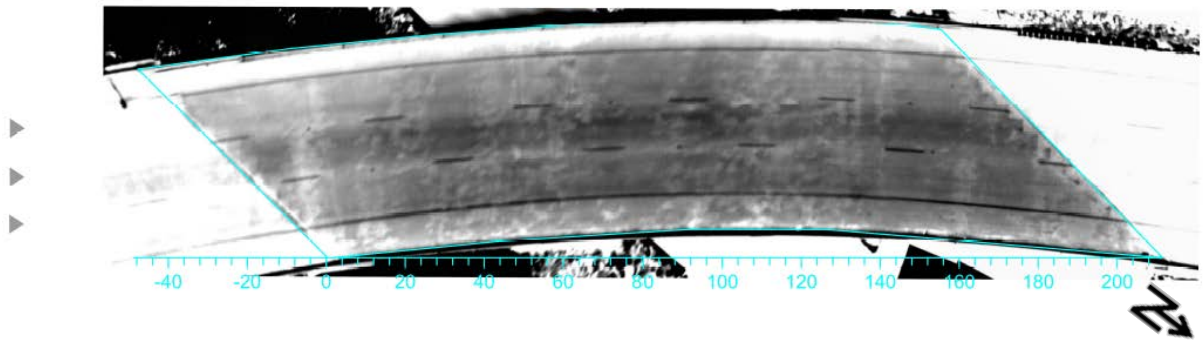

Bridge 36700

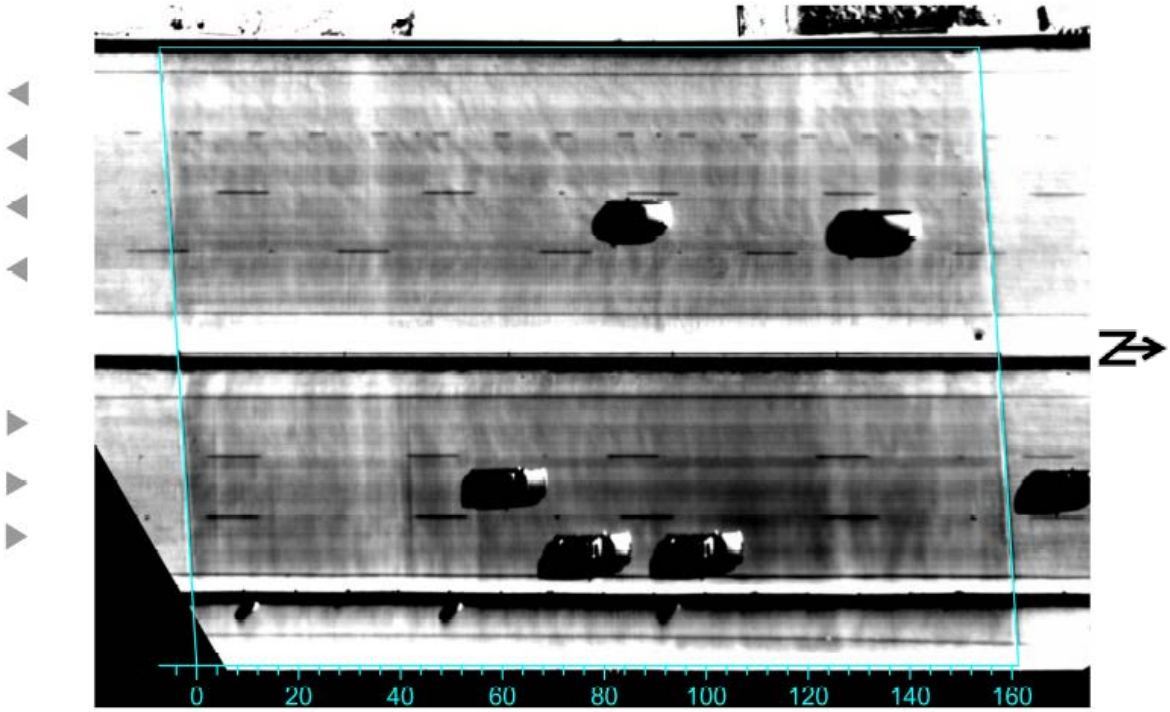

Bridge 36730

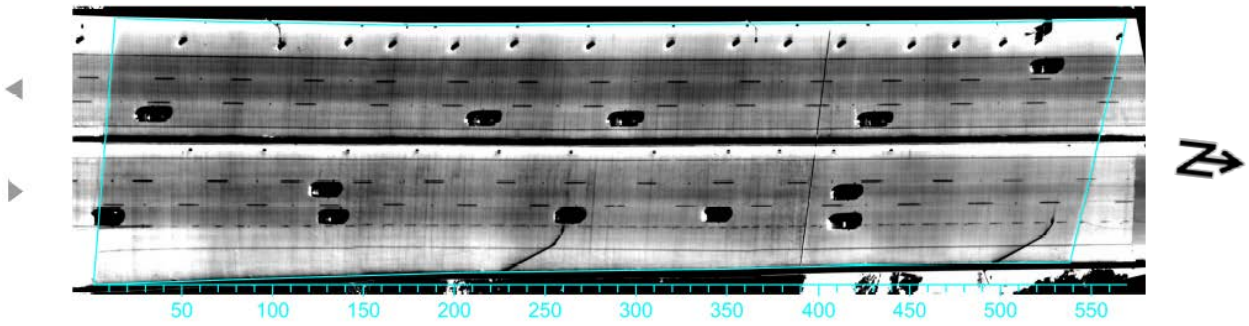

Bridge 36740

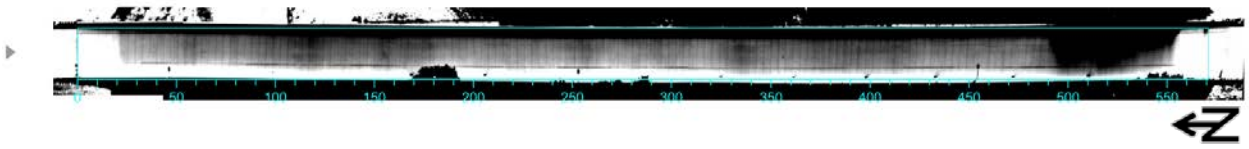

Bridge 36750

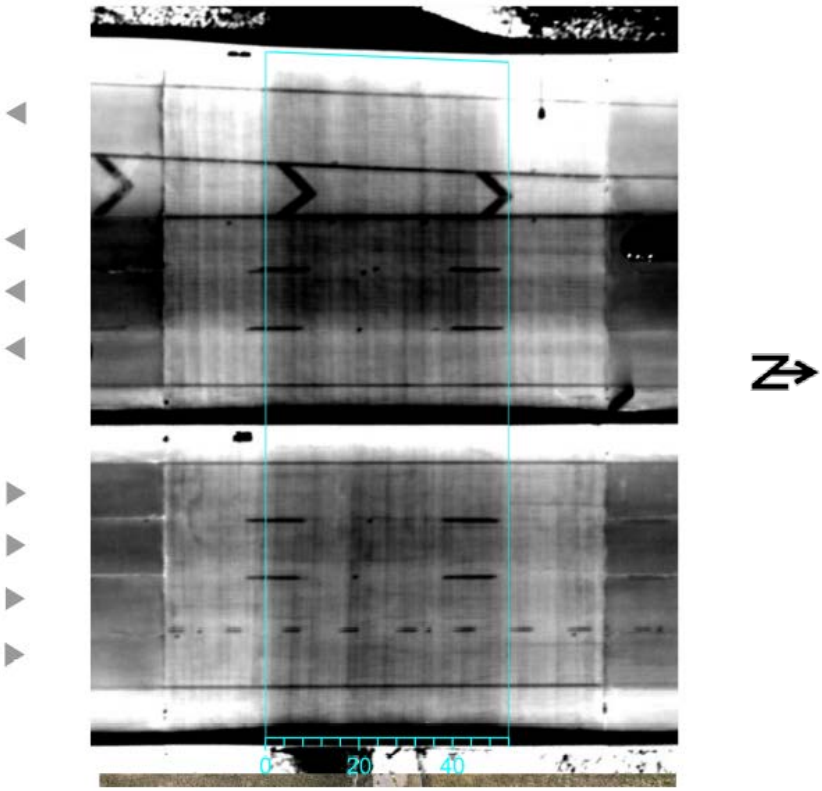

Bridge 36760

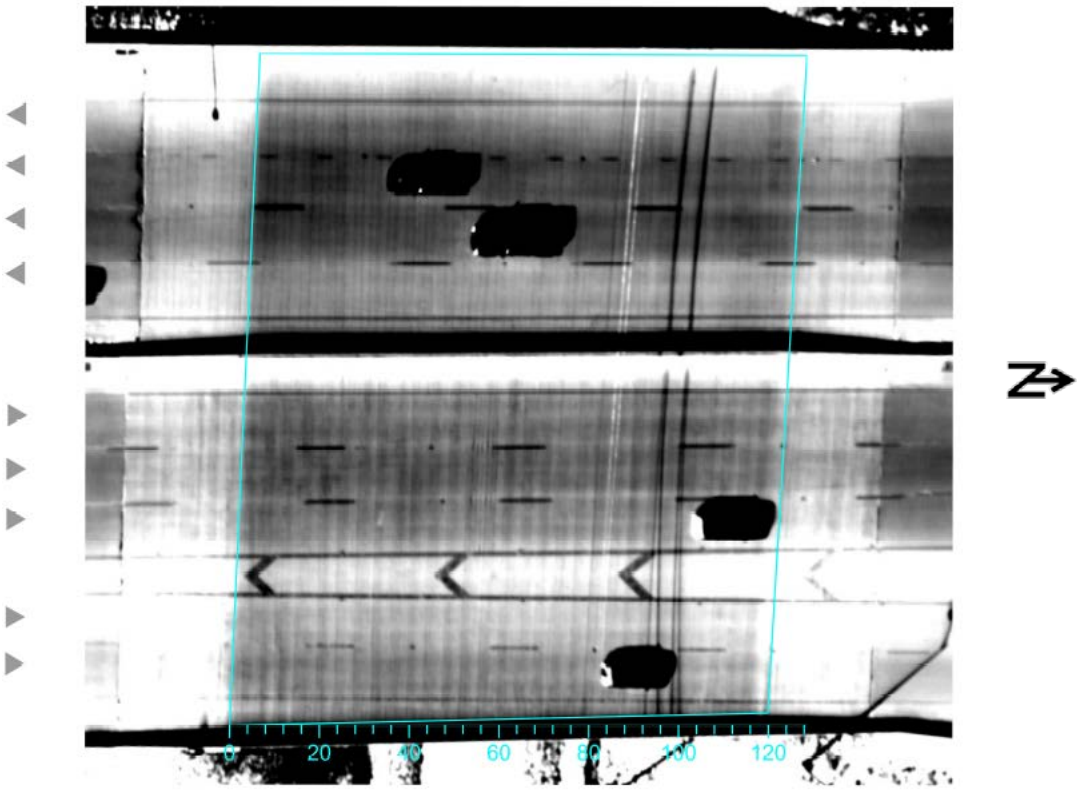

Bridge 36770

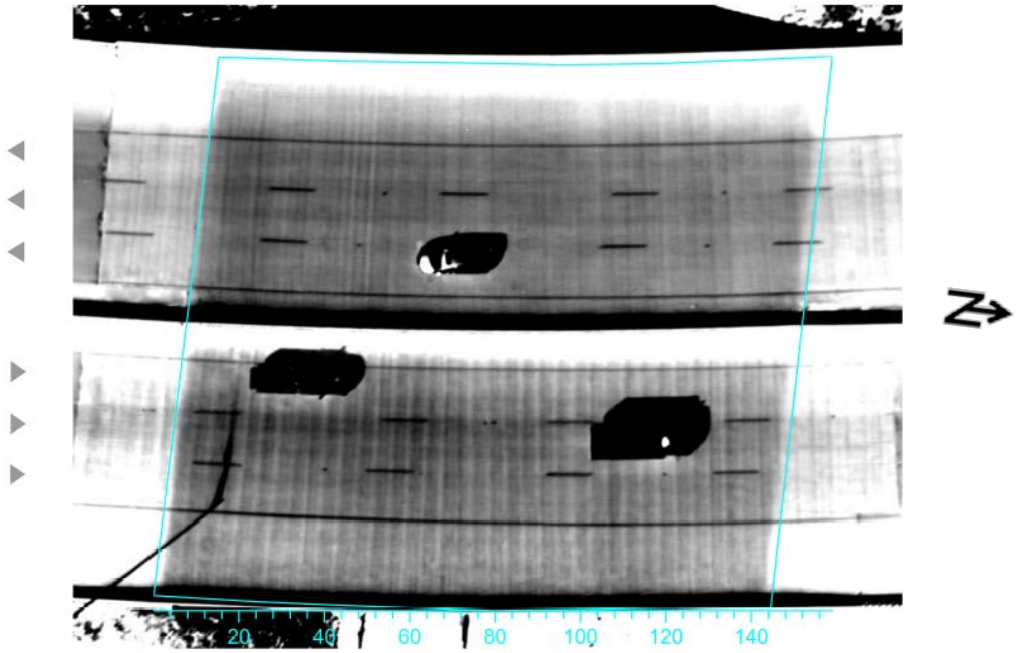

Bridge 36780

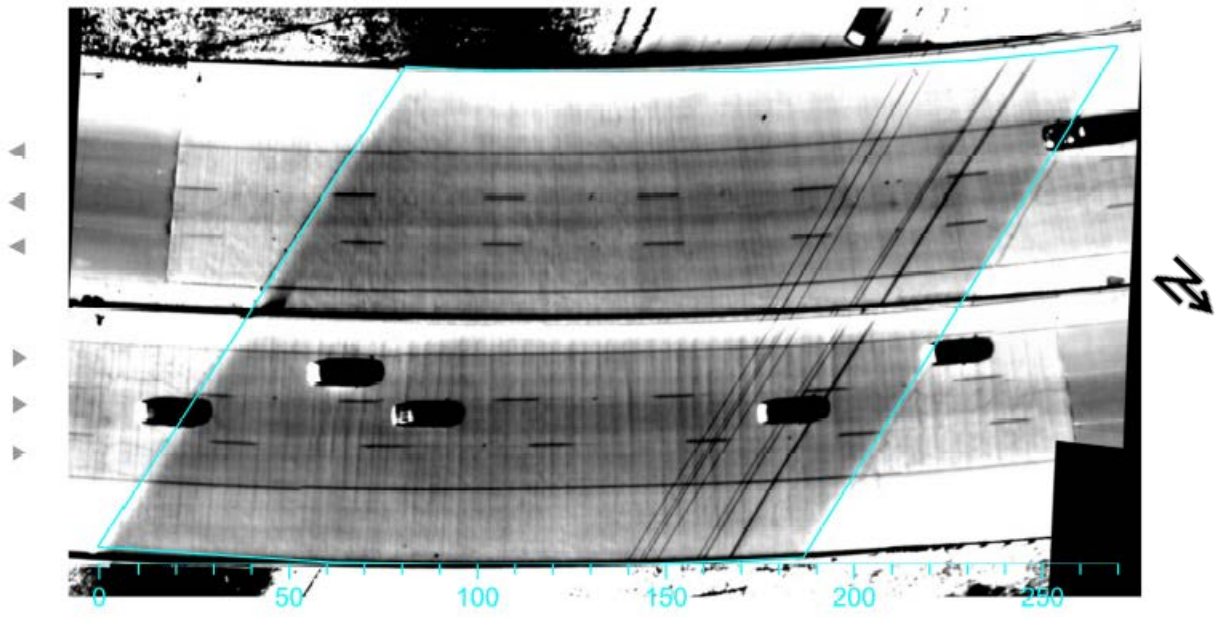

Bridge 36790

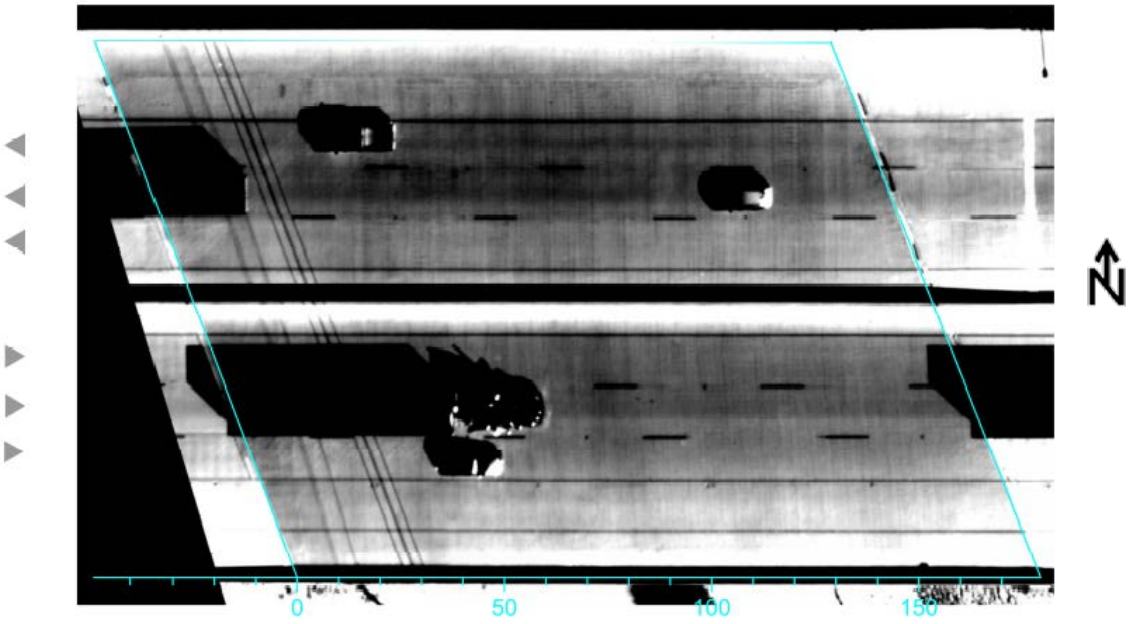

Bridge 36800

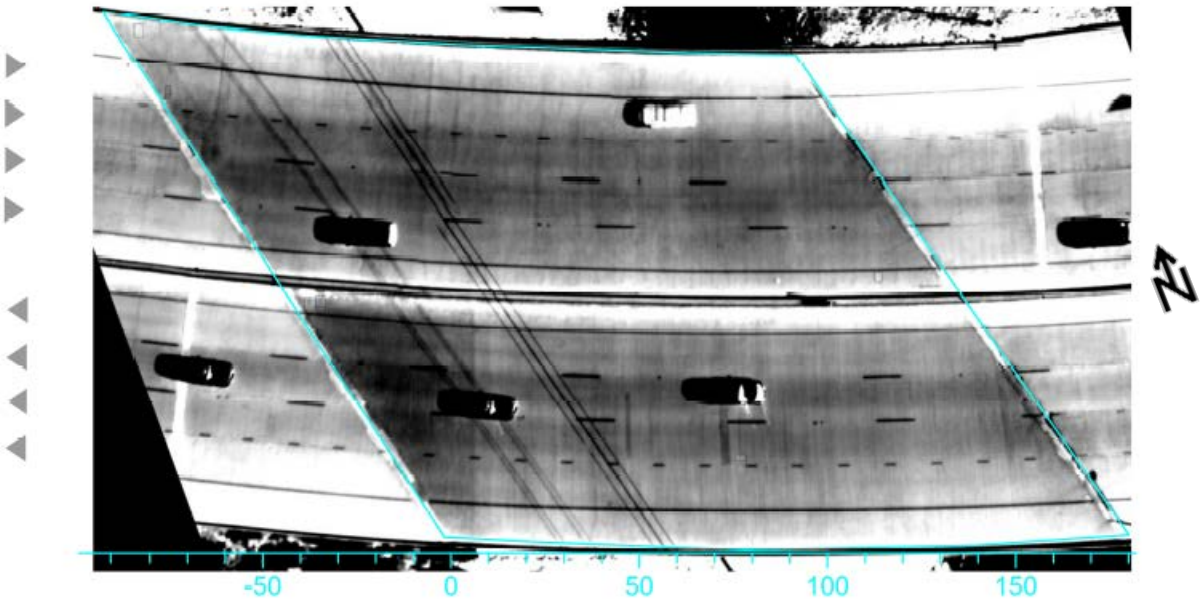

Bridge 36850

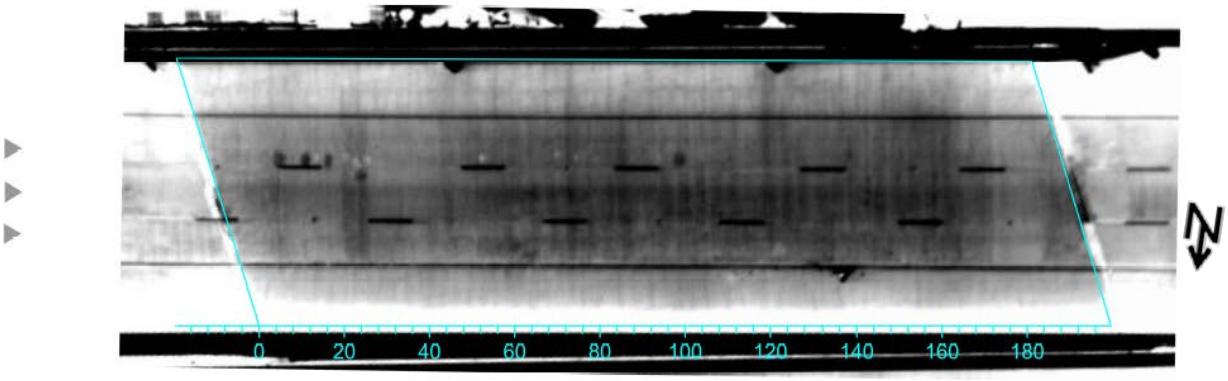

Bridge 36880

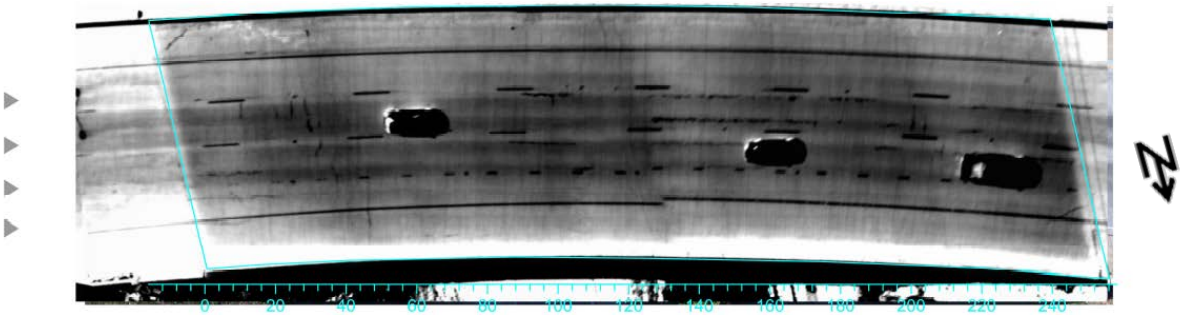

Bridge 36900

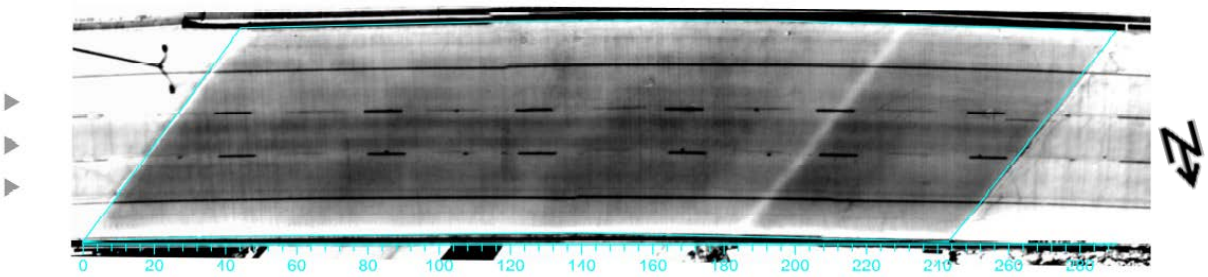

Bridge 36920

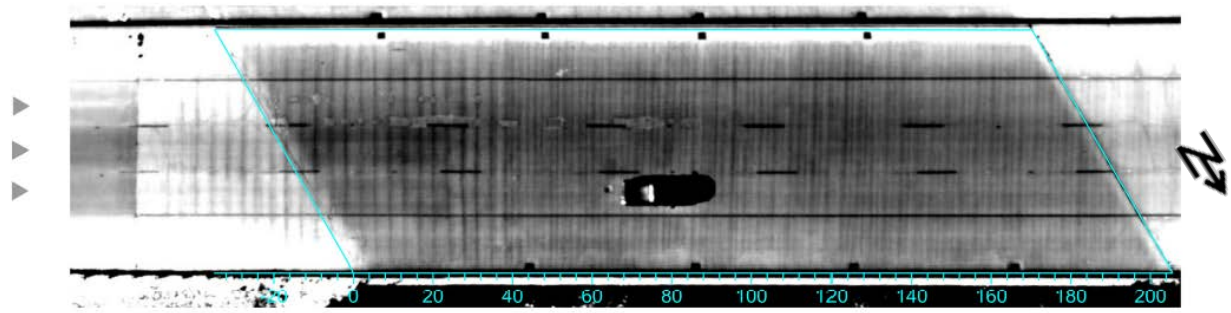

Bridge 36950

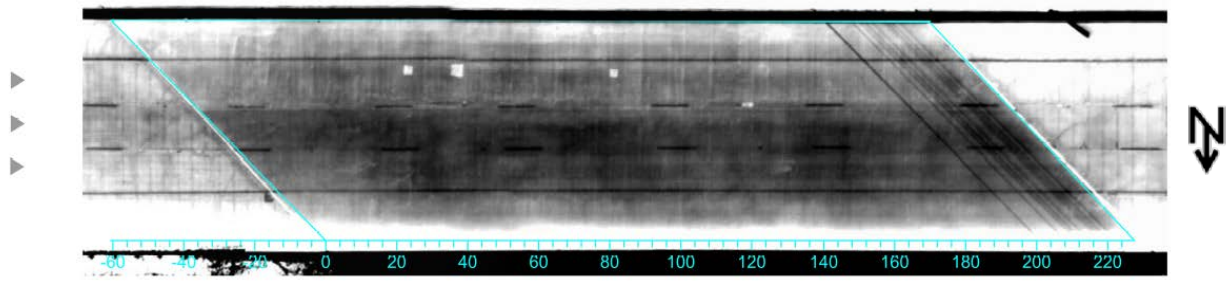

Bridge 36980

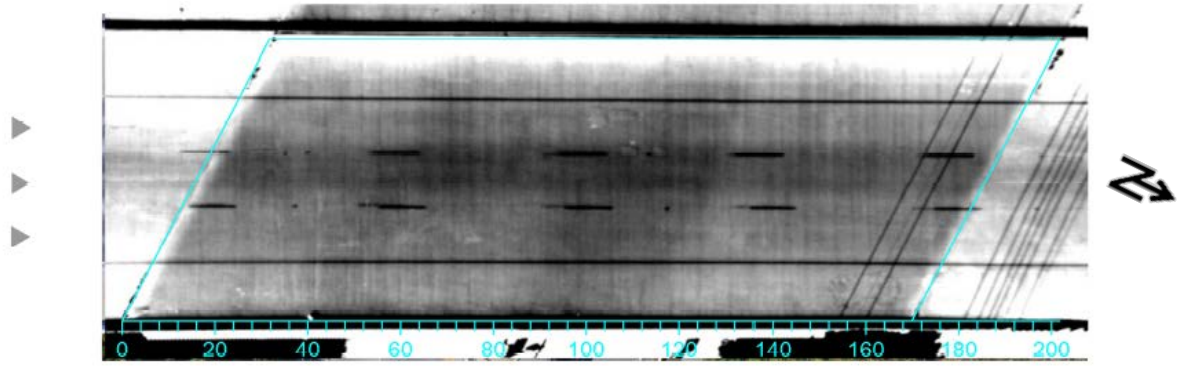

Bridge 37030

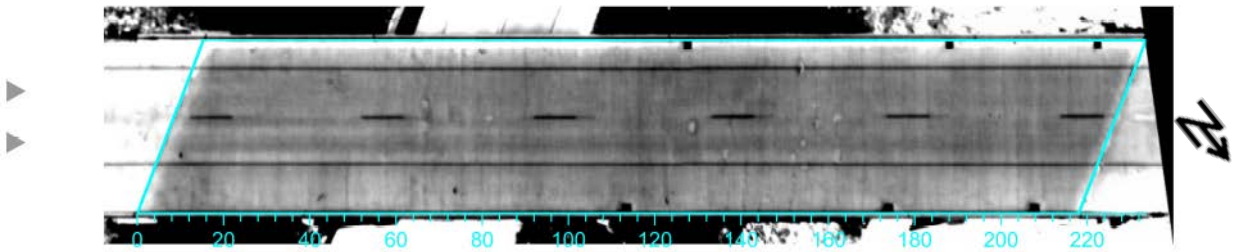

Bridge 37060

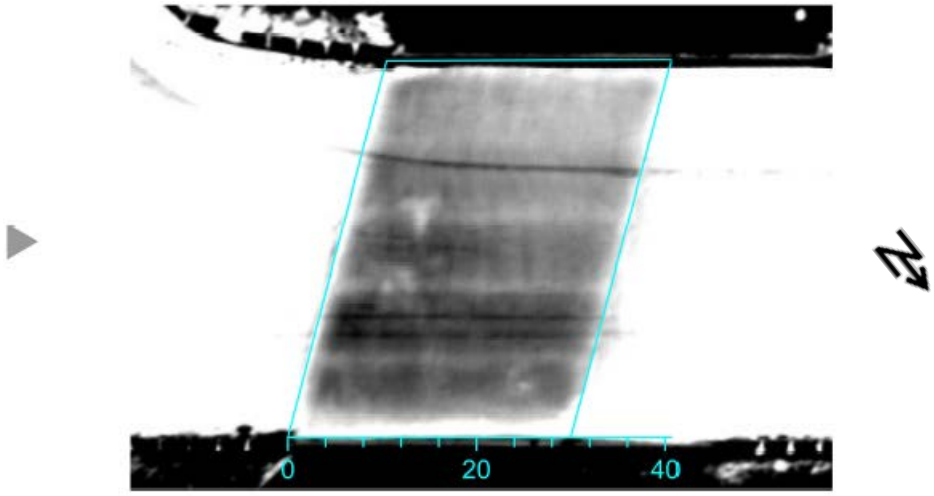

Bridge 37070

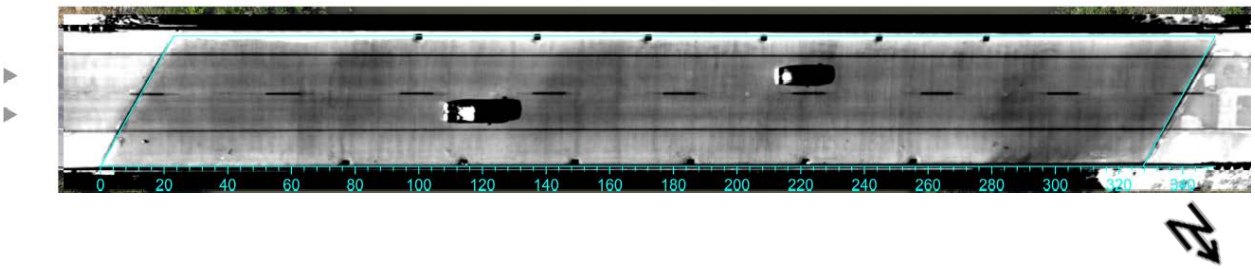

Bridge 37100

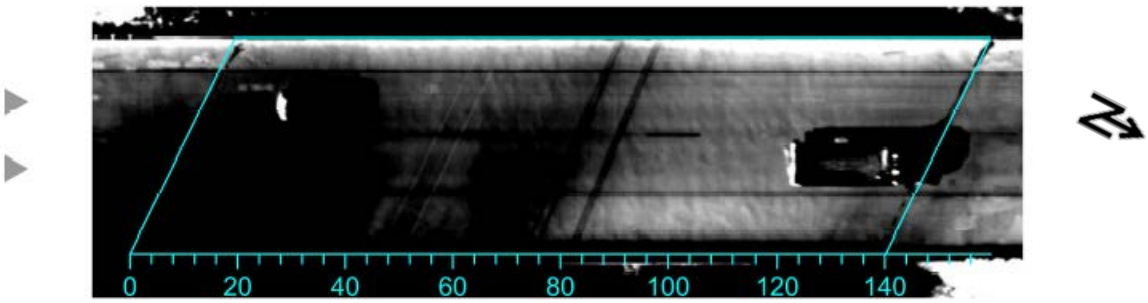

Bridge 37120

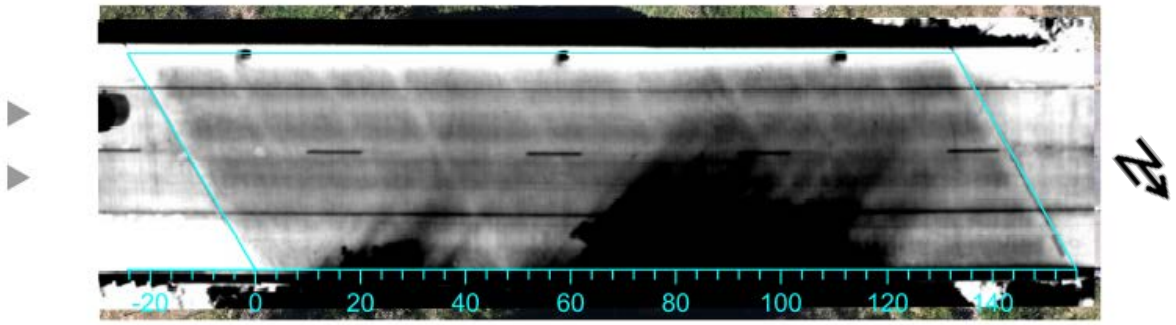

Bridge 50720

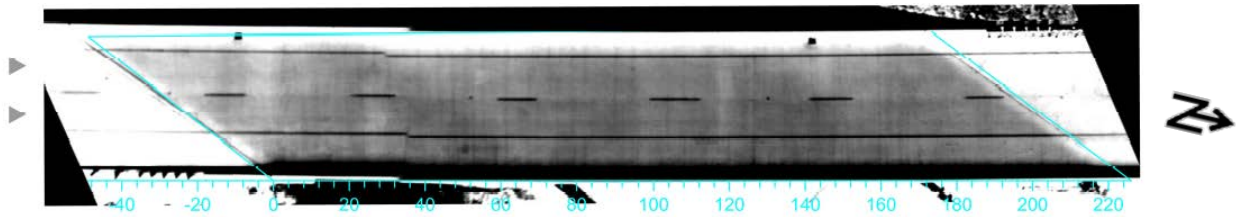

C.4.2 Consultant D (vehicle-mounted IRT)–First Round (see result maps at air-launched GPR)

See result maps.

C.4.3 Consultant E (Vehicle-Mounted IRT)–First Round

Bridge 01310

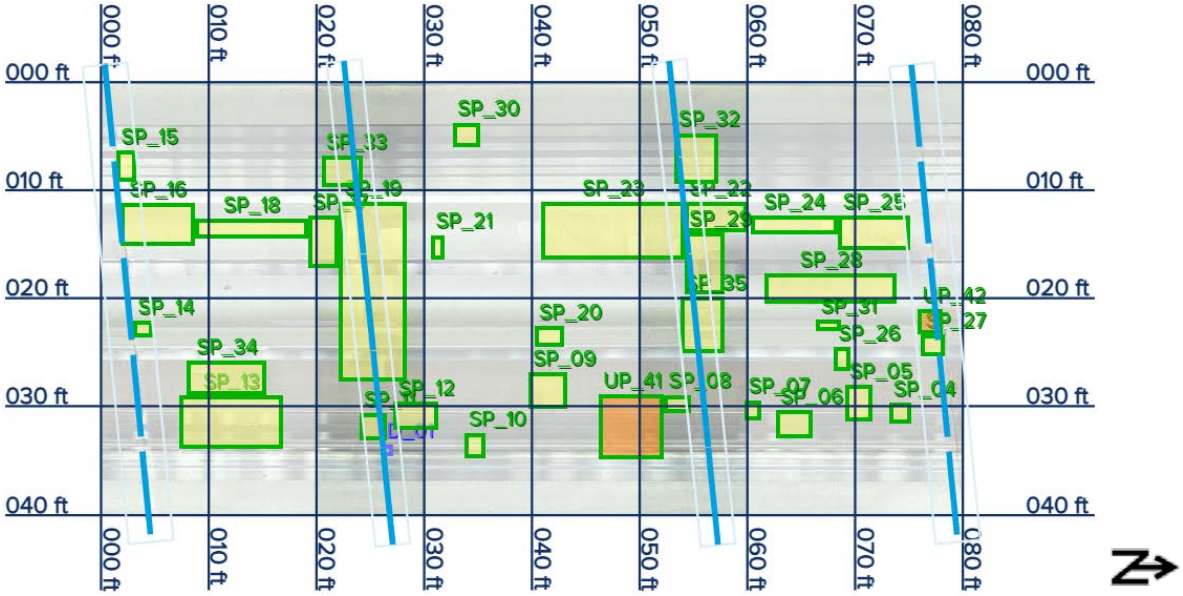

Bridge 01347

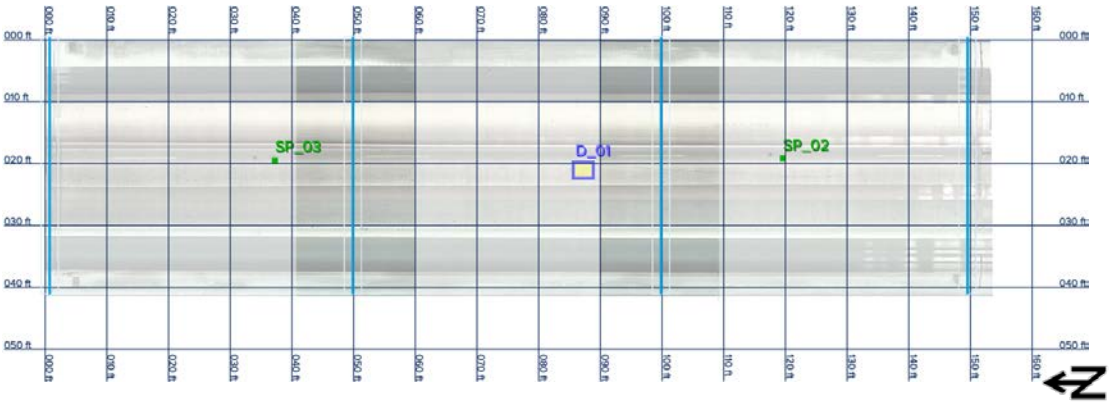

Bridge 05230

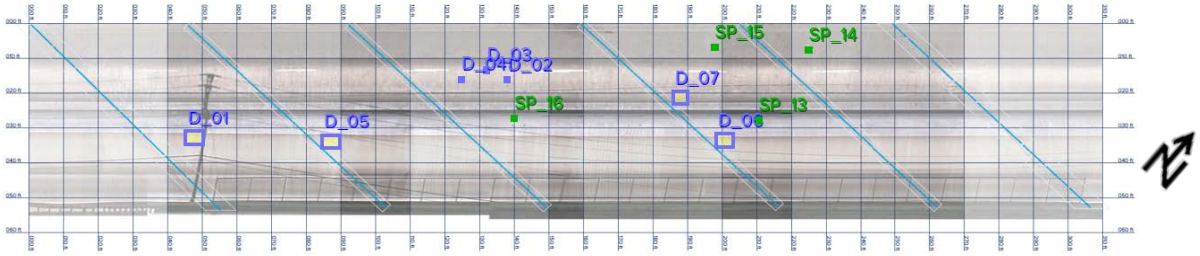

Bridge 11940

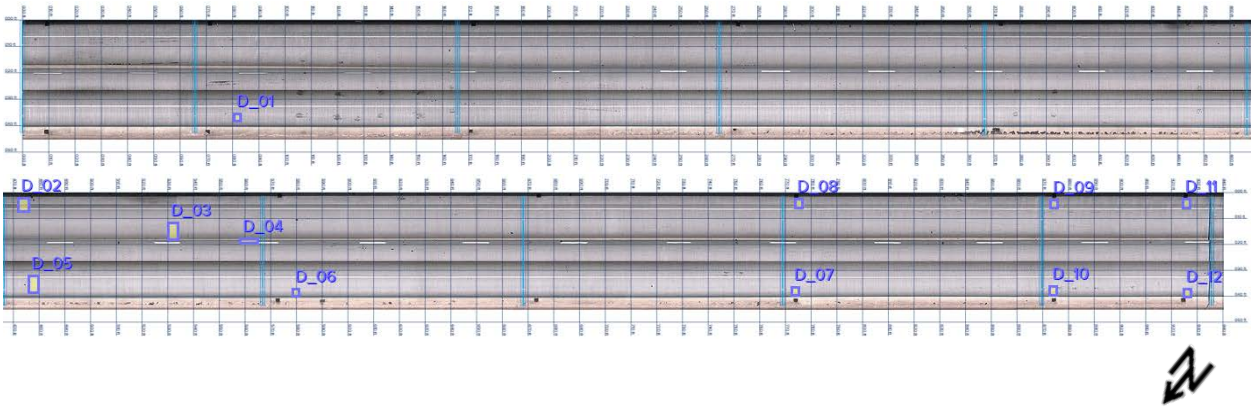

Bridge 16500

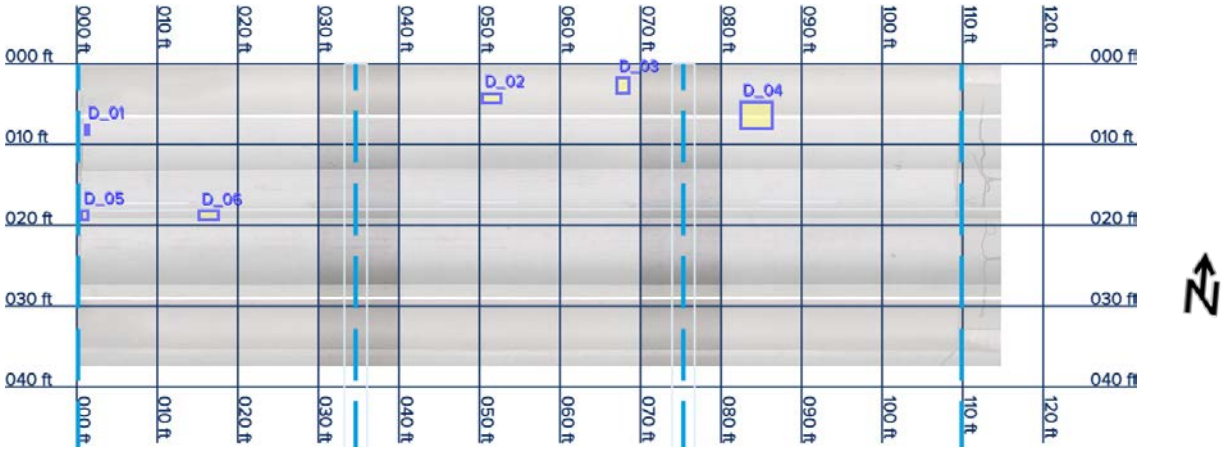

Bridge 17940

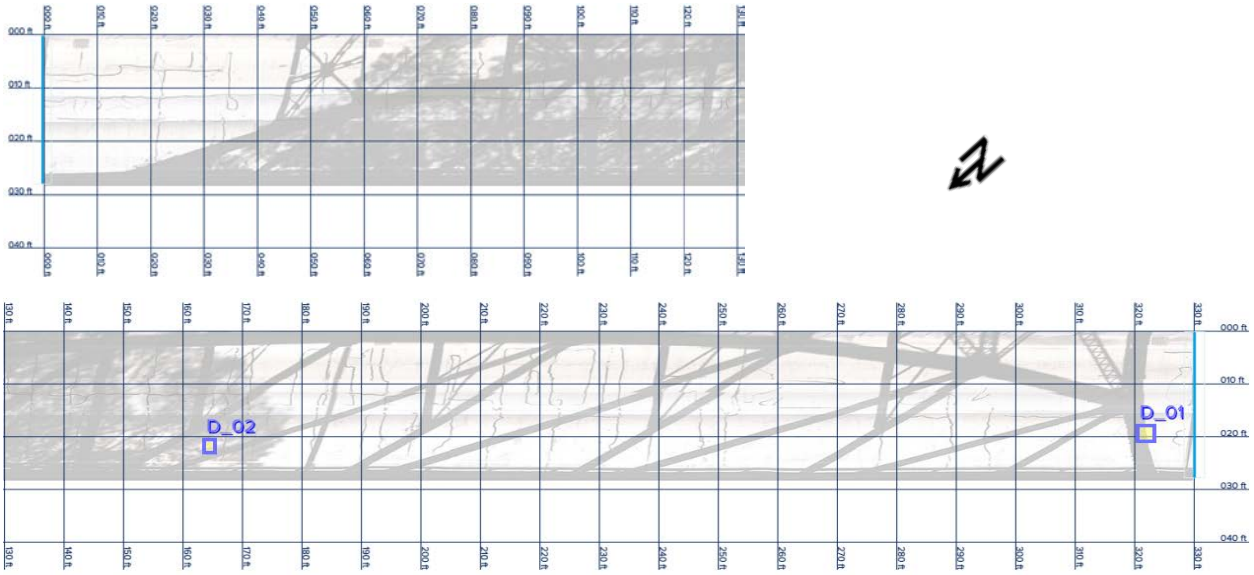

Bridge 18770

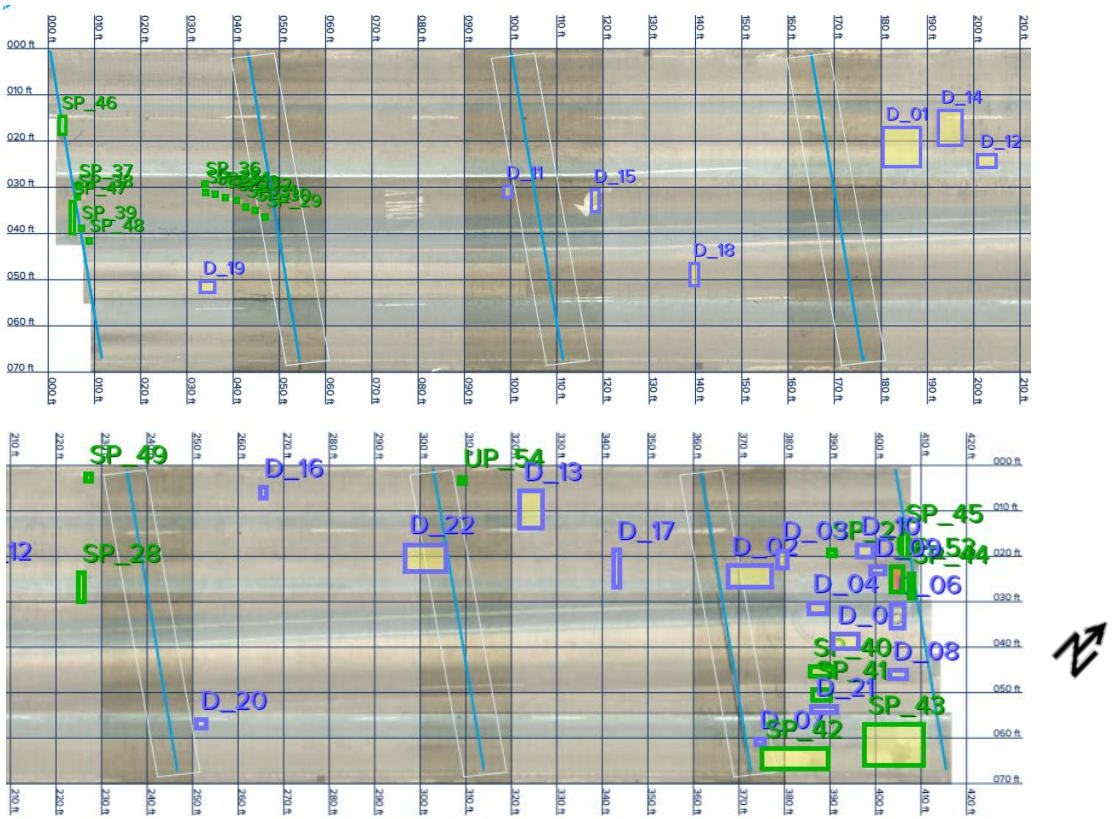

Bridge 18870

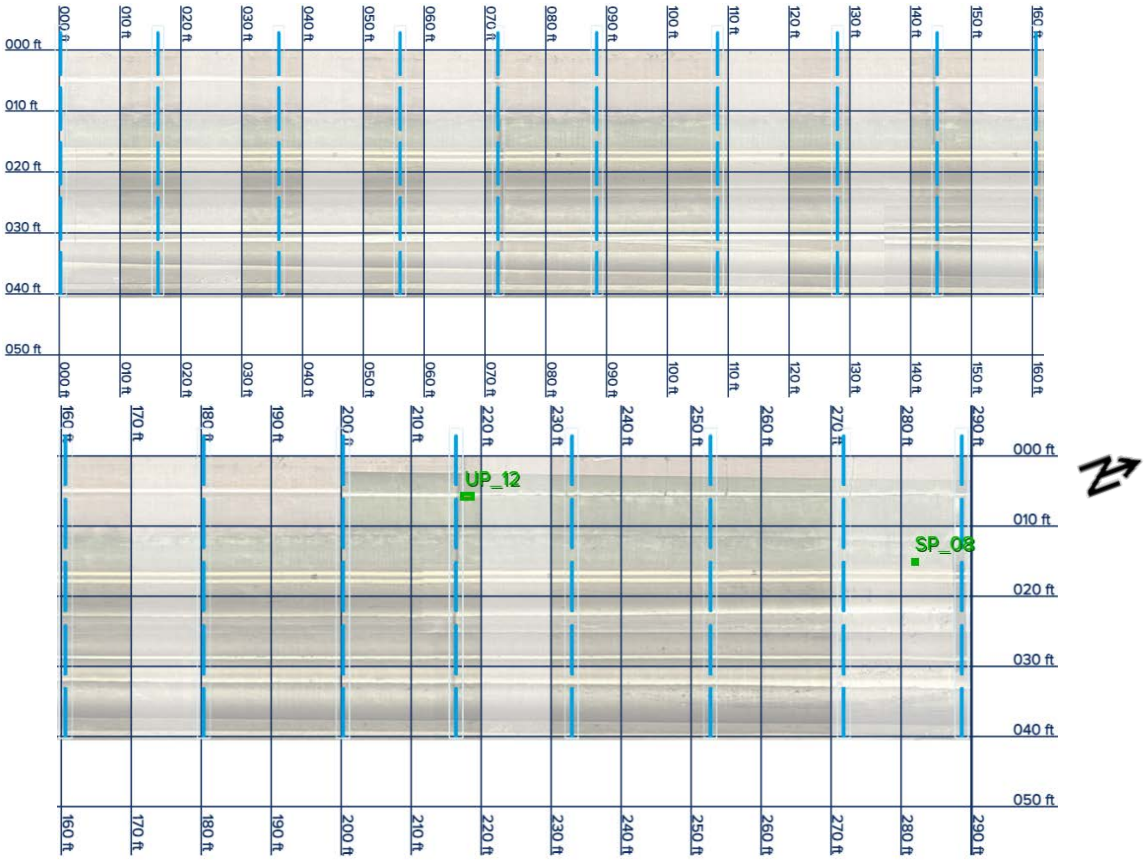

Bridge 19640

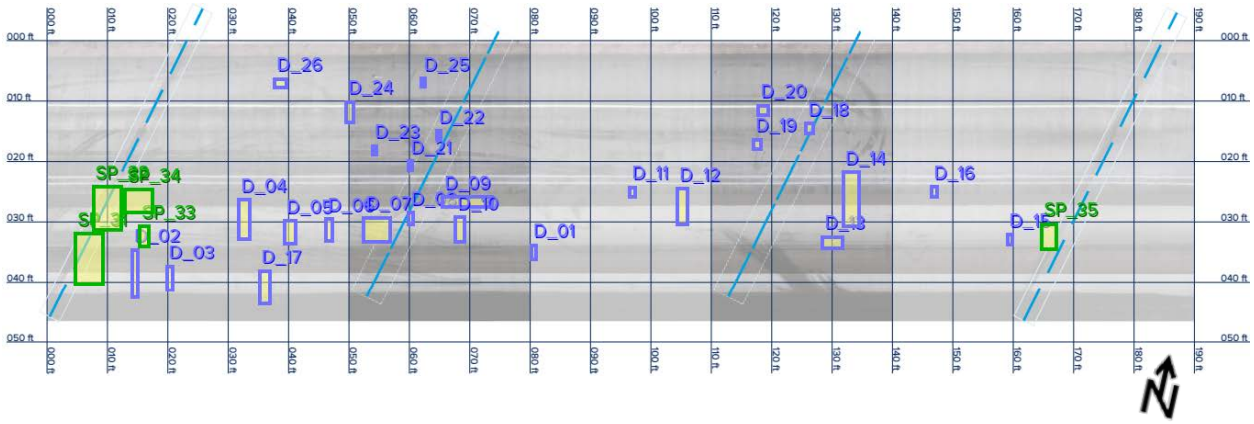

Bridge 20610

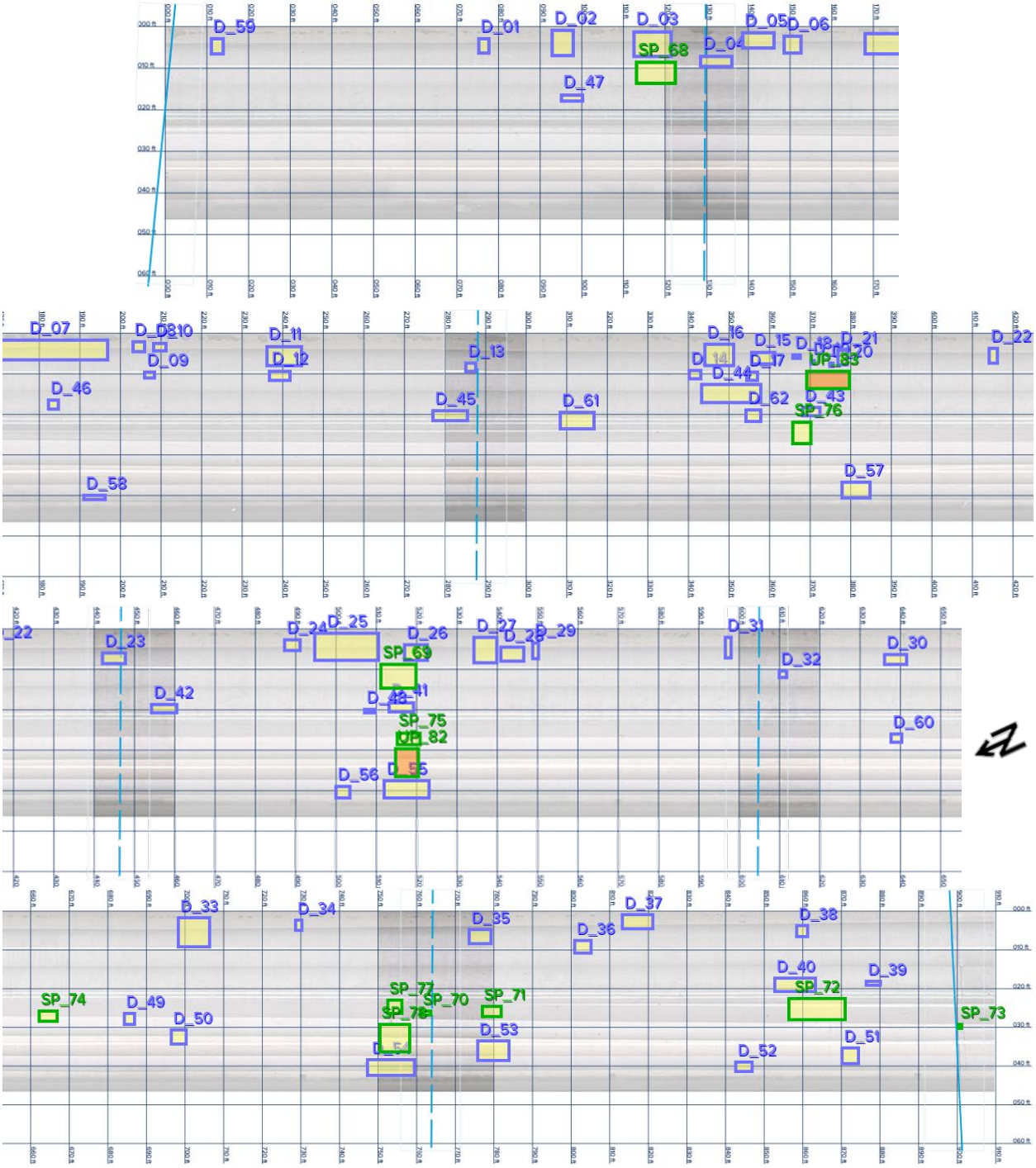

Bridge 22690

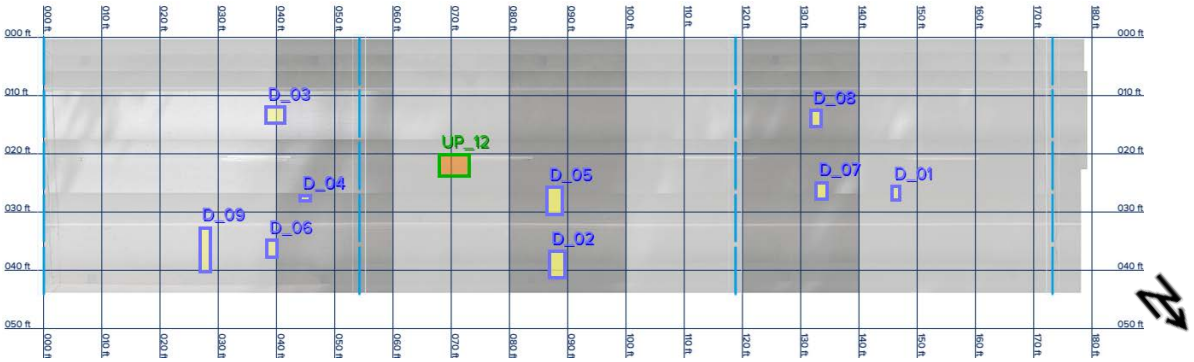

Bridge 31080

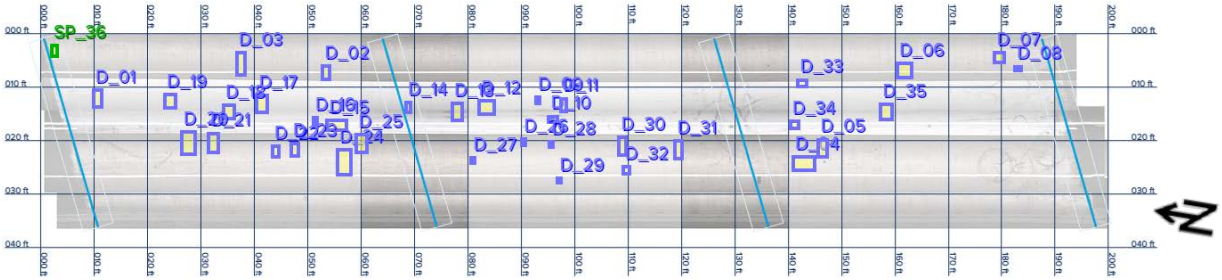

Bridge 35520

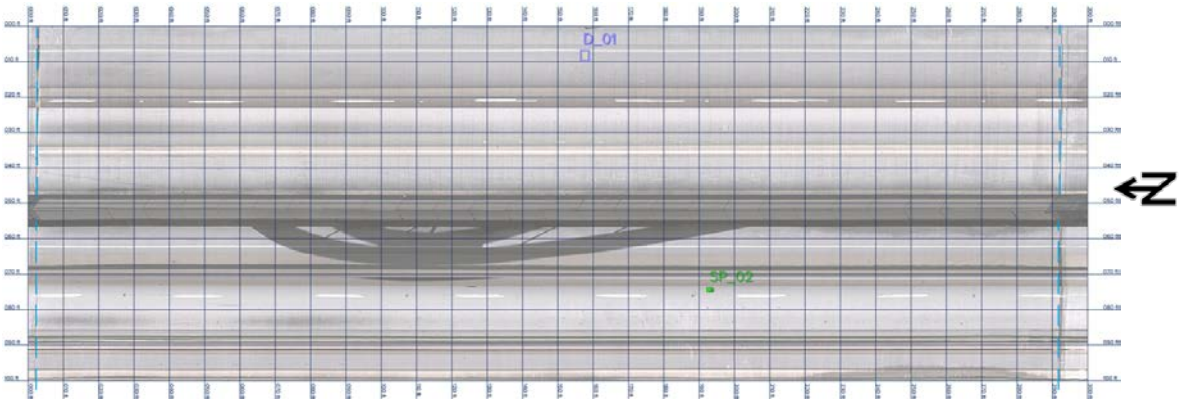

Bridge 37070

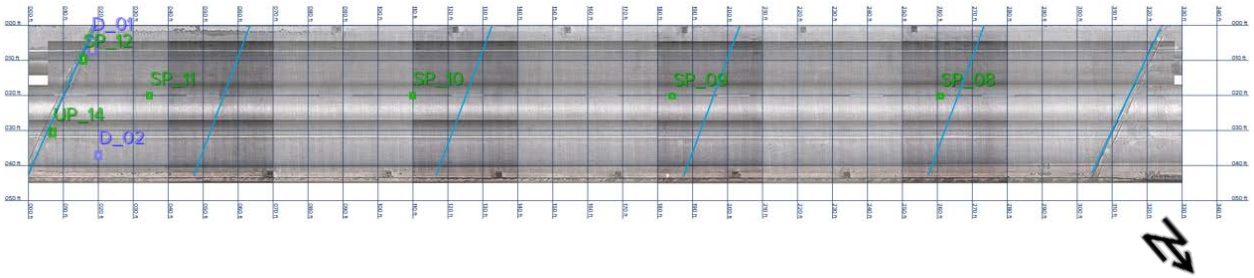

Bridge 37100

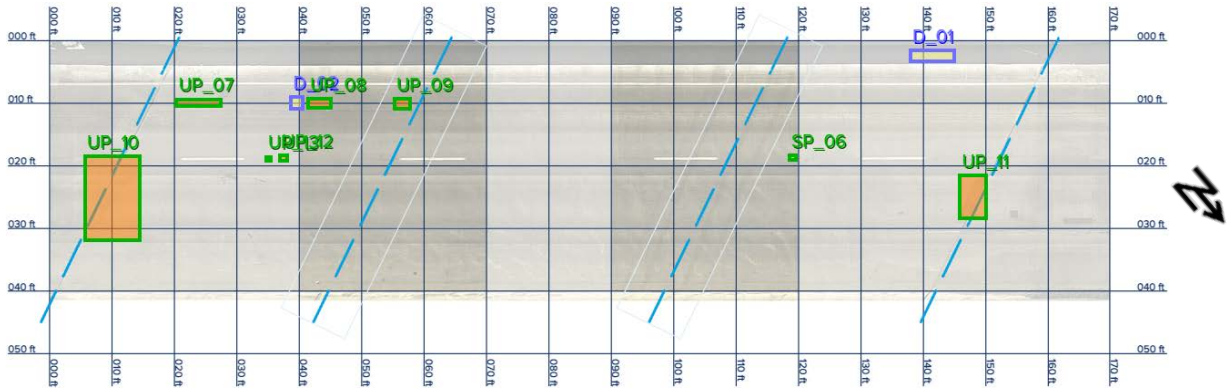

Bridge 37150

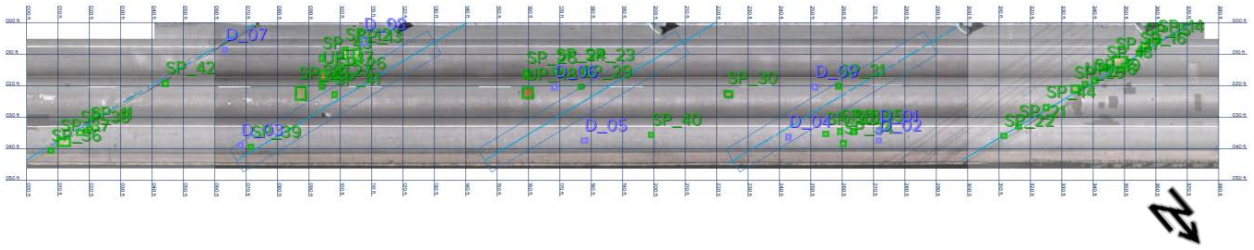

Bridge 41810

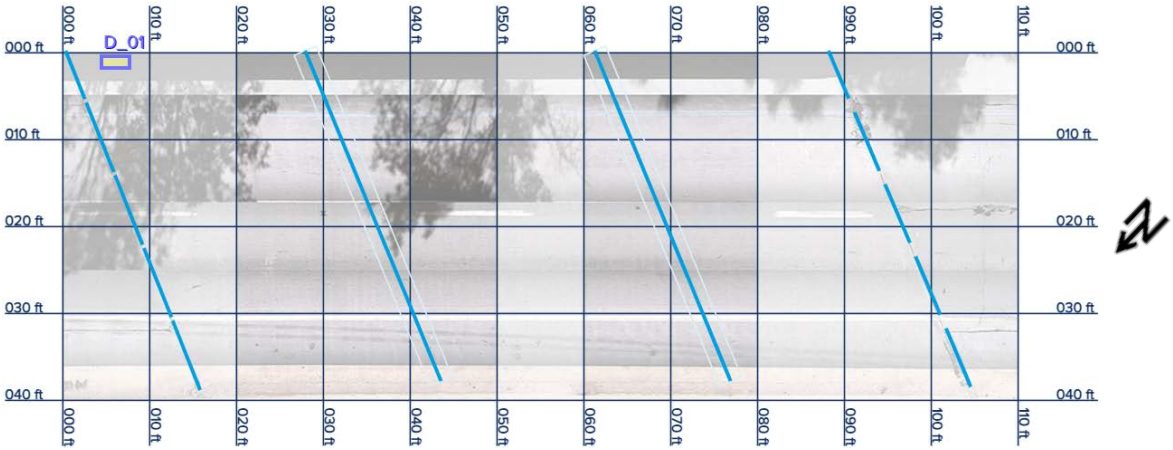

Bridge 41870

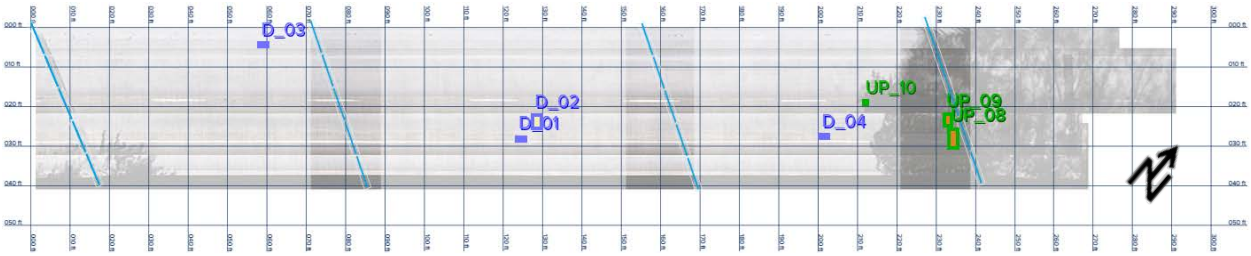

Bridge 49200

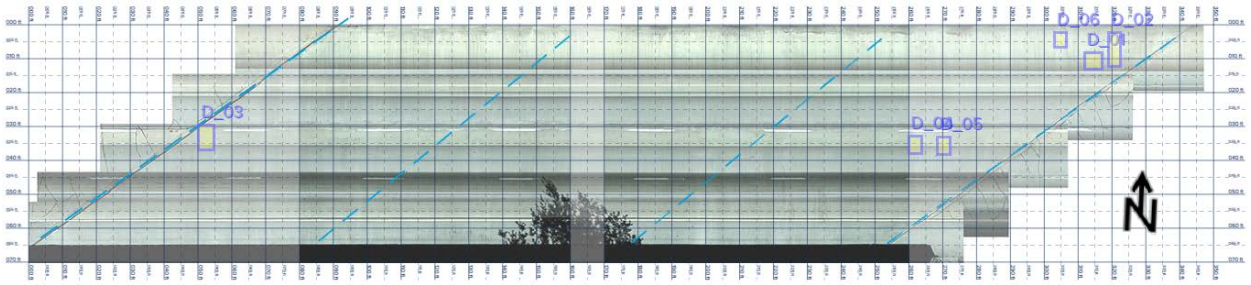

Bridge 76140

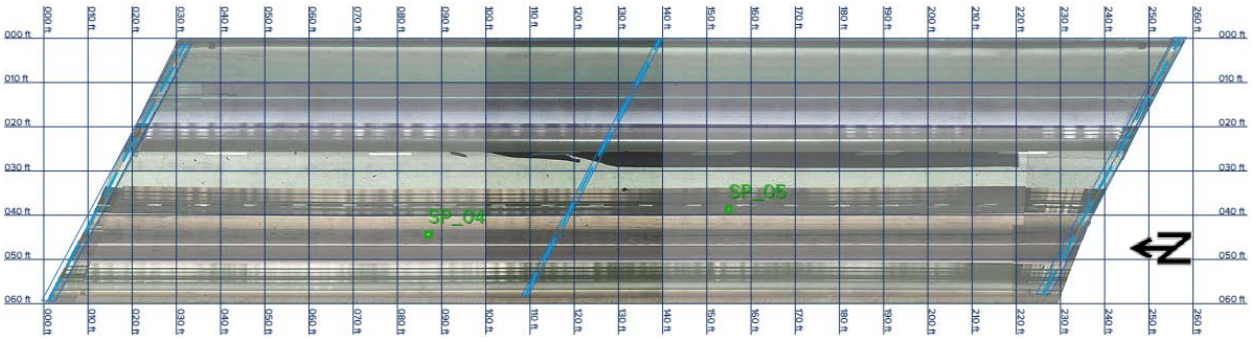

C.4.4 Consultant B (drone-mounted IRT)

Bridge 16500

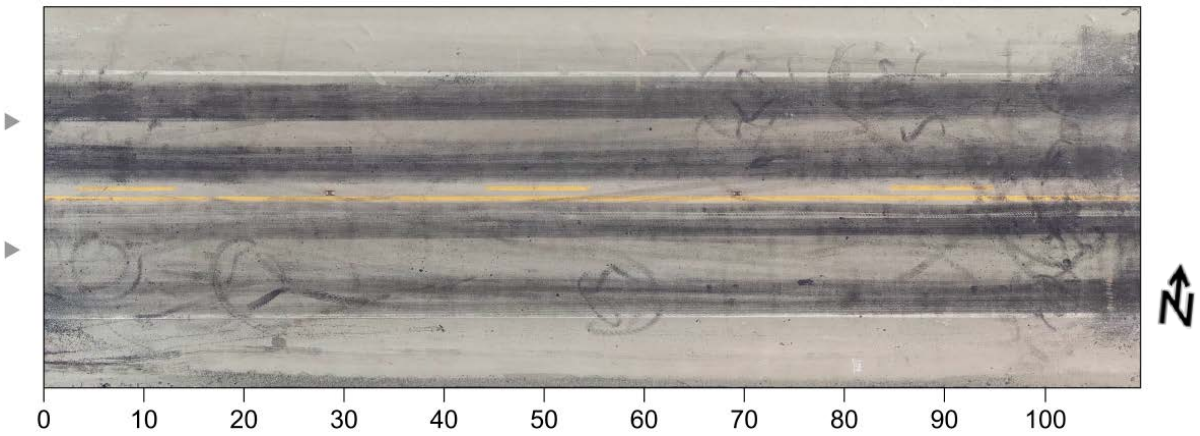

Bridge 18770

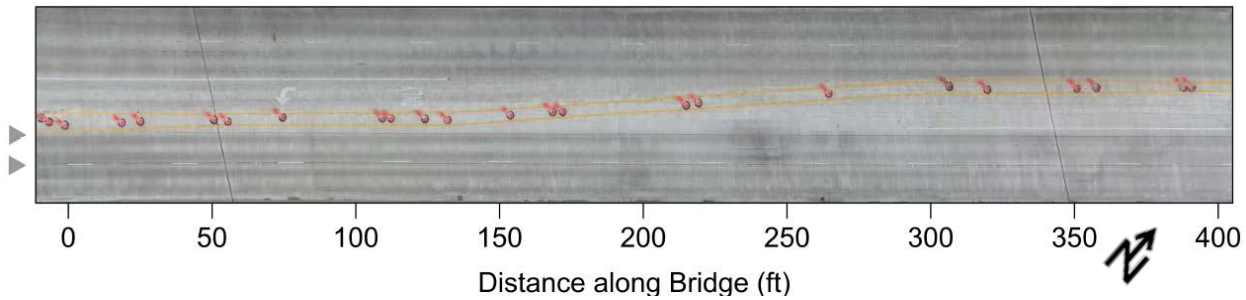

Bridge 22690

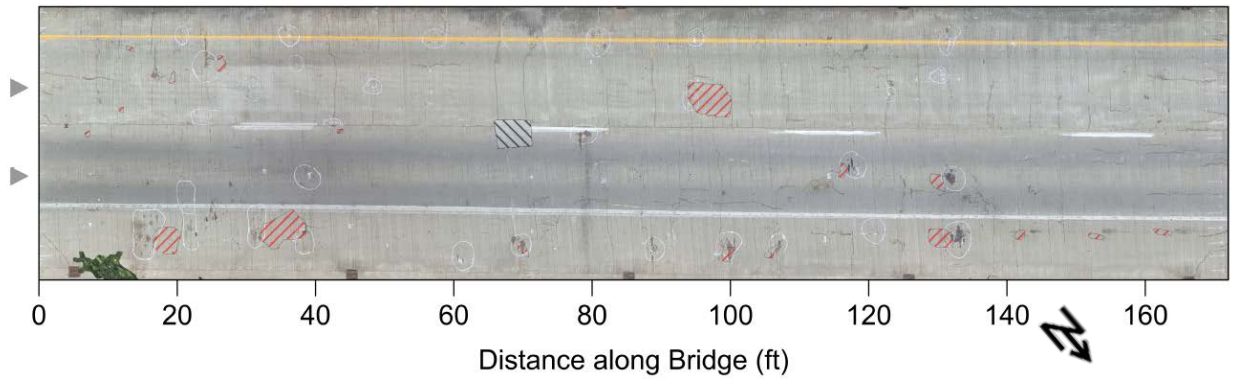

Bridge 31080

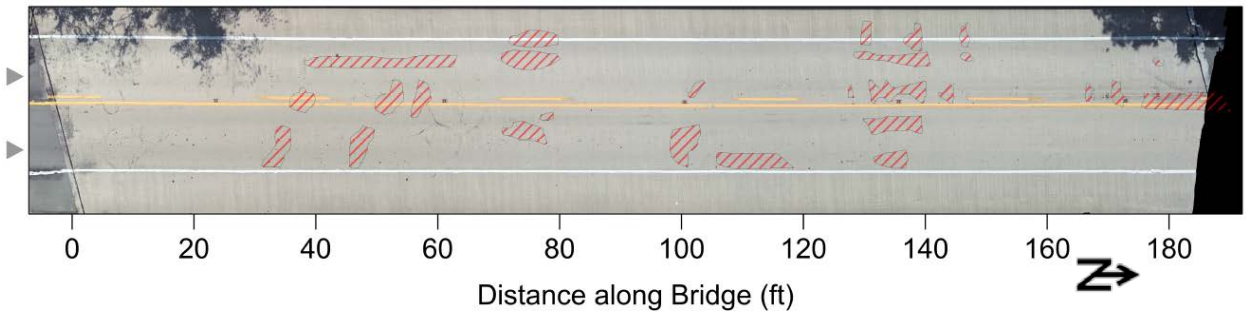

Bridge 35520

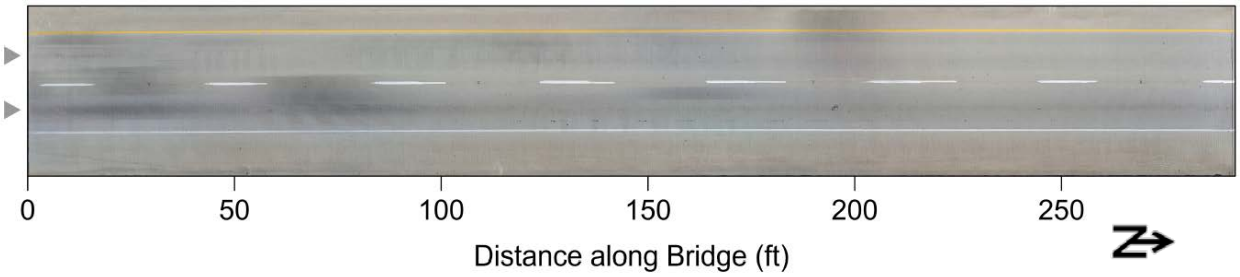

Bridge 37070

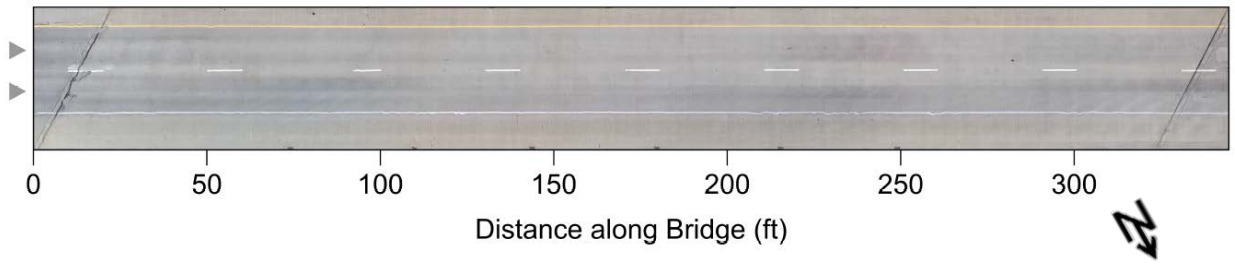

Bridge 37100

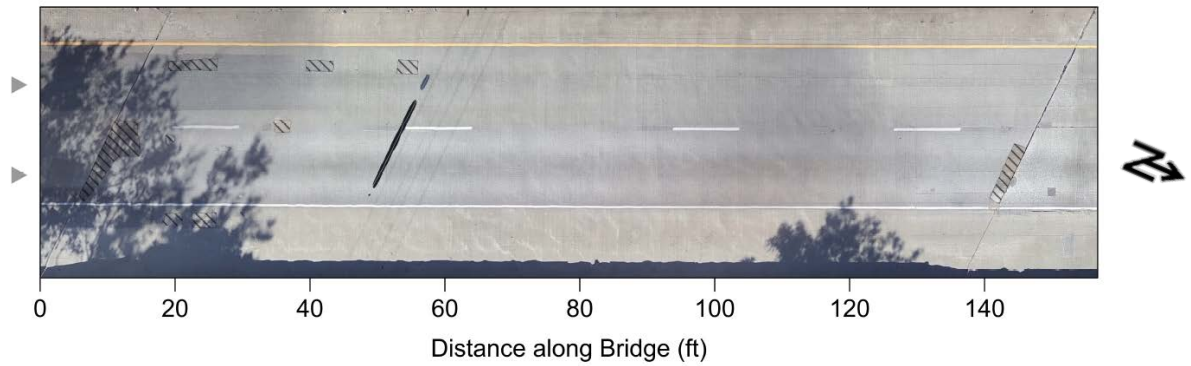

Bridge 37150

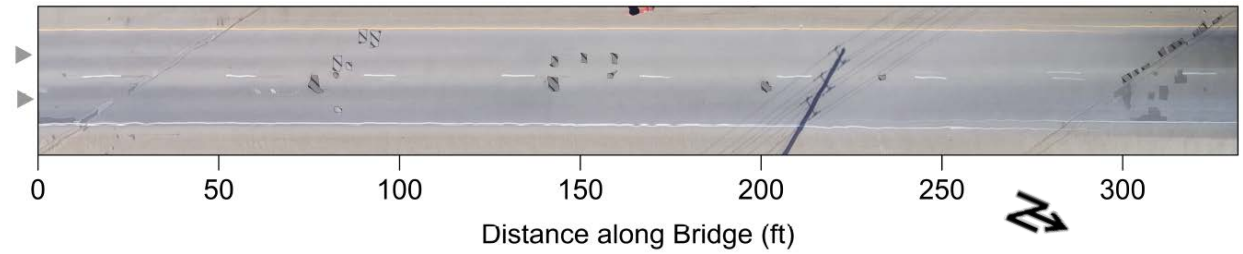

Bridge 41810

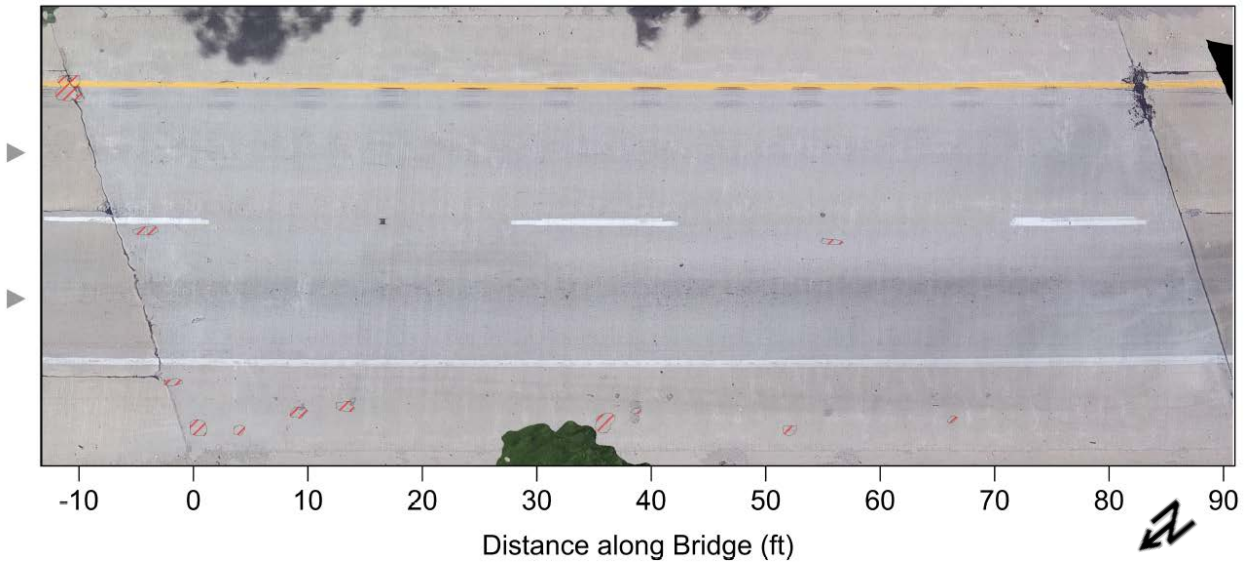

Bridge 41870

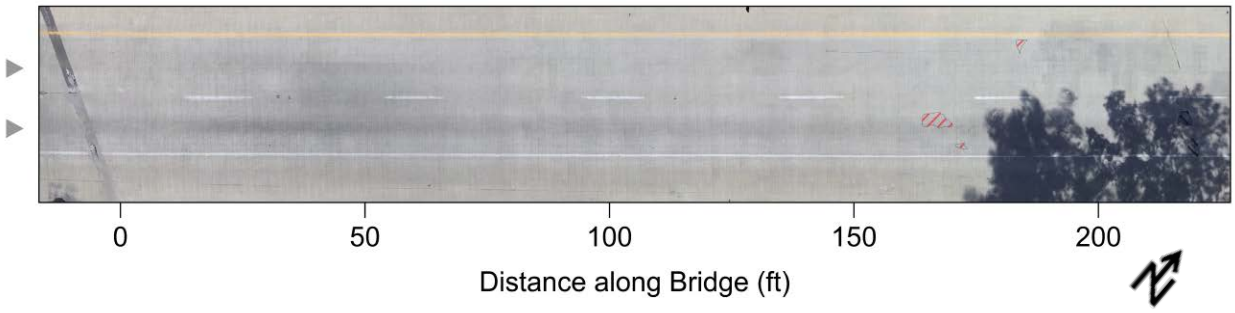

C.4.5 Consultant I (pole-mounted IRT)

Bridge 37070

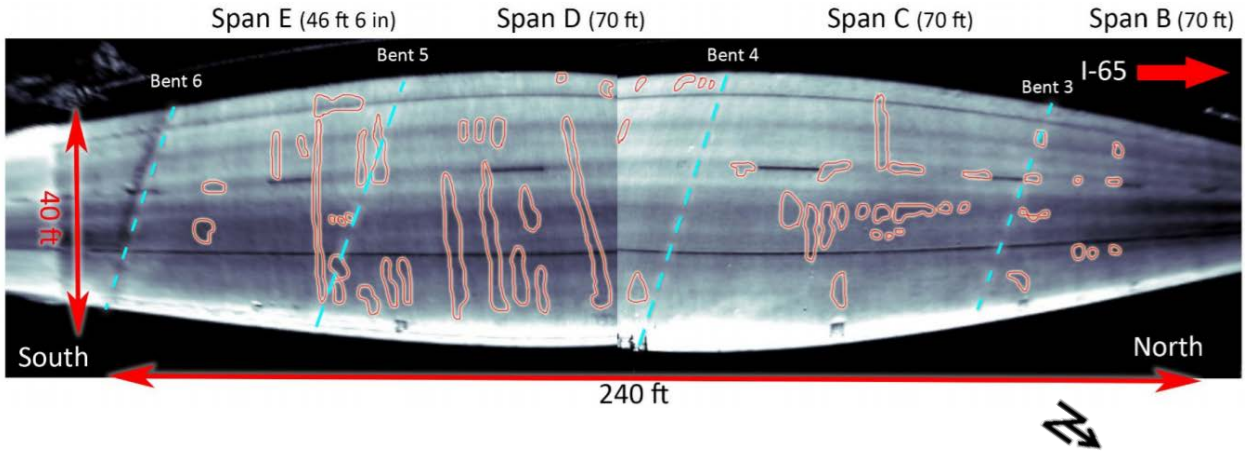

Bridge 42190

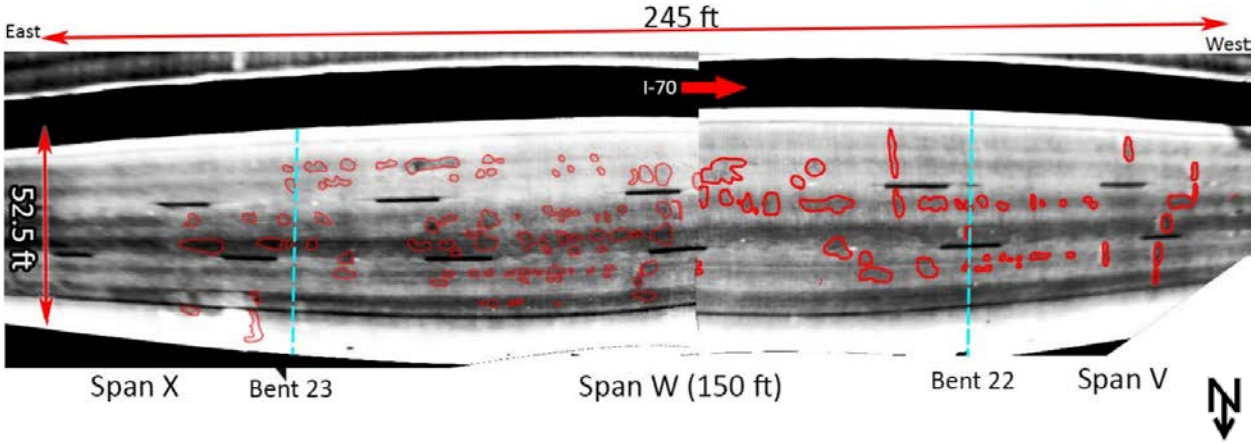

C.4.6 Consultant D (Aerial IRT)–Second Round

Bridge 04708

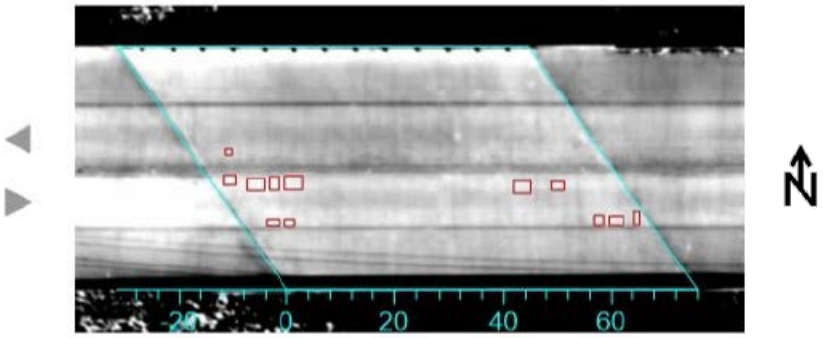

Bridge 04710

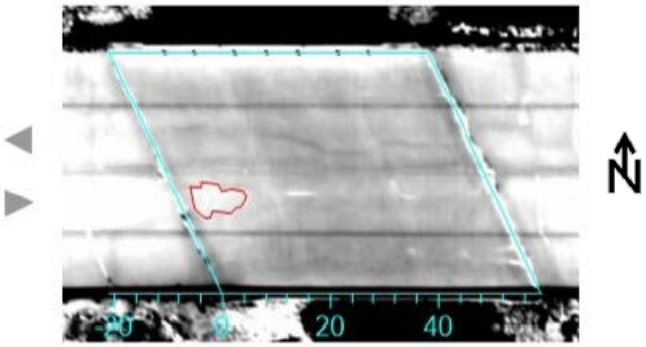

Bridge 04730

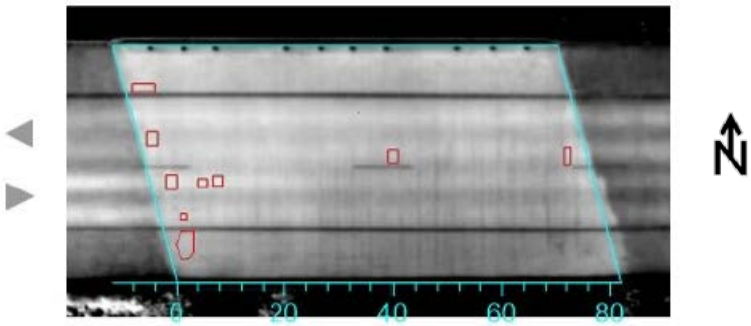

Bridge 04740

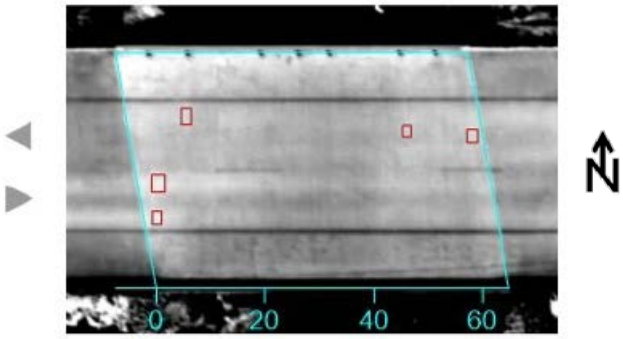

Bridge 04750

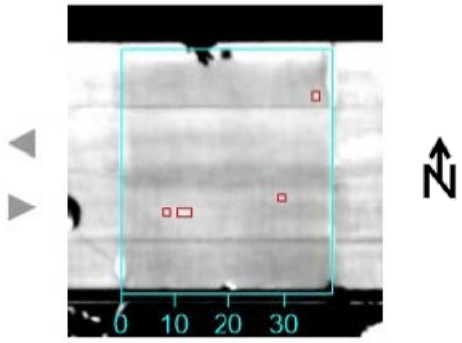

Bridge 04770

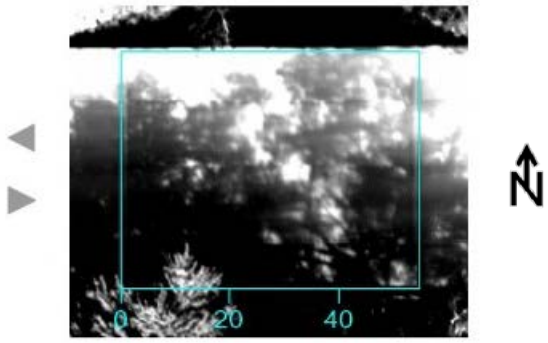

Bridge 04820

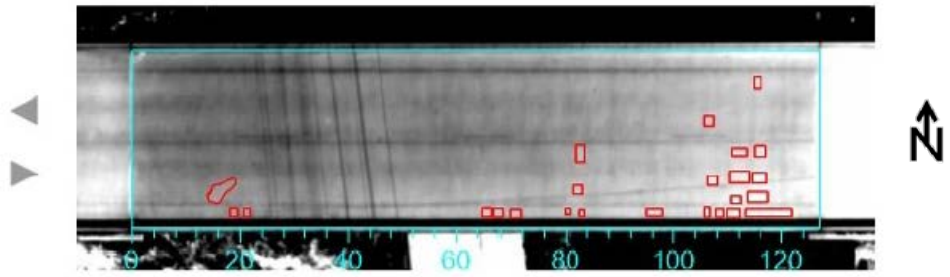

Bridge 04830

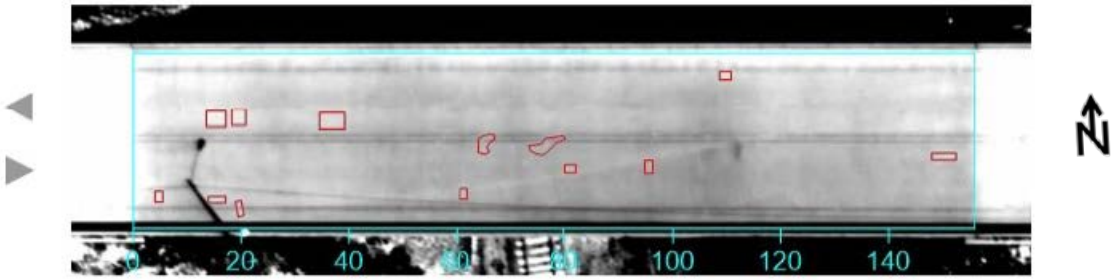

Bridge 04845

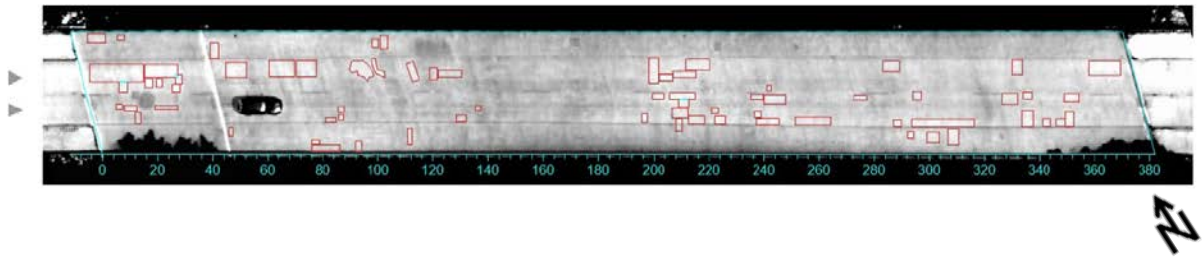

Bridge 04859

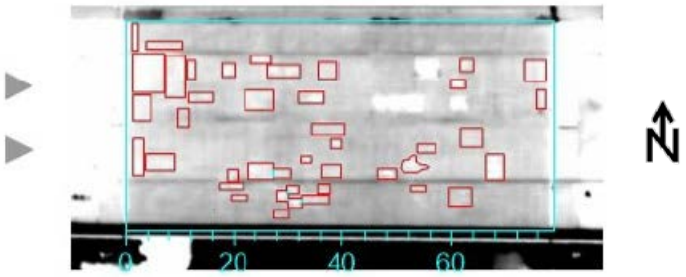

Bridge 04860

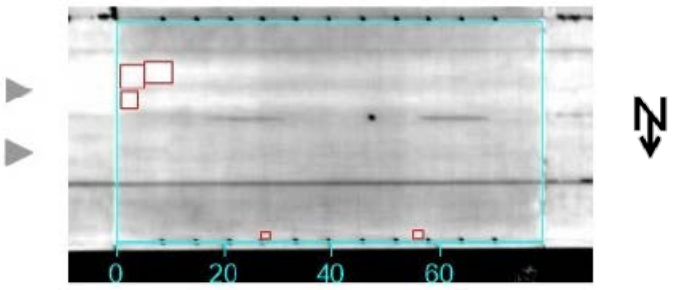

Bridge 04910

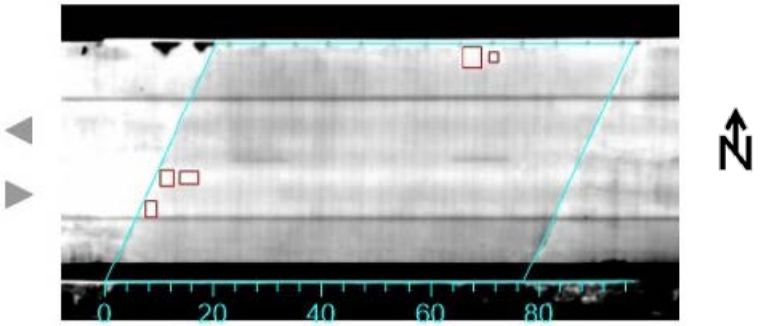

Bridge 04920

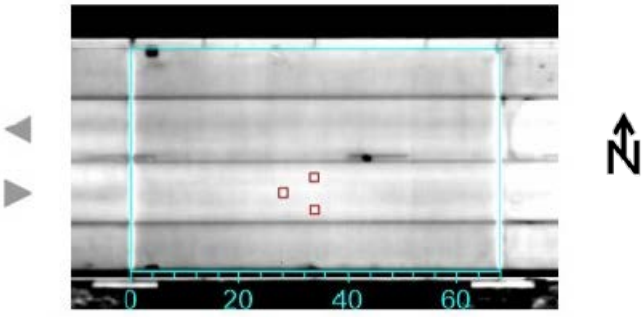

Bridge 04930

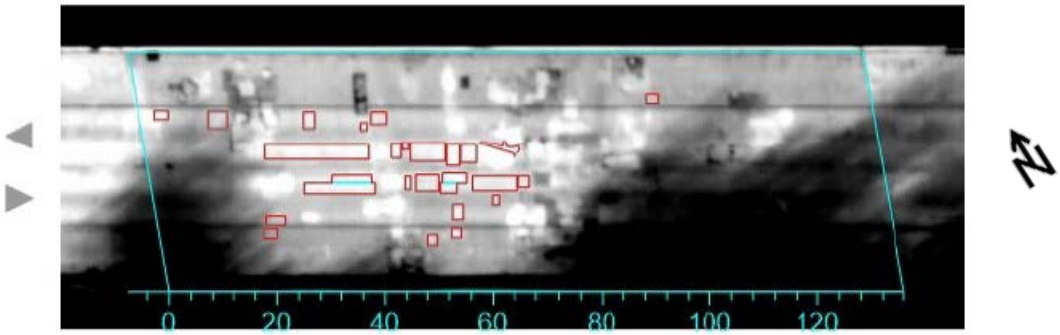

Bridge 39620

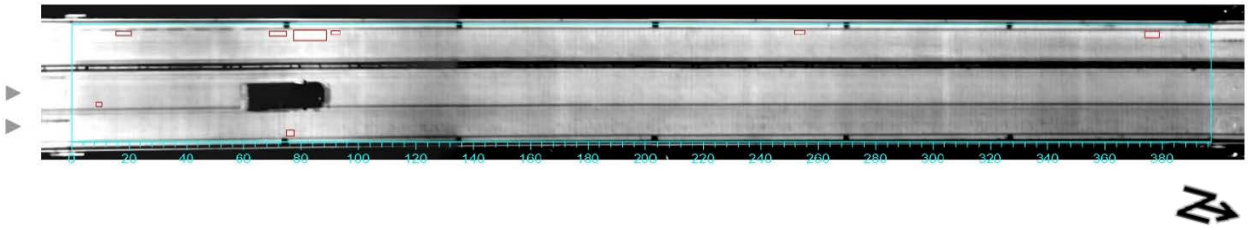

Bridge 39630

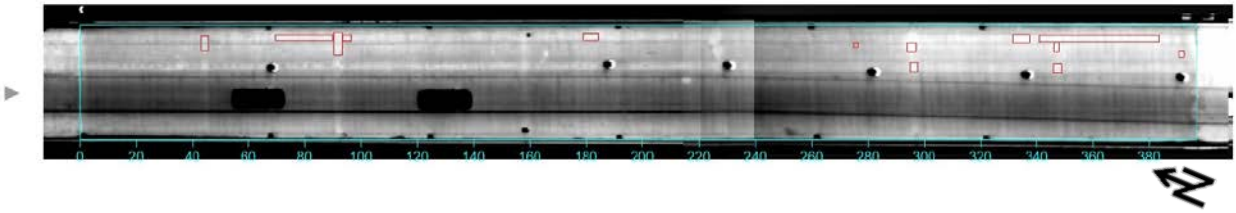

Bridge 39640

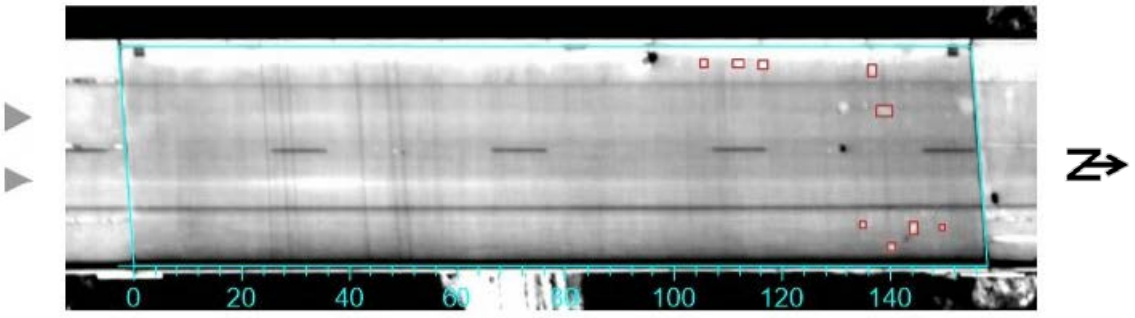

Bridge 39650

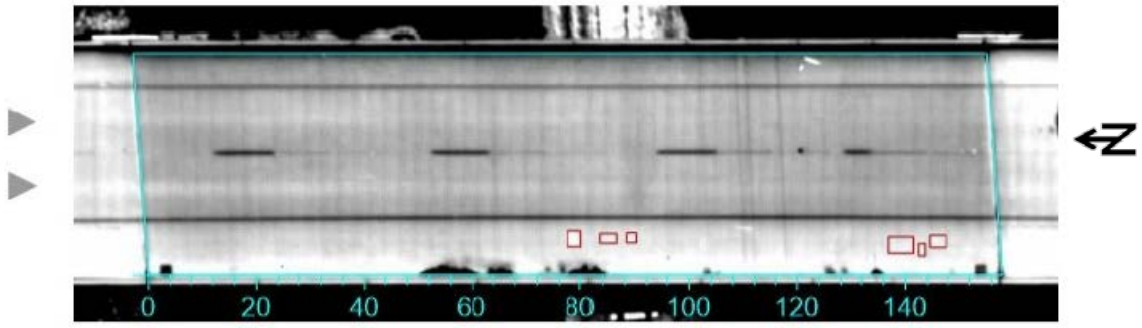

Bridge 39740

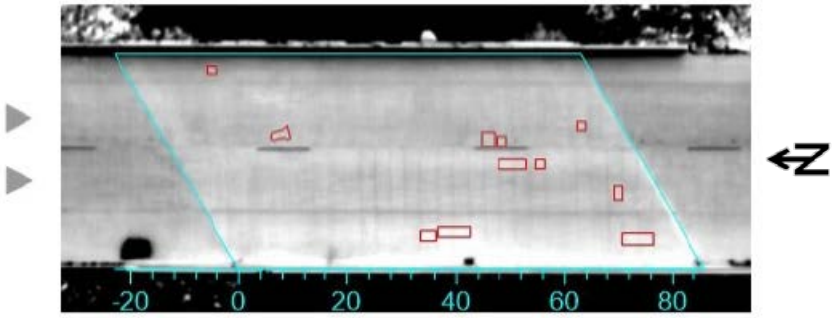

Bridge 39770

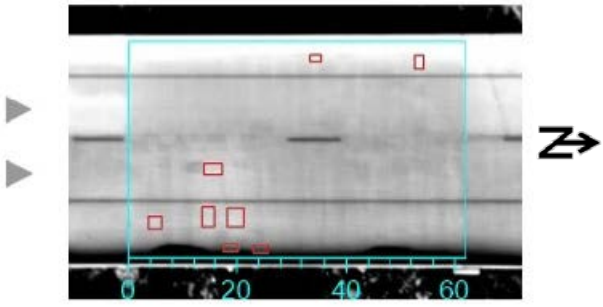

Bridge 39780

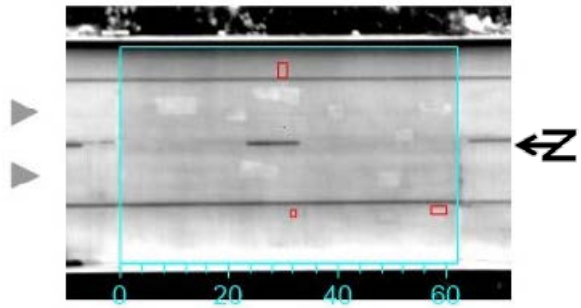

Bridge 39850

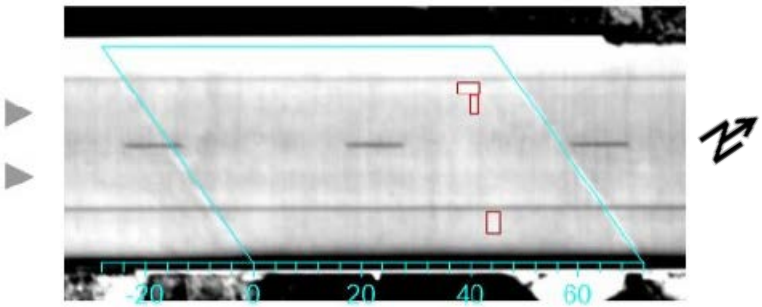

Bridge 39860

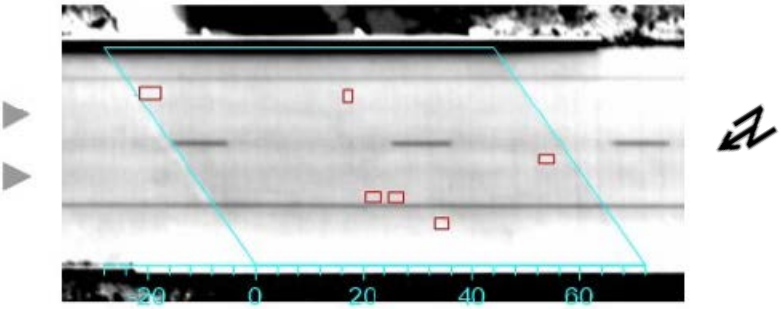

Bridge 39870

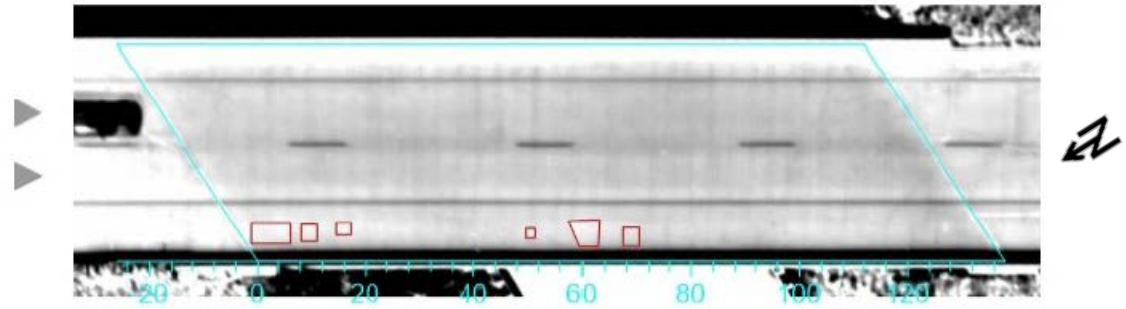

Bridge 39880

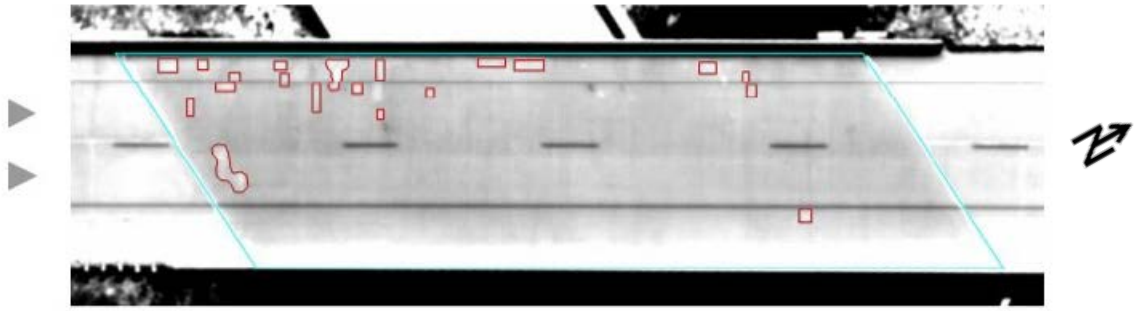

Bridge 39910

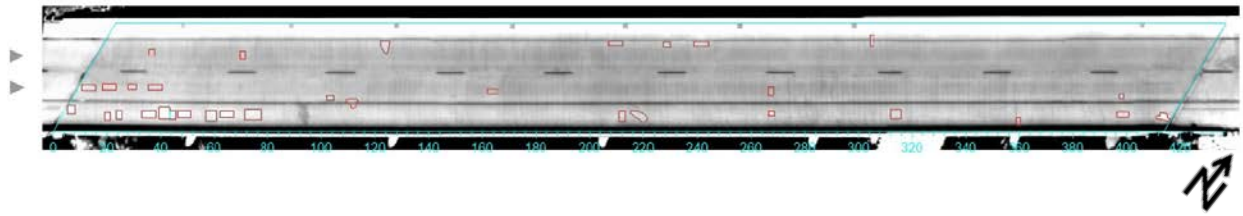

Bridge 39920

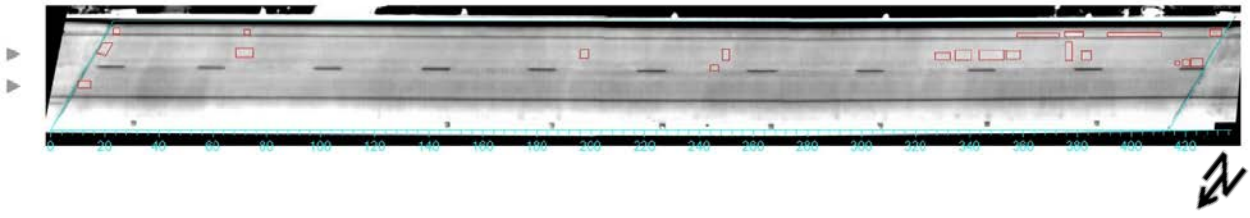

Bridge 40000

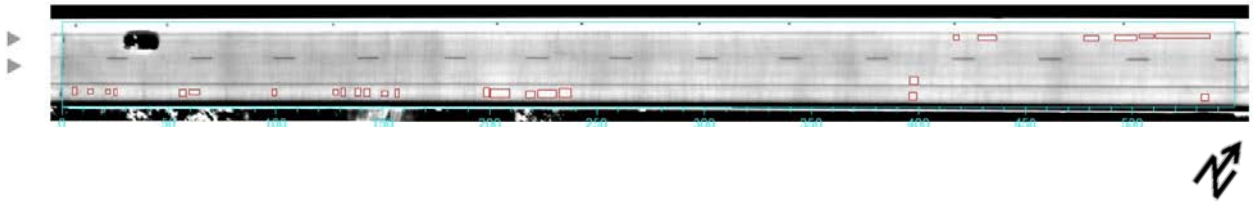

Bridge 40010

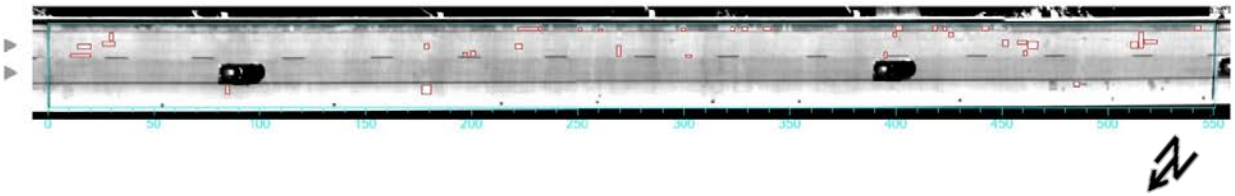

Bridge 40130

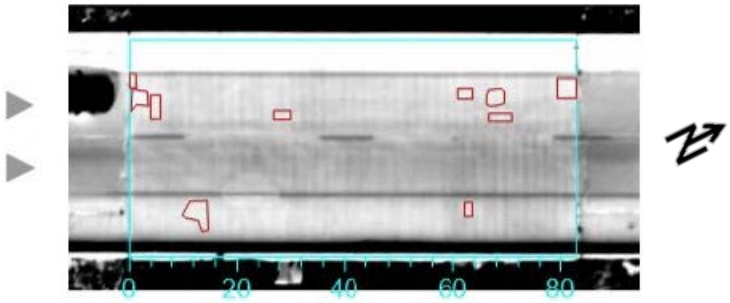

Bridge 40140

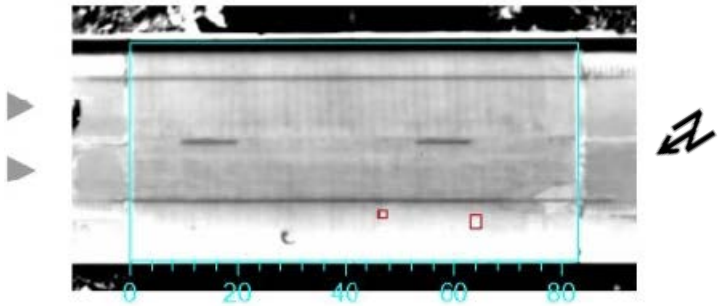

Bridge 40220

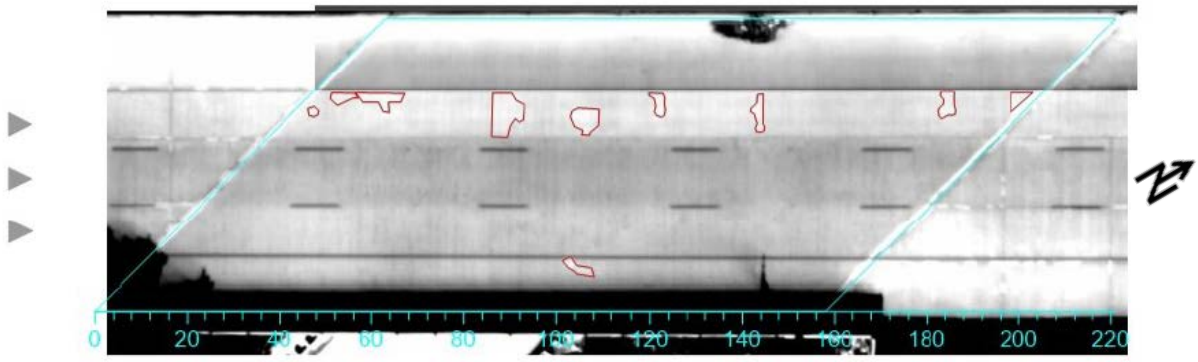

Bridge 40230

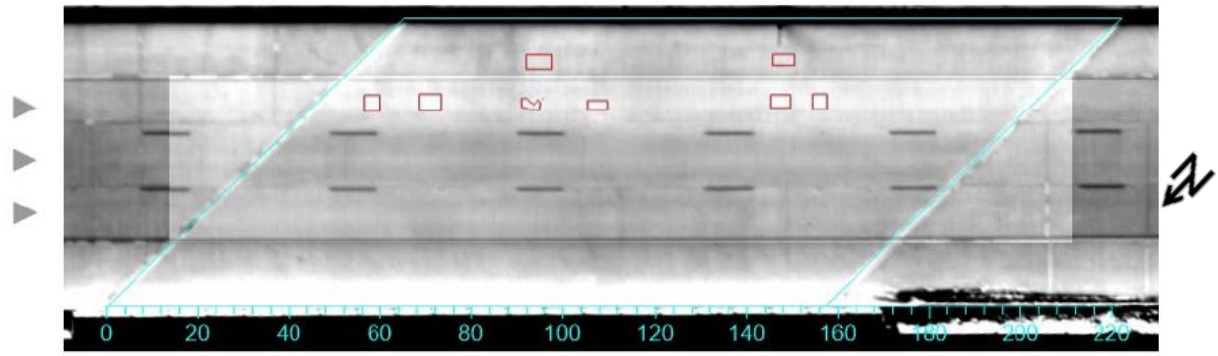

Bridge 40330

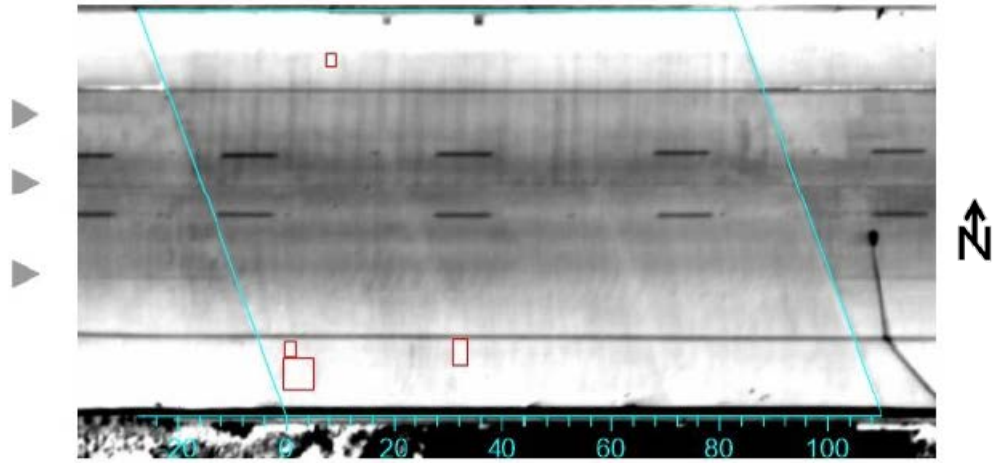

Bridge 40340

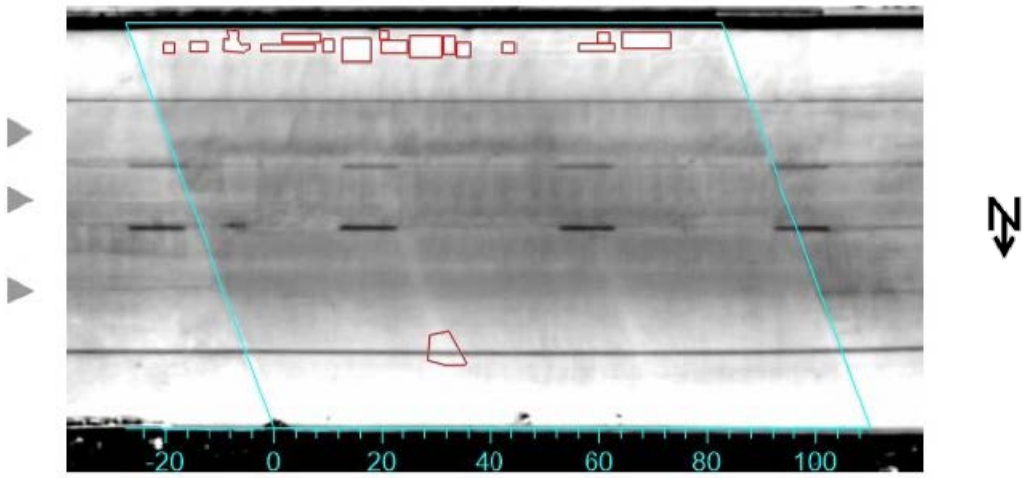

Bridge 40350

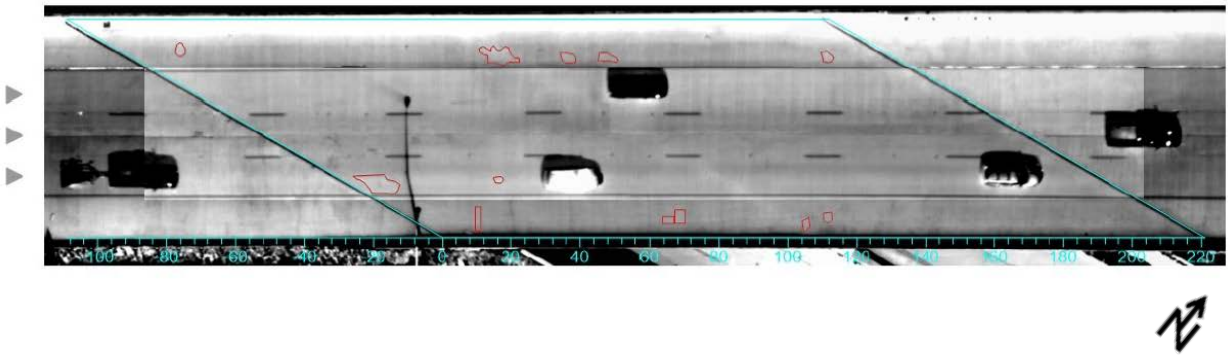

Bridge 40360

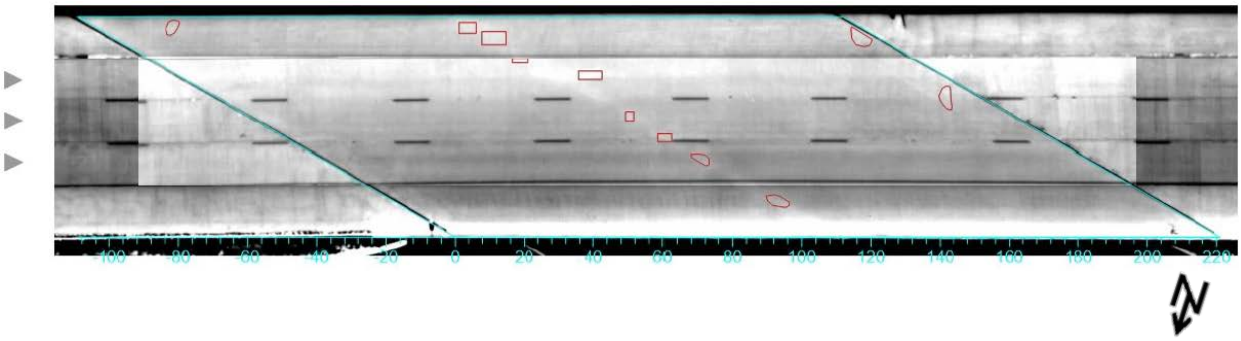

C.4.7 Consultant E (vehicle-mounted IRT)–Second Round

Bridge 01310

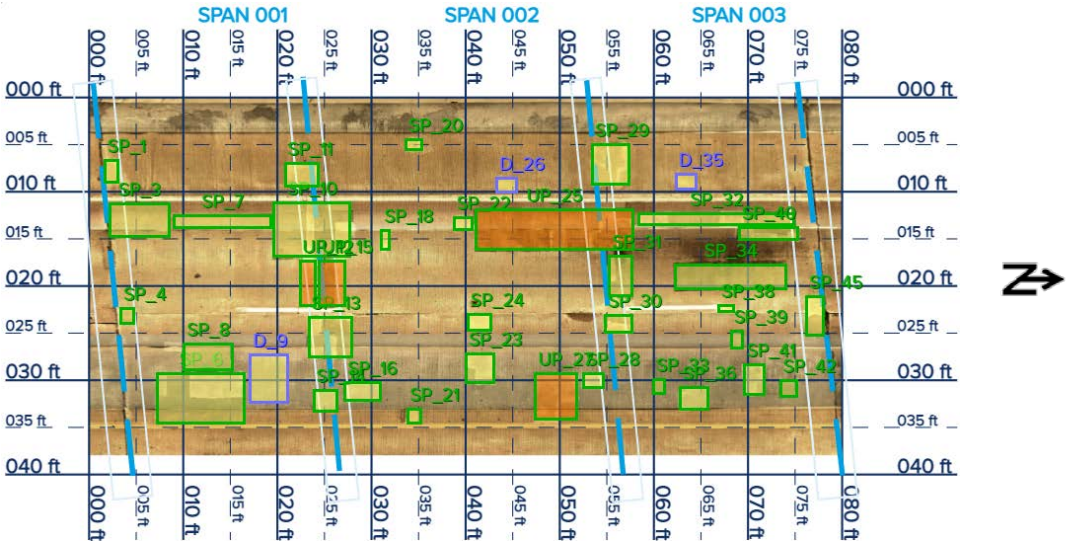

Bridge 01347

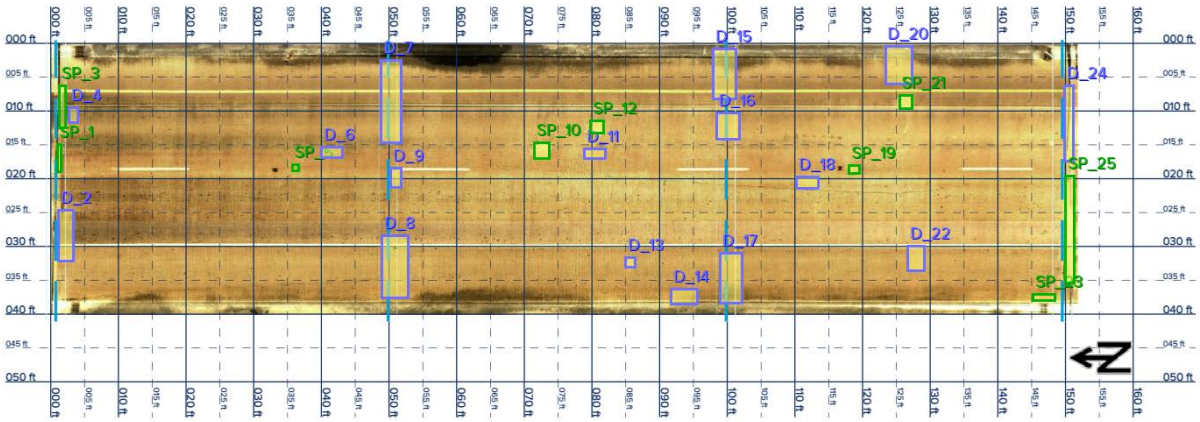

Bridge 04845

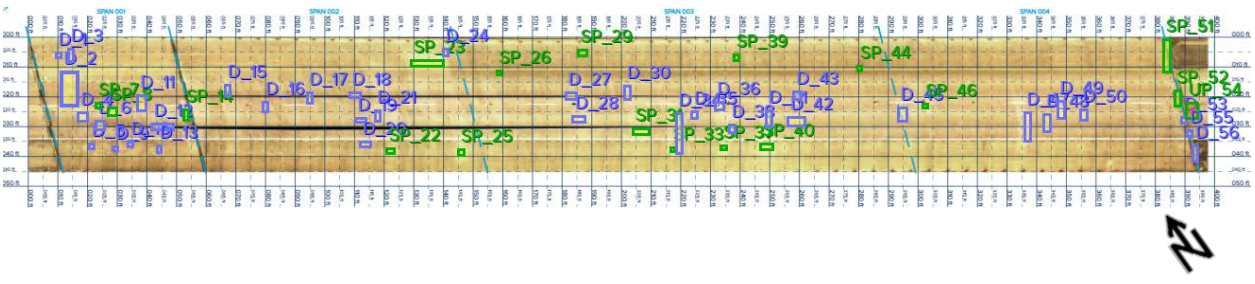

Bridge 04930

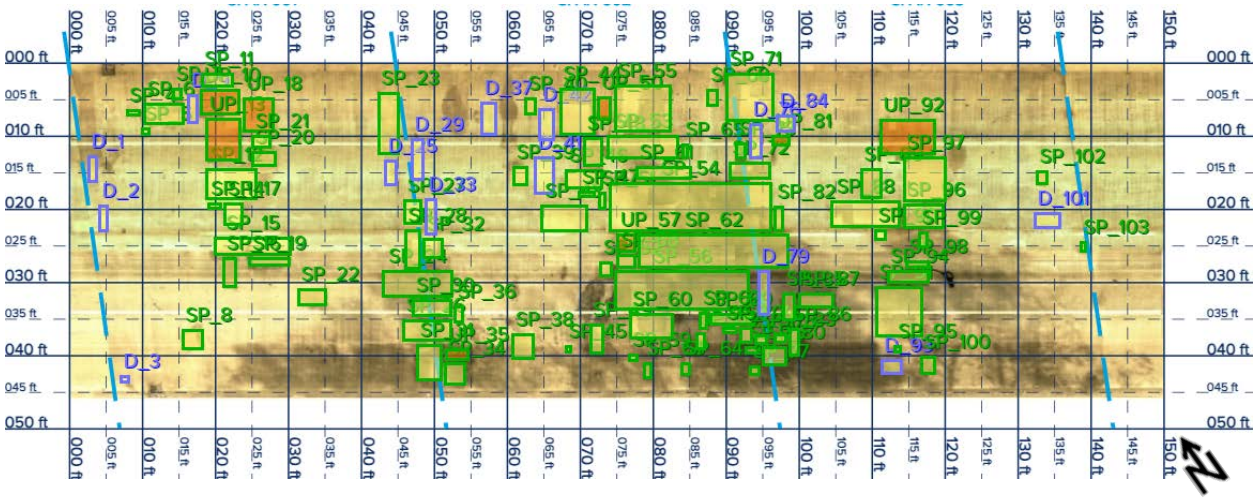

Bridge 08630

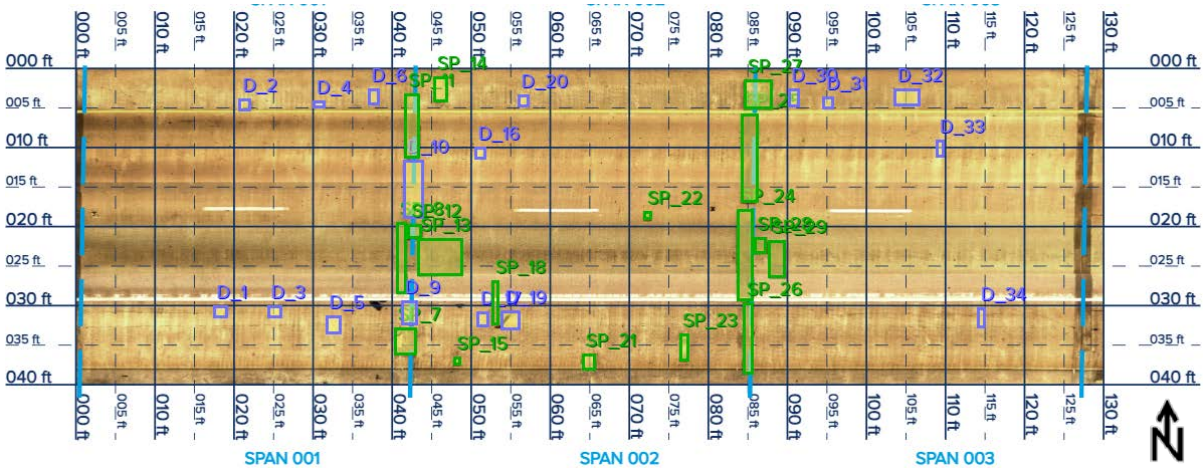

Bridge 17940

Bridge 19640

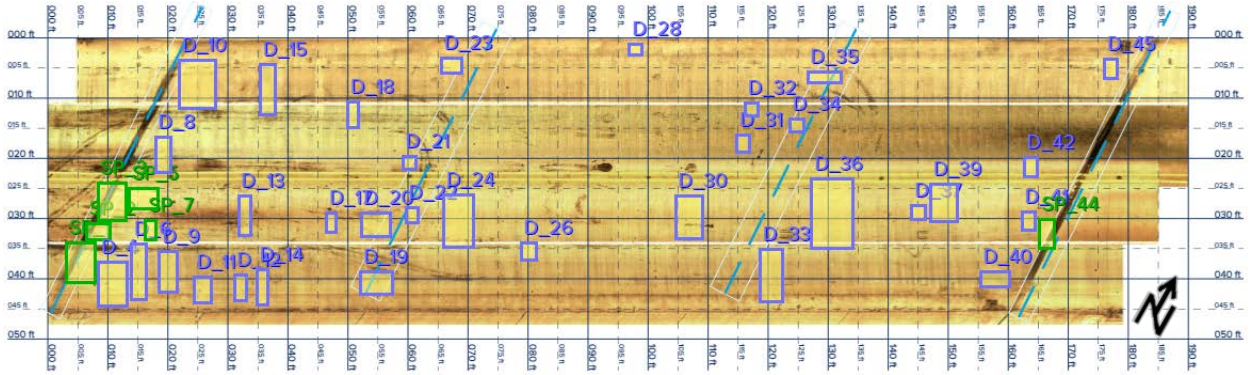

Bridge 20610

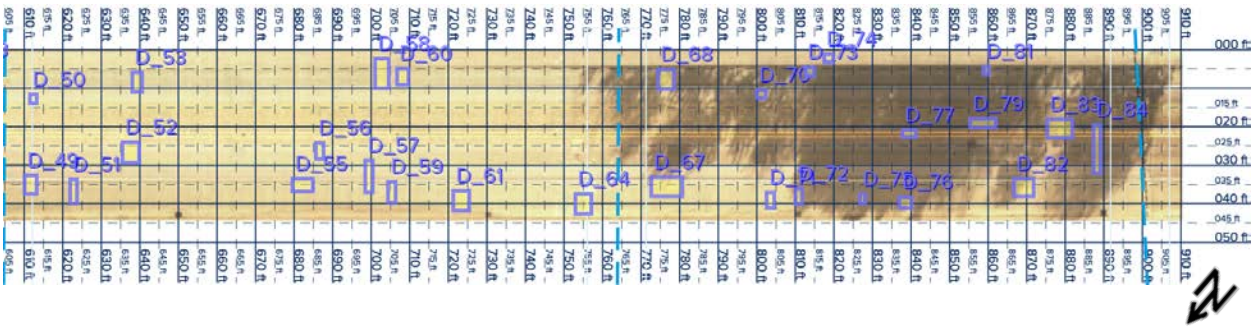

Bridge 24220

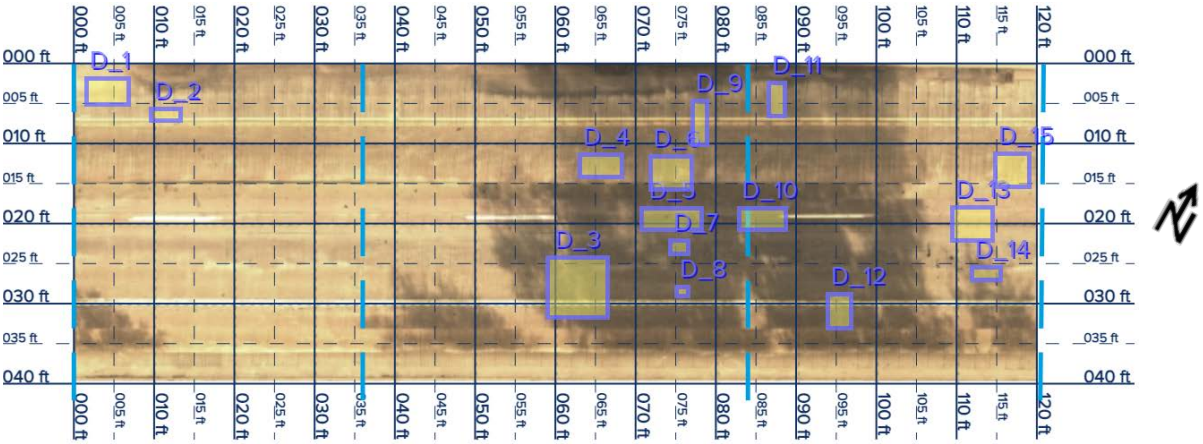

Bridge 49200

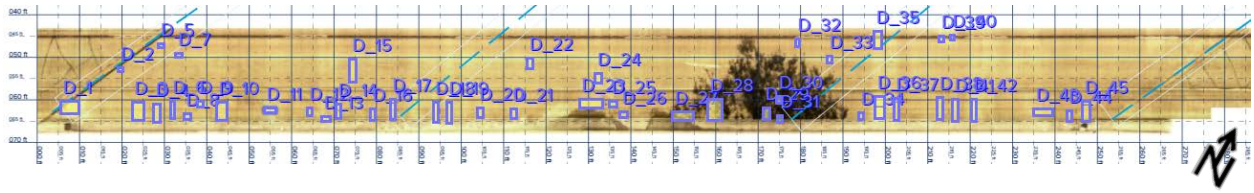

C.4.8 Consultant C (drone-mounted IRT)

Bridge 01310

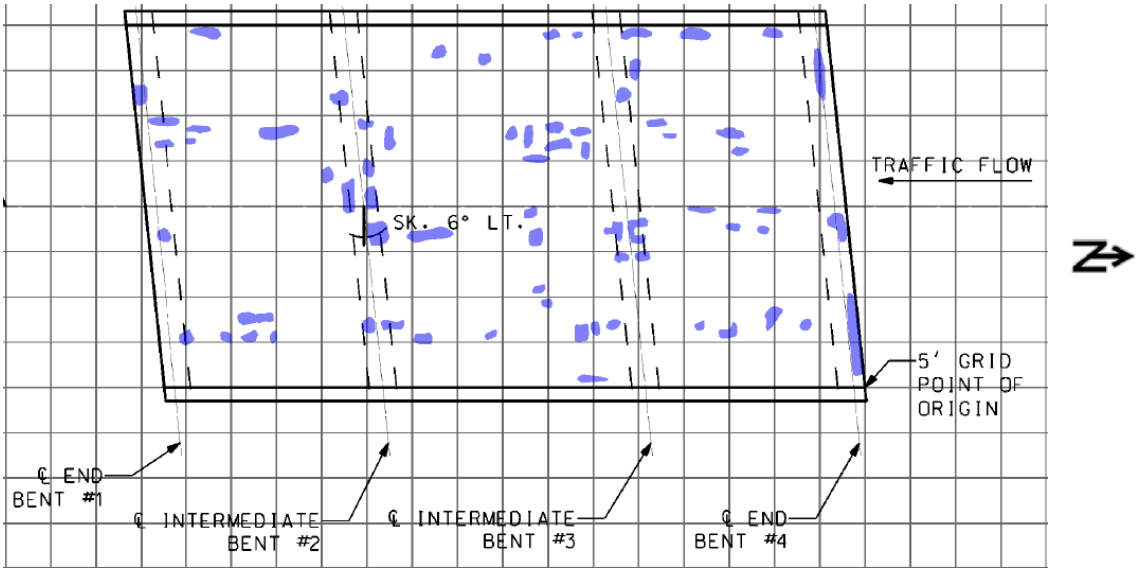

Bridge 01347

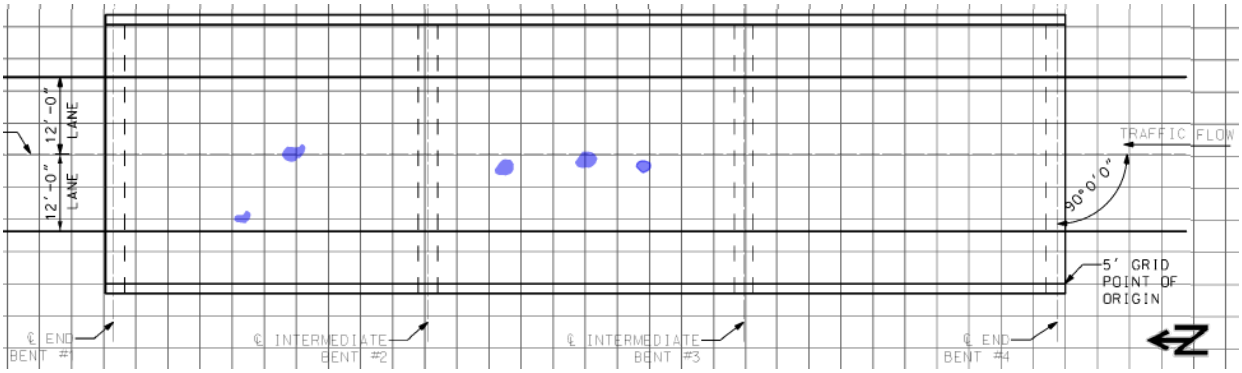

Bridge 04845

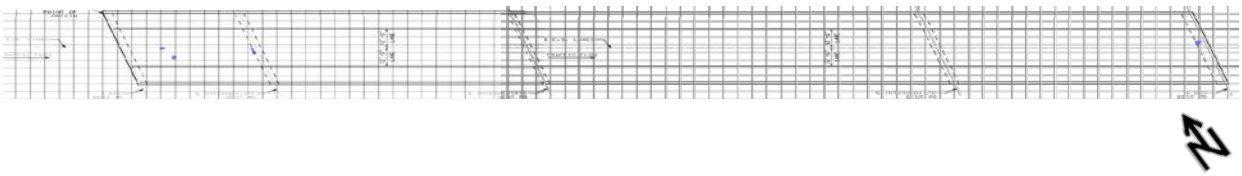

Bridge 04930

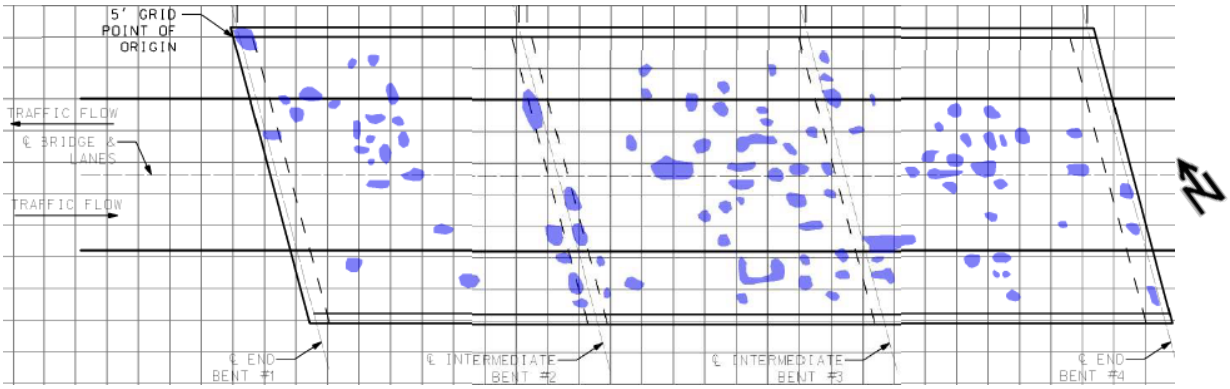

Bridge 08630

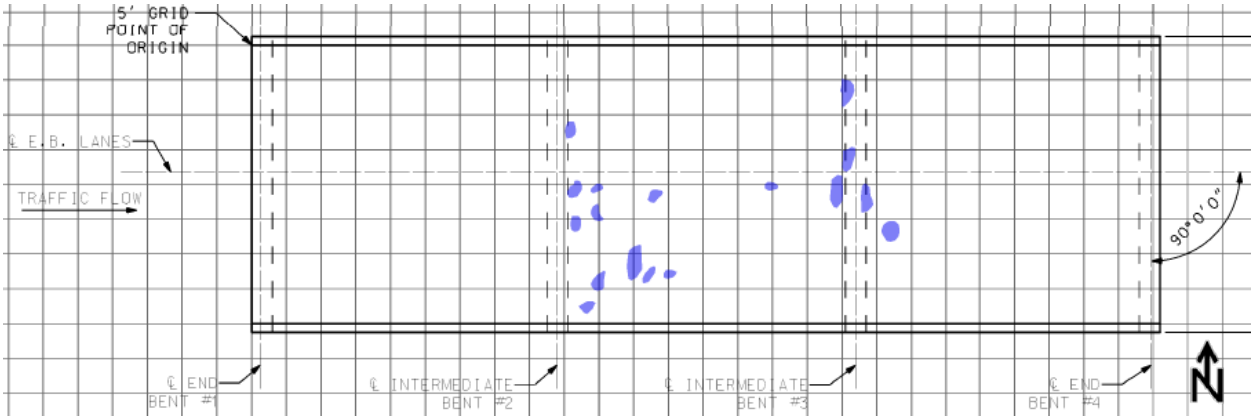

Bridge 17940

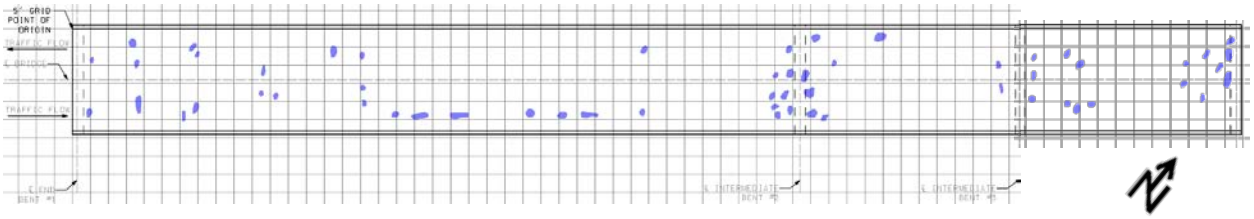

Bridge 19640

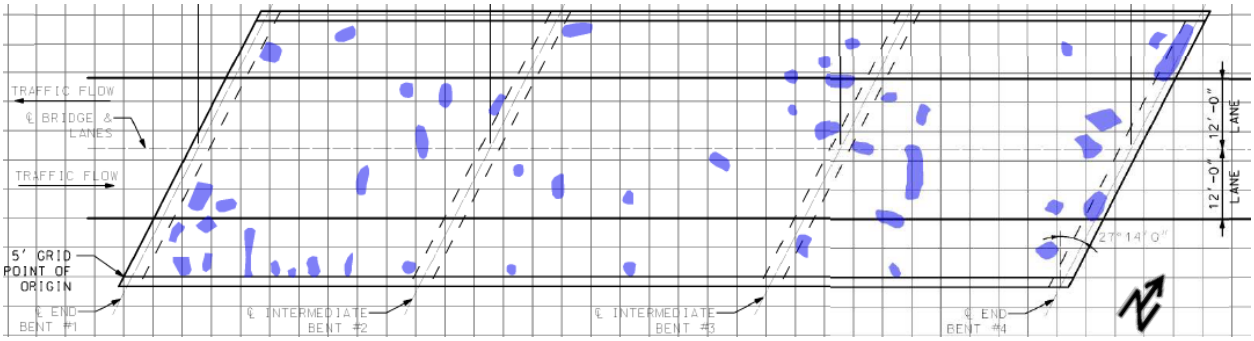

Bridge 20610

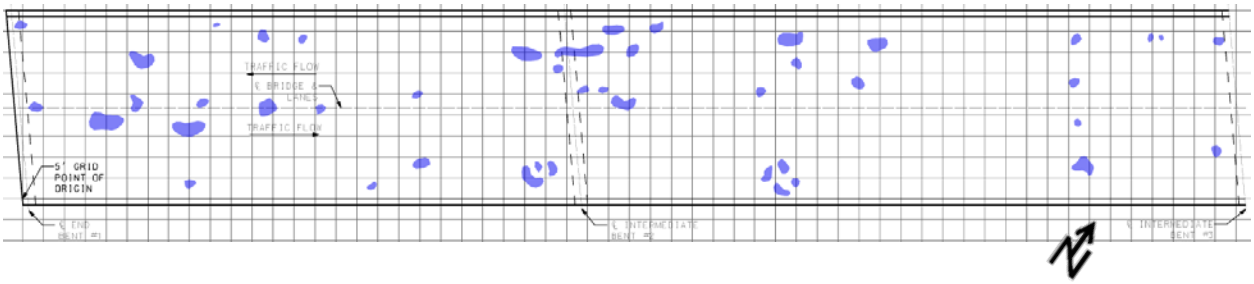

Bridge 24220

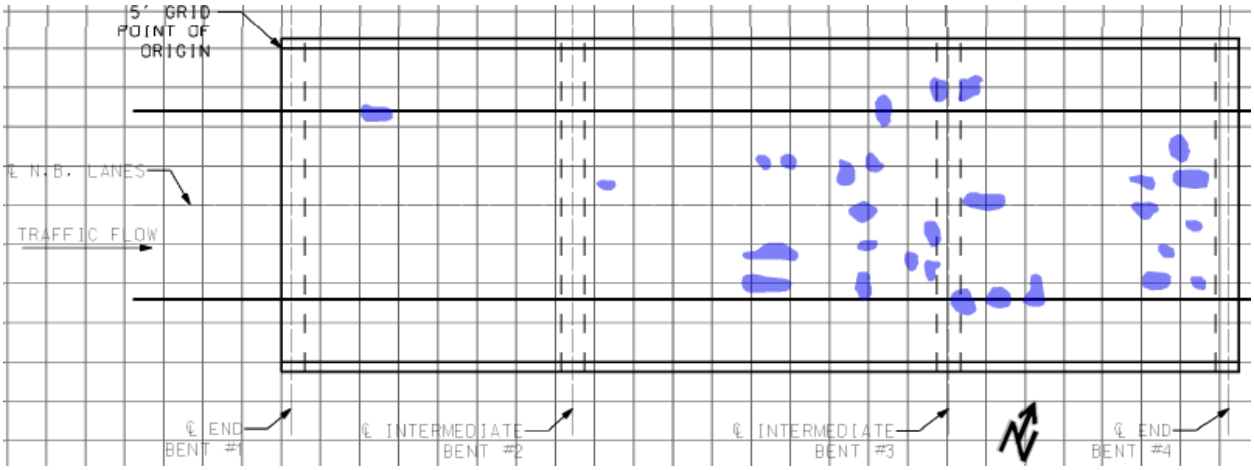

Bridge 49180

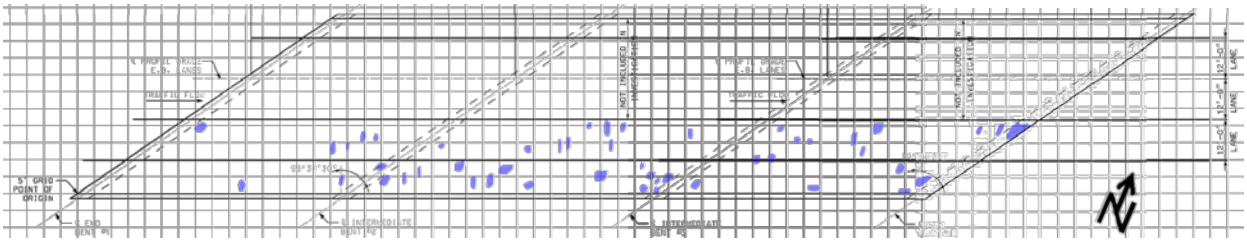

C.4.9 Consultant I (pole-mounted IRT)–Second Round

Bridge 01310

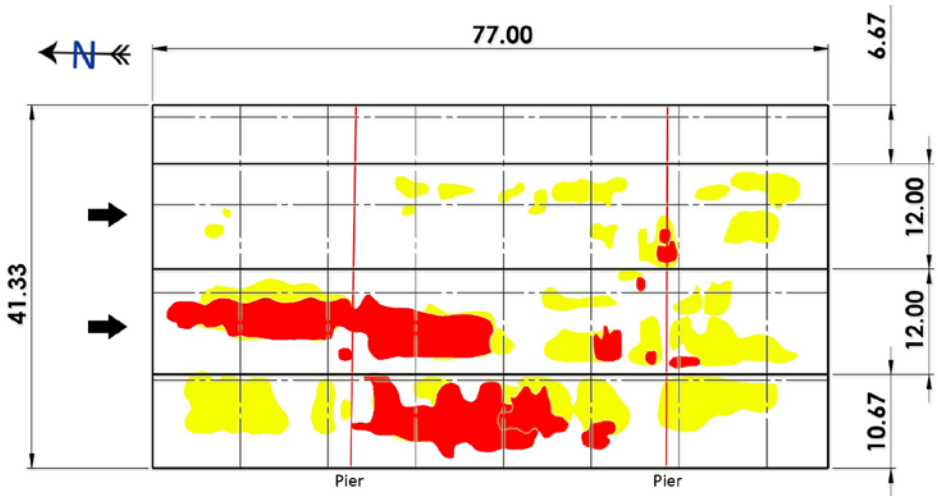

Bridge 01347

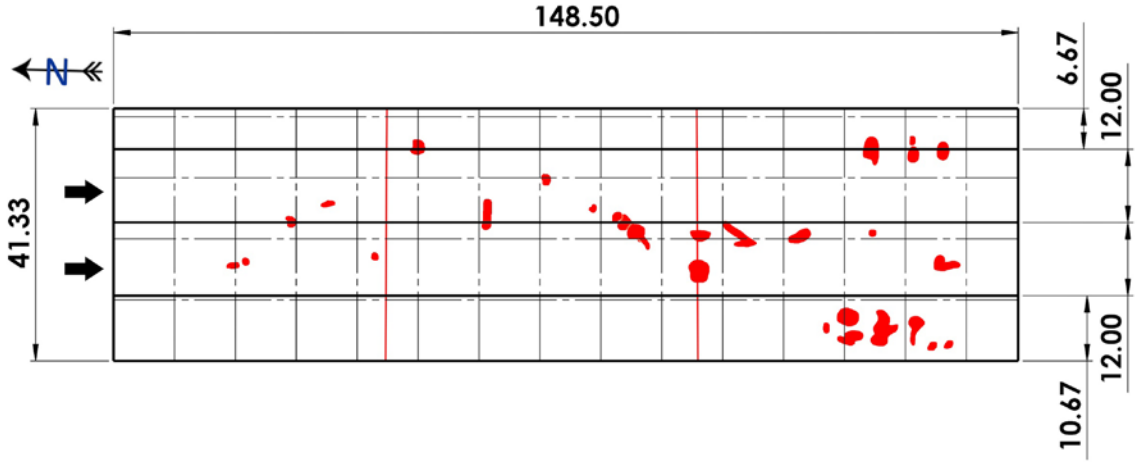

Bridge 24220

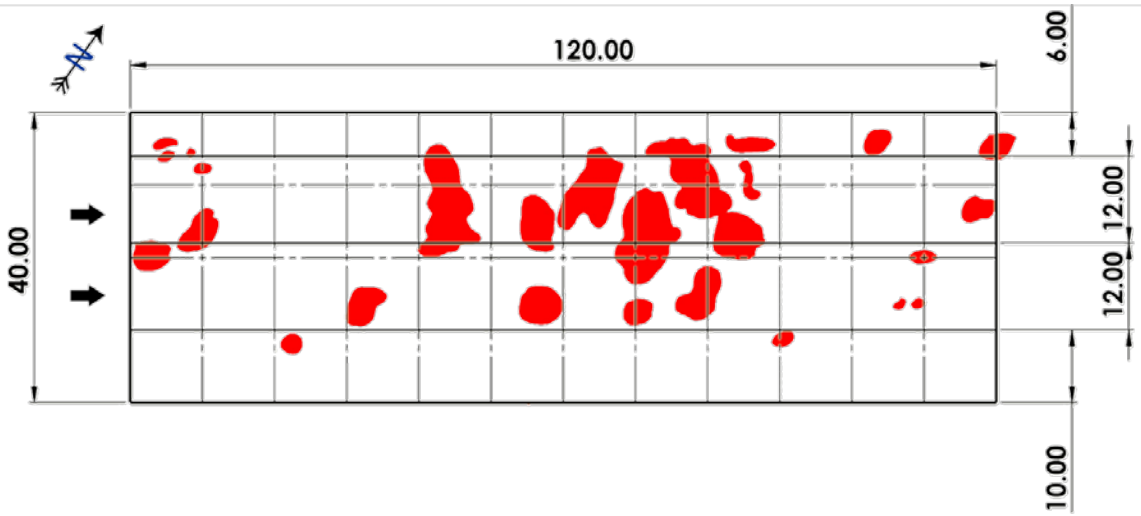

Bridge 49200

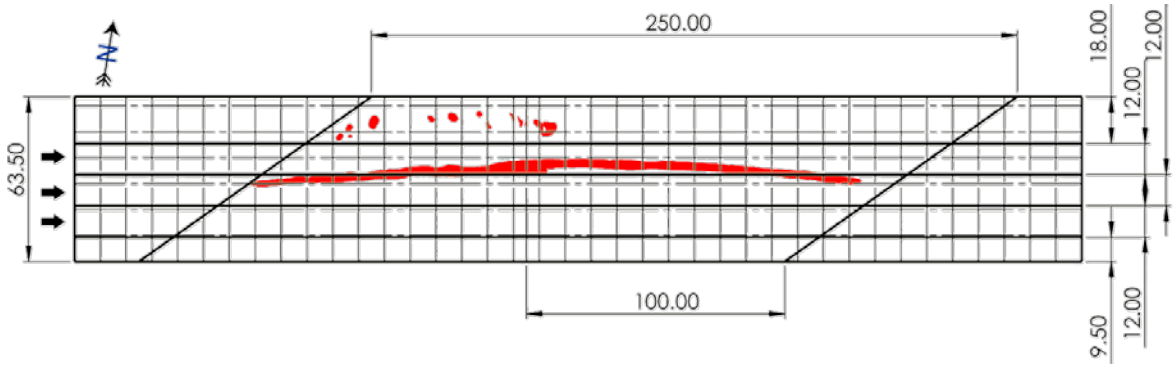

C.5 Automated Sounding

C.5.1 Consultant B

Bridge 16500

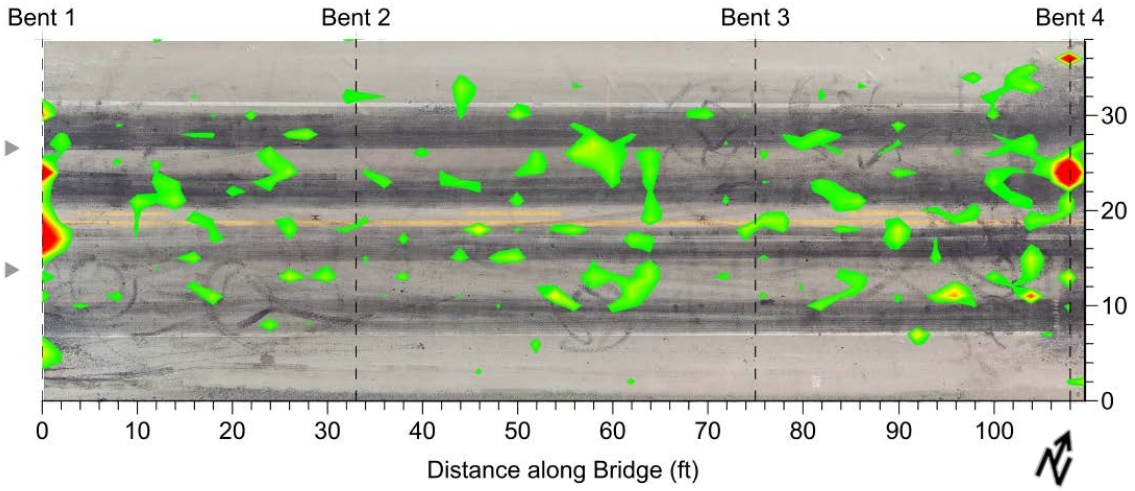

Bridge 18770

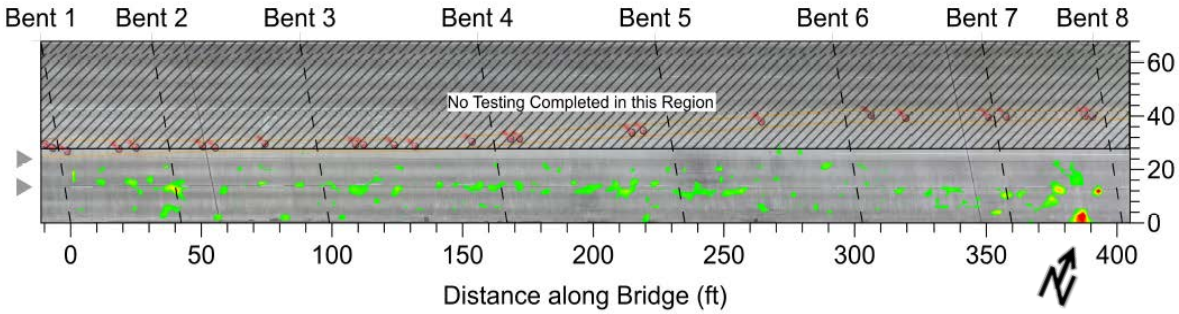

Bridge 22690

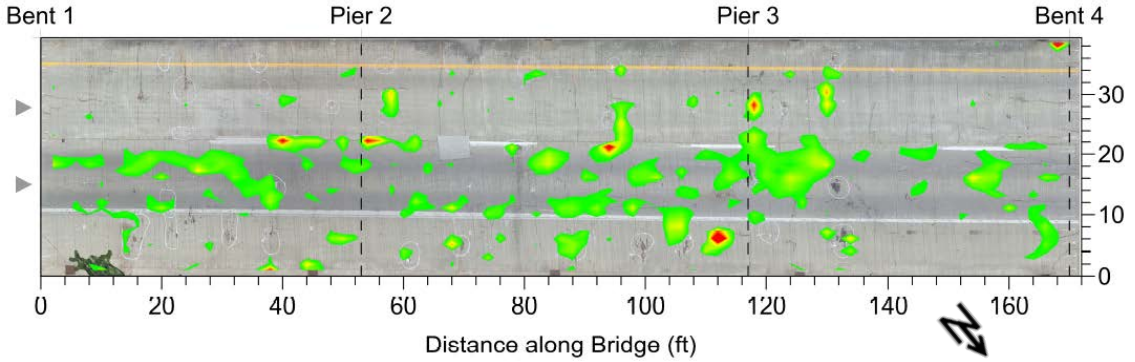

Bridge 31080

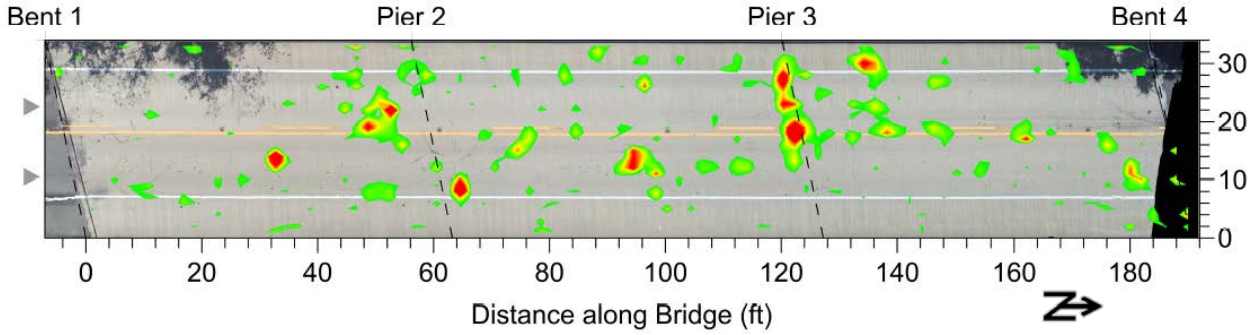

Bridge 35520

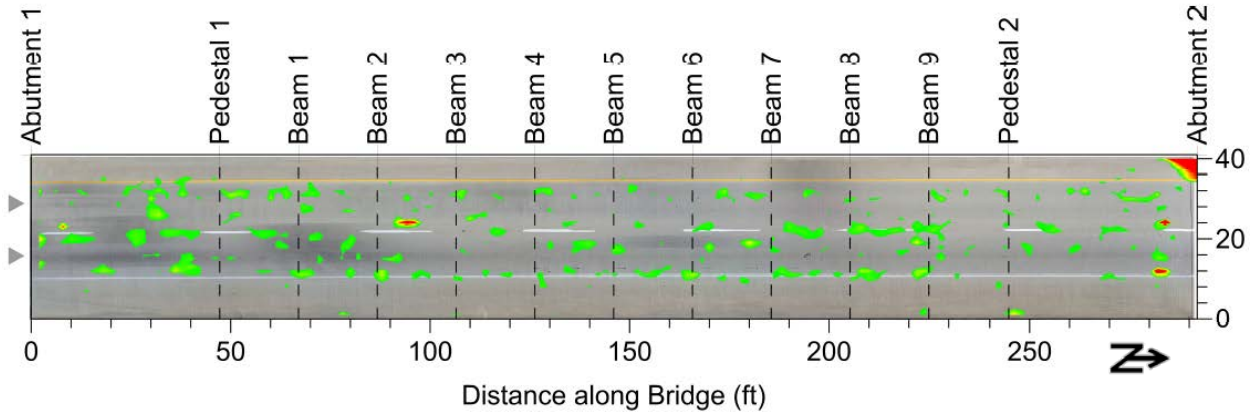

Bridge 37070

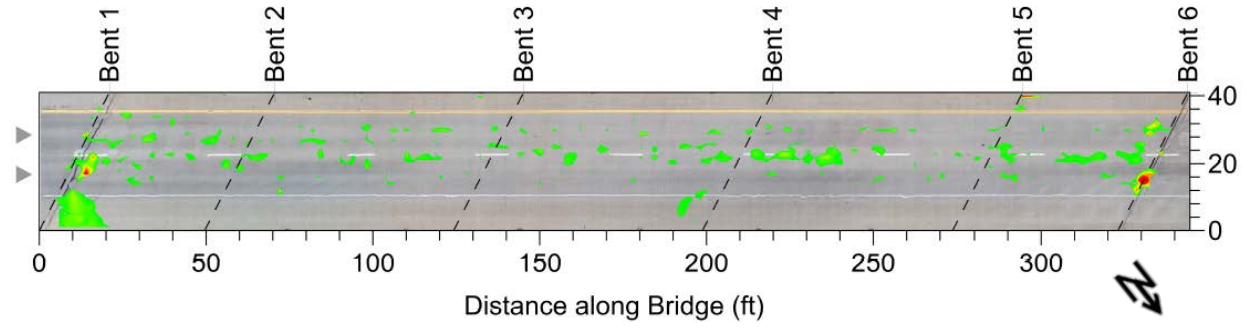

Bridge 37100

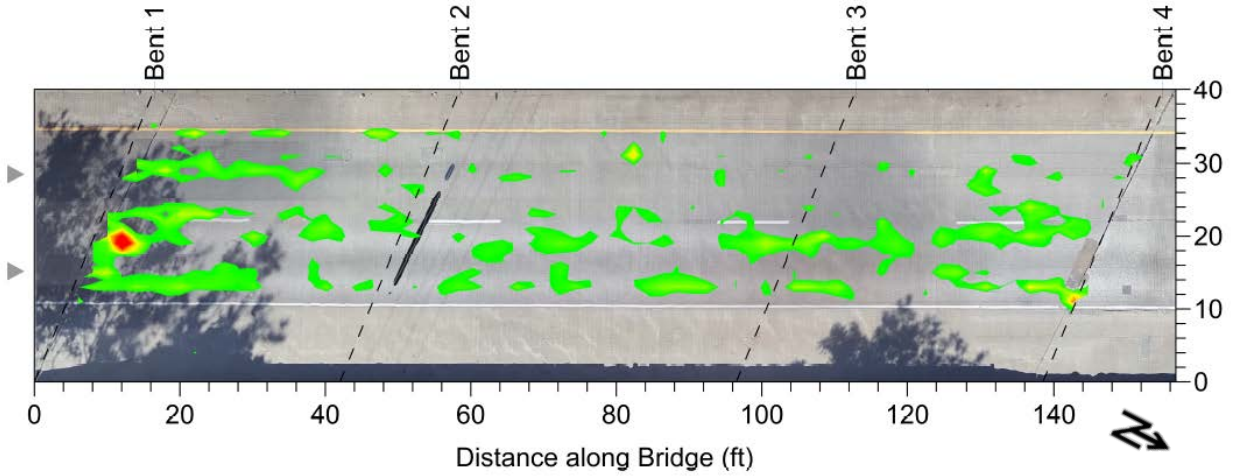

Bridge 37150

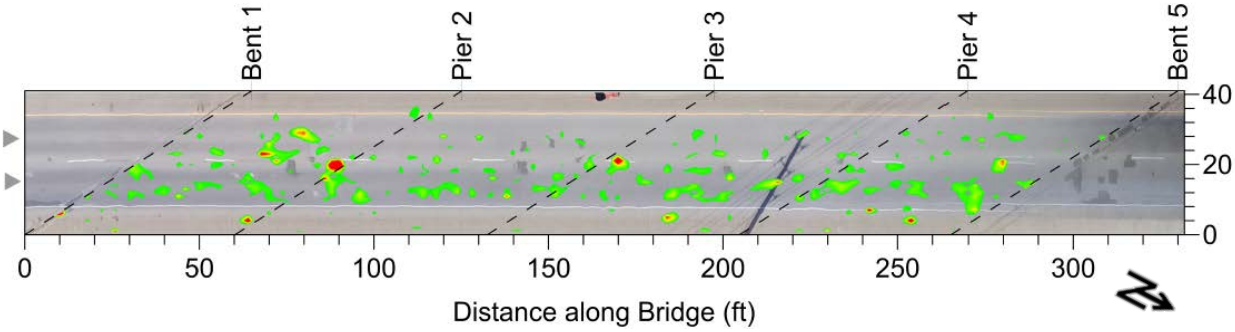

Bridge 41810

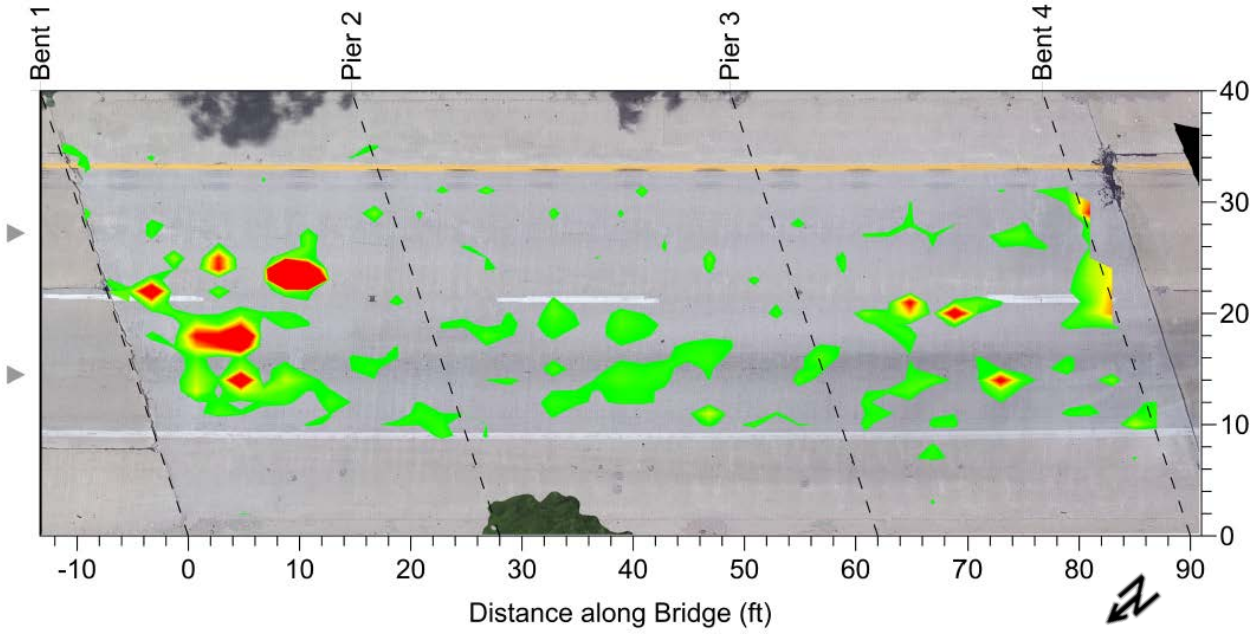

Bridge 41870

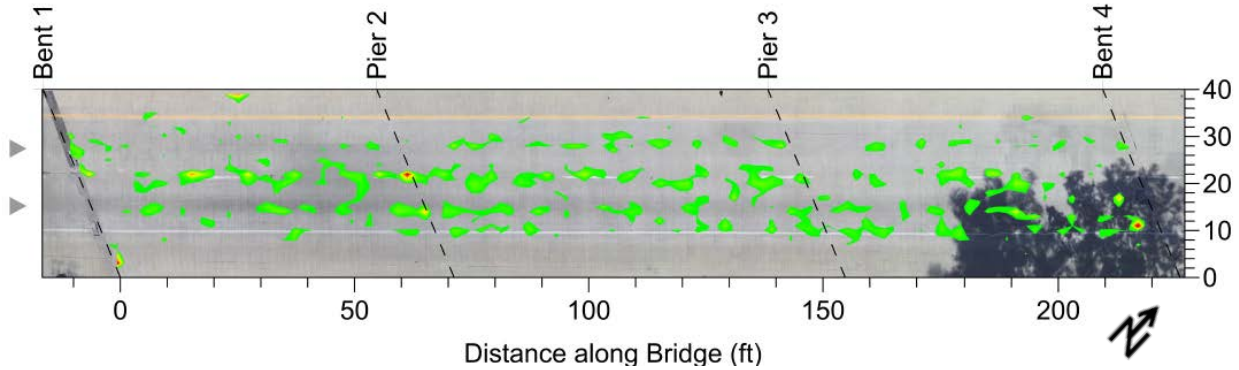

C.5.2 Consultant A

Bridge 01310

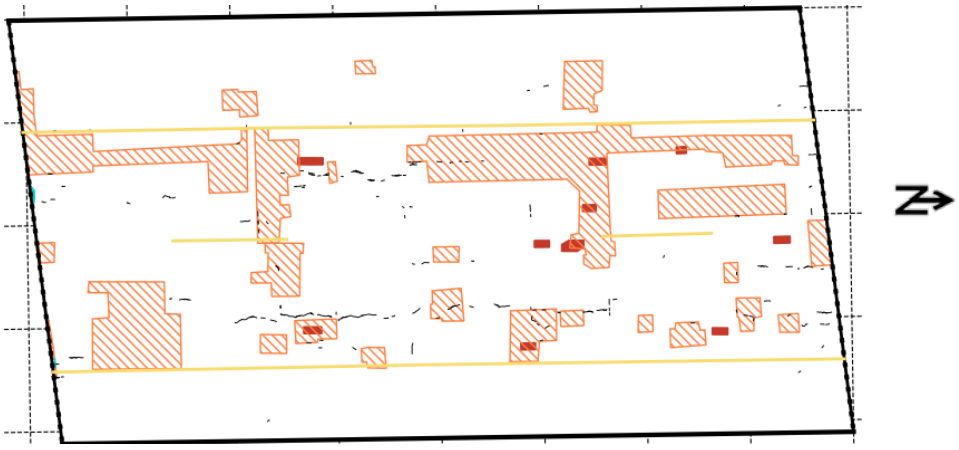

Bridge 01347

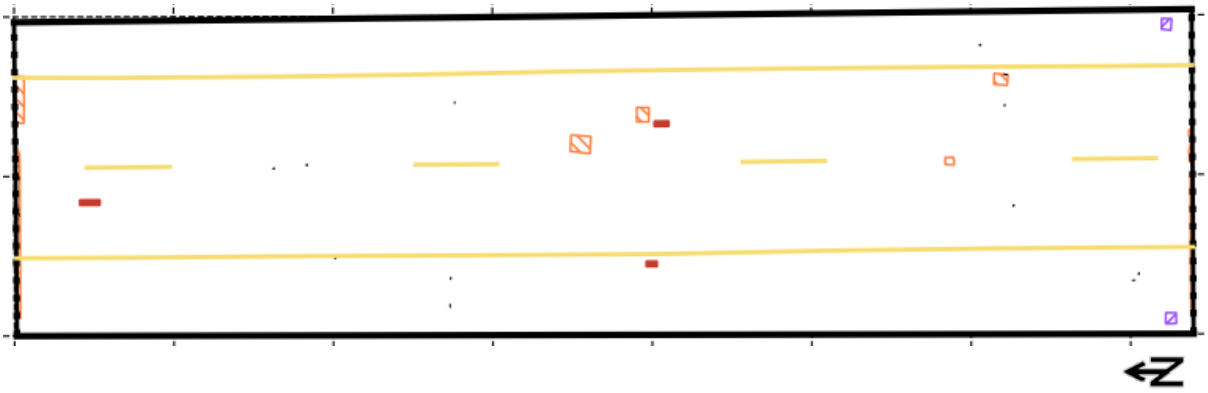

Bridge 04845

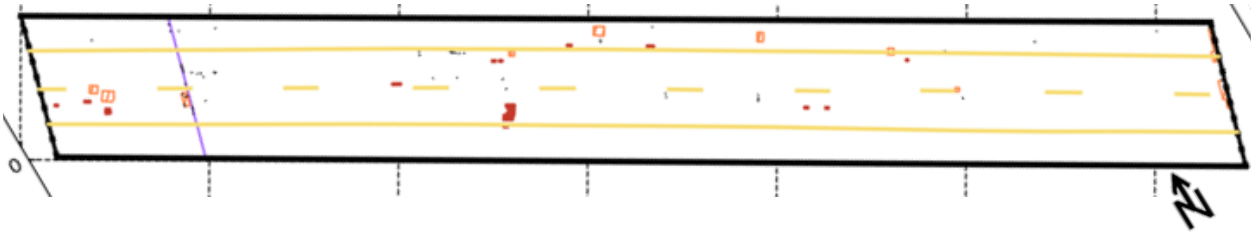

Bridge 04930

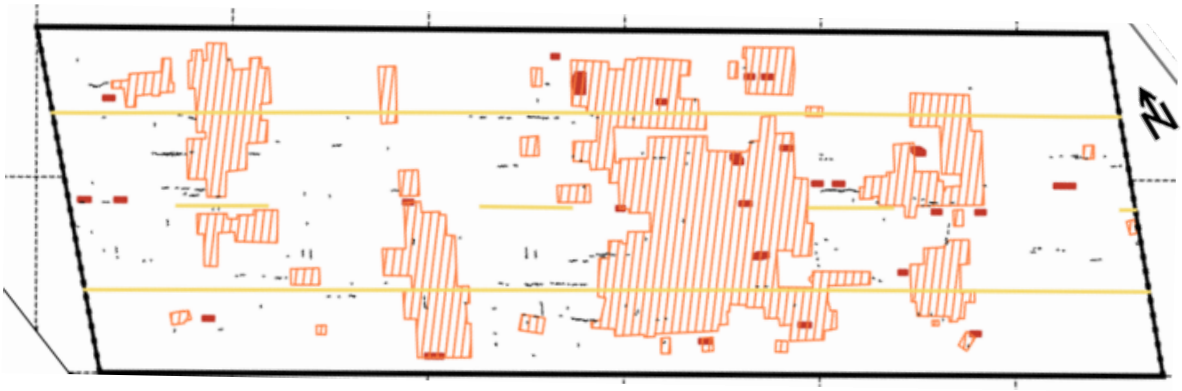

Bridge 08630

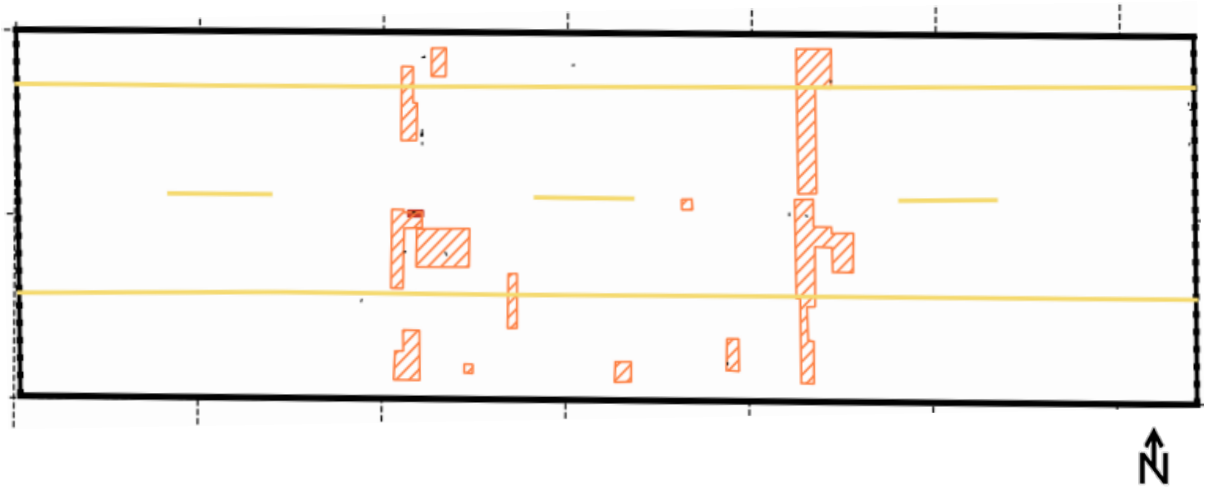

Bridge 16500

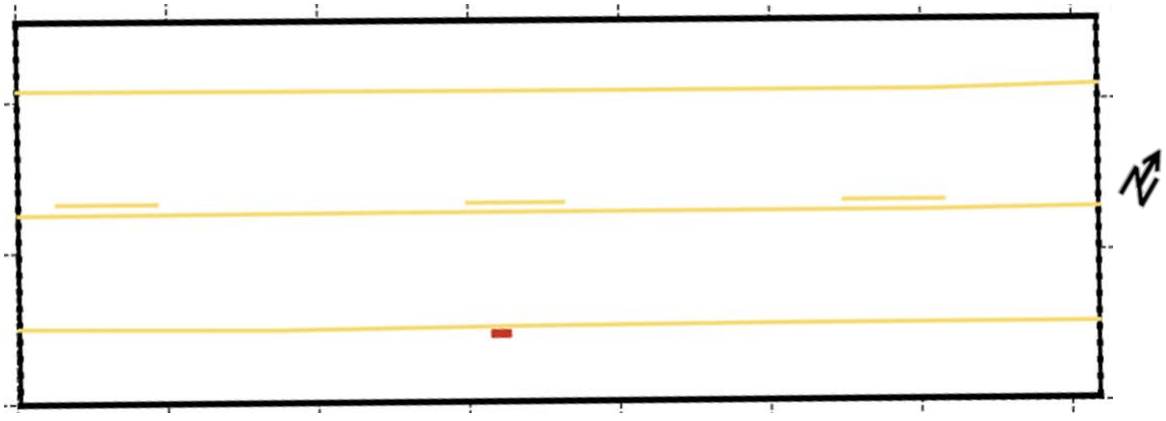

Bridge 17940

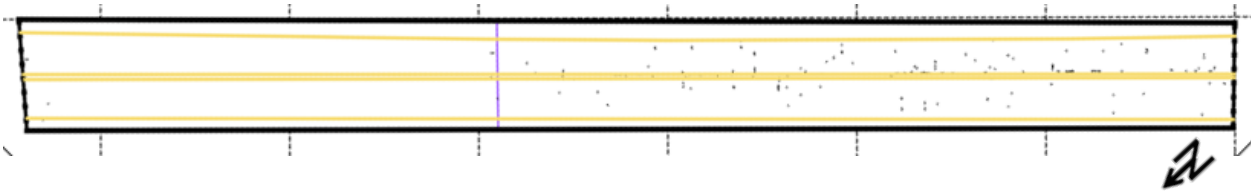

Bridge 18770

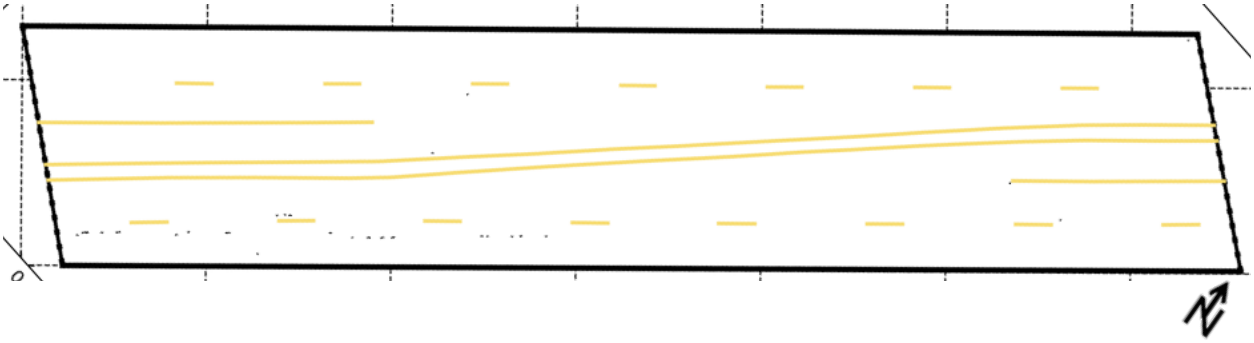

Bridge 19640

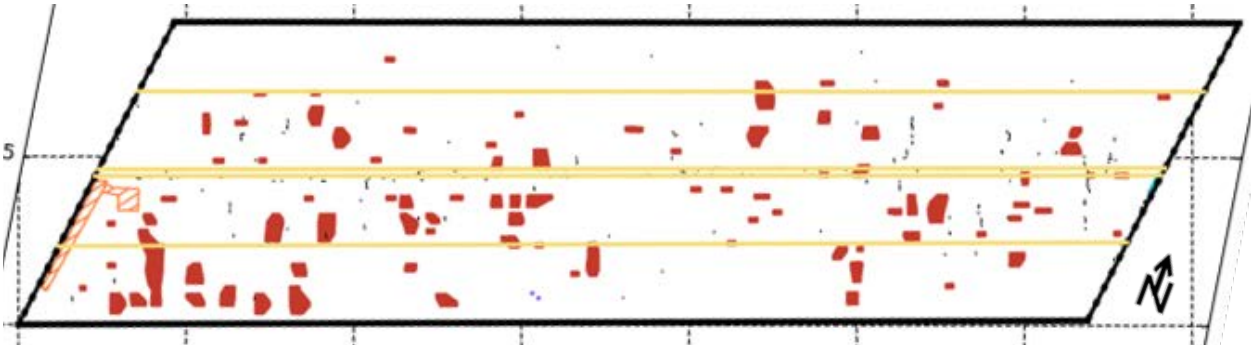

Bridge 20610

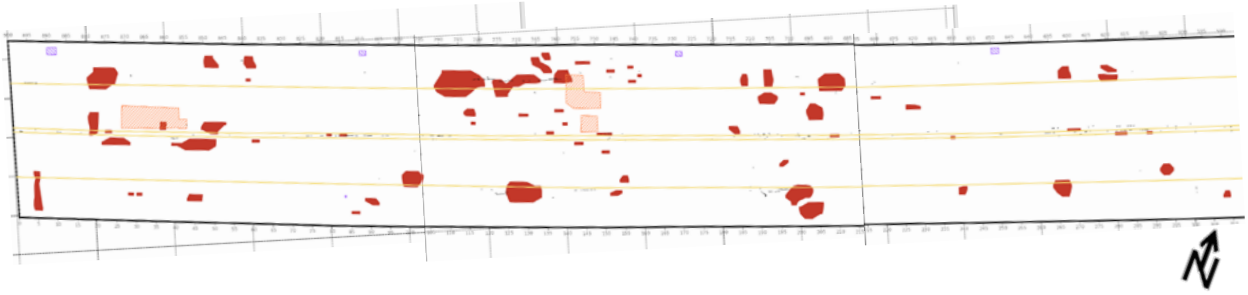

Bridge 22690

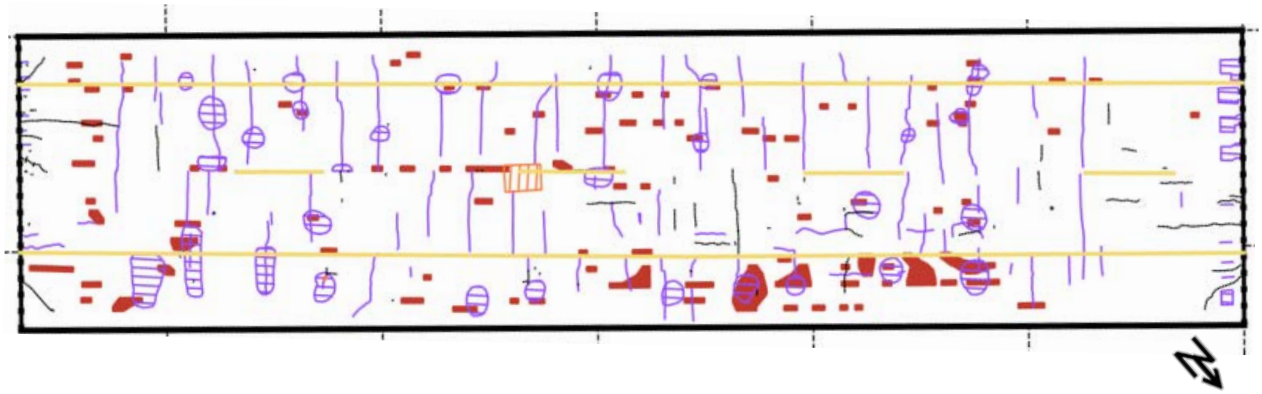

Bridge 24220

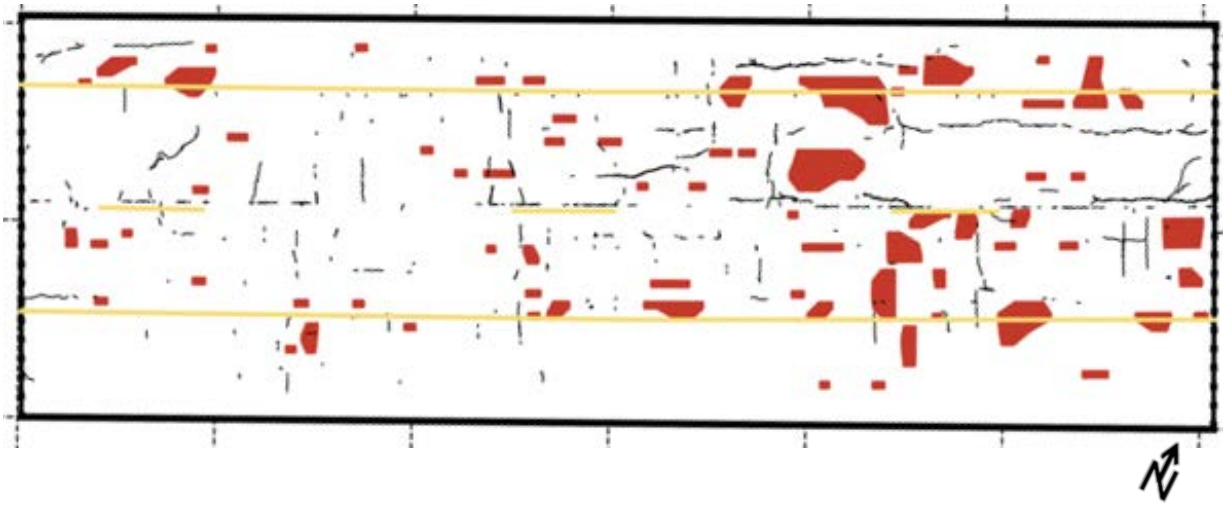

Bridge 35520

Bridge 37070

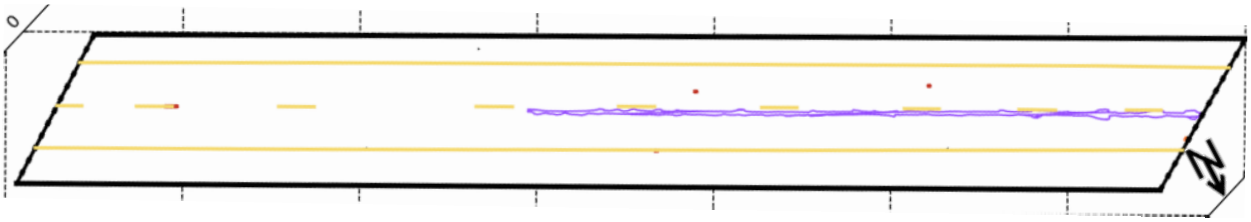

Bridge 37100

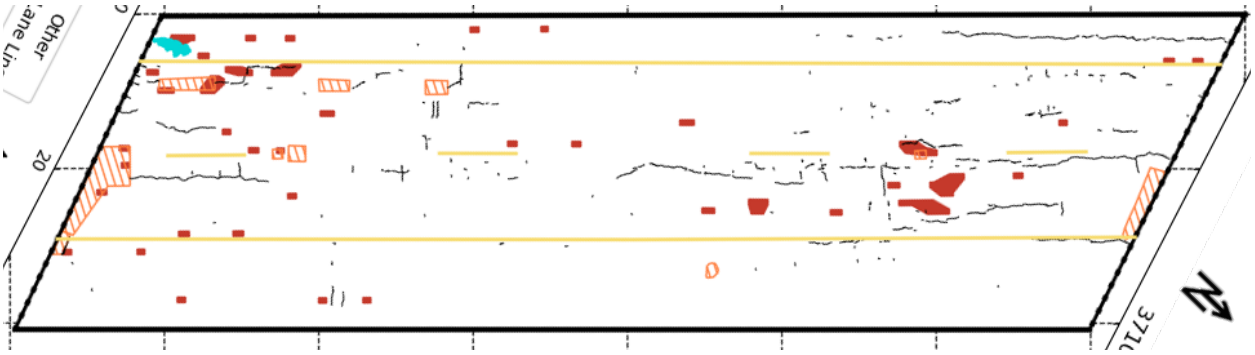

Bridge 37150

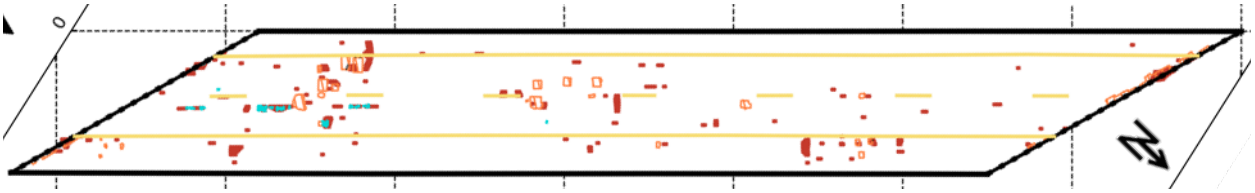

Bridge 41810

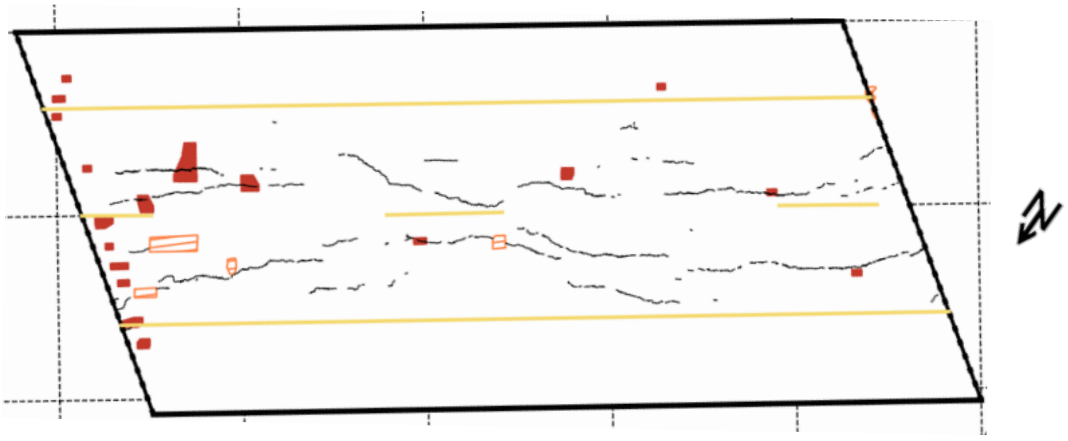

Bridge 41870

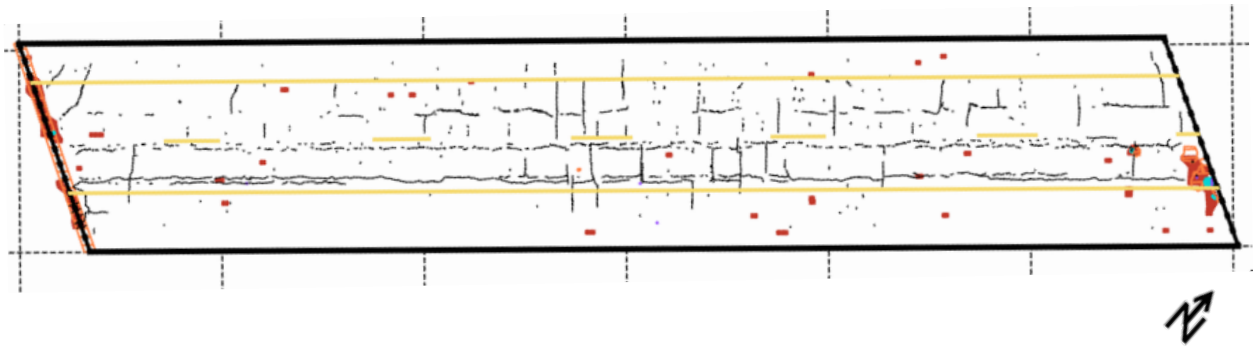

Bridge 49200

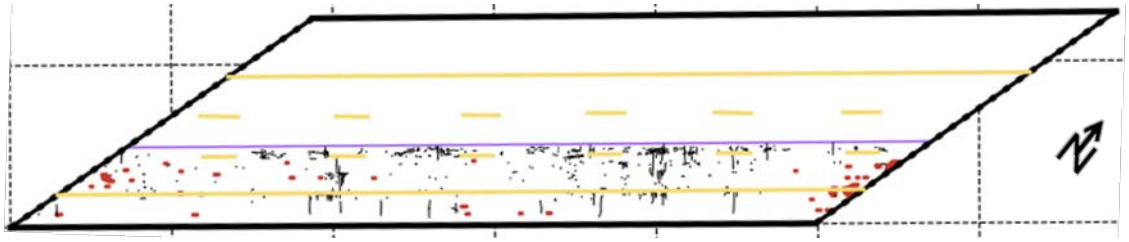

C.6 Concrete Cover Thickness

C.6.1 Consultant D (New bridges)

Bridge 13321

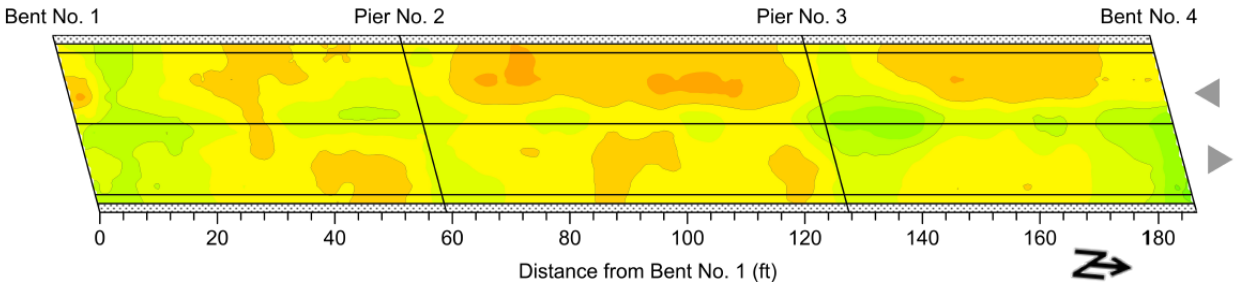

Bridge 16171

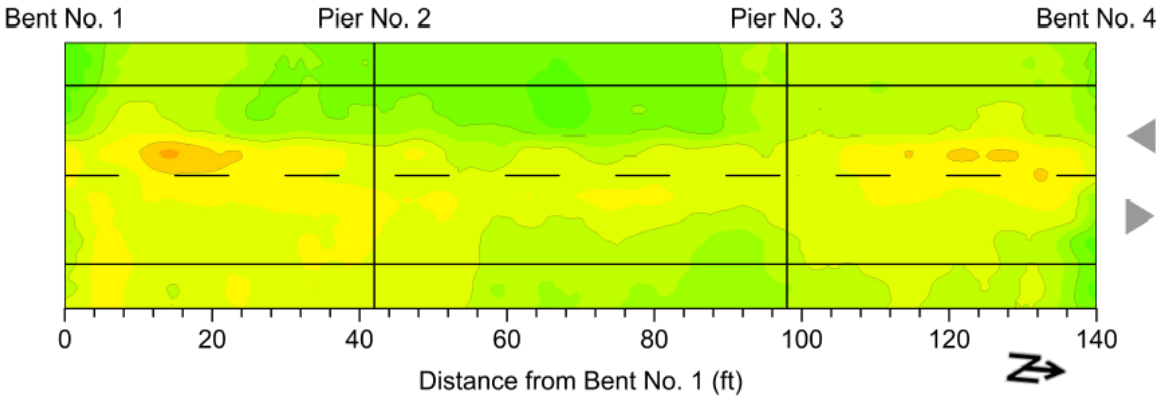

Bridge 16811

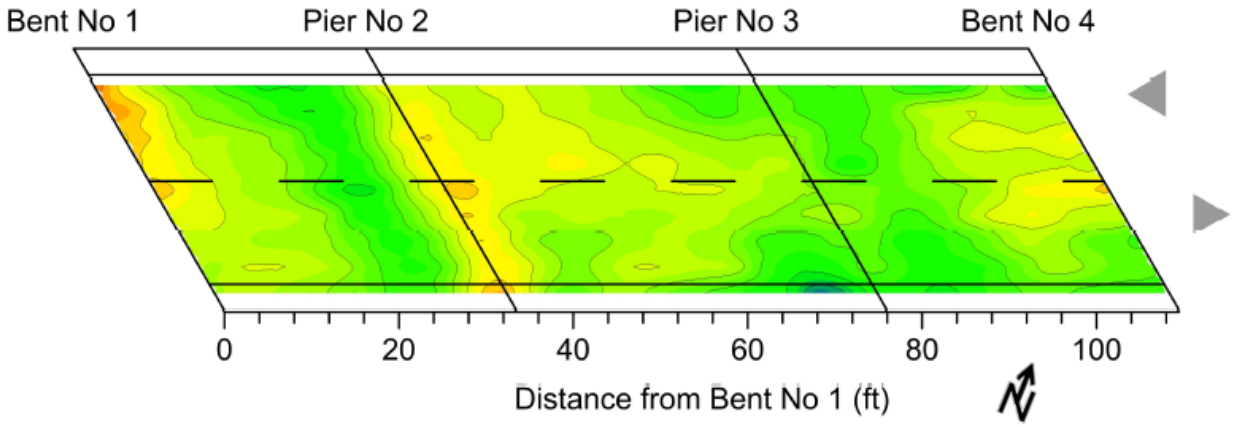

Bridge 17051

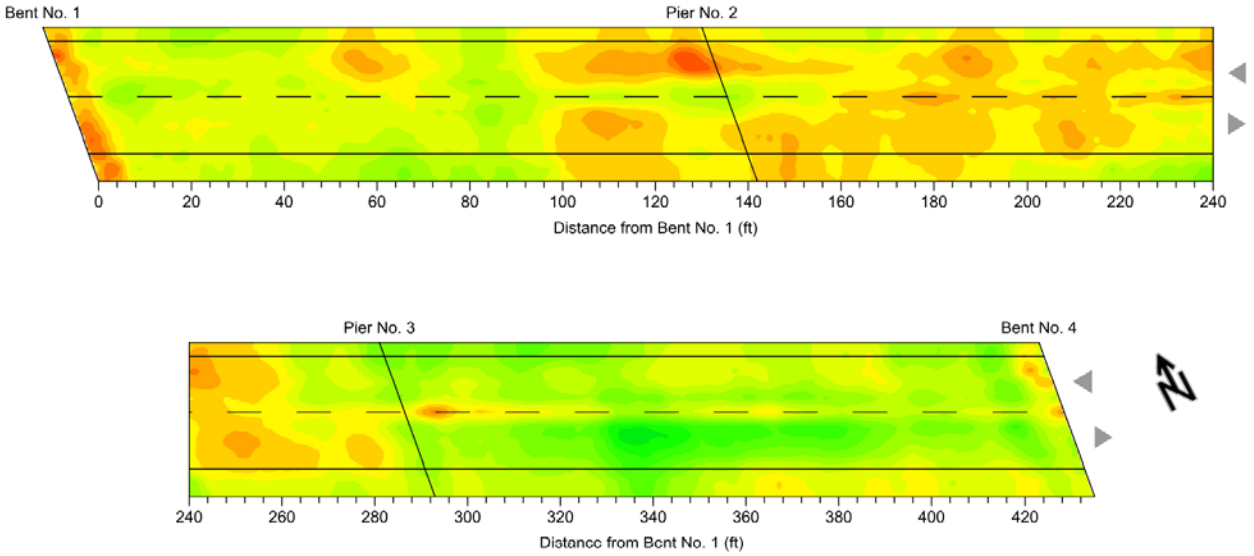

Bridge 28326

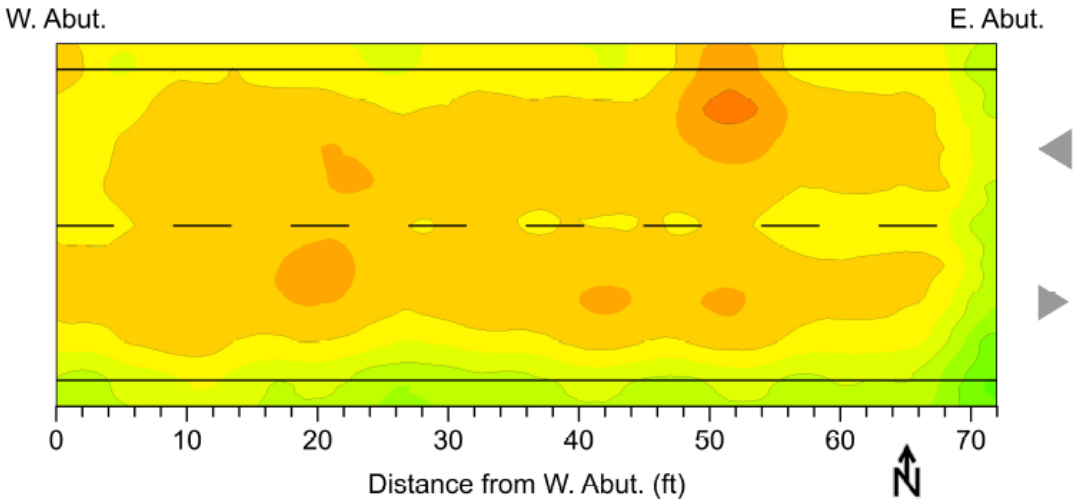

Bridge 28430

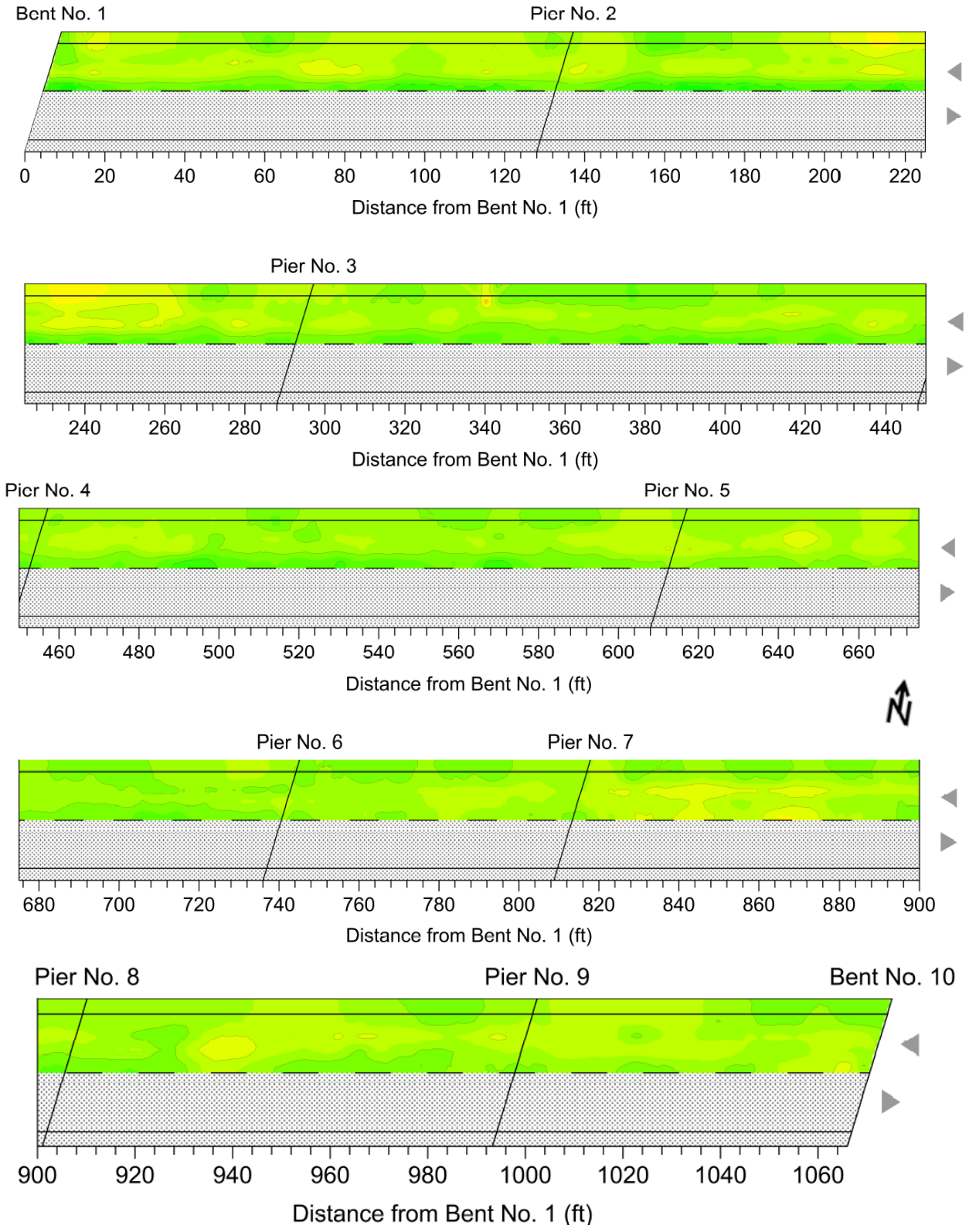

Bridge 32675

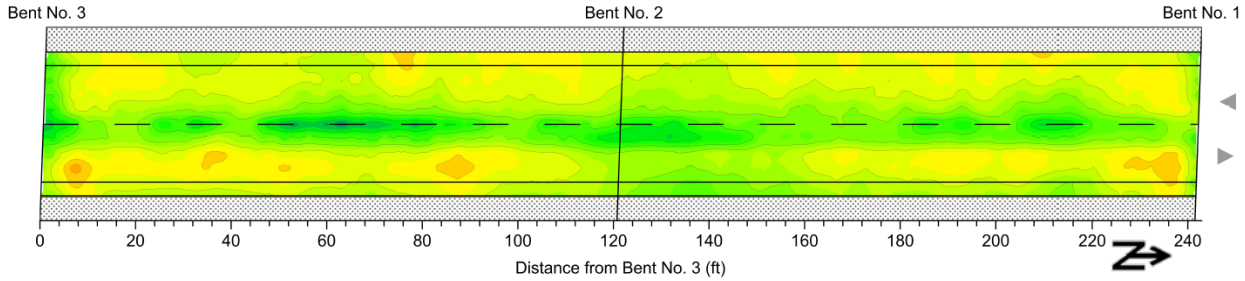

Bridge 33500

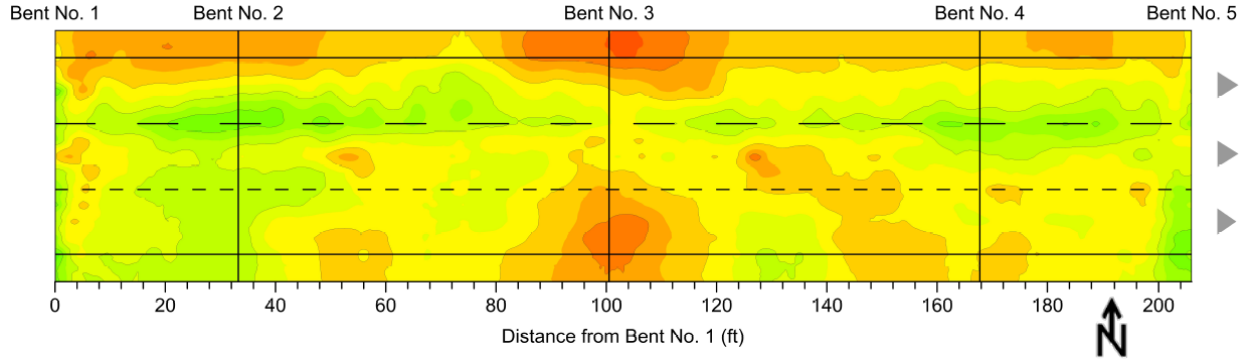

Bridge 44090

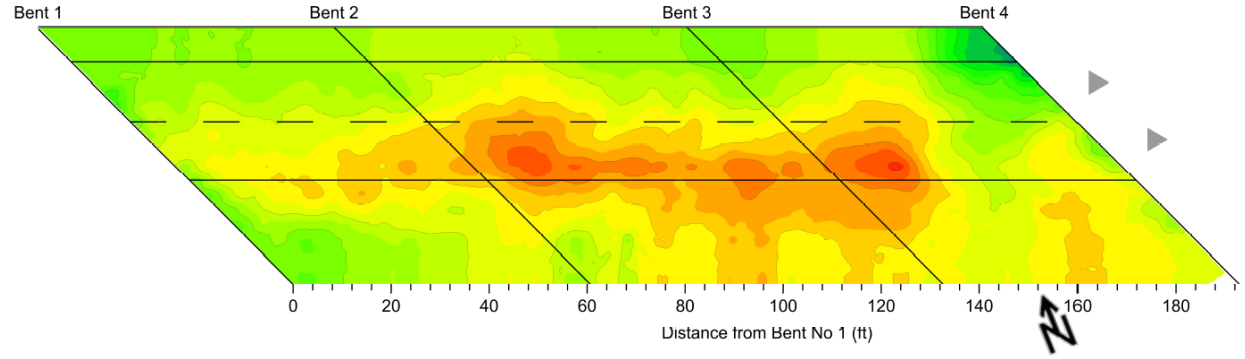

Bridge 44120

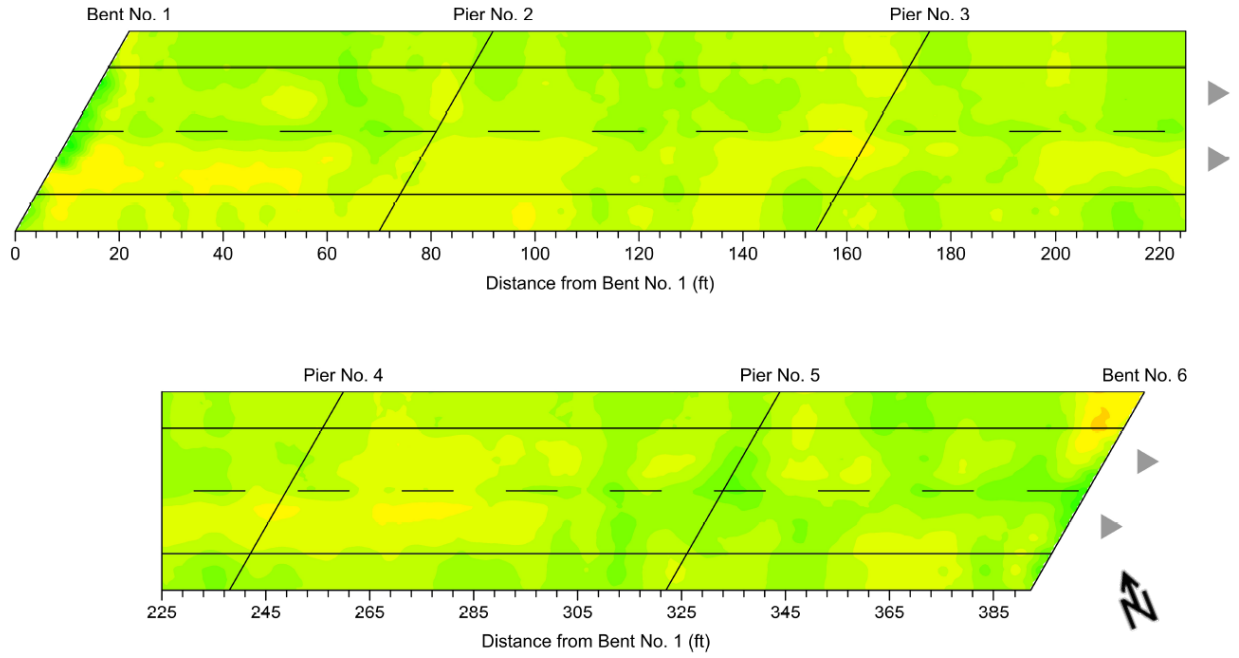

C.6.2 Consultant B

Bridge 16500

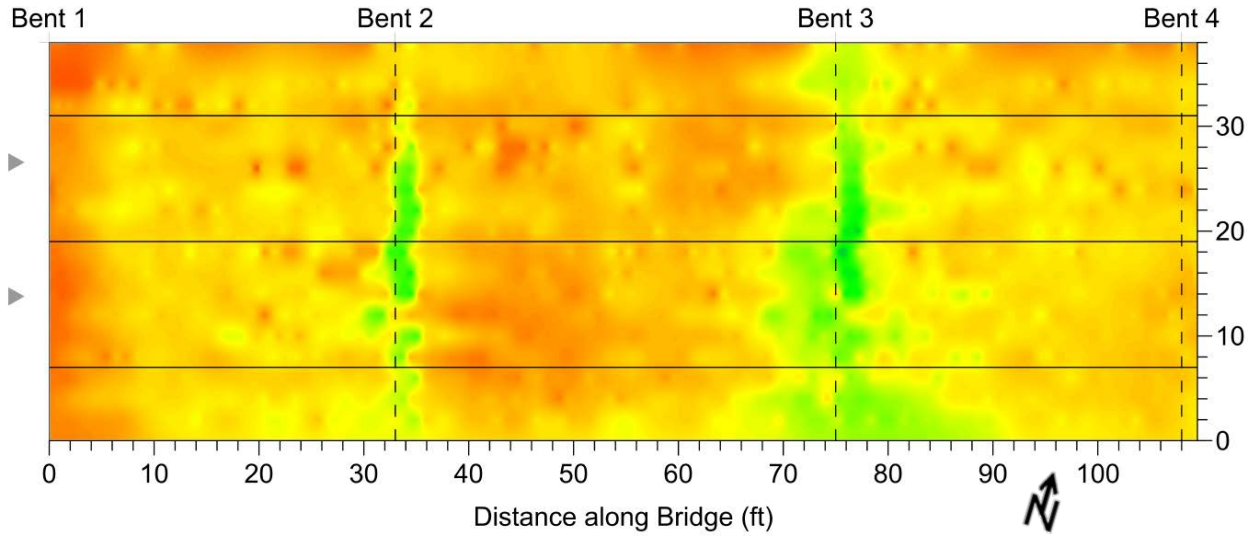

Bridge 18770

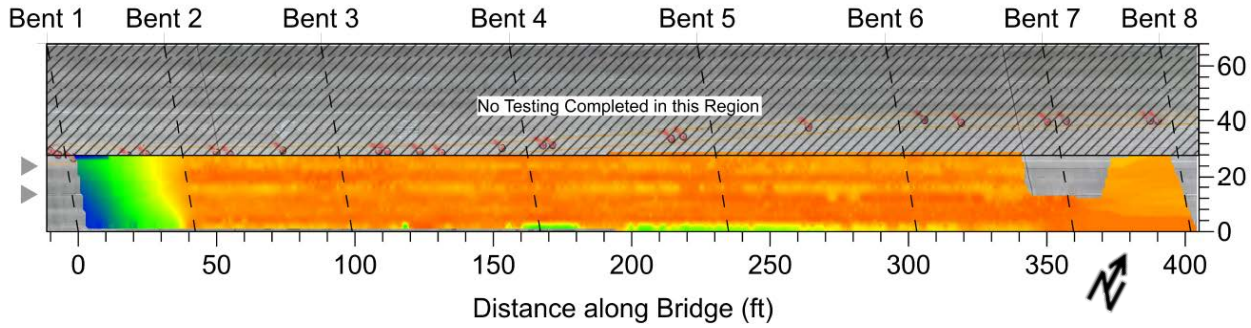

Bridge 22690

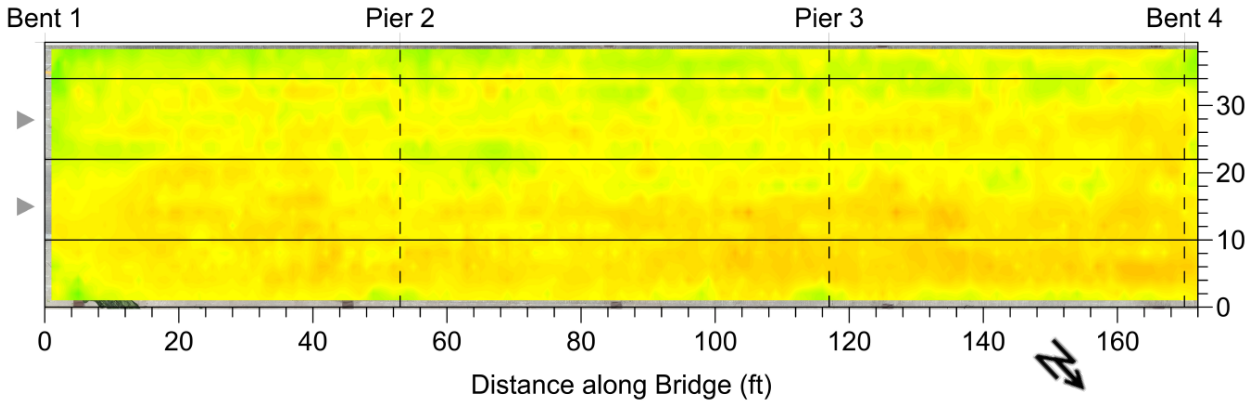

Bridge 31080

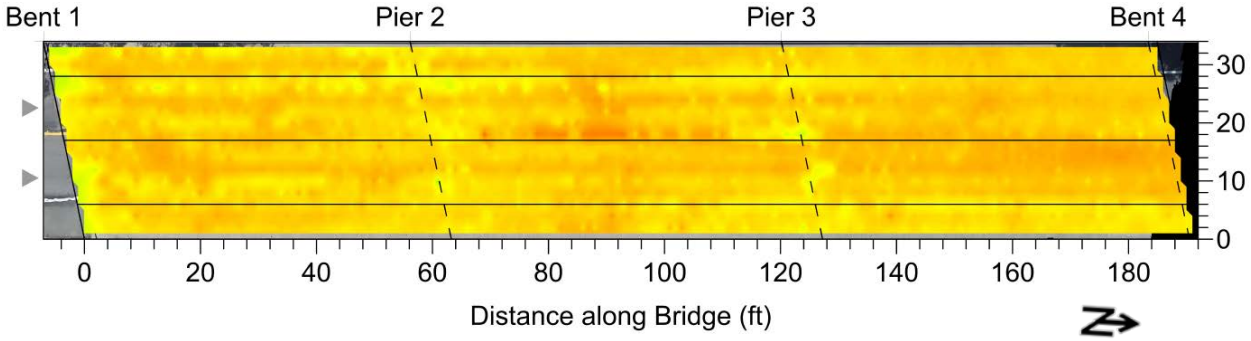

Bridge 35520

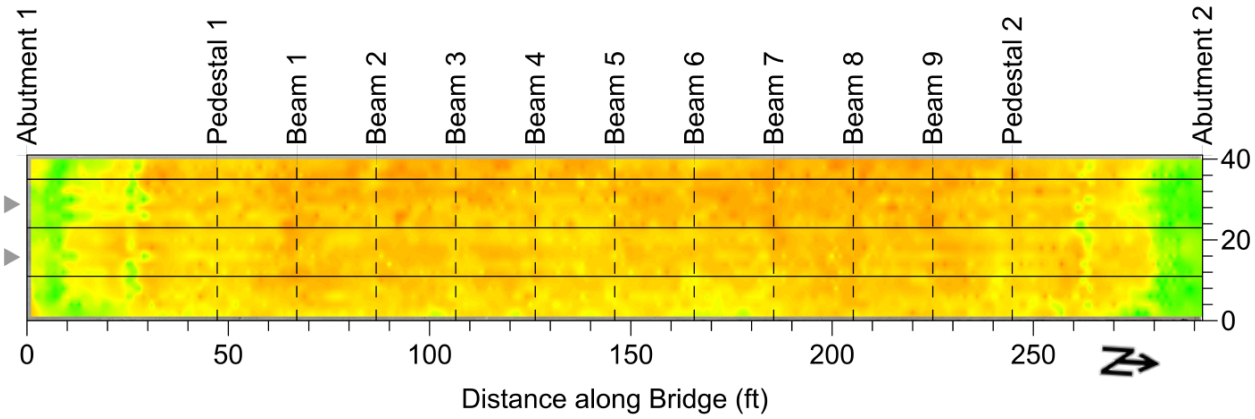

Bridge 37070

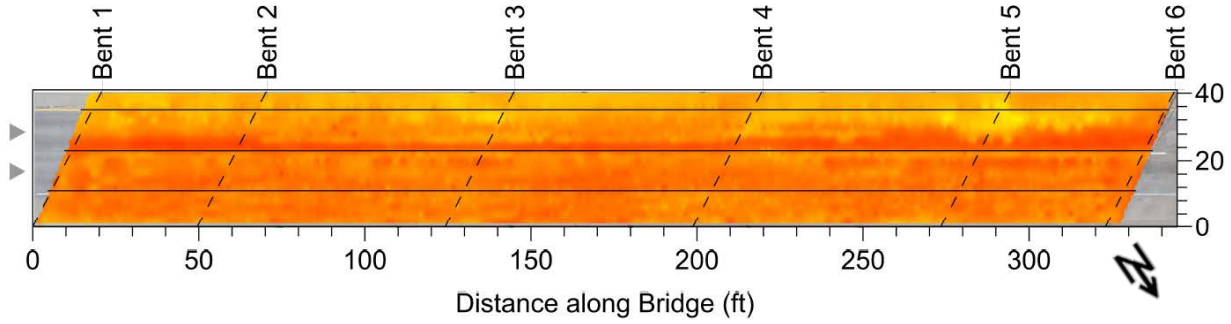

Bridge 37100

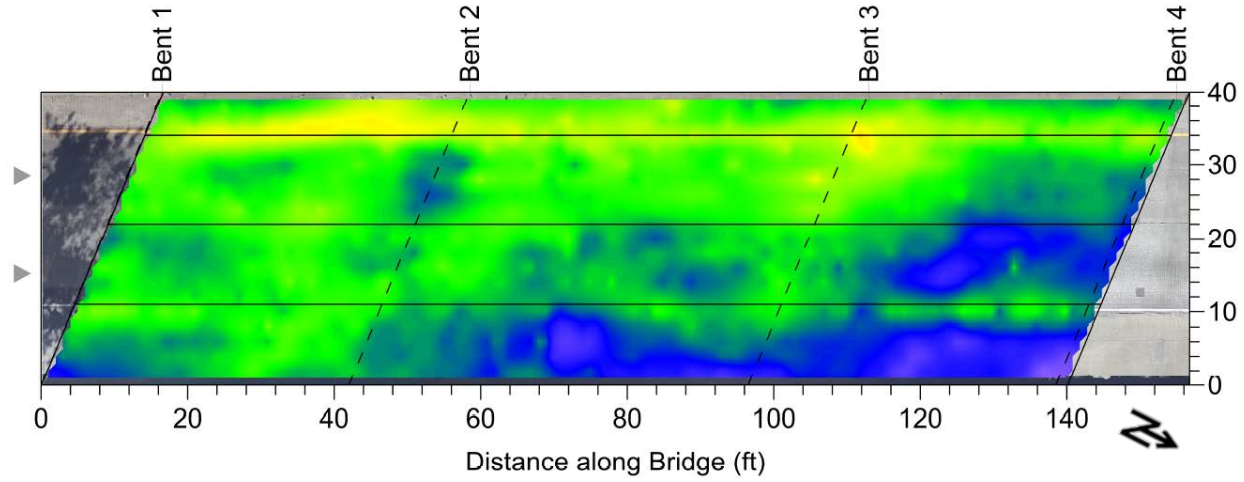

Bridge 37150

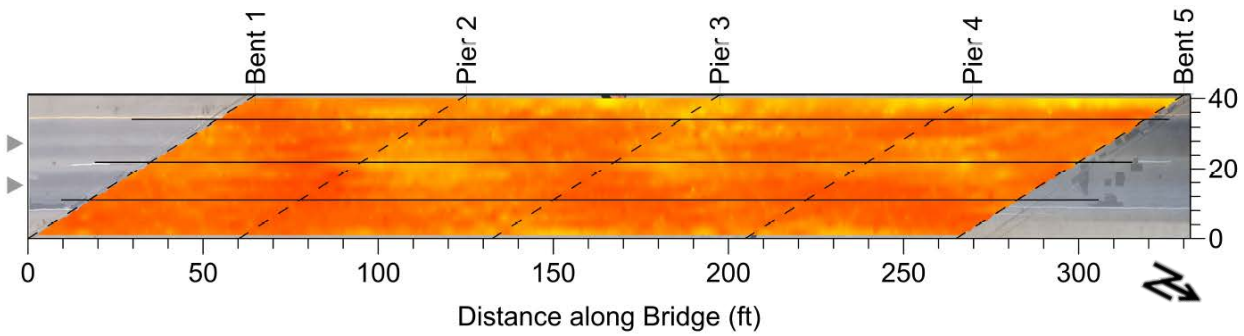

Bridge 41810

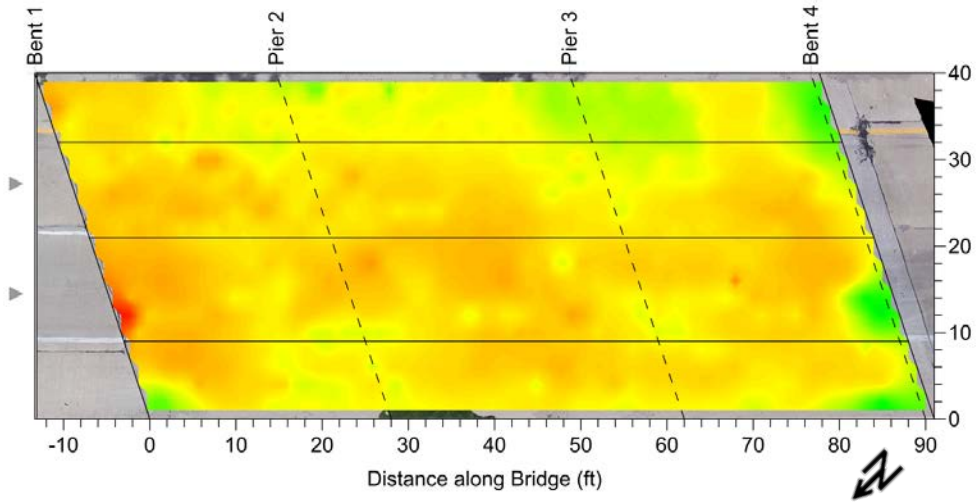

Bridge 41870

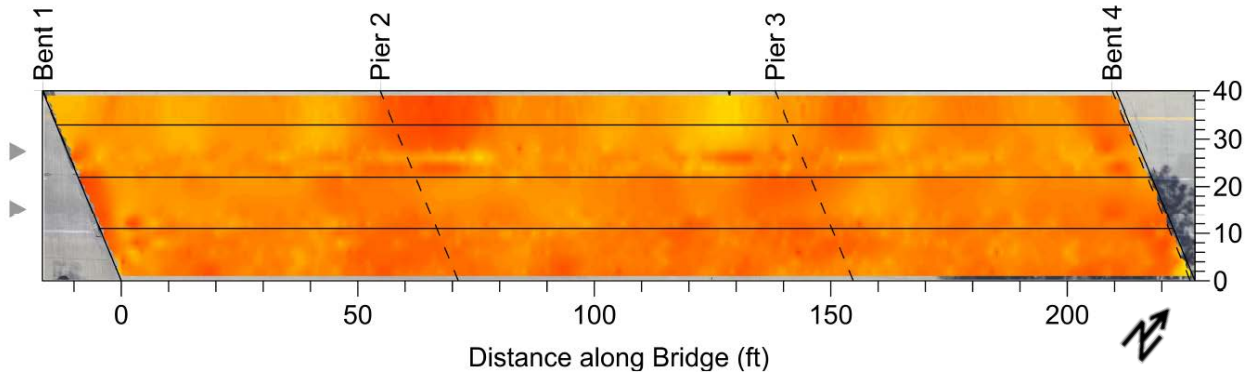

C.6.3 Consultant G

Bridge 16500

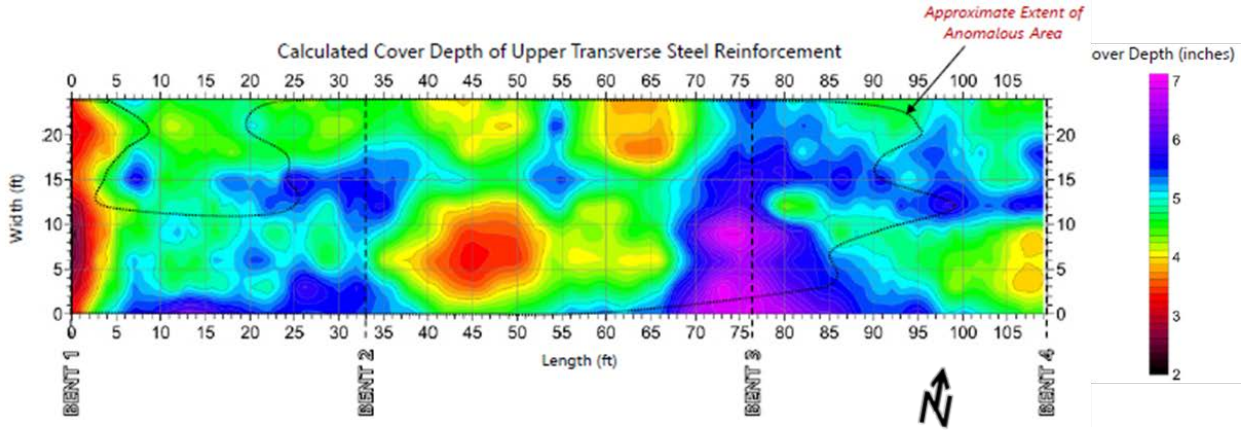

Bridge 18770

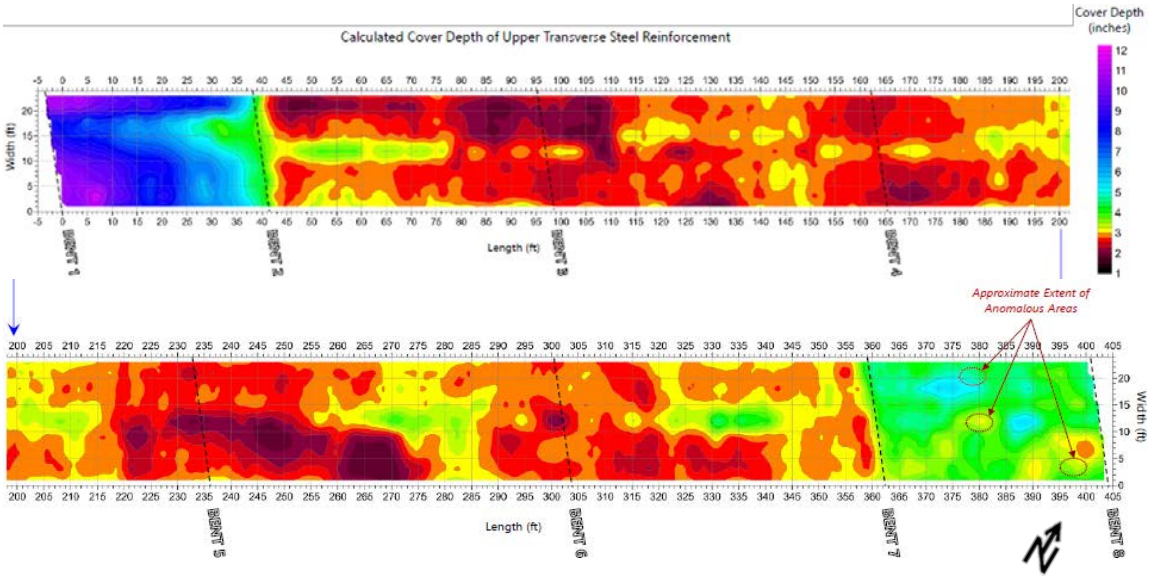

Bridge 22690

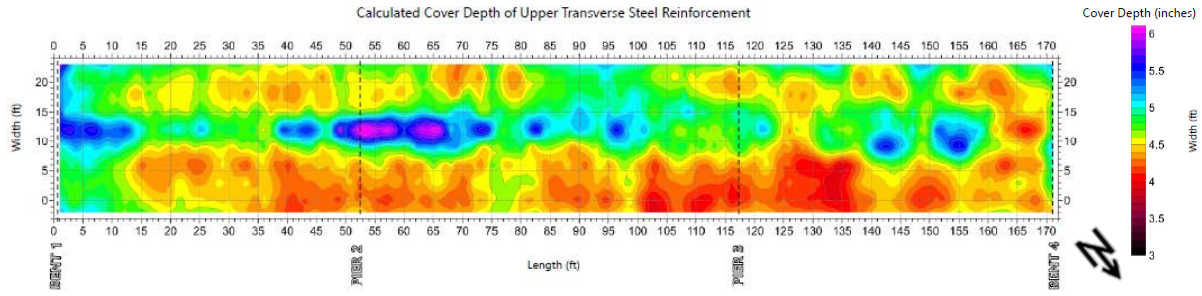

Bridge 31080

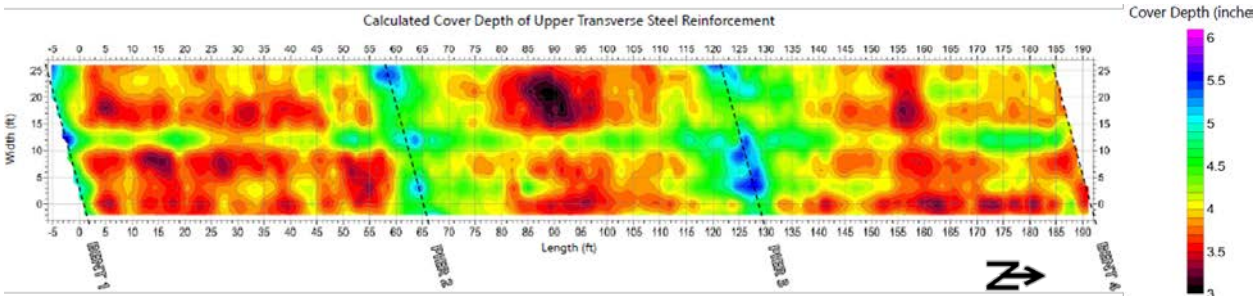

Bridge 35520

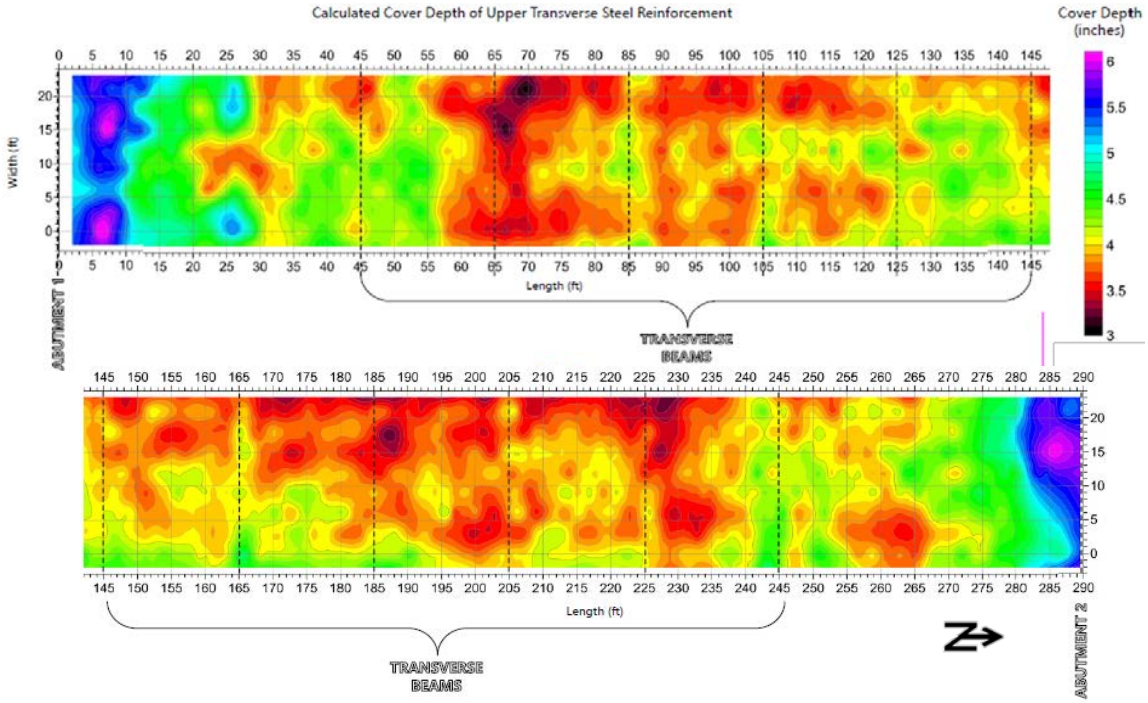

Bridge 37070

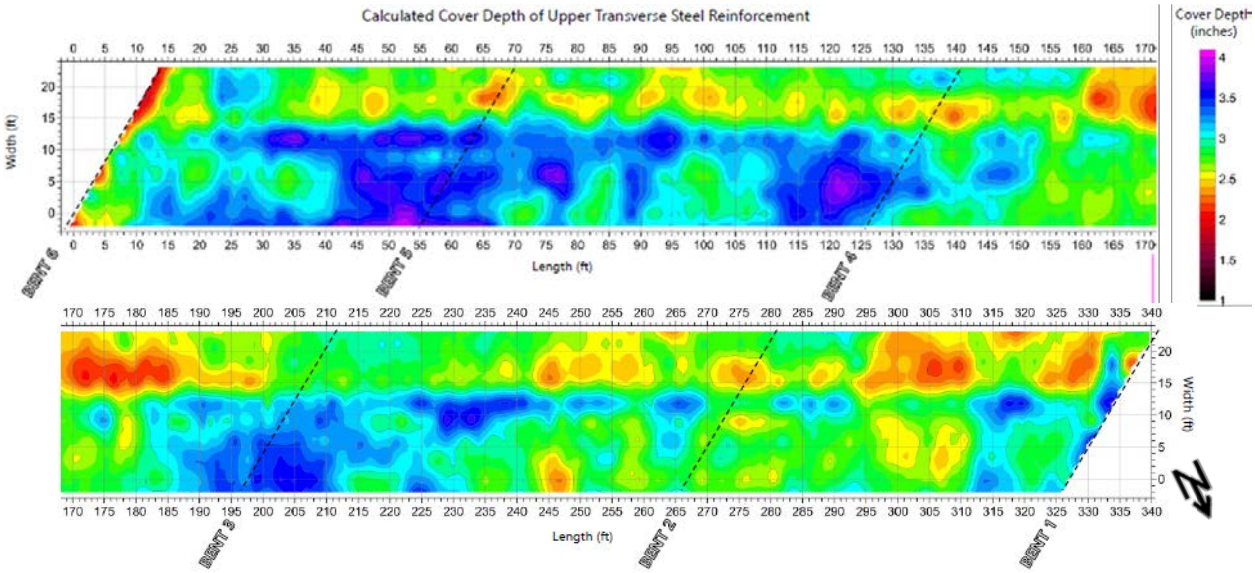

Bridge 37100

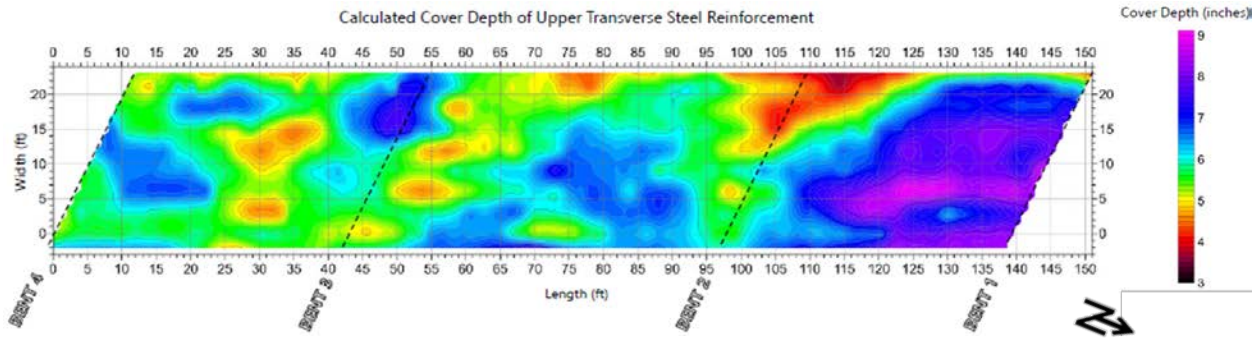

Bridge 37150

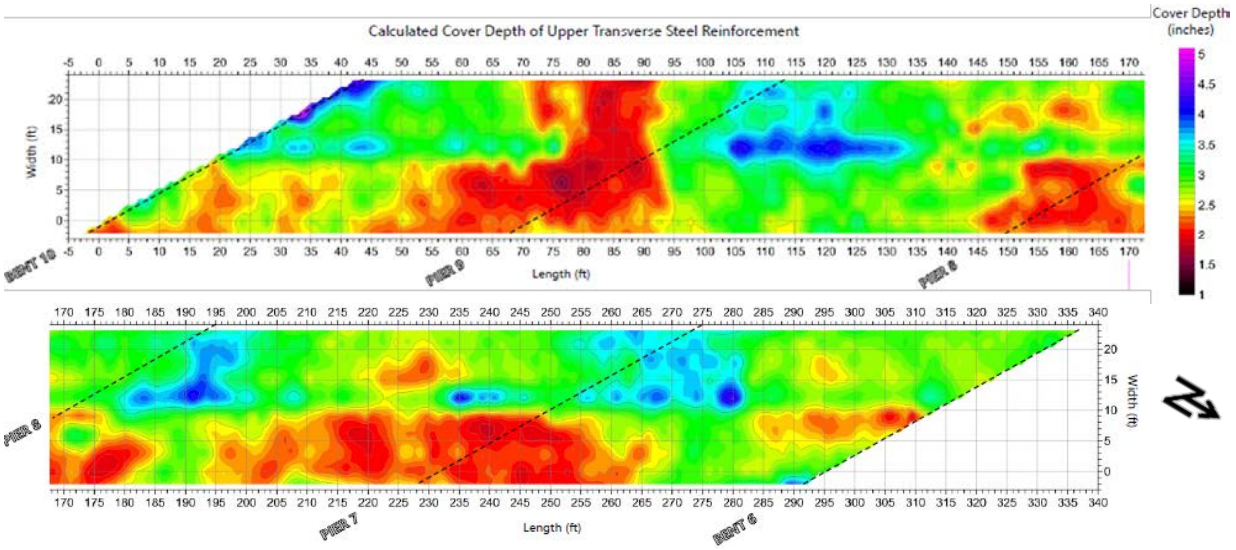

Bridge 41810

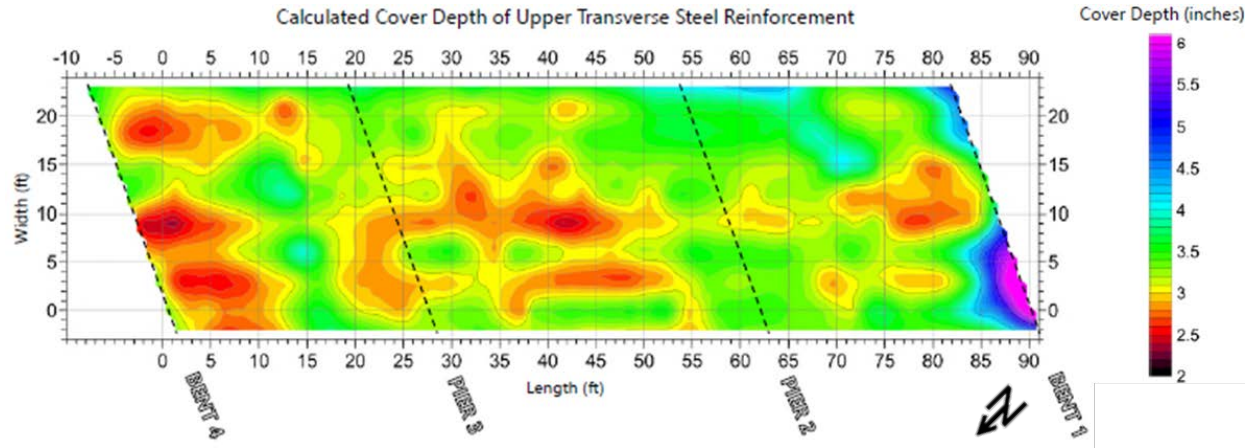

Bridge 41870

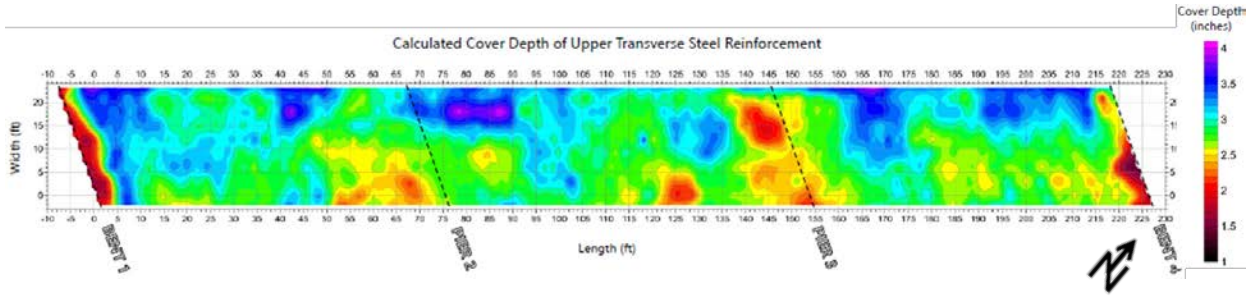

C.6.4 Consultant H

Bridge 01310

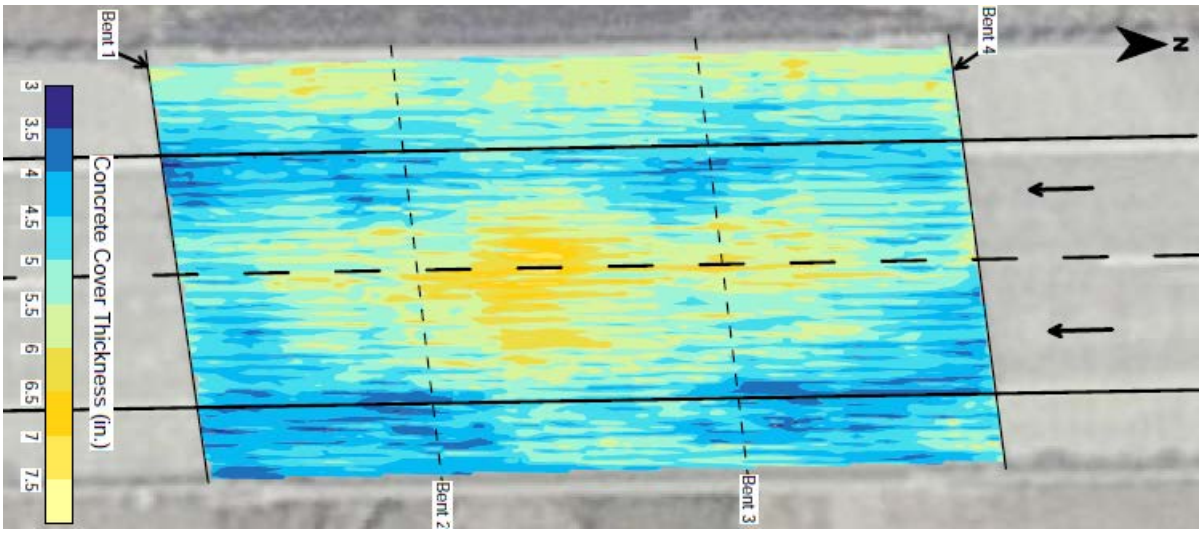

Bridge 01347

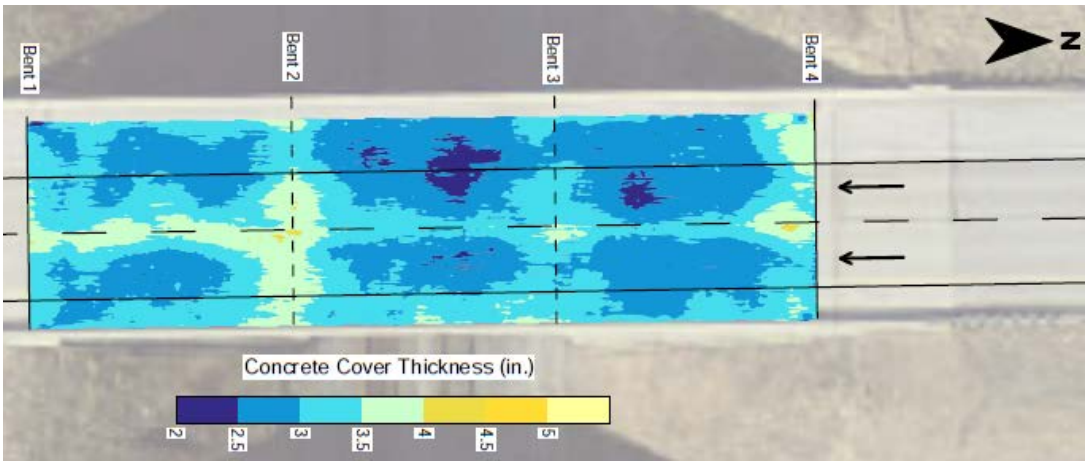

Bridge 04845

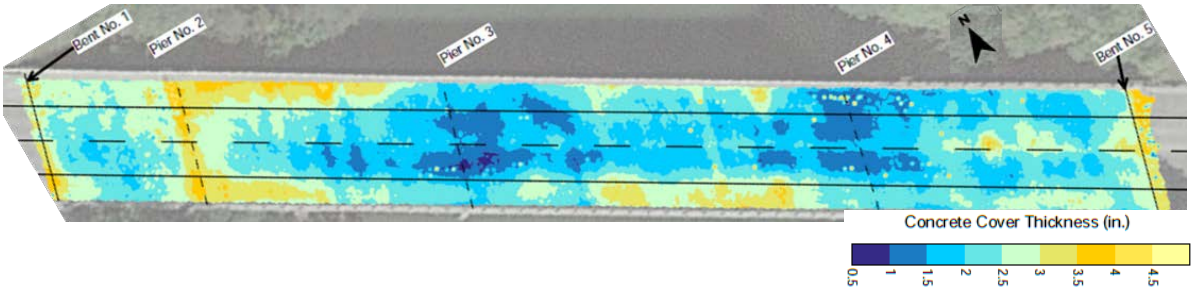

Bridge 04930

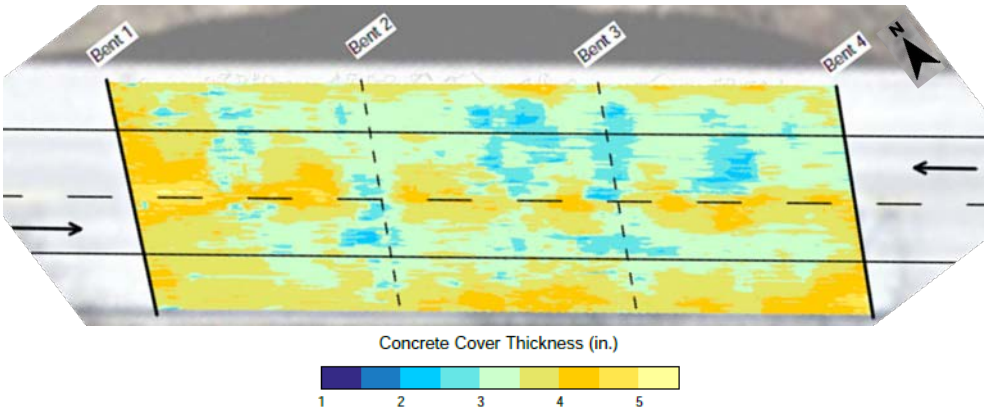

Bridge 08630

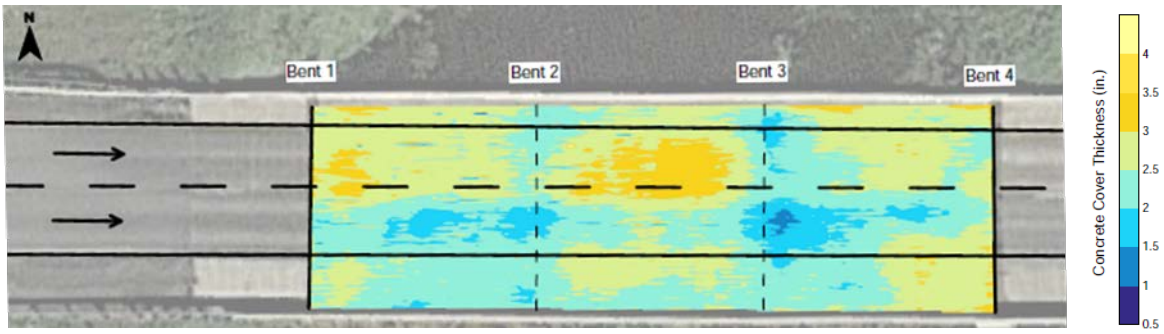

Bridge 17940

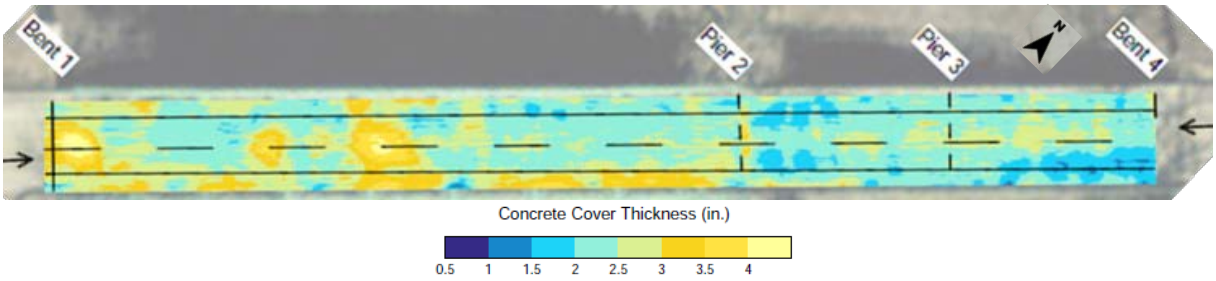

Bridge 19640

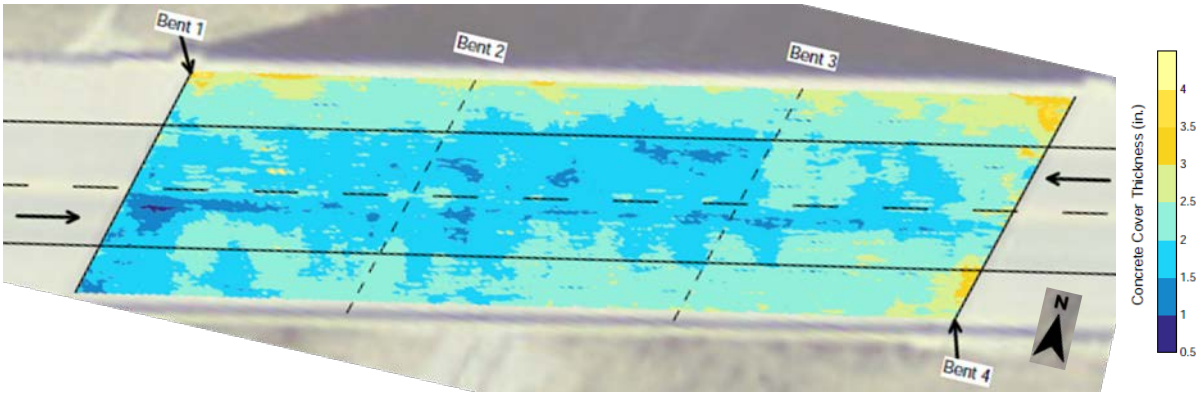

Bridge 20610

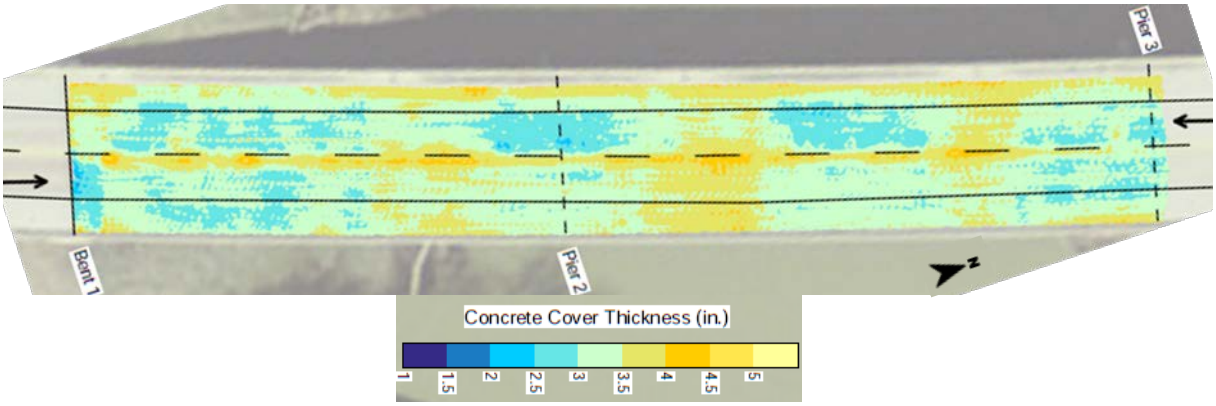

Bridge 24220

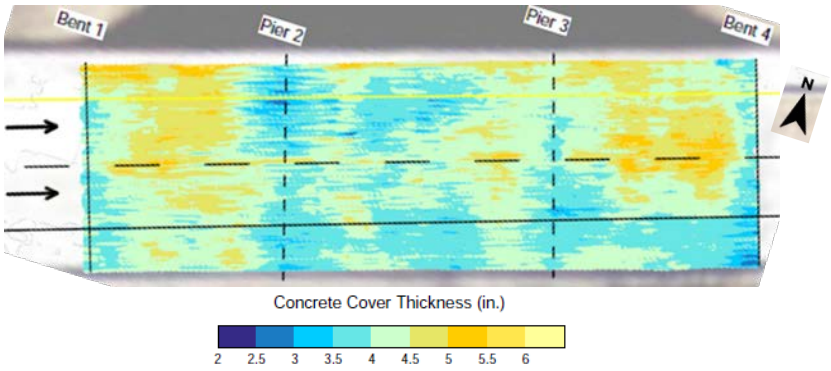

Bridge 49180

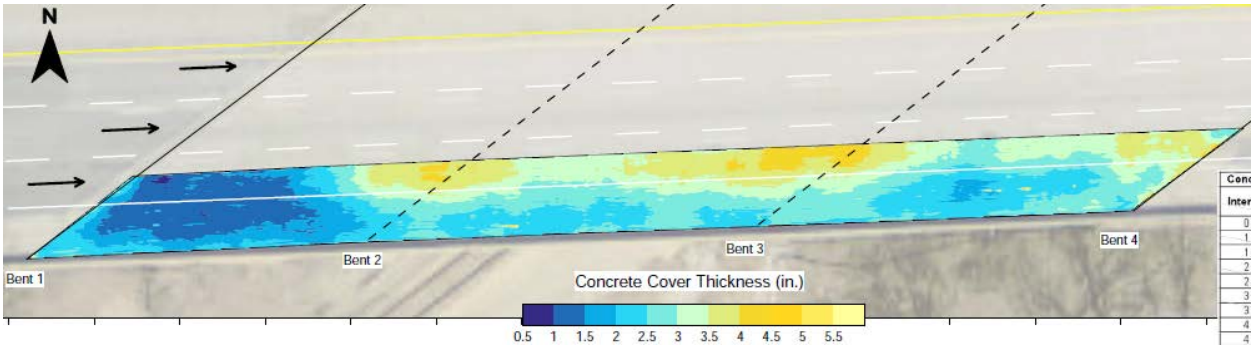

About the Joint Transportation Research Program (JTRP)

On March 11, 1937, the Indiana Legislature passed an act which authorized the Indiana State Highway Commission to cooperate with and assist Purdue University in developing the best methods of improving and maintaining the highways of the state and the respective counties thereof. That collaborative effort was called the Joint Highway Research Project (JHRP). In 1997 the collaborative venture was renamed as the Joint Transportation Research Program (JTRP) to reflect the state and national efforts to integrate the management and operation of various transportation modes.

The first studies of JHRP were concerned with Test Road No. 1—evaluation of the weathering characteristics of stabilized materials. After World War II, the JHRP program grew substantially and was regularly producing technical reports. Over 1,600 technical reports are now available, published as part of the JHRP and subsequently JTRP collaborative venture between Purdue University and what is now the Indiana Department of Transportation.

Free online access to all reports is provided through a unique collaboration between JTRP and Purdue Libraries. These are available at http://docs.lib.purdue.edu/jtrp.

Further information about JTRP and its current research program is available at http://www.purdue.edu/jtrp.

About This Report

An open access version of this publication is available online. See the URL in the citation below.

Jia, Y., William, C. S., Baah, P., & Bowman, M. D. (2022). *Long-term project and network-level NDT implementation plan for Indiana* (Joint Transportation Research Program Publication No. FHWA/IN/JTRP-2022/31). West Lafayette, IN: Purdue University. https://doi.org/10.5703/1288284317582